Flax fibres modification by cellulose nanocrystals and xyloglucan for the development of hierarchical biobased composites

Estelle Doineau

▶ **To cite this version:**

Estelle Doineau. Flax fibres modification by cellulose nanocrystals and xyloglucan for the development of hierarchical biobased composites. Materials. IMT - MINES ALES - IMT - Mines Alès Ecole Mines - Télécom, 2020. English. NNT : 2020EMAL0007 . tel-03634751

HAL Id: tel-03634751

https://theses.hal.science/tel-03634751

Submitted on 8 Apr 2022

HAL is a multi-disciplinary open access archive for the deposit and dissemination of scientific research documents, whether they are published or not. The documents may come from teaching and research institutions in France or abroad, or from public or private research centers.

L'archive ouverte pluridisciplinaire **HAL**, est destinée au dépôt et à la diffusion de documents scientifiques de niveau recherche, publiés ou non, émanant des établissements d'enseignement et de recherche français ou étrangers, des laboratoires publics ou privés.

THÈSE POUR OBTENIR LE GRADE DE DOCTEUR
ÉCOLE NATIONALE SUPÉRIEURE DES MINES D'ALÈS (IMT MINES ALÈS)

En Biomatériaux

École doctorale GAIA – Biodiversité, Agriculture, Alimentation, Environnement, Terre, Eau
Portée par l'Université de Montpellier

Unité de recherche Polymères et Composites Hybrides

Flax fibres modification by cellulose nanocrystals and xyloglucan for the development of hierarchical biobased composites

Présentée par Estelle DOINEAU
Le 10 Décembre 2020

Sous la direction de Jean-Charles BÉNÉZET
et Julien BRAS

Devant le jury composé de

Joël BRÉARD, Professeur, Université de Caen Normandie	Rapporteur
Jannick DUCHET-RUMEAU, Professeur, INSA de Lyon	Rapporteur
Tatiana BUDTOVA, Directrice de Recherche, Mines ParisTech	Présidente du jury
Hélène ANGELLIER-COUSSY, Maître de Conférences, Université de Montpellier II	Examinateur
Evelyne MAURET, Professeur, Grenoble INP	Examinateur
Jean-Charles BÉNÉZET, PR2, IMT Mines Alès	Directeur de thèse
Julien BRAS, Maître de Conférences, Grenoble INP	Co-directeur de thèse
Nicolas LE MOIGNE, Maître Assistant, IMT Mines Alès	Co-encadrant de thèse
Bernard CATHALA, Directeur de Recherche, INRAe Nantes	Co-encadrant de thèse / Membre Invité
Laurent HEUX, Directeur de Recherche, CERMAV – CNRS Grenoble	Membre Invité

UNIVERSITÉ DE MONTPELLIER

IMT Mines Alès
École Mines-Télécom

Remerciements

Je souhaiterais remercier dans un premier temps les membres du jury. La pandémie Covid-19 et l'instauration d'un nouveau confinement en France en novembre 2020 a fortement bouleversé le déroulement habituel d'une soutenance de thèse mais n'a entaché en rien les belles discussions qui ont eu lieu avec et entre les membres du jury, tous présents à distance. Pr Tatiana Budtova, merci d'avoir présidé ces 4 longues heures de soutenance et pour vos recommandations. Merci également aux Pr Jannick Duchet-Rumeau et Pr Joël Bréard pour le temps consacré au rapport de mon manuscrit de thèse et pour toutes les questions et remarques très enrichissantes énoncées lors de ma soutenance de thèse. Je tiens à remercier Pr Evelyne Mauret et Dr Hélène Angellier-Coussy pour avoir examiné mes travaux de thèse et pour tous leurs commentaires très constructifs. Je tiens également à te remercier Hélène pour ta bienveillance tout au long de ces trois années de thèse, en tant que référente de l'Ecole doctorale GAIA et membre de mes comités de suivis de thèse. De même, merci à Laurent Heux, directeur de recherche au CERMAV-CNRS, présent à ces comités et lors de ma soutenance en tant qu'invité ; j'ai apprécié les discussions et l'intérêt porté à mes travaux de thèse. Enfin, merci à Rodolphe Sonnier d'avoir accepté de participer à la réunion et aux discussions de mon 2ème comité de thèse.

Ce projet de thèse est né d'une collaboration entre 3 laboratoires de recherche, mais surtout 4 encadrants de thèse que je tiens à remercier tout particulièrement. Merci Jean-Charles pour ton soutien, ta confiance et tes nombreux conseils tout au long de ces trois années. Merci également à Julien pour ta confiance et pour avoir su trouver les mots avec ton éternel optimisme dans mes moments de doute, en début de thèse notamment. Chaque réunion se finissait par une liste d'idées et de voies nouvelles à explorer, qui me redonnaient dans un premier temps l'envie et la motivation d'avancer et qui, dans un second temps, me donnaient pas mal de fil à retordre… ;). Tu m'as donné l'opportunité d'aller à de nombreuses conférences en tant que spectatrice ou pour montrer mes travaux de thèse et je t'en remercie. Cela m'a permis d'ouvrir mon champ de vision sur des domaines de recherche scientifique éloignés de mon sujet de thèse, et donc d'accroître ma curiosité et ma culture scientifique. Bernard, je te remercie pour l'accueil chaleureux que tu me réservais à Nantes à chacun de mes passages et pour ton implication sans faille dans ce projet de thèse. Cette partie adsorption n'a pas été une mince affaire, cependant ta pédagogie, ta disponibilité et ton expertise m'ont permis de surmonter ces nombreux obstacles, et je t'en remercie

sincèrement. Enfin, merci Nicolas pour ton soutien également sans faille, ta forte implication et ta bonne humeur tout au long de cette thèse. J'ai appris énormément à tes côtés sur plein d'aspects scientifiques grâce à ta rigueur, ton expertise et ta disponibilité. Ta passion pour les sciences et la recherche est communicative et m'a donné l'envie de surpasser tous les problèmes rencontrés, d'aller plus loin dans les analyses et la compréhension des différents phénomènes impliqués. Tu t'es énormément impliqué dans cette thèse au niveau des idées, des relectures et corrections ou encore des nombreuses réunions et je t'en remercie infiniment. Jean-Charles, Julien, Bernard, Nicolas, j'ai énormément apprécié travailler à vos côtés pendant ces trois ans. Les réunions étaient fructueuses et très intéressantes scientifiquement avec beaucoup de discussions grâce à l'expertise de chacun. Vous m'avez tous apporté beaucoup et m'avez permis de m'épanouir sur le plan professionnel, mais également sur le plan personnel avec une plus grande confiance en moi.

Merci aux financeurs de ce projet : l'Ecole doctorale GAIA, le GDR SYMBIOSE et le GFP Méditerranée qui m'ont permis de mener à bien mes travaux de thèse et de partir à des conférences scientifiques internationales.

Je souhaite également remercier toutes les personnes qui m'ont apporté leurs connaissances techniques et leur bagage scientifique, et aidé lors des manipulations dans les différents laboratoires : Nadège Leray pour les manipulations sur l'adsorption du XG et des CNC (BIA à INRAe Nantes), Cécile Sillard (AFM et XPS, LGP2), Monica Francesca Pucci (tensiomètre K100SF et AFM, IMT Mines Alès), Bruno Novales (microscope confocal, BIBS à INRAe Nantes), Alain Diaz (préparation échantillons MEB, IMT Mines Alès), Jean-Claude Roux (MEB, IMT Mines Alès), Mohamed Karrouch (microcompounder et mini-presse à injection, 3SR Grenoble), Stéphane Corn (FDAS et IFSS, IMT Mines Alès), Maxime Terrien (mécanique et composites, LGP2), Alexandre Cheron (traction quasi-statique et choc Charpy, IMT Mines Alès), Benjamin Gallard (thermocompression, IMT Mines Alès), Loïc Dumazert (DSC et TGA, IMT Mines Alès). Merci à Guillaume Coqueugniot (stagiaire PFE ingénieur, LGP2), Guillaume Bauer (stagiaire M1, INRAe Nantes) et Léo Ensenlaz (stagiaire IUT, LGP2) pour leur investissement et leur aide précieuse sur les différents pans de ma thèse.

Evidemment, je tiens à remercier le personnel des trois laboratoires LGP2, IMT Mines Alès et INRAe Nantes (BIA), à savoir les permanents, les services administratif, technique et informatique pour leur disponibilité et leur aide.

Pour resituer le contexte, j'ai tout d'abord évolué dans les locaux du LGP2 de novembre 2017 à février 2019. Je tiens à remercier la direction et particulièrement Didier pour son écoute, sa bienveillance et sa gentillesse. Un merci amical à Cécile pour ta collaboration sur l'AFM, ton expertise mais aussi et surtout pour ta bonne humeur en toute circonstance et ta gentillesse. J'ai eu la chance de travailler dans ce laboratoire que l'on peut assimiler à une famille avec des personnes bienveillantes et toujours prêtes à aider. J'ai adoré les repas tous ensemble (barbecue, raclette, repas de noël) mais également la soirée ski nocturne à Chamrousse. Je tiens à remercier et embrasser les doctorants et post-doctorants (Manon, Gab, Hugo, Mathieu, Johanna, Hippolyte, Loreleï, Bastien, Lili, Flavien, Etienne G., Claire, Camille, Amina, Clémentine, Erwan, Axelle, Charlène, Maxime W., Eva) avec qui j'ai passé de super moments et sans qui ce séjour au LGP2 n'aurait pas été le même. Plus personnellement, big up à la team sport/trail (Hippolyte, Axelle, Camille, Vivien) et à notre performance au trail du Grand Duc en Chartreuse. Un grand merci à Manon, copine de bureau, pour ta bonne humeur contagieuse, tes conseils de « grande sœur » et ton soutien moral ! Enfin, merci à Hugo et Gab, les As du Carreaux, avec qui j'ai gagné le tournoi de pétanque du labo mais avec qui surtout j'ai gagné une amitié infaillible, permettant de surmonter les obstacles de la thèse sans problème ! Grosse pensée à vous ☺.

Puis, je suis arrivée à l'IMT Mines Alès en février 2019 pour y rester jusqu'à la fin de ma thèse. Merci à tous les doctorants et post-doctorants avec qui j'ai eu la chance de travailler mais pas que… : mots-croisés, soirées, sport, baignades etc. Merci donc à Haithem, Helena, Léa LM, Mathieu, Julie, Adrien, Rob, Wahab, Léa Floch, Raïssa, Angélique, Julien, Kübra, Valentin, Rachel. Merci à l'association l'ATHEMA qui a fait un boulot remarquable pour renforcer la cohésion des doctorants (Antoine au badminton, Valentin et Adrien au cardio/muscu par exemple). Ici aussi, j'ai rencontré des gens fantastiques qui sont devenus des amis et que je n'oublierai jamais. Tout particulièrement, merci à toi Haithem avec qui j'ai fini ma thèse à une semaine près ! Tu as le don de rassembler les gens de par ta gentillesse et ta bienveillance, cela ne m'étonne pas que ton bureau ait été re-baptisé « Le café du coin » ☺. Merci pour ton aide si précieuse durant cette seconde moitié de thèse. Merci aux chicas Helena et Julie, avec qui j'ai beaucoup ri, partagé de super moments au sein du C2MA mais aussi en dehors (la Fabrique à boire, les randonnées, les parties de pétanque, le badminton, les soirées à n'en plus finir et j'en passe !). Petit big up à Mathieu pour ces parties infinies au ping-pong, et Léa LM pour les dégustations de burgers cévenols à l'Urban Parc. J'ai également apprécié le temps passé avec les techniciens du C2MA et particulièrement Romain et Benji, toujours à courir dans tous les sens. Benji, merci pour ce weekend Rapaces en Lozère avec Jane, je n'oublierai pas cette belle journée ! Ces après-midis

barbecue, rivière et chill ou encore les soirées à la Fabrique ou Alès plage sont de beaux souvenirs ;).

Enfin, merci également à l'équipe Nano de BIA à l'INRAe Nantes qui m'a accueillie chaleureusement à mes 4 ou 5 brefs passages (1 à 2 semaines max) durant ces 3 ans. Je pense à Maud, Malika, Aurore, Somia, Nadège, Hugo et les stagiaires Baptiste, Sébastien, Guillaume, Antoine. Vous êtes une équipe dynamique, soudée et bienveillante et cela m'a permis d'apprécier mes séjours passés sur Nantes malgré la charge de travail monstrueuse que j'avais à réaliser sur place. Merci beaucoup !

J'ai aussi la chance d'avoir des amis à l'extérieur qui m'ont épaulé de loin. Je pense à Loulou, ma copine de la galère prépa, Lolotte partie du côté de la Catalogne à Barcelone, Paupau qui s'est envolée sur l'île de la Réunion, Philou partie à Barcelone puis Toronto, Arthur et ses rillettes du Mans et Jordy (#Neuchâtel). J'embrasse bien sûr la team de Grenoble (Gaby, Noémi, Nana, Lucas, Hugo et Gab) qui m'ont beaucoup soutenue et encouragée et avec qui j'ai passé et je passe toujours de super moments. Bisous aussi à la team de Solvay à Lyon avec ces weekends à boire des bières en terrasse, jouer au palet breton ou encore danser jusqu'au bout de la nuit. Cela m'a fait extrêmement plaisir que vous assistiez pour la plupart à ma soutenance de thèse, je vous sentais à mes côtés.

Bien sûr, je te remercie toi, Thibaut, qui est arrivé à mes côtés dans les mois difficiles de rédaction et soutenance… Tu as été le rayon de soleil qui me manquait pour finir cette thèse et tu m'as apporté la confiance nécessaire. Merci pour la personne que tu es, pour tout ce que tu fais au quotidien, ta joie de vivre, ton grand cœur et ta gentillesse. Je t'aime.

Bien sûr et enfin, tout cela n'aurait pas été rendu possible sans ma famille à qui je dois beaucoup. Merci à ma sœur Gaëlle et mon beau-frère Guillaume, pour m'avoir accueillie sur Nantes lors de mes nombreux déplacements à l'INRAe. Vous m'avez soutenue et donnée de l'énergie, notamment pour faire le trajet interminable maison-labo matin et soir ☺ Merci à vous Papa, Maman, pour votre aide depuis le début de ces longues études. Les deux mois de confinement passés à vos côtés m'ont permis de tenir dans cette rédaction et cette période angoissante. Vous avez toujours été présents à mes côtés et m'avez sans cesse poussée et encouragée à aller plus loin. Je vous dois beaucoup, je vous aime et je vous embrasse très fort ! <3

General table of contents

RÉSUMÉ FRANÇAIS

French Abstract

I. Composites biosourcés à base de fibres végétales

Un matériau composite est un matériau multi-phasé constitué d'une matrice, d'un renfort mais également d'une zone interfaciale renfort / matrice [1]. Le développement d'un matériau composite peut notamment avoir pour objectif d'alléger la pièce produite tout en conservant de bonnes propriétés physiques et mécaniques. Le marché des composites à matrice polymère et renforts fibreux est en plein essor au niveau mondial : 11,4 Mt en 2018 contre 8,5 Mt en 2010 avec une utilisation majoritaire des fibres de verre à 87,7 % (en volume), 11 % de fibres végétales (lin, chanvre, coton,…) et 1,2 % de fibres de carbone [2].

Dans le contexte environnemental actuel, il paraît indispensable de se tourner vers des matières premières plus respectueuses de l'environnement dans l'intégralité de leur cycle de vie. Le gouvernement français et l'Union Européenne (UE) ont financé depuis 2000, 195 projets liés aux composites à base de fibres végétales et plus de 560 millions d'euros ont été investis en grande partie dans les secteurs de la construction, l'automobile et l'emballage [3] (**Figure 1**).

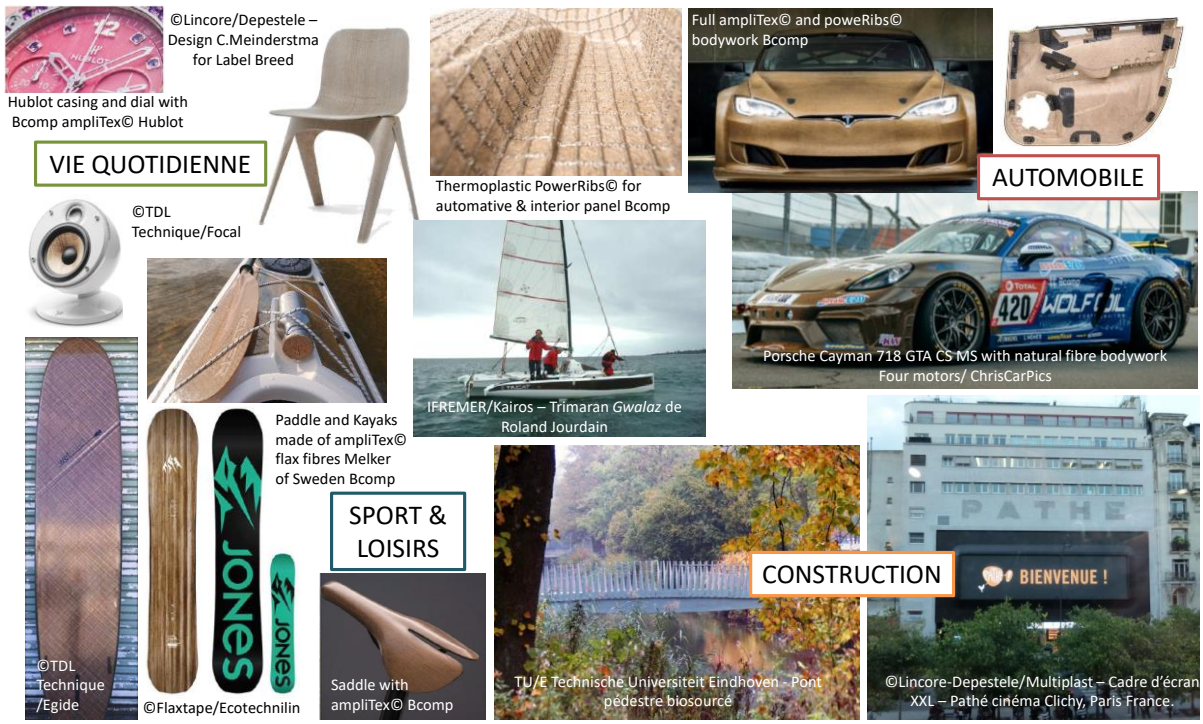

Figure 1 : Composites biosourcés réalisés à base de fibres de lin et/ou chanvre dans les secteurs de la construction, l'automobile, les sports et loisirs et la vie quotidienne (repris avec permission de CELC-Gomina [4] et Bcomp-Rion [5]).

La production de composites biosourcés, aussi appelés « biocomposites », a atteint en Europe 410 kT en 2017 contre 357 kT en 2012 [6]. Leur croissance annuelle moyenne est estimée à 3%, allant jusqu'à 30% dans certains domaines d'application, avec majoritairement la construction (terrasse, clôture…) représentant 49% du marché et l'automobile avec principalement des pièces intérieures (36% du marché). D'autres secteurs d'application innovants peuvent également être cités comme le mobilier et biens de consommation, les objets en impression 3D etc. La législation de l'UE suit ce chemin avec une réduction des émissions de CO_2 imposée à 95 g/km en 2020 contre 135 g/km auparavant dans le secteur automobile, poussant les constructeurs à alléger les véhicules [6]. Les fibres végétales telles que le lin sont de bonnes candidates (**Tableau 1**) avec une faible densité comparée aux fibres de verre et de carbone, permettant ainsi un allègement des pièces, un prix très attractif et des propriétés mécaniques compétitives avec notamment une très bonne rigidité spécifique.

Tableau 1 : Propriétés mécaniques et coûts moyens des fibres de verre (type E), de carbone et de lin.

Fibres	Résistance σ (MPa) / Spécifique σ/d	Rigidité E (GPa) / Spécifique E/d	Densité	Déformation à la rupture (%)	Prix (Euro/kg)	Références
Verre (type E)	2500 – 3500 / 960 - 1400	70 – 73 / 27 - 28	2,6	2,5 – 4,0	1,5 – 2,5	[7], [8]
Carbone	2500 – 6000 / 1400 - 3300	220 – 700 / 120 – 380	1,75 – 1,9	1,4 - 2	30 – 50	[7], [9]
Lin	595 – 1510 / 410 – 1040	37 – 75 / 26 – 52	1,4 – 1,5	1,6 – 3,6	0,5 – 1	[7], [10]

La particularité des fibres végétales réside dans leur plus faible impact environnemental (disponibilité de la ressource renouvelable, neutralité carbone, biodégradabilité) en comparaison aux fibres de verre avec notamment un faible impact sur le réchauffement climatique et la diminution de la couche d'ozone (**Figure 2**). Il a été estimé qu'un hectare de lin textile permet de stocker 3,5 tonnes de CO_2 [11].

Les composites à renfort végétal possèdent d'autres avantages comme une bonne isolation thermique et phonique ou encore un fort amortissement des vibrations [6], [10]. Cependant, l'étude de Coroller *et al.* (2013) sur la confection de composites époxy / verre et époxy / lin avec renforts unidirectionnels montre une différence des propriétés mécaniques des composites [12]: volume de fibres, module d'Young et résistance en traction de 45 %, 34 GPa et 550 MPa respectivement pour le composite à renfort en verre, contre 51 – 54 %, 26 – 34 GPa

et 290 – 410 MPa pour le composite à renfort en lin (selon la variété des fibres de lin, i.e. Hermès, Andrea ou Marylin). Cette différence est due d'une part aux différences de propriétés mécaniques intrinsèques des renforts mais aussi à la moins bonne compatibilité et adhésion interfaciale lin / résine époxy. En effet, les renforts en fibres de verre subissent systématiquement un ensimage ou « sizing » (traitement de surface) [13], [14], fruit de plusieurs années de développement et permettant l'amélioration de l'adhésion fibre / matrice. Les composites à base de fibres végétales ne disposent pas encore aujourd'hui d'un tel historique scientifique et technologique.

Figure 2 : Carte radar représentant les impacts environnementaux durant la production de fibre de lin peignées en comparaison aux fibres de verre (Le Duigou *et al.* 2011 [15], pas de permission de diffusion de l'image).

II. Problématique et enjeux

L'une des problématiques des composites biosourcés à renforts végétaux réside dans la mauvaise compatibilité entre les fibres végétales et la matrice polymère. La zone tridimensionnelle mise en jeu est appelée « interphase » ou « zone interfaciale », une extension de l'interface définie seulement par deux dimensions. Cette région de transition, d'une centaine de nanomètres jusqu'à quelques microns selon les matrices polymères

considérées, permet le transfert et la distribution des charges de la matrice vers les fibres lorsque le composite est soumis à une sollicitation mécanique [1]. Cette zone d'interphase est le siège de différents phénomènes chimiques et physiques. Ainsi, la qualité de l'adhésion interfaciale est gouvernée par les interactions (physico-)chimiques entre le renfort et la matrice polymère en lien avec le mouillage et la réactivité chimique de la matrice, ainsi que par la quantité d'interface et l'ancrage mécanique liés notamment à la surface spécifique et la topographie du renfort (**Figure 3**).

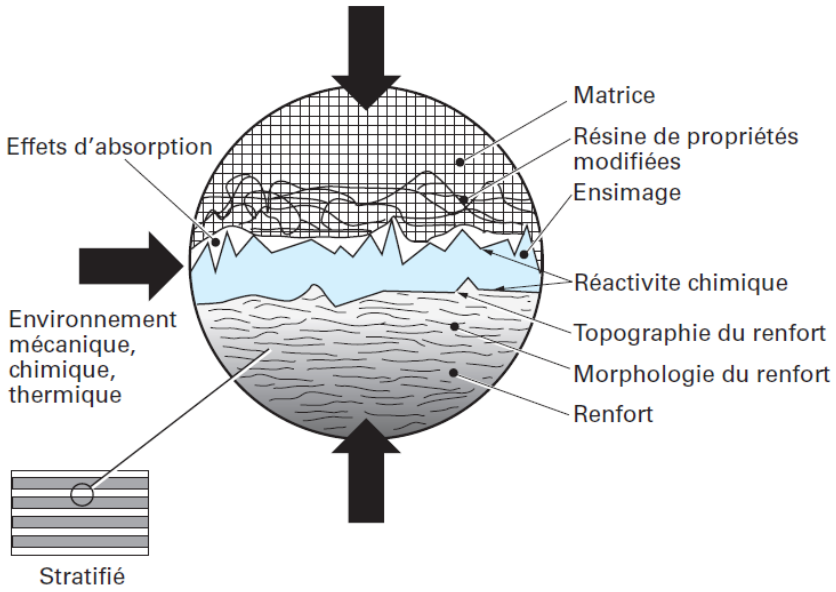

Figure 3 : Ensemble des phénomènes intervenant dans la zone d'interphase fibre / matrice dans un matériau composite (repris avec permission de Herrera-Franco et Drzal 1992 [16], Bergeret et Krawczak 2006 [1]).

Une interphase dite « faible » sera caractérisée par des ruptures adhésives à l'interface avec un déchaussement des fibres dans la matrice et une propagation de fissures le long de cette zone, impliquant une baisse des propriétés mécaniques et une possible augmentation de la fragilité du composite. Un compromis entre résistance et ténacité est toujours nécessaire et implique un choix adapté de la stratégie de compatibilisation entre fibres et matrice.

Le cas des fibres végétales est plus complexe car celles-ci sont en grande partie hydrophiles et polaires, en contact avec une matrice polymère majoritairement hydrophobe et apolaire. De plus, les renforts végétaux sont des matériaux complexes et multi-échelles, impliquant une chimie de surface hétérogène et la présence de multiples interfaces au sein du composite, (**Figure 4**), et donc de potentielles zones de défauts dans le matériau.

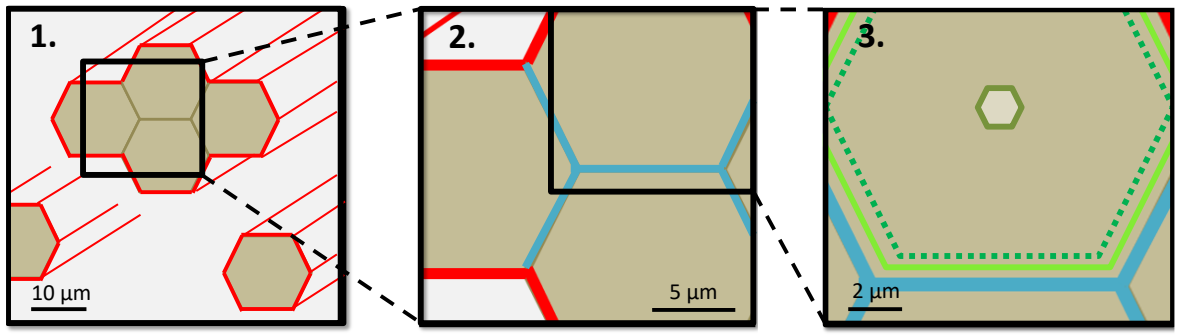

1. Interface **matrice / faisceaux ou fibres élémentaires de lin** (rouge)
2. Interface **entre les fibres élémentaires dans le faisceaux** (bleu)
3. Interface **entre les couches** dans les parois cellulaires de la fibre élémentaire (vert)

Figure 4 : Schéma des différentes interfaces présentes au sein d'un composite biosourcé à renfort végétal.

Pour tenter de répondre à cette problématique, de nombreuses stratégies ont été développées pour modifier les fibres végétales et améliorer leur affinité avec les matrices polymères [17], [18] : *(i)* prétraitements (rouissage, extraction par voie chimique ou solvant), *(ii)* fonctionnalisation chimique (acides gras, anhydrides d'acide, diisocyanates, organosilanes,…), *(iii)* fonctionnalisation physique (traitement plasma, irradiation gamma,…) ou encore *(iv)* traitements thermiques. Ces modifications ont permis d'augmenter les quantités d'interface fibre / matrice par une meilleure dispersion des fibres, ainsi qu'une meilleure compatibilité physico-chimique (**Figure 5**).

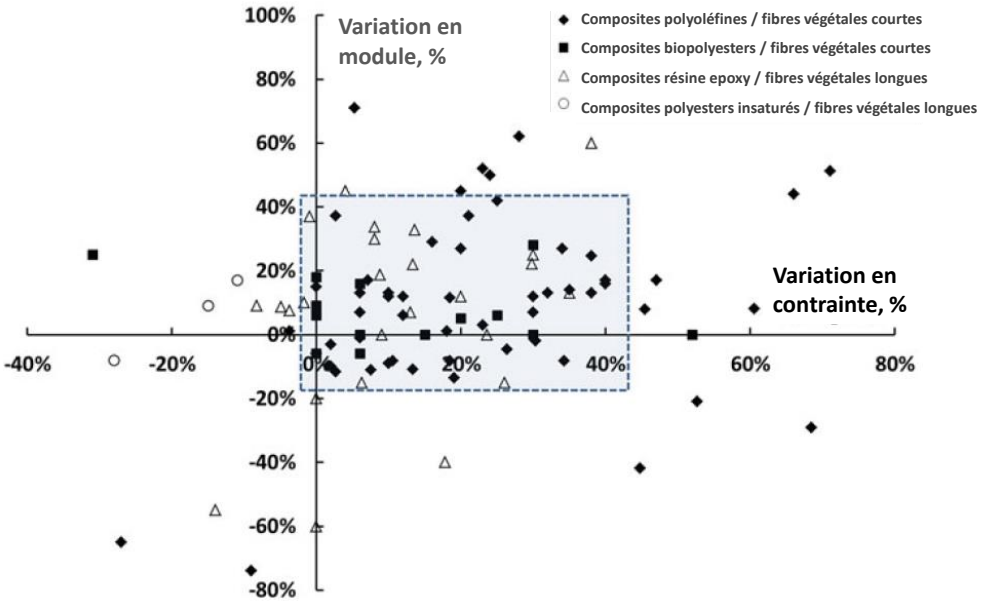

Figure 5: Diagramme d'Ashby – variation en module versus en contrainte (propriétés en traction ou flexion) des composites à renforts végétaux ayant subi des prétraitements et/ou fonctionnalisations de fibres. Ensemble de données non-exhaustif (repris avec permission de Le Moigne *et al.* 2018 [19]).

Une amélioration des propriétés mécaniques telles que le module d'Young ou la résistance en traction a été obtenue, mais ces performances ne permettent pas de cibler des pièces structurelles nécessitant des propriétés mécaniques plus élevées, ce qui est par exemple le cas dans le secteur automobile.

III. Projet de thèse : concept, verrous et démarche scientifiques

Dans ce contexte, ce projet de thèse porte sur la « *Modification de fibres de lin par des nanocristaux de cellulose et du xyloglucane pour le développement de composites biosourcés hiérarchiques* », fruit d'une collaboration entre 3 laboratoires français : l'IMT Mines Alès (Polymères, Composites et Hybrides, PCH), le LGP2 (Laboratoire Génie des Procédés Papetiers) à Grenoble et l'INRAe (Biopolymères Interactions Assemblages, BIA) à Nantes (**Figure 6**).

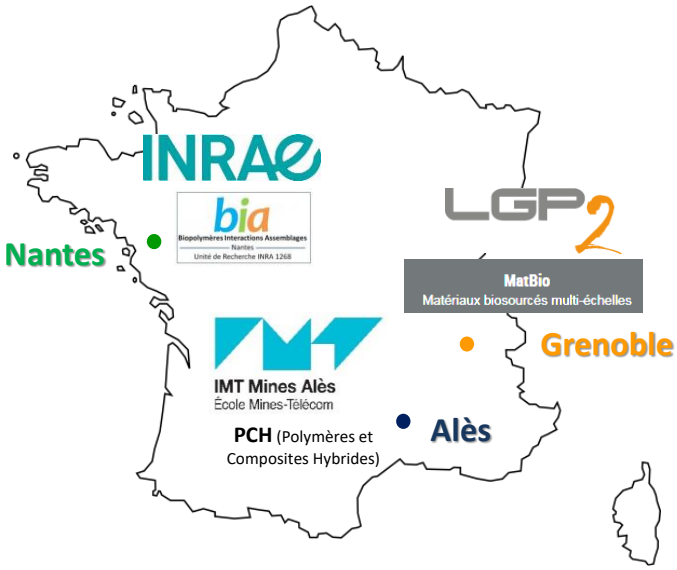

Figure 6 : Ensemble des laboratoires intégrés au projet de thèse.

III. 1. Concept du projet de thèse

Le concept développé dans ces travaux pour modifier les fibres de lin est directement inspiré de systèmes présents dans la nature (os, nacre, bois). En effet, ceux-ci possèdent des structures hiérarchiques se développant de l'échelle macroscopique à l'échelle nanoscopique [20]. Il a été démontré l'importance de l'architecture hiérarchique dans ces systèmes biologiques et particulièrement la présence de nano-objets qui améliorent de manière

considérable certaines propriétés du matériau telles que la résistance et la ténacité [21]. Des chercheurs se sont inspirés de ce concept dans la réalisation de composites hiérarchiques en déposant à la surface de fibres de renfort (fibres de carbone, de verre ou végétales) des nanoparticules telles que des nanotubes de carbone, des nanofils d'oxyde de zinc, des nano-argiles ou encore des nanocelluloses [22]–[24]. Le but de cette nanostructuration de surface étant notamment l'amélioration de la résistance interfaciale et de l'ancrage mécanique fibre / matrice, induisant un meilleur transfert de charges au sein du composite. En transposant ces structures pour la création de fibres hiérarchiques 100% biosourcées, une stratégie originale de nanostructuration des fibres de lin a été mise en place pour améliorer l'interphase fibre / matrice dans les biocomposites à l'aide de deux co-produits de la biomasse ligno-cellulosique : le xyloglucane (XG) et les nanocristaux de cellulose (CNC), illustrée avec l'exemple du tissu de lin (**Figure 7**).

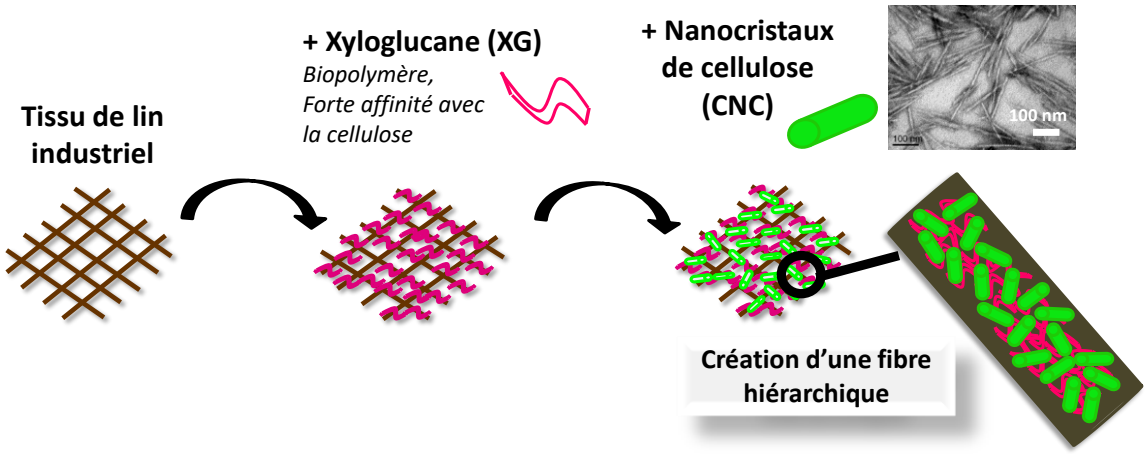

Figure 7 : Schéma de nanostructuration d'un tissu de lin par adsorption de nanocristaux de cellulose et de xyloglucane. Ce schéma n'est pas à l'échelle pour faciliter l'illustration.

En effet, le XG est un polymère naturel disposant d'une forte affinité avec les surfaces cellulosiques via des interactions hydrogène et van der Waals, et pouvant donc être utilisé en tant qu'agent interfacial pour l'auto-assemblage des CNC sur les fibres de lin. Les CNC possèdent par ailleurs des propriétés physiques très intéressantes avec un module d'Young de l'ordre de 100 à 130 GPa et une surface spécifique estimée entre 150 et 800 g/m² [25], [26], permettant un renfort de l'interphase fibre / matrice avec un ancrage mécanique augmenté. De plus, les CNC possèdent plusieurs groupements hydroxyle en surface pour une possible fonctionnalisation, toujours dans le but de compatibiliser les fibres et la matrice polymère.

Enfin, l'atout de cette stratégie de nanostructuration est l'utilisation de l'eau comme solvant non-toxique.

III. 2. Démarche scientifique et déroulé du manuscrit de thèse

Ce projet de thèse se divise en trois grands volets qui structurent le manuscrit de thèse :

(1) La création de fibres de lin hiérarchiques ou nanostructurées par l'adsorption de xyloglucane et de nanocristaux de cellulose à leur surface ;

(2) L'apport de la combinaison de deux stratégies de modification de l'adhésion interfaciale, à savoir les fibres hiérarchiques CNC ou XG/CNC et l'ajout d'un agent de couplage chimique au sein de la matrice, sur le comportement mécanique de composites thermoplastiques polypropylène / fibres courtes de lin, préparés par extrusion bi-vis et injection ;

(3) L'analyse multi-échelle de composites thermodurcissables stratifiés époxy / tissus de lin unidirectionnels (UD) modifiés CNC et XG/CNC, préparés par thermocompression.

Le ***Chapitre I*** porte sur l'état de l'art avec une section ***I.1.*** décrivant la fibre de lin de sa croissance et sa structure jusqu'à son utilisation comme renfort dans les matériaux composites. Cette section traite également du XG, des CNC et de l'importance des interactions XG / cellulose. La section ***I.2.*** détaille le rôle de la zone d'interphase fibre / matrice dans les composites. Elle décrit également les principales stratégies de modification des fibres végétales en vue de leur compatibilisation avec les matrices polymères. Enfin, la section ***I.3.*** met l'accent sur le concept bio-inspiré de la création de fibres hiérarchiques avec différents exemples allant des composites synthétiques jusqu'aux composites biosourcés à fibres végétales, en passant par des systèmes hybrides. Cette dernière section a pour but de comprendre l'apport du dépôt de nano-objets à la surface de fibres de renfort sur les propriétés de matériaux composites et plus précisément dans la zone d'interphase.

Les Chapitres de ce manuscrit de thèse sont basés sur des publications acceptées (***Chapitre I, Chapitre II***, ***Chapitre III)*** ou en cours d'écriture (***Chapitre IV)*** et couvrent, dans l'ordre, les 3 grands volets du projet de thèse présentés ci-dessus.

Le ***Chapitre II*** du manuscrit de thèse porte sur la compréhension des processus d'adsorption XG/CNC sur les fibres de lin. La démarche scientifique est détaillée dans le **Tableau 2**.

Tableau 2 : Questions de recherche et stratégies/techniques utilisées dans le ***Chapitre II*** pour l'étude du processus d'adsorption de XG et/ou CNC sur un tissu de lin.

Questions de recherche	Stratégies/Techniques mises en œuvre
• **Localisation** de XG et CNC sur le tissu ? **Pénétration** des composants dans l'architecture du tissu ?	Couplage d'images en microscopie à balayage électronique **(MEB)** + **Microscopie confocale** avec un greffage de marqueurs fluorescents (rhodamine B et fluorescéine) sur XG et CNC 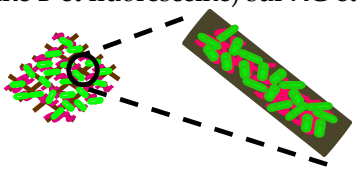
• **Quantification** de XG et/ou CNC adsorbés sur les fibres ? • **Cinétique d'adsorption (ou sorption)** du XG et des CNC sur les fibres de lin **?**	Utilisation de XG et CNC greffés avec le marqueur fluorescent rhodamine B et analyse du surnageant en **spectroscopie UV** → obtention d'**isothermes d'adsorption**
• **Architecture et adhésion lin / XG / CNC** obtenues ?	Mesures de la **force d'adhésion** par microscopie à force atomique **(AFM)** → fonctionnalisation de pointes avec XG ou CNC pour mesures d'adhésion sur fibres de lin 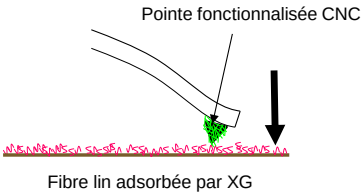

Comme détaillé ci-dessus, le ***Chapitre II*** se base sur l'utilisation de marqueurs fluorescents greffés sur XG et CNC pour localiser et quantifier leur adsorption (environ 20mg/g_{fibres}). Il permet également une mise en lumière de la complexité de l'adsorption du XG et des CNC sur un matériau tel qu'un tissu de lin industriel avec des phénomènes de pénétration dans les mèches, de gonflement et de déstructuration. Enfin, des mesures de force d'adhésion en AFM ont permis de révéler la création d'un réseau extensible XG/CNC en surface de la fibre de lin.

Les Chapitres suivant, à savoir le ***Chapitre III*** et le ***Chapitre IV***, utilisent le procédé de traitement des fibres par CNC et XG/CNC étudié dans le ***Chapitre II*** et adapté à plus grande échelle au type de renfort utilisé. Le ***Chapitre III*** du manuscrit de thèse est consacré à l'étude

de l'incorporation de fibres courtes de lin modifiées CNC ou XG/CNC dans une matrice thermoplastique polypropylène, par extrusion bi-vis. Ce chapitre a pour objectif d'étudier l'apport de la combinaison de deux stratégies de modification de l'interface fibres / matrice sur le comportement mécaniques des composites, à savoir le traitement CNC ou XG/CNC des fibres de lin et l'ajout d'agent de couplage chimique polypropylène greffé anhydride maléique (PP-g-MA) dans la matrice. Afin de mieux comprendre le rôle de la nanostructuration de surface des fibres de lin, des analyses micro- et macroscopiques ont été réalisées sur les composites, telles que détaillées dans le **Tableau 3**.

Tableau 3 : Questions de recherche et stratégies/techniques utilisées dans le ***Chapitre III*** pour l'étude des microstructures et du comportement mécanique des composites thermoplastiques PP / fibres courtes de lin.

Questions de recherche	Stratégies/Techniques mises en œuvre
• **Imprégnation et adhésion interfaciale fibre/matrice** dans les conditions de mise en œuvre du composite ?	→ **Tensiomètre K100SF** : immersion d'une fibre élémentaire dans des liquides choisis pour l'obtention de l'énergie de surface (composantes polaires et dispersives) des fibres modifiées → **Calcul du travail d'adhésion** entre le PP ou PP-g-MA et les fibres de lin modifiées à la température de mélange (190°C) selon les modèles OWRK [27] et Wu [28]
• Effet de la **combinaison de 2 stratégies de modification de l'adhésion interfaciale sur la microstructure et le comportement mécanique** du composite ? 1) nanostructuration des fibres de lin par adsorption de CNC et XG/CNC 2) ajout d'un agent de couplage polypropylène greffé anhydride maléique (PP-g-MA)	→ Échelle micro : tests de **micro-traction sous MEB** *(20% fibres en massique)* - Mesure du travail à la rupture - Observation de la propagation de fissures au sein du matériau 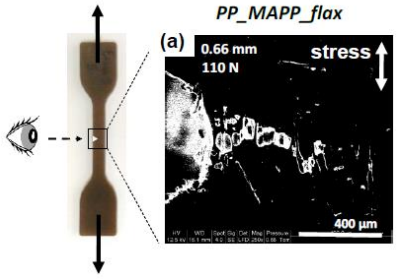 → Échelle macro : tests de **traction uni-axiale** *(5, 20 et 30% fibres en massique)* - Mesure de la contrainte maximale et du module d'Young - Mesure du travail à la rupture → Étude microstructurale : - **Taux de cristallinité Xc** de la matrice - **Facteur de forme L/d** et dispersion des fibres de lin dans les composites

Le ***Chapitre III*** a révélé que l'adsorption de CNC à la surface de fibres de lin diminue leur caractère polaire en surface et améliore le travail d'adhésion avec la matrice PP / PP-g-MA. De plus, la combinaison des modifications interfaciales avec la nanostructuration des fibres via l'adsorption de CNC et XG/CNC à leur surface ainsi que l'utilisation de l'agent de couplage PP-g-MA apporte vraisemblablement des liaisons covalentes avec les fibres, ce qui améliore les propriétés en rupture des composites. Des fissures locales plus progressives ont été observées ainsi qu'une amélioration des contraintes et travaux à la rupture en traction : augmentation de 12,5 % et 21,6 % du travail à la rupture des composites mesuré par tests micromécaniques pour les traitements CNC et XG/CNC, respectivement.

Enfin, le ***Chapitre IV*** du manuscrit de thèse porte sur une étude multi-échelle de composites stratifiés thermodurcissables à matrice résine époxy et tissus UD lin modifiés CNC ou XG/CNC. Il met également l'accent sur le procédé de traitement des tissus et son impact sur les microstructures et les performances mécaniques du composite stratifié final. Les méthodes/techniques utilisées pour appréhender au mieux les questions de recherche posées sont détaillées sur le **Tableau 4**.

Tableau 4 : Questions de recherche et stratégies/techniques dans le ***Chapitre IV*** utilisées pour l'étude multi-échelle des composites stratifiés thermodurcissables époxy / tissus UD lin.

Questions de recherche	Stratégies/Techniques mises en œuvre
• Effet du traitement CNC et XG/CNC sur la **morphologie des fibres et des mèches** au sein du tissu UD lin ?	→ Observations **MEB** des mèches de lin issues des tissus UD traités → **Analyse dimensionnelle/gravimétrique** de l'effet du procédé de traitement (trempage, séchage) et de l'adsorption de CNC et XG/CNC.
• **Phénomènes d'imprégnation** des plis de lin traités CNC et XG/CNC par la résine époxy	→ **Tensiomètre K100SF** : mesure de l'énergie de surface (composantes polaires et dispersives) des fibres modifiées et de l'angle de contact avec la résine époxy → Calcul du **travail d'adhésion** Equation de Young-Dupré [29], [30] et modèles de OWRK et Wu 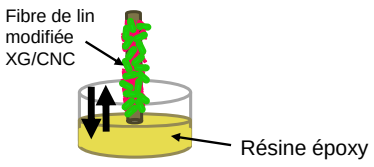 → Microstructure : **Etat de dispersion** des fibres et mèches dans la matrice (MEB) + Détermination des **volumes de porosité et de fibres** dans le composite

• Effet du **procédé de traitement des tissus (trempage et séchage)** sur les propriétés du composite final ?	→ **Alignement des plis de tissu de lin** dans le composite stratifié sur surfaces polies (MEB) → Utilisation de **deux procédés de séchage** différents (libre ou sous tension) 
• **Comportement mécanique** des composites stratifiés et effet des traitements CNC et XG/CNC ?	→ **Comportement visco-élastique :** rigidité en traction uni-axiale dans le sens longitudinal, analyse thermo-mécanique dynamique en transverse → **Comportement à la rupture :** résistance en traction uni-axiale dans les sens longitudinal et transverse, observations MEB des faciès de rupture en traction transverse → **Utilisation de lois de mélange** pour analyser l'effet des traitements sur les propriétés mécaniques

Une analyse multi-échelle a été réalisée dans le ***Chapitre IV*** pour étudier l'effet des traitements CNC et XG/CNC du tissu UD lin sur la fibre élémentaire, la mèche et la microstructure des composites. Ces analyses ont permis de mieux comprendre les comportements (visco-)élastique et à rupture des composites en lien avec les traitements réalisés sur les tissus de lin. Une amélioration du travail à la rupture en traction sens longitudinal a été mesurée avec des augmentations de 11 % et 14 % pour le traitement CNC, séchage libre et sous tension respectivement. En revanche, le traitement XG/CNC a généré la formation de structures/réseaux polymères autour des fibres dans les mèches du tissu, induisant une moins bonne dispersion et imprégnation des fibres dans la résine époxy et de la porosité au sein du composite laminé. Enfin, les traitements appliqués aux tissus de lin pouvant modifier leur structure, des composites de « contrôle » ont été étudiés afin de prendre en compte l'effet du procédé de traitement, à savoir les étapes de trempage et de séchage des tissus.

Ainsi, les ***Chapitre III*** et ***Chapitre IV*** étudient l'utilisation de fibres de lin hiérarchiques modifiées CNC et XG/CNC dans des composites thermoplastique et thermodurcissable. Les procédés de mise en œuvre des thermoplastiques et thermodurcissables étant relativement

différents, ce choix a permis de mettre en évidence certains avantages ou limitations de ce type de traitements. En effet, le procédé de mélange par extrusion des fibres courtes de lin dans le PP implique une concentration en fibres maîtrisée et des volumes de porosité très faibles dans le composite. Il facilite donc l'analyse de la zone d'interphase avec peu de paramètres influents qui découlent du procédé de mise en œuvre. En revanche, le procédé de thermocompression implique des volumes de fibres et de porosité variables, influencés par la qualité de l'imprégnation fibre / matrice, et pouvant grandement modifier le comportement mécanique des composites stratifiés préparés.

L'ensemble de ces travaux a permis d'étudier les procédés à mettre en œuvre pour élaborer des fibres de lin hiérarchiques et leur incorporation dans des matériaux composites, et d'évaluer le potentiel de ces renforts végétaux hiérarchiques pour le développement de biocomposites structuraux.

IV. Références

[1] A. Bergeret et P. Krawczak, « Liaison renfort/matrice - Définition et caractérisation », *Techniques de l'Ingénieur*, vol. AM5305v1, 2006.

[2] F. Reux, « Overview of the global composites market 2018-2023: continuing growth. JEC Composites », présenté à 5e Colloque « Fibres Naturelles et Polymères », Troyes, sept. 19, 2019.

[3] FRD & IAR, « Matériaux fibres naturelles : réalités de marchés et enjeux en matière d'innovation », présenté à 5ème colloque « Fibres naturelles et polymères », Troyes, sept. 19, 2019.

[4] M. Gomina, « CELC - Flax & hemp fiber composites, a market reality - The biobased solutions for the industry », présenté à 5ème colloque « Fibres naturelles et polymères », Troyes, sept. 19, 2019.

[5] J. Rion, « Bcomp - Composites à fibres de lin et technologie powerRibsTM : du sport automobile aux pièces intérieures de voitures », présenté à 5ème colloque « Fibres naturelles et polymères », Troyes, sept. 19, 2019.

[6] C. Géradon, « Biocomposites : un marché en développement ? », *Valbiomag*, janv. 05, 2019.

[7] N. Ramli *et al.*, « Natural fiber for green technology in automotive industry: A brief review », *IOP Conference Series: Materials Science and Engineering*, vol. 368, p. 012012, juin 2018, doi: 10.1088/1757-899X/368/1/012012.

[8] P. Wambua, J. Ivens, et I. Verpoest, « Natural fibres: can they replace glass in fibre reinforced plastics? », *Composites Science and Technology*, vol. 63, nº 9, p. 1259-1264, juill. 2003, doi: 10.1016/S0266-3538(03)00096-4.

[9] D. Gay et S. V. Hoa, *Composite materials: design and applications*, 3. ed. Boca Raton, Fla.: CRC Press, 2014.

[10] Bourmaud, J. Beaugrand, D. U. Shah, V. Placet, et C. Baley, « Towards the design of high-performance plant fibre composites », *Progress in Materials Science*, vol. 97, p. 347-408, août 2018, doi: 10.1016/j.pmatsci.2018.05.005.

[11] Masters of linen et AGPL, « Le lin, piège à CO2 », *Le lin côté nature*, 2019. .

[12] G. Coroller *et al.*, « Effect of flax fibres individualisation on tensile failure of flax/epoxy unidirectional composite », *Composites Part A: Applied Science and Manufacturing*, vol. 51, p. 62-70, août 2013, doi: 10.1016/j.compositesa.2013.03.018.

[13] J. L. Thomason, « Glass fibre sizing: A review », *Composites Part A: Applied Science and Manufacturing*, vol. 127, p. 105619, déc. 2019, doi: 10.1016/j.compositesa.2019.105619.

[14] *Glass Fibre Sizings by James L. Thomason | Blurb Books UK*. 2015.

[15] A. Le Duigou, P. Davies, et C. Baley, « Environmental Impact Analysis of the Production of Flax Fibres to be Used as Composite Material Reinforcement », *Journal of Biobased Materials and Bioenergy*, vol. 5, nº 1, p. 153-165, mars 2011, doi: 10.1166/jbmb.2011.1116.

[16] P. J. Herrera-Franco et L. T. Drzal, « Comparison of methods for the measurement of fibre/matrix adhesion in composites », *Composites*, vol. 23, nº 1, p. 2-27, janv. 1992, doi: 10.1016/0010-4361(92)90282-Y.

[17] N. Le Moigne, B. Otazaghine, S. Corn, H. Angellier-Coussy, et A. Bergeret, *Surfaces and Interfaces in Natural Fibre Reinforced Composites*. Cham: Springer International Publishing, 2018.

[18] N. E. Zafeiropoulos, C. A. Baillie, et J. M. Hodgkinson, « Engineering and characterisation of the interface in flax fibre/polypropylene composite materials. Part II. The effect of surface treatments on the interface », *Composites Part A: Applied Science and Manufacturing*, vol. 33, nº 9, p. 1185-1190, sept. 2002, doi: 10.1016/S1359-835X(02)00088-X.

[19] N. Le Moigne, B. Otazaghine, S. Corn, H. Angellier-Coussy, et A. Bergeret, « Modification of the Interface/Interphase in Natural Fibre Reinforced Composites: Treatments and Processes », in *Surfaces and Interfaces in Natural Fibre Reinforced Composites: Fundamentals, Modifications and Characterization*, N. Le Moigne, B. Otazaghine, S. Corn, H. Angellier-Coussy, et A. Bergeret, Éd. Cham: Springer International Publishing, 2018, p. 35-70.

[20] F. Barthelat, R. Rabiei, et A. K. Dastjerdi, « Multiscale toughness amplification in natural composites », *MRS Online Proceedings Library Archive*, vol. 1420, ed 2012, doi: 10.1557/opl.2012.714.

[21] H. Gao, B. Ji, I. L. Jager, E. Arzt, et P. Fratzl, « Materials become insensitive to flaws at nanoscale: Lessons from nature », *Proceedings of the National Academy of Sciences*, vol. 100, nº 10, p. 5597-5600, mai 2003, doi: 10.1073/pnas.0631609100.

[22] O. Zabihi, M. Ahmadi, Q. Li, S. Shafei, M. G. Huson, et M. Naebe, « Carbon fibre surface modification using functionalized nanoclay: A hierarchical interphase for fibre-reinforced polymer composites », *Composites Science and Technology*, vol. 148, p. 49-58, août 2017, doi: 10.1016/j.compscitech.2017.05.013.

[23] J. Karger-Kocsis, H. Mahmood, et A. Pegoretti, « All-carbon multi-scale and hierarchical fibers and related structural composites: A review », *Composites Science and Technology*, vol. 186, p. 107932, janv. 2020, doi: 10.1016/j.compscitech.2019.107932.
[24] K.-Y. Lee, P. Bharadia, J. J. Blaker, et A. Bismarck, « Short sisal fibre reinforced bacterial cellulose polylactide nanocomposites using hairy sisal fibres as reinforcement », *Composites Part A: Applied Science and Manufacturing*, vol. 43, nº 11, p. 2065-2074, nov. 2012, doi: 10.1016/j.compositesa.2012.06.013.
[25] E. J. Foster *et al.*, « Current characterization methods for cellulose nanomaterials », *Chemical Society Reviews*, vol. 47, nº 8, p. 2609-2679, 2018, doi: 10.1039/C6CS00895J.
[26] A. Dufresne, *Nanocellulose: From Nature to High Performance Tailored Materials*. Walter de Gruyter GmbH & Co KG, 2017.
[27] D. K. Owens et R. C. Wendt, « Estimation of the surface free energy of polymers », *Journal of Applied Polymer Science*, vol. 13, nº 8, p. 1741-1747, 1969, doi: 10.1002/app.1969.070130815.
[28] S. Wu, « Calculation of interfacial tension in polymer systems », *Journal of Polymer Science Part C: Polymer Symposia*, vol. 34, nº 1, p. 19-30, 1971, doi: 10.1002/polc.5070340105.
[29] M. E. Schrader, « Young-Dupre Revisited », *Langmuir*, vol. 11, nº 9, p. 3585-3589, sept. 1995, doi: 10.1021/la00009a049.
[30] D. H. Bangham et R. I. Razouk, « Adsorption and the wettability of solid surfaces », *Transactions of the Faraday Society*, vol. 33, p. 1459, 1937, doi: 10.1039/tf9373301459.

CHAPTER I

Literature Review

Table of contents - Chapter I

I. 1. Flax: A multi-scale material

I. 1. 1. Contextualization

I. 1. 1. 1 History

Flax or *Linum L.* is a large genus of around 200 species comprising the most widely used, the domesticated flax (*Linum usitatissimum L.).* The first discovered wild flax fibres dates from the Upper Paleolithic (36,000 B.C.), and have been found in a cave in Georgia. These flax fibres were colored, indicating the early producing of colorful textiles at this period [1]. Natural fibres and more especially flax fibres have really contributed to the development of the sedentarization of humans in the Neolithic period (about 10,000 years ago) [2], [3] with the making of cords, garments and weaving yarn. The European and more especially Flanders linen industry became to be prospering in the Middle Ages.

All this history confers to these bast fibres a real advantage in the artisanal knowledge and know-how in the harvesting and producing of textiles and other linen objects. However, flax fibres have been gradually replaced by cotton fibres in the nineteenth century and largely since the twentieth century by cotton, artificial (viscose, lyocell etc.) and synthetic fibres (polyester, polyamid etc.). Today, flax fibres are mostly used in the textile industry but also in paper industry and more recently in biocomposite materials [4].

I. 1. 1. 2 Geographical area and production market

Natural fibre type and production quantity are very different considering the geographical area and climatic conditions, illustrated in **Figure I-1**. The major part of the flax cultivation is based in temperate region, requiring humidity and mild temperatures. The maritime coast of the Western Europe (Netherlands, Belgium, and France) is well appropriated for this cultivation [5].

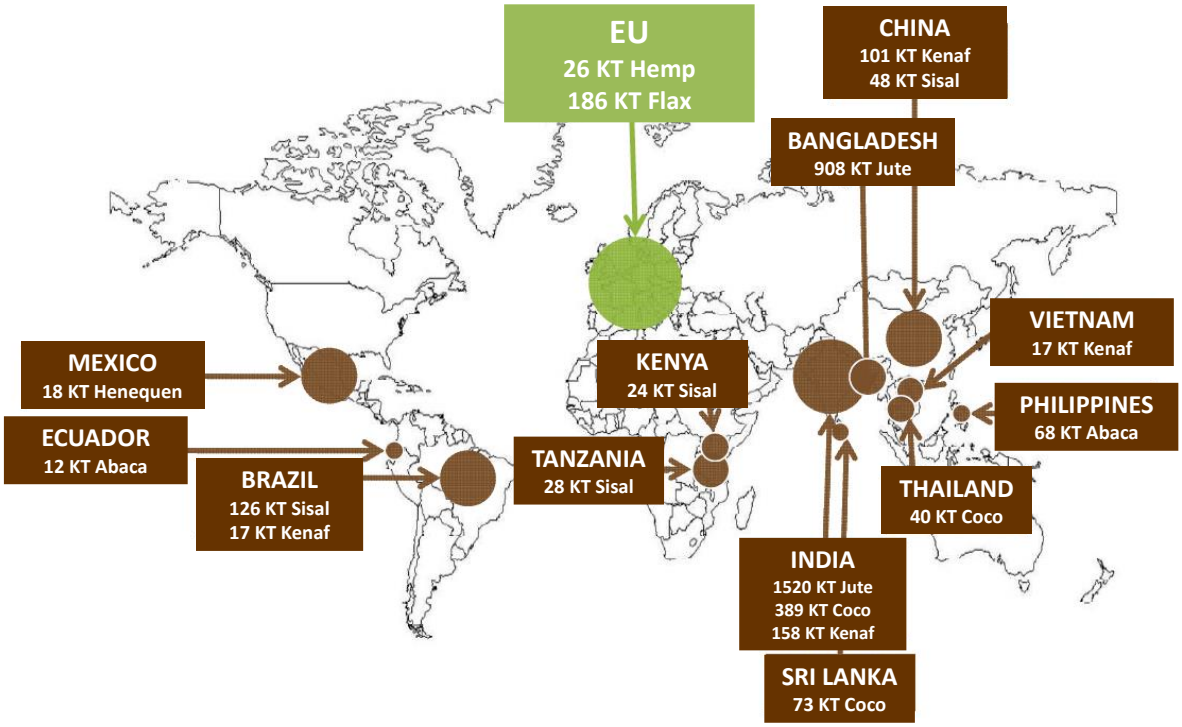

Figure I-1: Distribution of the world production of natural fibres (cotton and wood excluded) 2001 – 2008 (translated and reprinted with permission from the report of ADEME and FRD in 2011 [6]).

The European Union is largely the 1st producer in the world with 85 % of the production distributed in three countries: France with 80 %, Belgium with 15 % and Netherlands with 5 %, representing around 141,000 tons of scutched flax fibres. The inter-branch committee of the flax production Cipalin publishes regularly the key figures [7], [8]. The production of flax fibres is increasing since few years with an increase of the harvesting surfaces (**Figure I-2**) showing the renewed interest in this natural fibre with notably the emergency of the biocomposite sector.

This diversity of applications and the strong interest in flax based innovative materials result to a growing industrial involvement and numerous emerging projects mixing industries and academic scientists. Some studies are directly focused on the plant growth, the development and the structure of the stem and fibres, while the majority aims at the development of high-performance biocomposites or the improvement of specific criteria for the textile application [9], [10].

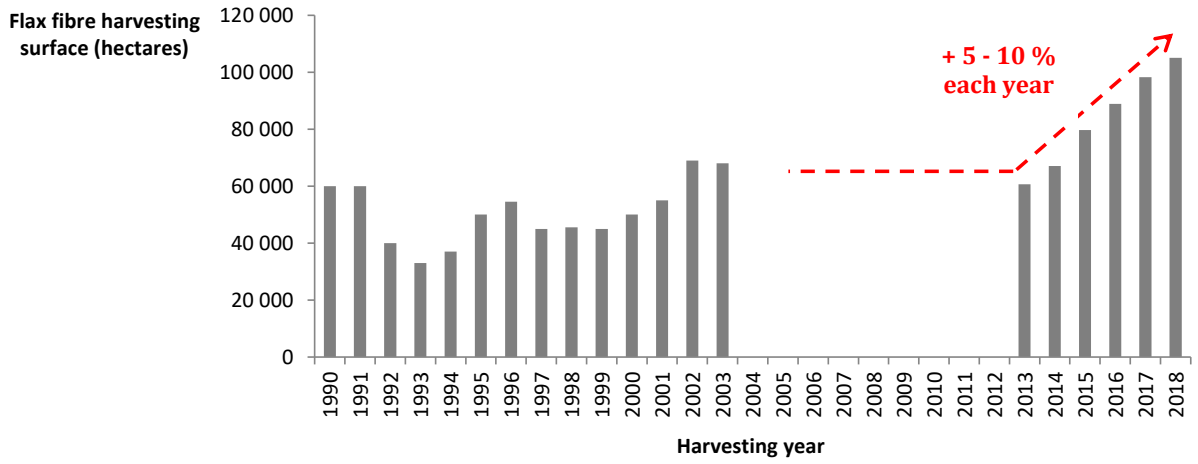

Figure I-2: Histogram of the harvesting surfaces of flax fibre from 1990 to 2018 (data taken from websites [7], [11] and report from FRD [12]).

I. 1. 2. Flax plant building and organization

In order to well understand the interesting morphological and mechanical properties of the flax fibre, it is necessary to come back to its original role that is reinforcement of the flax stem [13]. First, farmers and scientists have worked closely for one century [14] on the control of the flax plant growth and the crossing and selecting of varieties, to reach a varietal selection with an exceptional slenderness giving its interesting properties [15]. This selection of high yielding flax fibres covers especially the textile industry but more recently the composite sector with the development of natural fibre based composites [16]. The flax plant is also considered as a composite structure with a hierarchical structure developed at different scales (**Figure I-3**). The next section will explain more precisely the creation of this complex architecture, going from the seeding of the flax plant to the flax fibre maturity.

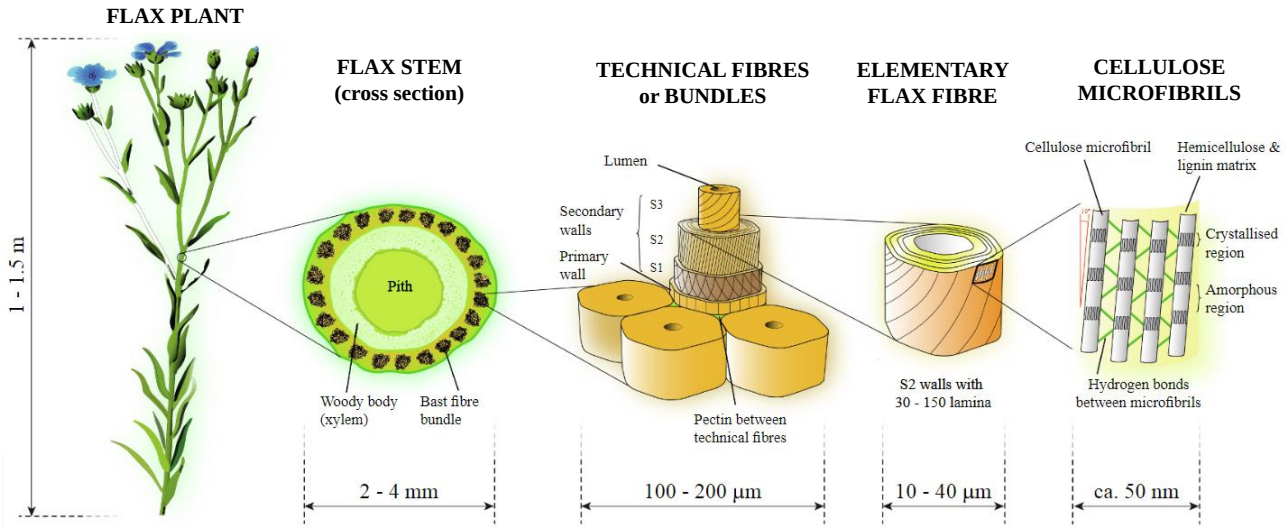

Figure I-3: Hierarchical architecture of the flax plant (reprinted with permission from Woigk *et al.* 2019 [17]).

I. 1. 2. 1 The flax plant

The growth of the plant, a period of about 100 – 120 days, is divided in different stages going from the sowing (15th March - 15th April in France [18]) to the fibre maturity [13]. Growth conditions can be influenced by many parameters like cultivation methods (inputs, seeding etc.), the nature of the soil, the harvesting time or even the weather (temperature, amount of rainfall etc.). This growth and the gene pool variety have a real impact on the flax stem and consequently on flax fibres in terms of morphology and mechanical properties.

I. 1. 2. 2 The flax stem

The main functions of the flax stem in the plant are the water and nutrients conduction and also the mechanical support. The stem is highly hierarchical structured with different parts detailed in **Figure I-4**. The bark surrounding the stem protects the plant against fungi and insects. The pith, the cambium and the xylem are mainly composed of vascular tissues and carries water and nutrients. The particularity of the flax stem is the incredible slenderness, corresponding to the ratio between the height and the diameter of the stem. Indeed, with a length of around 1 m and a diameter between 1 and 3 mm [19], the ratio L / d may exceed 1,000. This slenderness is partially possible thanks to peripheral fibres, allowing the support and the stability of the plant with a huge elongation capacity of the cell walls compared with other bast fibres [20], [21].

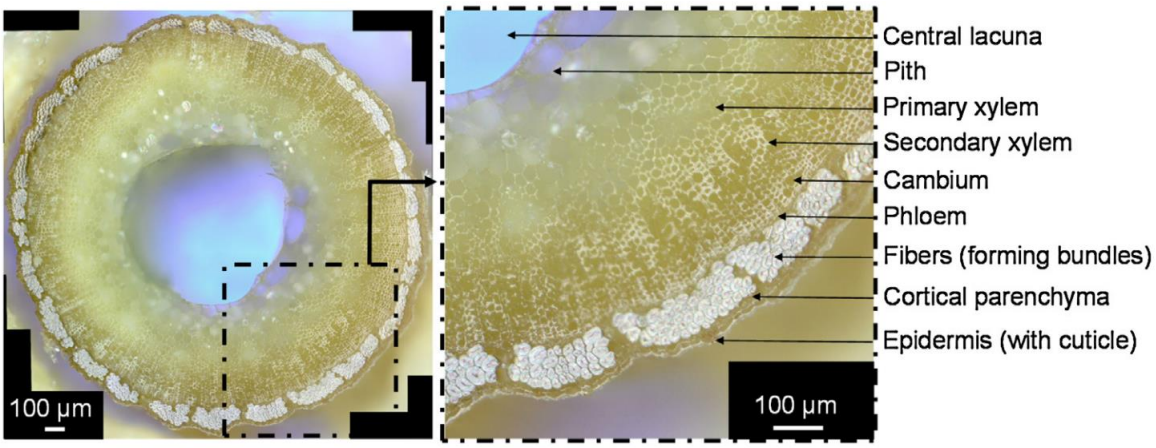

Figure I-4: Transverse section of flax stem (Ariane variety) with the different components of the stem (reprinted with permission from Goudenhooft *et al.* 2017 [15]).

Flax fibre bundles, corresponding to so-called technical fibres or bast fibres, are located at the periphery. This thin parenchyma cell wall contains between 15 and 40 bundles of fibres, depending on the variety. These bundles are composed of 10 to 40 elementary flax fibres, bonded with the parenchyma cell walls, a matrix composed in majority of pectins and low amount of lignin [22], [23], **Figure I-3**.

I. 1. 3. Flax fibre growth, structure and chemical composition

I. 1. 3. 1 Building of the elementary fibres and morphological properties

During the growth of the plant, cell tissues are growing within the stem in different steps. Tissues at the periphery of the stem will formed the so-called technical fibres mainly used in natural reinforced composites. Indeed, the flax bast fibres are very long with extremely thickened cell walls. The elongation stage corresponds to a short time of the fibre growth and restricted to the top of the stem. This stage is crucial and determines the maximal length of the bast fibres, reaching up 8 cm. This fibre-cell elongation is divided in two steps: (1) fibre-cell multiplication at the top of the stem with a different number of fibres depending on the plant variety, (2) the intrusive growth of each fibre (0.5 – 2 cm/day during 2 - 4 days) [24] in the top of the stem, above the snap-point (SP), **Figure I-5 A**.

The last and extending stage of the fibre building, called cell-wall thickening, occurs below the snap-point and lasts around 2 months. During this step, the radial expansion of the fibre

and the thickening of the walls can be observed with a significant increase of the stiffness of the stem. The formation of a secondary cell wall corresponds to layered deposition of cellulose fibrils, which act as reinforcing agent, inducing a strong increase of the mechanical strength of tissues. In fact, a specific layer S2 is created in the tripartite secondary cell wall of the fibre, detailed in **Figure I-5 B**. Therefore, flax fibres have non circular but polygon cross-sections, which can be a problem for their use as reinforcement in biocomposites, such as the impregnation process.

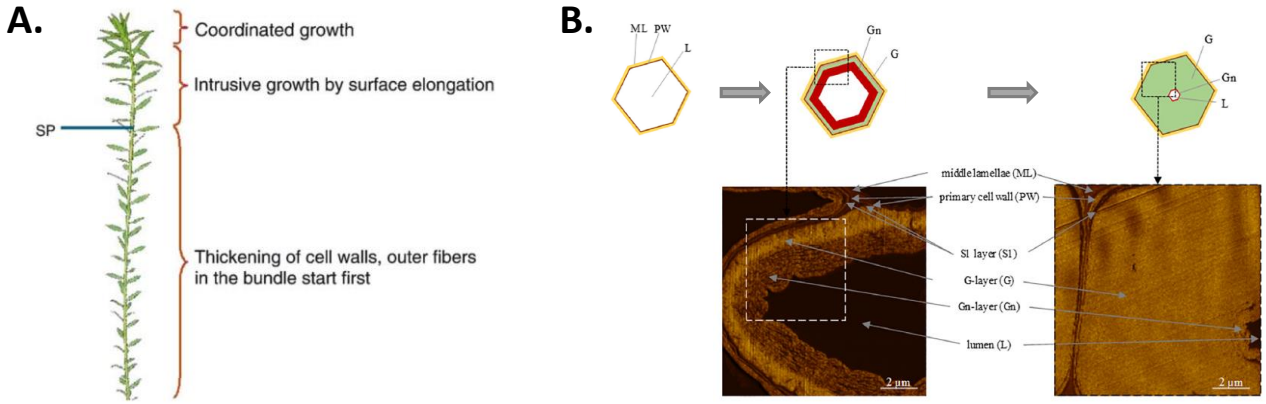

Figure I-5: A. Localization of the different stages of the fibre growth in the flax stem during the fast growth period. SP: snap-point; **B.** Cell-walls thickening stage until the maturity flax fibre and cell walls organization in the elementary flax fibre (adapted with permission from Goudenhooft *et al.* 2019 [13]).

These two main stages in the growing of the cells give to the flax fibre exceptional morphological properties, i.e. 6 – 80 mm length, 12.4 – 23.9 µm diameter with a low density around 1.53 – 1.54 g/cm^3 [25].

I. 1. 3. 1 Structure and biochemical composition

I. 1. 3. 1. 1. Hierarchical structure of cell walls

The architecture of matured flax fibres is very complex with a hierarchical organization at different length scales, illustrated in **Figure I-6**.

Three main layers can be described [26]:

- The Middle Lamella (ML) is the first layer formed during the cells division. This adjoining area between fibres provides a good cohesion and is fully composed of

pectins, lignin in woody secondary wall and low amount of cellulose. In the case of flax fibre, lower amount of lignin is observed than in woody primary wall.

- The Primary Wall (PW) corresponds to the deposited wall in the growing cell. This thin layer is closely linked to the ML and composed of cellulose microfibrils randomly dispersed in a matrix containing mainly hemicelluloses and pectins.
- The Secondary Wall (SW) is formed during the cell-walls thickening. This is the major part of the fibre which can be divided in three layers S1, S2 and S3 [27] particularly characterized by the orientation of cellulose that is measured by the microfibril angle (MFA). The layer S2 is the thicker one, up to 15 µm, and plays a key role in the mechanical and morphological properties of the flax fibres.

Finally, the Lumen (L), a small channel at the middle of the fibre, contributes essentially in the water uptake.

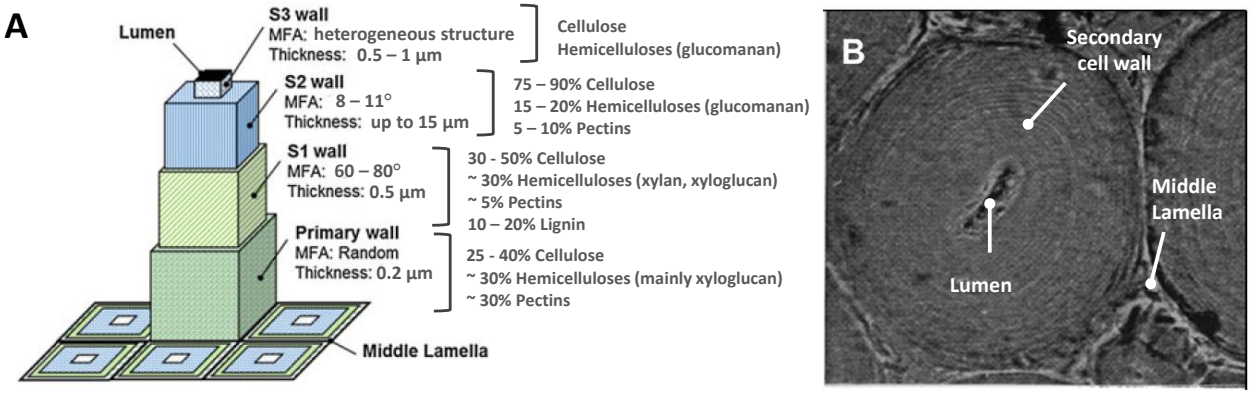

Figure I-6: A. Cell wall structure of mature flax fibres, with: middle lamella, primary wall, secondary S1 wall, secondary S2 wall (main body), secondary S3 wall, lumen (adapted with permission from Nicolas Le Moigne *et al.* 2018 [28]). Indications about thickness, microfibrillar angle and biochemical composition are given according to Goudenhooft *et al.* 2019 [13]; **B.** Microscopic view of flax cell walls (adapted from Hock 1942 [29] and reprinted with permission from Bourmaud *et al.* [25]).

In a summarized form, the structure of the flax fibre can be compared with a composite network with cellulose microfibrils as reinforcements embedded in an amorphous matrix mainly composed of pectins, hemicelluloses, proteins, lipophilic extractives and lignin (**Figure I-7**).

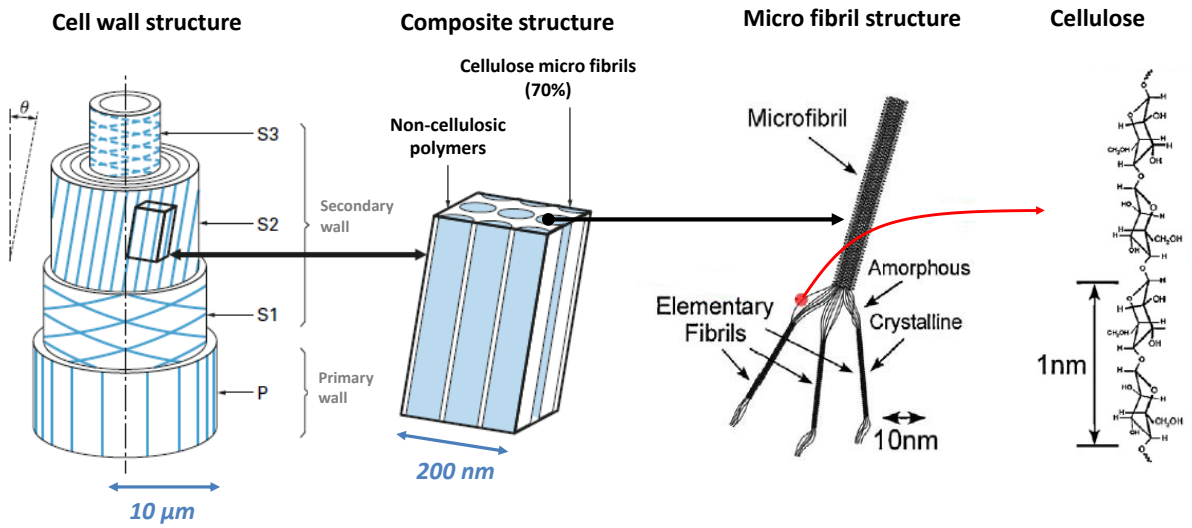

Figure I-7: Hierarchical organization of flax fibre cell walls and cellulose microfibrils (reprinted from Moon *et al.* 2006 and with permission from Baley 2020 [30], [31]).

I. 1. 3. 1. 2. Cellulose microfibrils as reinforcements

Cellulose is the most abundant biobased polymer on the Earth with more than half of the total biomass [32]. The production of cellulose by the nature via the photosynthesis is estimated at 10^{10} to 10^{11} tons per year [33]. This polymer can be extracted from many biomass sources, mainly from wood but also from seed fibres, bast fibres, fruits, tunicates etc. The chemical structure of the cellulose, formula $C_6H_{10}O_5$, can be described as a linear homopolymer composed of anhydro-D-glucopyranose units (AGU) covalently connected by β-(1-4) glycosidic linkages, detailed in **Figure I- 8**. The cellobiose is considered as the structural repeating unit of cellulose and is a combination of two AGU which is the chemical repetition unit [34]. The two extremities of the chain of cellulose are chemically different with one reducing end bearing aldehyde group and one non-reducing end. The chain length of cellulose, commonly named degree of polymerization (DP), is the number of AGUs, and depends on the origin of the cellulose and the treatment method. It varies from 300 – 1,700 for wood pulp and 800 – 10,000 for cotton and other plant fibres such as flax or hemp [34].

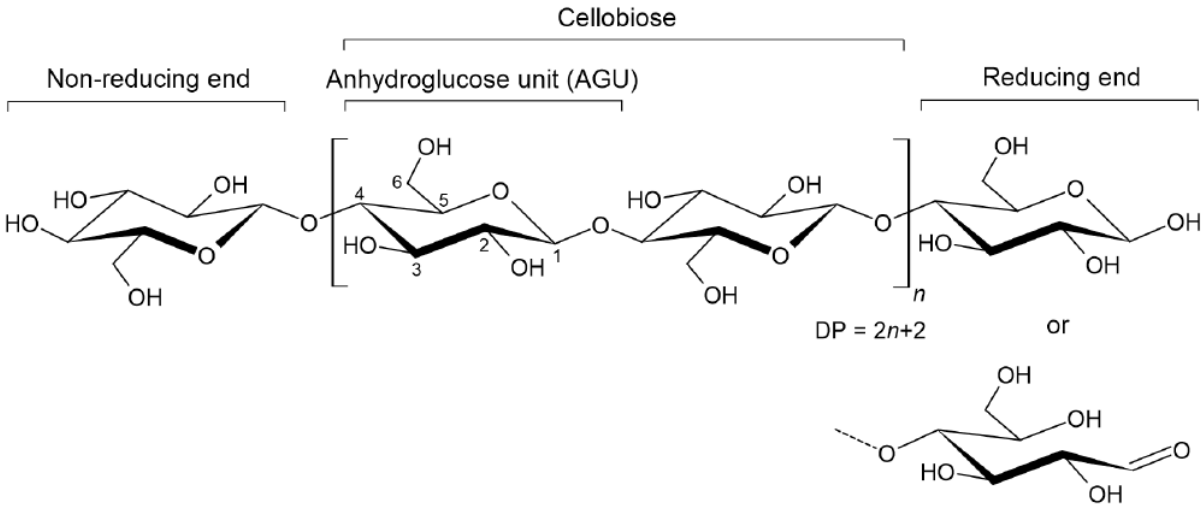

Figure I- 8: A. Chemical structure of the cellulose polymer and B. Interactions between glucan chains in cellulose microfibrils (reprinted with permission from Banvillet 2021 [35]).

The degree of crystallinity of cellulose in flax fibres measured by Bonatti *et al.* was 64 % [36]. In fact, cellulose chain are constituted of highly ordered crystalline arrangements but also disordered amorphous-like regions, due to the presence of defects in the structure [37]. Four principal allomorphs have been identified: cellulose I (I_α and I_β), II, III and IV [38]. The cellulose I is considered as the natural form of cellulose (so-called native cellulose) and is the most abundant crystalline form. The cellulose is the major constituent of the flax fibres and can represent until 85 % of the weight, reported below in **Table I-1**. High cellulose content seems to increase significantly the mechanical properties of the fibre [39]. In fact, the Young's Modulus of the crystalline cellulose can reach 100 - 130 GPa [40]. The major part of the cellulose is located in the layer S2 of the secondary wall, the main part of the flax fibre. The cellulose microfibrils are oriented along the axis of the fibre with an angle of 8.3 – 11° [25]. This angle MFA is very low in the flax fibres comparing to other biomass sources and displays a unidirectional structure and consequently high mechanical properties in the longitudinal axis.

I. 1. 3. 1. 1. Non-cellulosic matrix entangled with cellulose microfibrils

In the cell walls of periphery flax fibres, cellulose fibrils are entangled in a non-cellulosic matrix, mainly composed of hemicelluloses, pectins and also lignin and extractives, their content values being reported in **Table I-1** and compared with other natural fibres.

Contrary to cellulose, hemicelluloses and pectins are synthetized in the Golgi by enzymatic complexes and carried to the extracellular matrix via Golgi vesicles merging the plasma membrane. The non-cellulosic polymers are assembled in the inner surface of cell walls at the same time as the microfibrils cellulose biosynthesis [41].

Table I-1: Biochemical composition of lignocellulosic fibres (reprinted with permission from Bourmaud *et al.* 2018 [25]).

	Cellulose (%)	Hemicellulose (%)	Lignin (%)	Pectin (%)	Fat and Wax (%)
Musa textilis (Abaca)	60.8–68.0	17.5–21	5–15.1	< 1	< 1
Stipa tenacissima (Alfa)	43.9–48.0	25.7–38.5	14.9–23	1	1–3
Bambusoideae (Bamboo)	36.1–54.6	11.4–16.6	20.5–28.5	< 1	1–4
Cocos nucifera (Coir)	32.0–43.4	0.3	40–45.8	3	0–6
Gossypium sp. (Cotton)	82.7–98.0	4.0–5.7	0.7	4	2–3
Linum Usitatissimum L. (Flax)	60–85	14.0–20.6	1–3	1.8–15.0	1–6
Cannabis Sativa (Hemp)	55–90	12	2–5	3	1.7
Corchorus capsularis (Jute)	58.0–71.5	13.6–24.0	11.8–16	2	< 1
Ceiba pentandra (Kapok)	13–35	23–32	13–21	7–23	< 1
Hibiscus cannabinus (Kenaf)	52.0–61.2	18.5–29.7	12.9–16.1	3–5	< 1
Boehmeria nivea (Ramie)	61.8–76.2	5.3–16.7	0.6–9.1	0.3	< 1
Agave sisalana (Sisal)	52.8–65	19.3	11.1–13.5	10–14	< 1
Wood (different species)	38–45	19–39	22–34	0.4–5	< 1

Hemicelluloses

Hemicelluloses are low-molecular weight branched heteropolysaccharides constituted of an osidic β-(1-4)-linked linear backbone literally substituted with different sugars units with a DP of 100 – 200 [42]. The nature of hemicelluloses varies according to the cell wall of the flax fibre: majority of xyloglucan in the primary wall and xylan and glucomannan in the secondary wall. Hemicelluloses, in contrary to the cellulose, are amorphous with very limited mechanical properties [43]. Even if these polysaccharides are non-crystalline, they contribute strongly to the support of the plant and the organization of the cell walls [23], [44]. Moreover, hemicelluloses are very hydrophilic components.

Pectins

Pectins are high molecular weight acidic polysaccharides constituting a large part of the cell wall of plants [45], [46]. They are synthesized in the Golgi vesicles, probably involving a lot

of different enzymes. These pectic polysaccharides have a complex structure but can be gathered in three principal groups: homogalacturonans (HG), rhamnogalacturonans type I (RG-I) and rhamnogalacturonans type II (RG-II), illustrated in **Figure I-9**. They are principally located in the primary wall of non-wood plant fibres and are also abundant in the middle lamellae, playing a role in the cohesion between cells. According to the **Figure I-6 A**, they are also present in the secondary wall but in small proportion around 5 %. This anionic polymer can sometimes form gels in the presence of calcium, which is the case in flax fibres.

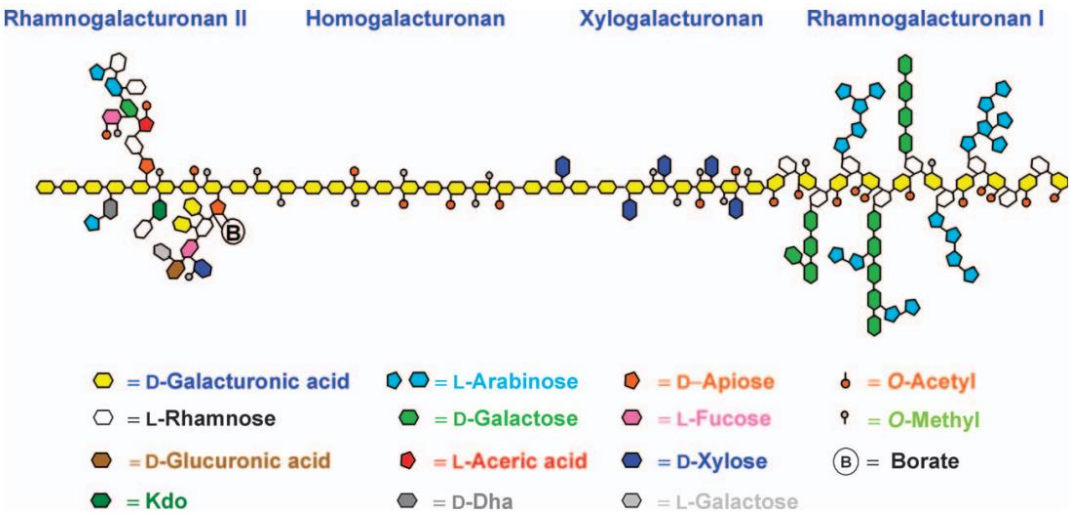

Figure I-9: Schematic structure of main pectins (reprinted with permission from Henrik Vibe Scheller *et al.* 2007 [46]).

Proteins and lipophilic extractives

Structural proteins are gathered considering the main amino acid: proline-rich (PRP), glycine-rich (GRP) and hydroxylamine-rich (HRGP) proteins [26]. These proteins have the capacity to create covalent bonds between them or with the non-cellulosic matrix and so participate to the building of the plant cell wall and structure [23], [47].

The lipophilic extractives are the non-polar extractable fraction from lignocellulosic crops including alkanes, fatty acids, fatty alcohols, free and conjugated sterols, terpenoids, triglycerides and waxes [48], mainly illustrated in **Figure I-10**. Waxes, for example, can also be added on the surface during the process of flax fabrics manufacturing, requiring a good resistance during the manipulation of the product for a biocomposite application. The

extraction of such components is possible thanks to treatments with water, ethanol or ethanol / toluene, and induces an increase of the hydrophilicity of the flax fibres [49].

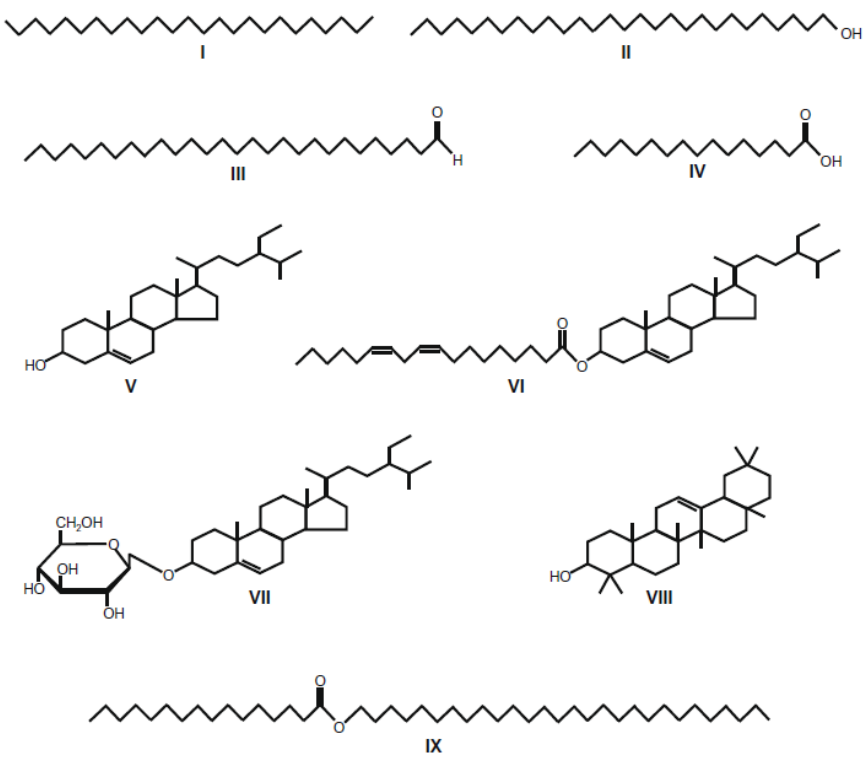

Figure I-10: Chemical structures of compounds representing the main classes of lipophilic extractives found in lignocellulosic fibres: (I) pentacosane; (II) octacosanol; (III) octacosanal; (IV) palmitic acid; (V) sitosterol; (VI) sitosteryl linoleate; (VII) sytosteryl 3β-D-glucopyranoside; (VIII) β-amyrin and (IX) octacosyl hexadecanoate (reprinted with permission from Marques *et al.* 2010 [48]).

Lignin

Lignin is a complex polyphenolic polymer and exhibits both distinct sub-cellular localization and monomeric composition [50]. It is created by the enzymatic polymerisation of three monomers leading to three phenolic building blocks: guaiacyl (G), *p*-hydroxyphenyl propane (*p*-H) and syringyl (S).

The lignification occurs during the formation of the second wall and is essentially located in the middle lamella (ML) and the primary wall (PW). This complex assembly is interconnected via non-covalent and covalent bonds and gives a strong cohesion between the elementary flax fibres gathered in bundles. In the case of the flax, the lignin is present in very low content and is rich in guaiacyl units and condensed bonds, implying an increase of the hydrophobicity [51].

I. 1. 4. Transformation steps: flax stem to final product

The peripheral flax fibres play a role in the nutrients transport and the support of the plant. The extraction process is crucial and consists of the extraction of fibres from the stem, via enzymatic, chemical and/or mechanical processes. The main challenge is to keep the physical and structural integrity of the fibres to obtain the best properties for biocomposite application. In the case of the flax plant, there are strong knowledge and know-how coming directly from the textile flax industry. Three main steps are required:

- **Pre-treatment** to decrease the cohesion between elementary flax fibres inside bundles and start the separation;
- **Defibrillation mechanical processes** to extract the flax fibre bundles, separated from the other components of the plant;
- **Post-treatment** to refine and prepare fibres to be used for different applications (textile, biocomposite, semi-product etc.).

It can be noticed that all the components of the flax plant are used and required different characteristics and qualities considering the desired applications, which have to be preliminary defined.

I. 1. 4. 1 Flax plant harvesting

In June-July, the flax is at the maturity state with a brownish color of the heads and no more leaves. At this state, the flax plant is mechanically extracted from the soil, action called "pulling", and deposited homogeneously on the soil in windrows (**Figure I-11**). This specific method is necessary to obtain the entire fibre, going from the root to the top of the stem. The plant is turned over several times to have a homogenous and efficient retting.

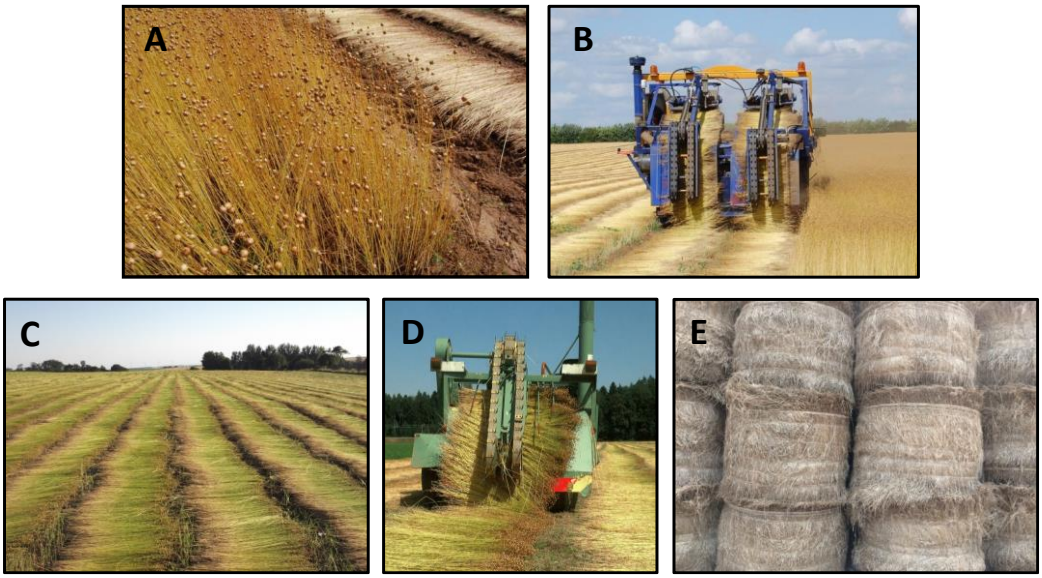

Figure I-11: Different steps of the flax plant harvesting: A. Flax fibres in the maturity state; B. Pulling; C. Windrows on the soil for retting; D. Turning of the flax plants; E. Flax straw bales. (reprinted with permission from the following sources: *https://linfibredeprintemps.wordpress.com/la-recolte/; http://lejardindenanny2.over-blog.com/album-1422124.html).*

The dew retting is a current and natural method and the first step of the transformation of the plant. It is driven by the alternation between sun and rain, essential climatic conditions to allow the development of micro-organisms and bacteria present naturally in the soil. A good retting is observed with the harvesters' expertise and knowledge via the color, the homogeneity, the divisibility and the resistance under the hand. This enzymatic action will modify the biochemical composition of the flax plant, decreasing pectins, phenolic compounds and hemicelluloses contents. In fact, micro-organisms will attack the pectic matrix and the lignin, present in the middle lamella surrounding the elementary flax fibres. This step is crucial to weaken the stem structure and begin the separation of bundles from the woody core and other tissues (more details on other retting methods in section ***I. 2. 5. 1***). After several weeks of dew retting and the reach of the optimal quality of fibres, the flax is ready to be collected. Flax straw bales are formed and stored, waiting for the defibrillation steps. This pretreatment is essential to begin the defibrillation and strongly contributes to the efficiency of mechanical treatments.

I. 1. 4. 2 Defibrillation and refining

The scutching [25], [26] is the combination of successive mechanical operations used to extract selectively the flax fibres from the stem, trying to have as little impact as possible on the morphological and mechanical properties [52], illustrated in **Figure I-12**.

Figure I-12: Different operations present on the scutching line
(reprinted with permission from the following source: *https://blog.libecohomestores.com/fr/metier-de-lin-fr/extraire-la-fibre/*).

The flax bale is unwound in a sheet: flax stems are parallelized and homogenized in thickness via the grinding and the stretching. Then, flax straws are crushed under fluted rolls with different tooth sizes and an angle close to 90°. These rolls lead to repeated pull-off forces and bending of the stems, that increases the disintegration of the more rigid woody core (epidermis, xylem), separated from the smoother fibres. Wastes, called "shives" composed mainly of xylem, are collected and stocked in bales. Finally, the threshing is made on a drum and removes the remaining shives and tows. The noble part is obtained at the end of the scutching line in a discontinuous form. These operations are delicate because they can induce damages and defects on the flax fibres, implying a decrease of the quality of the final product.

The long fibres obtained after the scutching are composed of bundles of less separated flax fibres with remaining attached intern and extern tissues of the stem. These fibres can provide from 15 to 20 wt% of shives and need to be post-treated in order to reach a higher quality, essential for textile and biocomposite applications. These steps of refining are adapted considering the application and can be modified to open new grades of fibres.

The hackling is used to align, untangle the bundles, remove residual shives or seeds and partly separate the elementary fibres inside bundles. Indeed, bundles run through more and more thin hackles to obtain at the end individualized, smooth and entangled long fibres stored in a continuous ribbon, illustrated in **Figure I-13**. The fractions of the fibres retained by the hackles, called "hackled tows", are collected for non-woven and reinforcement in biocomposites or ropes.

Figure I-13: Hackling operation with the obtention of a continuous ribbon of flax fibres (reprinted with permission from the following sources: *https://www.embrin.fr/*; *https://blog.libecohomestores.com/fr/metier-de-lin-fr/extraire-la-fibre/*).

Recent studies have highlighted that the decrease of the mechanical properties of fibres occurs in majority during the retting and the mechanical processes of scutching and hackling [53], [54]. So, these steps have to be well controlled and optimized to obtain biocomposites with high mechanical properties to compete with synthetic fibre reinforced composites.

The mechanical treatment of the flax plant is a model of circular economy with no wastes and the desire to optimize all the plant. All the products and co-products obtained by these different operations are used in many applications, illustrated in **Figure I-14**. Following the model of circular economy, a research team from the LOMC French lab of Le Havre studied recently the valorisation of shives, wastes from the flax plant defibrillation, by the production of nanocellulose, i.e. cellulose nanofibrils and cellulose nanocrystals [55]. This production of derived products from plant cell walls is welcomed in the realisation of green materials.

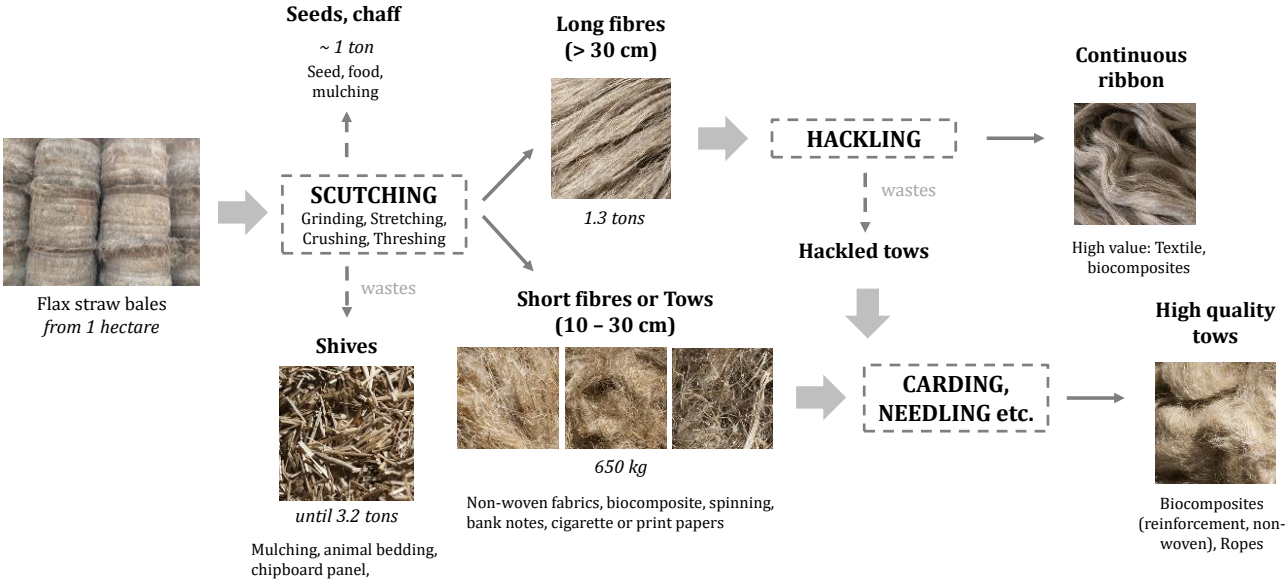

Figure I-14: Illustration of the products and co-products obtained during the mechanical processes of defibrillation and post-treatment of the flax plant; their obtained weight proportions for 1 hectare and the different applications. (Images reprinted from the following Source: https://www.lelin-cotenature.fr/FR/Pour-que-le-lin-donne-le-meilleur-de-lui-meme-32.html).

I. 1. 5. Derived products from plant cell wall for material applications

This section will focus on nanocellulose, especially "cellulose nanocrystals", and "xyloglucan", derived products from plant cell wall and used in the framework of the PhD project, getting a strong interest in the scientific community, highlighted in **Figure I-15**, *for their interesting and specific properties applicable to numerous sectors.*

Derived products from plant cell wall have raised a huge interest for the last decades in the conception of new products and materials. Many examples can be cited as bioethanol, biochar, lignin, hemicelluloses, nanocellulose targeting numerous applications such as energy, pharmaceutical, food, packaging, biobased plastic and composites [56]–[62].

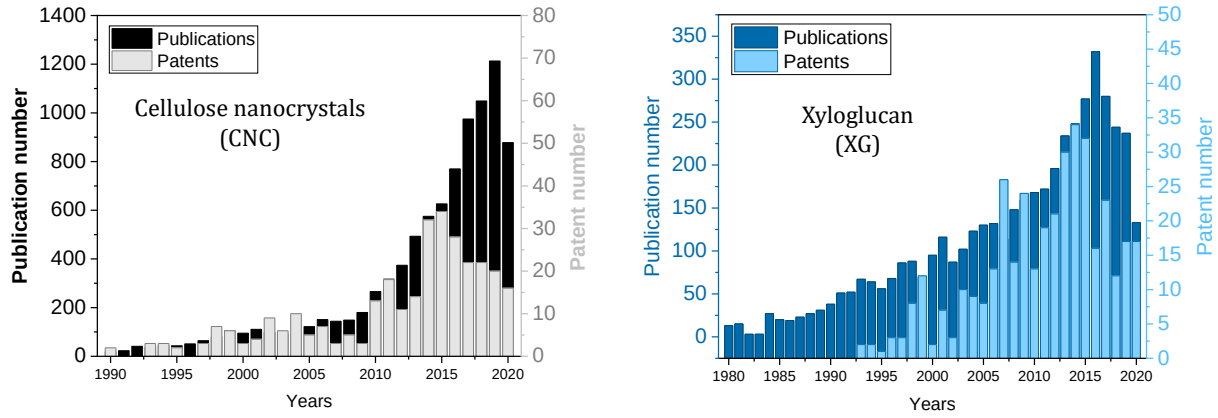

Figure I-15: Non-cumulative evolution of the number of publications and patents dealing with cellulose nanocrystals (CNC) (Source: SciFinder, July 2020 – Descriptors: cellulose nanocrystals, cellulose nanorod, cellulose nanowire, cellulose crystallite, cellulose whiskers, nanocrystalline cellulose, microcrystalline cellulose – Language: English) and xyloglucan (Source: SciFinder, July 2020 – Descriptor: xyloglucan – Language: English).

I. 1. 5. 1 Cellulose nanocrystals (CNC) and cellulose nanofibrils (CNF)

Nanocellulose can be divided in two types differing by their extraction procedure, properties and applications: (i) **cellulose nanofibrils (CNF)** and (ii) **cellulose nanocrystals (CNC)** [63].

CNF are long and flexible, semi-crystalline with one nanometric dimension, mainly influenced by the cellulose source and the type of pre-treatments (mechanical, enzymatic,…). CNC have a rod-like shape, a high crystallinity rate and possess two nanoscale dimensions, providing a high specific surface area up to 100 m^2/g and a high Young's modulus around 100 – 130 GPa [40]. The use of sulfuric acid to obtain CNC from cellulose is the most common way that induces the presence of sulfuric groups $–OSO_3^-$ on their surface.

- **Isolation of cellulose nanocrystals**

Cellulose nanocrystals (CNC) are extracted from biomass (wood, cotton, tunicate,…) by hydrolysing (ligno)cellulosic fibres with sulfuric acid, the most common process, to dissolve most of the amorphous regions of cellulosic chains with defined concentration, temperature and reaction time. Highly crystalline rod-like nanoparticles are obtained displaying two nanoscale dimensions [63] (**Figure I-16**).

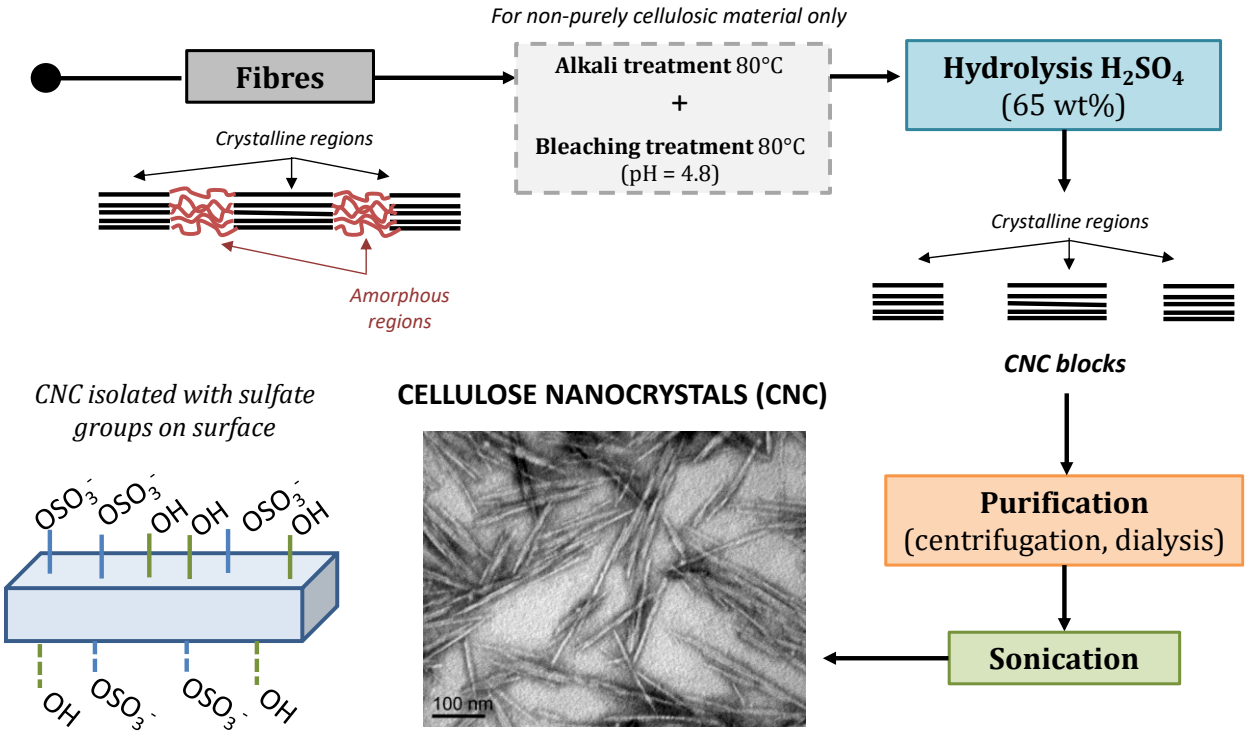

Figure I-16: Schematic of the general procedure of acid hydrolysis of (ligno)cellulosic fibres until the achievement of cellulose nanocrystals (CNC) with the sulfuric acid process.

Indeed, in the amorphous regions, cellulose chains are not tightly packed, which allows easier diffusion of acid in the cellulose network compared to crystalline part [64]. The sonication step allows the separation between intact crystalline regions and leads to isolated CNC bearing anionic half-sulfate ester groups $–OSO_3^-$ randomly distributed on their surface. These surface charges come from the esterification reaction between surface hydroxyl groups of cellulose and sulfuric acid.

CNC are renewable biobased nanomaterials and can be obtained from various sources of cellulose. They display interesting properties and target many applications and industrial sectors, detailed in the following section.

- **Properties and applications of cellulose nanocrystals**

We have to keep in mind that the properties of cellulose nanocrystals described below in the **Table I-2** are strongly dependant on the cellulose sources and isolation processes of (ligno)cellulosic fibres.

Table I-2: Principal physico-chemical and morphological properties of cellulose nanocrystals.

Properties	Features	References
Renewable, biobased, low toxicity	Non-toxicity by injection, dermal contact and for aquatic organisms but pulmonary diseases and cytotoxicity depending on shapes (powder form). → **Prioritize wet-state or in composites**	*Lin & Dufresne (2014), Roman (2015)* [65], [66]
Specific surface area	**A_{sp} = 150 – 800 m²/g** (very high due to the nanosize) → difficult to determinate due to aggregates upon drying	*Dufresne (2017), Foster et al (2018)* [63], [67]
Aspect ratio L/d	Length **L = 100 nm – few micrometers**; Diameter **d = ~ 5 to several tens of nanometers;** **L/d ≈ 10 – 30** (from cotton) and **70** (from tunicate)	*Habibi et al (2010)* [68]
Surface chemical groups	**Mainly –OH groups** but presence of other groups such as **$–OSO_3^-$** (low amount 80 – 350 µmol / g), -COO^-, -CHO and others (from isolation processes) 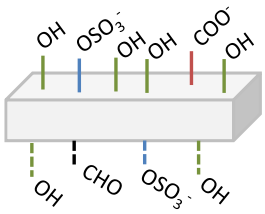 **Anionic groups $–OSO_3^-$ induce repulsive forces** between negatively charged CNC → **colloidal stability** and dispersion in **water** solvent → **decrease the thermostability** of CNC	*Julien et al (1993), Kim et al (2001),Habibi et al (2010),Tang et al (2017)* [68]–[71]
Hydrophobicity	High rate of crystallinity increases the hydrophobicity (less amorphous regions sensitive to humidity)	*Dufresne et al (2015)* [72]
Density	Low density compared to other organic materials **d = 1.61 g/cm³** *(for pure crystalline cellulose I_β)*	*Foster et al (2018)* [67]
Crystallinity	**X_{CNC} = 54 – 88 %** depending on isolation process	*Lin et al (2012)* [66]
Mechanical properties	Young's modulus **E = 100 - 130 GPa;** Tensile strength **σ = 7.5 ± 0.5 GPa**; → *Almost same properties than Kevlar-49 fibres providing E = 124-130 GPa and σ = 3.5 GPa*	*Moon et al (2011), Klemm et al (2011), Dufresne* [73], [74]

In this PhD, a commercial batch of CNC is used and was obtained via acid hydrolysis from wood. It was supplied by CelluForce (Canada) and more details will be given in section "Materials & Methods" of following Chapters.

I. 1. 5. 2 Xyloglucan and xyloglucan-cellulose interactions

Xyloglucan (XG) is a polysaccharide and precisely an important group of hemicelluloses located in the primary cell wall of higher plants (around 20 % of the dry mass). In food and related industries, tamarind seed xyloglucan is mainly used as thickener and stabilizer, gelling agent, starch modifier [75].

XG is composed of repeated units with a β-(1-4)-glucosyl backbone like cellulose, with attached substituents / sugars such as xylose, galactose and more rarely fucose (linked to galactose substituent) [76]–[78]. One of the possible tetrasaccharide backbones (XLLG) obtained after the hydrolysis of tamarind XG is illustrated in **Figure I-17**. XG hydrodynamic radius is estimated to 51 nm with a weight-average molecular mass of 470 kg/mol [79].

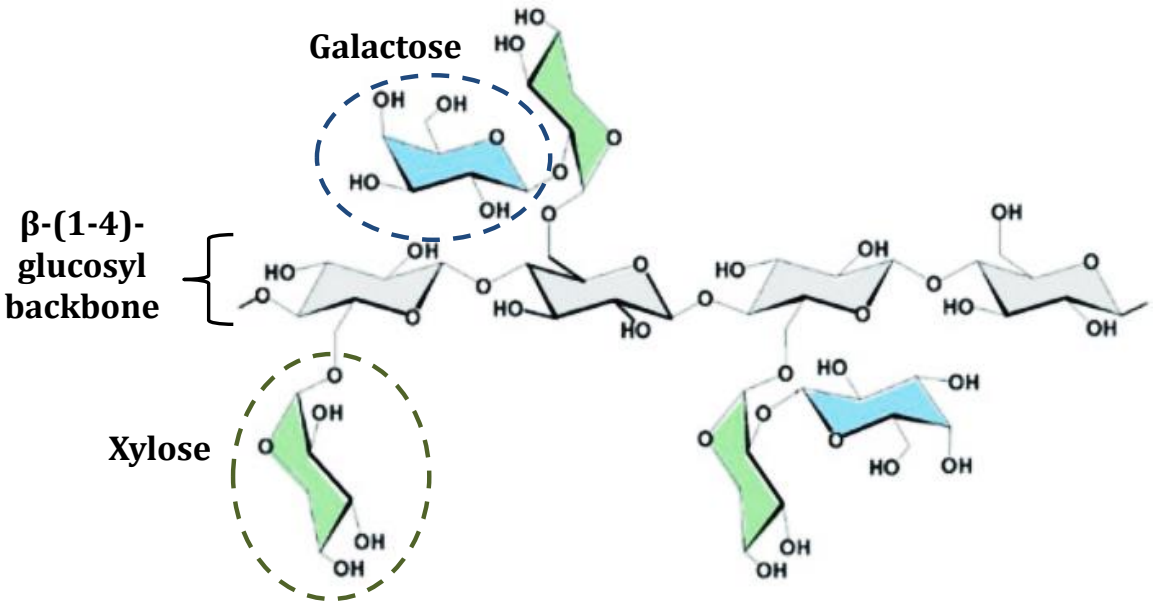

Figure I-17: Structure of the XLLG oligosaccharide xyloglucan showing the β-(1-4)-glucosyl backbone (gray) with side chains made of xylose (green) and galactose (blue). Adapted with permission from Park and Cosgrove 2015 [44].

In this PhD, a commercial batch of XG is used and was obtained from tamarind seed gum. It was supplied by DSP Gokyo - Food and Chemical (Japan) and more details will be given in section "Materials & Methods" of following Chapters.

In vivo, hemicelluloses are located around cellulose microfibrils within the amorphous matrix acting as an intermediate between lignin and cellulose. The role of xyloglucan in the plant cell walls is dual: *(i)* energy storage in seed, *(ii)* structural thanks to its tight interaction with cellulose. The precise role of the XG/cellulose network is still a matter of debate in the community but the model recently reported by Park and Cosgrove proposes the occurrence of three different assembly domains for XG/cellulose: *(1)* XG chains are not directly in interaction with cellulose (bridges, loops and tails between MFC), *(2)* XG is in interaction at the surface of cellulose and *(3)* XG is intimately located within MFC or between them acting such as a "glue" [44], **Figure I-18**. Nevertheless XG/Cellulose interactions have been investigated extensively *in vivo* and *in vitro* in literature [80]–[83]. XG interacts with cellulose microfibrils through hydrogen, van der Waals and polar bonds, the adsorption being entropically and kinetically driven [84], [85]. More precisely, the hydroxyl groups, in majority on the glucan chains, interact each other and create physicochemical interactions. The binding capacity between cellulose and xyloglucan is significantly related to concentrations of the building blocks, the molar mass and other adsorption processing parameters [84], [86]–[88].

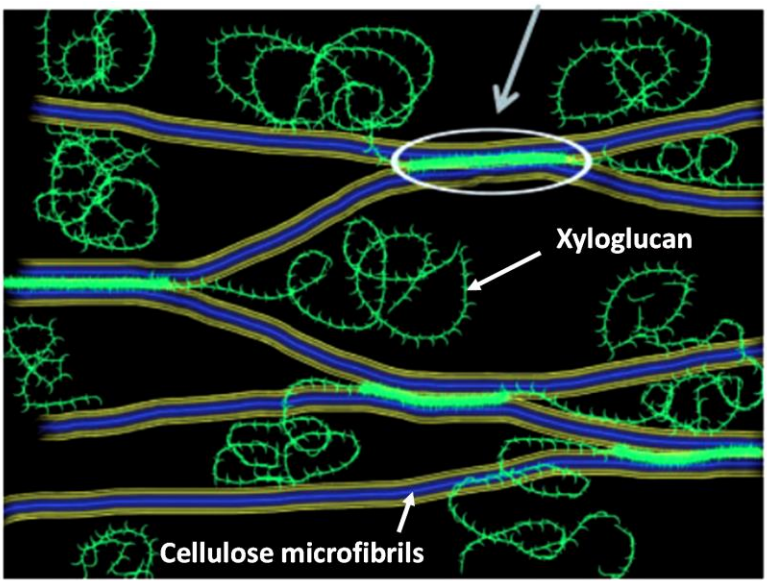

Figure I-18: Biomechanical hotspot model with cellulose microfibrils depicted as rods with hydrophilic (yellow) and hydrophobic (blue) surfaces and extended xyloglucan chains (green) (reprinted with permission from Park and Cosgrove (2015) [44]).

To go further in this way, friction measurements have been performed by AFM between cellulose and XG [89], [90]. These studies show the irreversibility side of the adsorption of XG to cellulose. Moreover, the adhesion between cellulose surfaces in water, which is often very small, is increased with the presence of XG on the surfaces. It appears that specific bonds are formed between XG and cellulose surfaces, creating a strong bridging between cellulose fibres.

I. 1. 5. 3 XG/cellulose interactions for the creation of innovative materials

This part will present some examples of innovative materials integrating the strong affinity between XG and cellulose and dealing with the framework of this PhD thesis.

First, scientists worked on the adsorption of XG on pulp fibres for paper application. For example, the addition of XG by spraying on a bleached birch kraft pulp increases its wet web strength, tension holding, drying tension and also its smoothness [91]. Similarly, when XG is used as a wet end additives in paper making process, paper formation is facilitated and final paper strength is increased [92], [93]. In fact, fibre bonds in pulps treated with XG seem to give high adhesion levels.

Berglund's team worked on the addition of the combined XG and CNF in wood pulp fibres for the manufacturing of sheet papers [94] and aerogels [95]. Considering the paper material, the addition of enzymatically pre-treated CNF (10 wt%) in wood pulp fibres increased the toughness by around 60 % due to the higher stress transfer by the preservation of fibre-fibre bonds. Moreover, the addition of XG (5 wt%) to the CNF-paper increased the toughness even more by 210 %, compared to the reference. They went further in this concept in the development of bionanocomposites. They adsorbed partly oxidised XG on TEMPO oxidized CNF, forming a core-shell CNF, to prepare wood fibre / CNF nanocomposites from a vacuum filtered suspension. The CNF or XG-CNF suspension is treated with wood pulp fibres and a cellulose nanofiber network is created in the pulp fibre structure, as shown in the schematic **Figure I-19**. The density, the strength and the modulus of the pulp fibre network composite have been strongly improved with the addition of CNF-XG, acting as a binder between fibres. It can also be noticed that the carboxylate content in CNF (CNF_5 or

CNF_{10}) has an impact on the mechanical properties of the composite with a stronger reinforcement for high charge content.

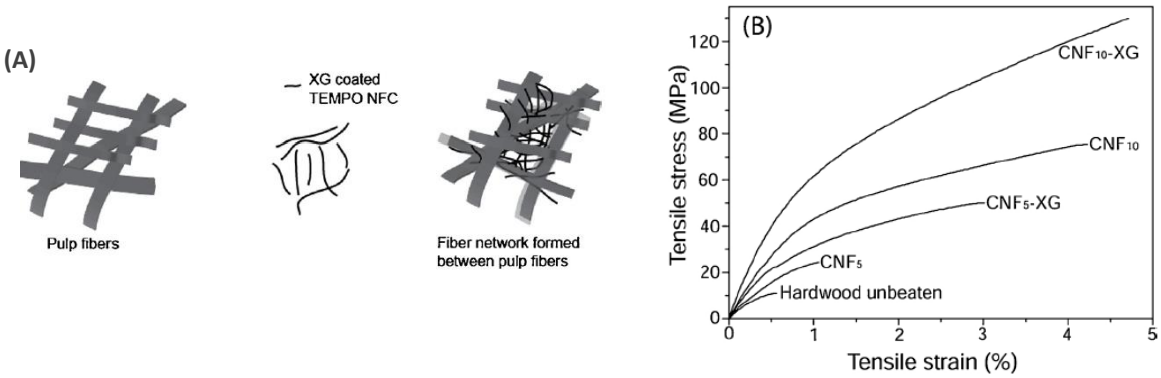

Figure I-19: (A) Schematic representation of XG coated CNF network in pulp fibre composite; (B) Tensile curves of hardwood unbeated wood fibre networks reinforced with 10 wt% of CNF. Note that the difference between the two grades of CNF is the density of charged carboxyls on the fibril surface (reprinted with permission from Vilaseca *et al.* 2020 [95]).

Jaafar *et al.* (2020) used the combination of CNC and XG to construct aerogels inspired by the hierarchical organization of the wood tissue [96] (**Figure I-20**).

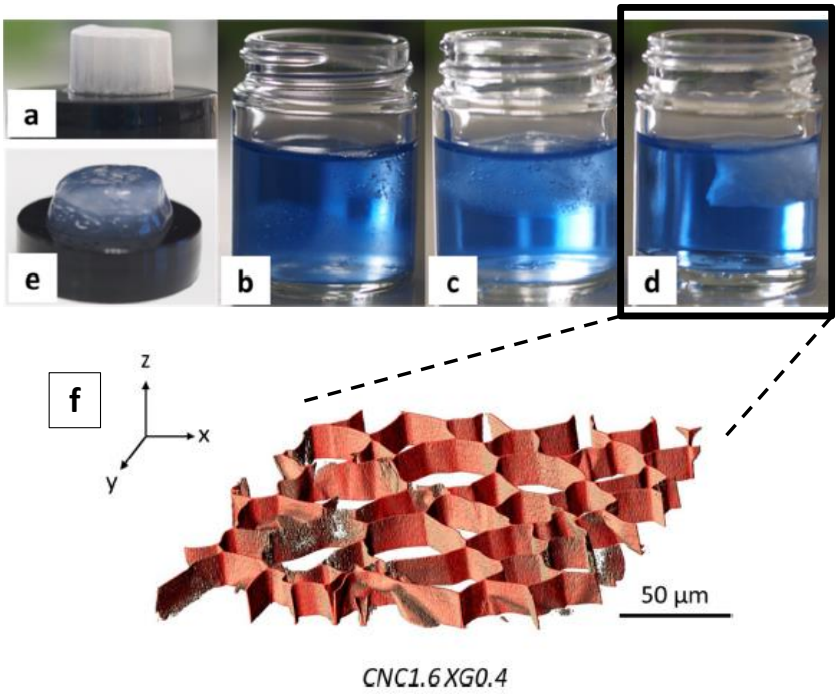

Figure I-20: Images of the unidirectional freeze-cast aerogel in water **(a)** before immersion, **(b, c, d)** after 4 h and **(e)** 2 weeks. The aerogels used in this experiment consist of **(b)** CNC2 XG0, **(c)** CNC1.9 XG0.1 and **(d, e)** CNC1.6 XG0.4. **(f)** 3D reconstruction of CNC/XG aerogel from confocal microscopy of the XG-RBITC channel, imaged after lyophilisation (adapted with permission from Jaafar *et al.* 2020 [96]).

The addition of XG amount in the unidirectional freeze-dried CNC aerogel improved clearly the mechanical properties of the structure with a Young's modulus increasing by around 340 % from 138 kPa to 610 kPa. Moreover, aerogels containing the highest proportion of XG, i.e. CNC/XG (1.6/0.4 wt%) for a final concentration of CNC/XG suspensions at 2wt%, keep their structural integrity in water.

If we focus on this combination of xyloglucan and cellulose nanocrystals, two derived products from the plant cell wall, they have been investigated in the literature and spurred the interest for developing innovative eco-friendly materials with the specific and interesting properties of the two components (**Figure I-21**).

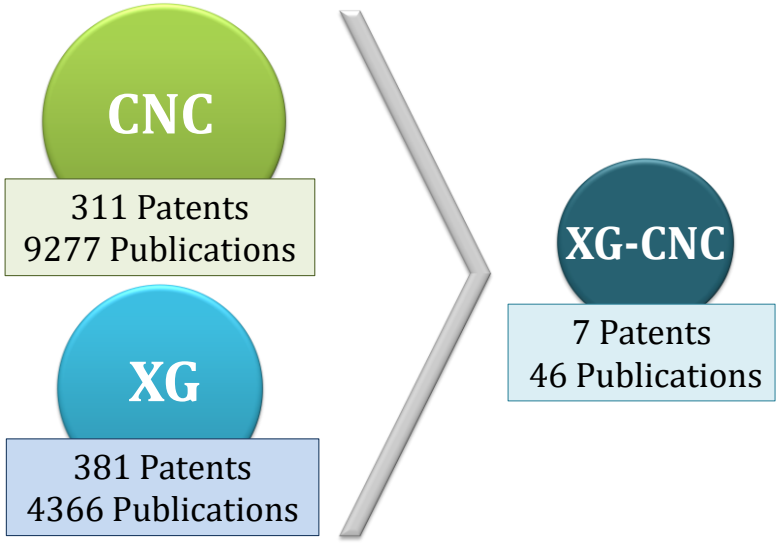

Figure I-21: Cumulative number of publications and patents dealing with cellulose nanocrystals (Source: SciFinder, August 2020 – Descriptors: cellulose nanocrystals, cellulose nanorod, cellulose nanowire, cellulose crystallite, cellulose whiskers, nanocrystalline cellulose, microcrystalline cellulose – Language: English) and xyloglucan (Source: SciFinder, August 2020 – Descriptor: xyloglucan – Language: English) since 1990.

I. 2. Interfaces and fibre modifications in natural fibre reinforced biocomposites

Mechanical properties of fibre reinforced composites are strongly linked to the fibre content and their intrinsic properties, such as strength, stiffness, biochemical composition and humidity and temperatures sensitivity, but also to the fibre / matrix interface. The interface in composites has a huge importance and impacts strongly the macroscopic properties of the materials. In the case of biocomposites, different types of interfaces occur at different scales providing complex failure mechanisms during mechanical loading. In order to enhance the compatibilization between natural fibres and matrix, modifications of fibres are performed following different paths. This section will present the properties of flax fibres influencing final biocomposite properties, the different types of interfaces within biocomposites with the role of the interphase region fibre / matrix, and finally present the different strategies of modification to improve the interfacial adhesion between natural fibres and the polymeric matrix.

I. 2. 1. Properties of flax fibres: biocomposite application

The preparation of biocomposites with natural fibres implies to well know the intrinsic properties of the fibres, reported in **Table I-3**, and their aptitude to resist to the transformation processes in order to keep their morphological and mechanical properties. These properties are in general highly variable that can be partially explained by their dependence to the seeding method, the climatic conditions during their growth, the retting etc. [10], [97], [98]. In fact, these fibres have different selection variety [15], location in the stem conditioning [99], diameter [100], biochemical composition and cell wall organization that decrease the reproducibility of their functional properties.

This particularity is often blamed on the natural fibres and is viewed as a limitation in their use as reinforcement in biocomposites. However, Baley *et al.* [101] have compared 4298 flax fibre mechanical tests from 17 varieties between 1993 and 2017 and have shown stable mechanical properties despite very different climatic conditions, which is positive for the manufacturing of industrial products. The average tangent modulus is 52.3 ± 8.3 GPa, the

average strength is 945 ± 200 MPa and the average failure strain value is 2.4 ± 0.4 %, with a mean diameter of 16.64 ± 2.65 µm. In their point of view, this variability in mechanical properties is also present in the synthetic fibres like E glass fibres. In fact, the tensile strength of freshly drawn 10 microns diameter E glass fibres is 3200 – 3400 MPa, against 2200 – 2400 MPa for sized fibres from a yarn and 1200 – 1550 MPa for a yarn with numerous fibres. It is therefore important to take into account all the mechanical extraction processes (scutching, combing, hydrothermal conditions) and the manufacture of semi-products for textile or biocomposite applications (spinning, weaving, bundles production, preform manufacture, carding, needling, post-treatments etc.), which have also a real impact on the final mechanical properties of the fibres

Table I-3: Diameter and mechanical properties of lignocellulosic fibres (elementary fibres or bundles), (reprinted with permission from Bourmaud *et al.* 2018 [25]).

	Elementary fibre or bundle	Diameter (µm)	Young's Modulus (GPa)	Strength at break (MPa)	Strain at break (%)
Musa textilis (Abaca)	Bundle	179–230	17.1–18.4	755–798	8.8–6.2
Stipa tenacissima (Alfa)	Elementary and bundle	24.3	31.0–71.0	679–1480	2.4–2.8
Bambusoideae (Bamboo)	Elementary	13.4	32.0–43.7	1200–1610	3.8–5.8
Cocos nucifera (Coir)	Bundle	100–460	3.39–17.3	131–343	3.7–44.7
Gossypium sp. (Cotton)	Elementary	No bundle	5.5–13.0	287–800	3–10
Linum Usitatissimum L. (Flax)	Elementary	12.4–23.9	37.2–75.1	595–1510	1.6–3.6
Cannabis Sativa (Hemp)	Elementary/Bundle	10.9–42.0	14.4–44.5	285–889	0.8–3.3
Corchorus capsularis (Jute)	Bundle	60–110	10–31.2	114–629	1.5–1.8
Ceiba pentandra (Kapok)	Elementary	23.6	1.7–4.0	45–93	1.2–4.0
Hibiscus cannabinus (Kenaf)	Elementary	13.3	19	983	4.5
Boehmeria nivea (Ramie)	Elementary	34–50	24.5–65	560–900	1.2–2.5
Agave sisalana (Sisal)	Bundle	25–252	9.0–25.0	347–577	2.3–5.45
Wood (different species)	Elementary	15.5–22.6	15.4–27.5	553–1300	3–7

I. 2. 1. 1 Different flax fibre properties influencing biocomposite mechanical properties

The diameter and the tensile mechanical properties of flax fibres are reported in the **Table I-3**. Comparing with the other lignocellulosic fibres, flax fibres seem to have very high Young's Modulus 37.2 – 75.1 GPa and tensile strength 595 – 1510 MPa. In fact, they are located in the

periphery of the stem, as explained in the part ***I. 1. 2. 2***, and have the role of mechanical support of the plant. However, flax fibres are not continuous fibres such as glass or carbon fibres, which can induce defects and lower tensile strength of natural fibre reinforced biocomposites.

The biochemical composition and the cell wall organization may also influence the mechanical properties of fibres. The presence of cellulose microfibrils as reinforcement in the secondary wall of the fibre is mainly responsible of the high stiffness. More specifically, the high cellulose content, the high degree of crystallinity and their quasi-parallel orientation with respect to the axis of the fibre (MFA around 10°) explain mainly the high mechanical properties of the flax fibres [102].

Because of the composition of the natural fibres, their mechanical properties are also directly linked to environmental factors as relative humidity and temperature. For example, flax fibres under usual storage conditions contain around 7 wt% of water at equilibrium at 65% RH and 21°C [103], [104]. Garat *et al.* [105] have highlighted two different processes of water uptake in natural fibres: *(i)* a microscopic swelling due to the sorption of bound water at the scale of cell walls, *(ii)* a macroscopic swelling with the formation of free water in lumens and pores (**Figure I-22 A**).

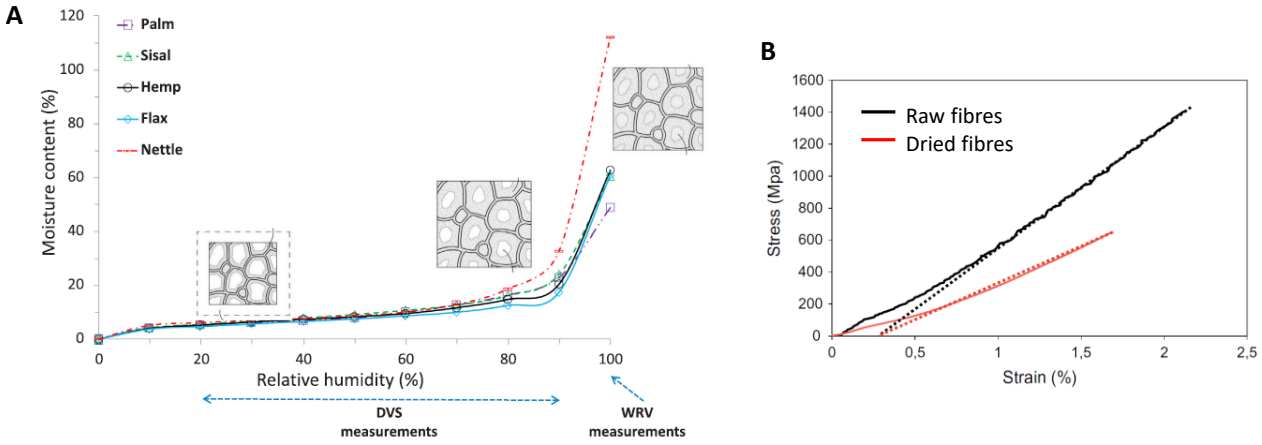

Figure I-22: A. Moisture content of natural fibre bundles in relative humidity (DVS) and in immersion (WRV) conditions at 23°C (reprinted with permission from Garat *et al.* 2020 [105]); **B.** Typical stress-strain plots comparing raw and dried flax fibres at 105°C during 14 hours (reprinted with permission from Baley *et al.* 2012 [106]).

The presence of this water in the cell wall, acting as a plasticizer, is a real challenge in the manufacturing of biocomposite materials [107]–[109]. High temperatures used in thermoplastic manufacturing processes (twin-screw extrusion, injection molding etc.) decrease considerably the properties of flax fibres and also biocomposites. In fact, it will affect directly the fibre / matrix interface and initiate defects such as porosities. On the other hand, the removing of water from flax fibres can cause mechanical stresses within the fibres with a strong decrease of their tensile strength [106], [110] (**Figure I-22 B**). Considering the thermoset biocomposites, the drying of flax fabrics before the impregnation can be a solution to remove water but will strongly influence the mechanical properties of the biocomposite in terms of microstructure, moisture sorption and desorption behaviour, swelling, shrinkage [106], [111].

Elementary flax fibres may have a large number of defects which can be some dislocations, misorientations of cellulose fibrils, sliding plane, kink-bands or knees [112]. These impacts on the fibre integrity are coming from the growth and the bending of the fibres [113], [114], the retting step or from the extraction and refine processes [115], [116] and impact strongly the mechanical properties of the flax fibres, especially the tensile strength (**Figure I-23**). All these defects imply stress concentrations, which can form micro-cracks in the matrix and also initiate the debonding of fibres at the fibre / matrix interface [117].

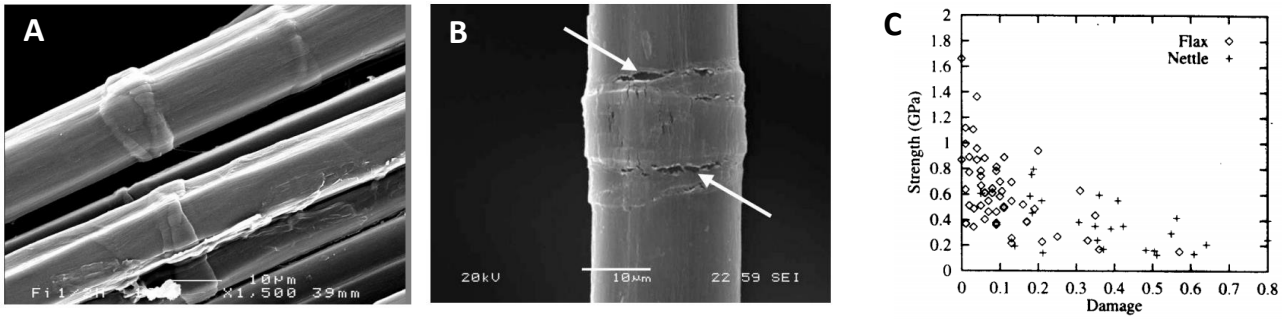

Figure I-23: A. Bundle of flax fibres with kink-bands; **B.** Tensile test in a SEM with the start of cracks in a flax fibre arounf the kink-band (reprinted with permission from Baley 2004 [118]); **C.** Variation of strength with damage for flax and nettle ultimates (reprinted with permission from Davies *et al.* 1998 [114]).

I. 2. 1. 2 Surface properties and porosities of natural fibres

The surface of natural fibres is the first contact zone between the fibres and the matrix and plays a key role in the adhesion and wetting mechanisms in composite processing. Physico-chemistry, chemistry and topography of flax fibre surfaces have a huge importance and will be detailed below.

In this section, all the technics used to analyse natural fibre surfaces have been listed and a focus will be done on methods used in the frame of the PhD work.

I. 2. 1. 2. 1. Physico-chemistry

In order to analyse the physico-chemistry of natural fibres, several technics can be relevant: the contact angle measurement techniques and the Inverse gas chromatography (IGC).

The surface physico-chemistry of natural fibres can be evaluated with the contact angle techniques, i.e. sessil drop, drop-on-fibre, vertically immersed fibre(s) with the Wilhelmy method, capillary rise in a bed of powder or fibres with the Washburn method. These methods provide the determination of the surface free energy γ_{SV} with the dispersive γ_{SV}^{d} and non-dispersive components comprising polar γ_{SV}^{p}, acid-base γ_{SV}^{AB}, γ_{SV}^{+}, γ_{SV}^{-} and Lifshitz-van der Walls γ_{SV}^{LW} components. It consists in measuring the contact angle θ at the intersection of the liquid, gas and solid phases to study the surface wettability of the fibre in the defined liquid. All these values are further used to characterize the fibre / matrix interactions with the interfacial tension γ_{SL} and the theoretical work of adhesion W_A. This work of adhesion is considered as the measure of the strength of physico-chemical interactions between two phases, which can be natural fibres and polymer matrix [119].

It should be noticed that the determination of the surface free energy of natural fibres is challenging because of the highly porosity of fibres and the surface roughness. Moreover, the distribution of cell wall components within the fibre is very heterogeneous [120] with mostly cellulose microfibrils in the bulk and non-cellulosic components at the surface. This surface seems to be more hydrophobic with the presence of lipophilic components and waxes [121], more or less present following the separation and treatment processes like retting, scutching, semi-products manufacturing etc. Finally, many treatments like chemical extractions, adsorption, temperature etc. can be used on natural fibres, and in our case flax fibres, in

order to obtain the most adapted and compatible surface physico-chemistry to the matrix [49], [107], which will be detailed in section *I. 2. 5*. As it can be observed on the **Figure I-24**, the thermal treatment of flax fibres seems to decrease a large amount of cracks present in the biocomposite on the left comparing to only microcracks in the biocomposite on the right.

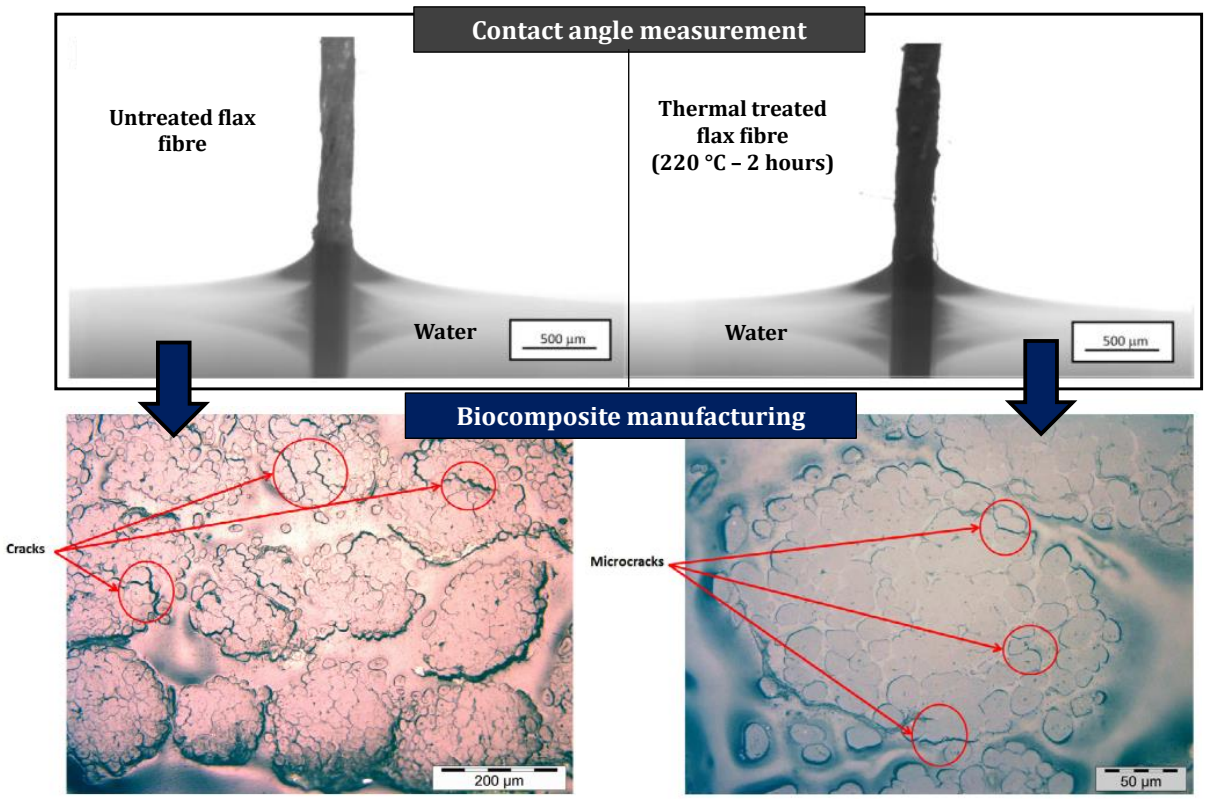

Figure I-24: Influence of the thermal treatment on the surface physico-chemistry of flax fibres and so the microstructure of the final biocomposite materials (adapted with permission from Pucci *et al.* 2015 [107]).

I. 2. 1. 2. 2. Chemistry

The surface chemistry of natural fibres is very complex because of the various biochemical components constituting the fibres and so implies a wide variety of functional groups at their surface. In this way, many technics have been used to characterize natural fibre surfaces and are reported **Table I-4**.

Some measurements have been made on flax fibres considering only few nanometres of the surface corresponding to the primary cell wall and residual middle lamellae [122]–[124]. It has been found a high amount of hydrocarbon compounds such as waxes and waxe-like components, a very few amount of lignin (no aromatic compounds), hemicelluloses and

0.5 – 1 % of calcium indicating the presence of pectins. Cellulose is also present but less than expected for a cellulosic material. It can be mostly explained by the presence of cellulose mainly in the secondary cell-wall of the flax fibre and less at the surface being in the major part the primary cell-wall and the middle lamellae. Le Duigou *et al.* achieved to determine the chemical elements ratios present at the surface of flax fibres from two different varieties from the C1s peak decomposition by X-ray Photoelectron Spectroscopy (XPS) [123]: 76 – 78 % Carbon, 19 – 21 % Oxygen, 1.9 % Nitrogen, 0.5 – 1 % Calcium with O/C ratios of 0.24 – 0.27.

Table I-4: Different experimental techniques used to characterize chemically natural fibre surfaces.

Experimental techniques	
Elementary analysis	**Elemental analysis** Time of Flight – Secondary Ion Mass Spectrometry **(ToF-SIMS)** X-ray Photoelectron Spectroscopy **(XPS)** Energy-dispersive X-ray spectroscopy **(EDX)** X-ray diffraction **(XRD)** Solid state magnetic resonance **(NMR)**
Spectroscopy analysis	**IR spectroscopy** **Raman spectroscopy**
Thermal analysis	Thermogravimetric analysis **(TGA)** Pyrolysis – Gas Chromatography - Mass Spectrometry **(Py-GC/MS)** Pyrolysis Combustion Flow Calorimetry **(PCFC)**

All the potential functional groups on flax fibre surfaces are illustrated **Figure I-25** but chemical groups present at the surface are very difficult to identify with precision, depending in particular on the extraction processes and the variety. This entire chemical environment has to be taken into account in order to well understand the interactions between the fibre and the polymeric matrix in biocomposites to adapt the compatibilization.

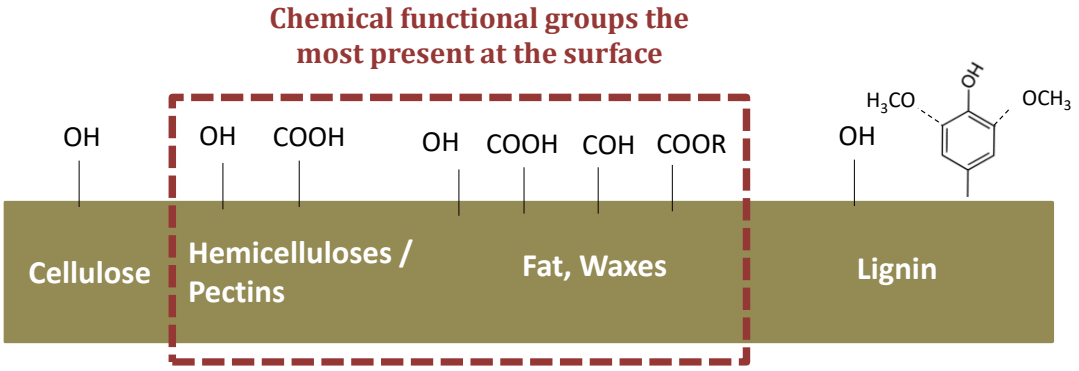

Figure I-25: Overall biochemical composition of the surface of flax fibres with possible reactive functional groups.

I. 2. 1. 2. 3. Topography

Natural fibres are very complex structures with pores and capillaries difficult to measure and quantify [125]–[127]. This porosity induces high available total pore volume and specific surface area which have to be considered in the functionalizing of lignocellulosic fibres with the migration of molecules, additives or biopolymers. Different technics are used to analyse porosities and specific surface area, i.e. Small angle X-ray scattering (SAXS), Mercury porosimetry, water vapour adsorption, Brunauer-Emmett-Teller (BET) or Nitrogen adsorption, size-exclusion chromatography or calculation apparent density measurements. The flax fibre has a porosity of around 11 % with a specific surface area ranging from 0.31 to 1.4 m^2/g (BET technique) [128]–[130]. Moreover, natural fibres have a non-negligeable surface roughness, illustrated **Figure I-26**, which can play a key role in the wettability and the interfacial adhesion in biocomposites. The interfacial interlocking with the matrix is enhanced but on the other hand, this topography will affect the wettability during the composite processing with the difficulty of the matrix to embed entirely the surface of fibres. In comparison, glass fibres have a very low root mean square roughness between 2.4 and 3.3 nm against 10.8 – 35 nm for flax fibres, measured by Atomic Force Microscopy (AFM) [110]. We have to keep in mind that modifications of natural fibres can induce a change of the topography in the positive or negative way. In fact, biopolymers adsorption or chemical grafting on the surface of natural fibres can induce porosities in the yarns or fibre bundles with difficulties in impregnation, compromising the desired gain in interfacial adhesion and wettability.

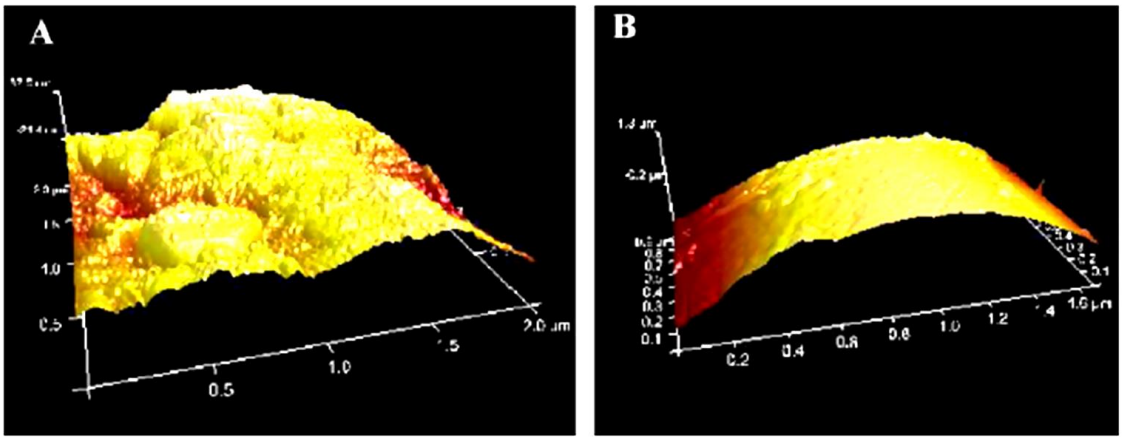

Figure I-26: TM-AFM phase of (A) raw flax fibre and (B) de-sized E-glass fibre (reprinted with permission from Le Duigou *et al.* 2012 [110]).

I. 2. 2. Multi-scale and various interfaces within biocomposites

The extracted flax fibres are in reality bundles constituted of several elementary fibres bonded via the middle lamellae mainly composed of lignin and pectins. It has been demonstrated that higher lignin content inside middle lamellae drives to lower dispersion state and more aggregated elementary fibres within the polymeric matrix [131]. Indeed, during the biocomposite manufacturing, flax fibres are dispersed inside the matrix, schematized **Figure I-27.1**, and can be found in three different shapes i.e. *(i)* fibres bundles, *(ii)* elementary fibres and *(iii)* particles (low aspect ratio) [132].

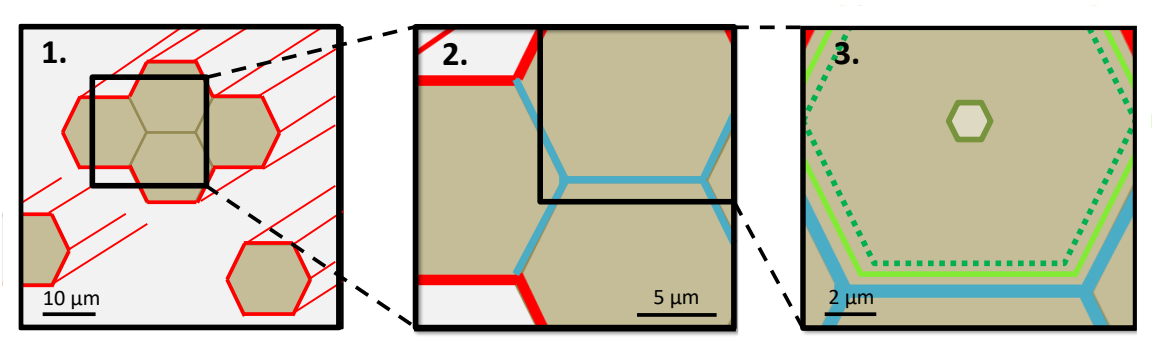

1. Interface **matrix / elementary or flax fibre bundles** (red)
2. Interface **between elementary flax fibres in bundles** (blue)
3. Interface **between layers** within the cell walls in flax fibres (green)

Figure I-27: Schematic of the different interfaces within natural fibre reinforced biocomposites.

However, the presence of bundles in the matrix decreases the dispersion state and creates defects and damages in the material [133]. Indeed, it seems that the failures occur preferentially within bundles during mechanical solicitations (**Figure I-28**). A better dispersion induces more fibre / matrix interactions, less fibre / fibre interactions and so a higher interfacial coupling with the matrix with a higher available surface in contact. Finally, we have to keep in mind the complex architecture of elementary flax fibres with multiple cell wall layers and so inter and intra-cellular interfaces, schematized **Figure I-27.3**, which may involve fibre breakage and peeling effects among the cell walls [106], [110], [123], [134], [135]. All these interfaces, *(1)* between matrix and elementary or flax fibre bundles, *(2)* between elementary fibres within bundles and *(3)* between layers within the cell walls in elementary fibres are potential defect zones inducing multiple and heterogeneous rupture mechanisms in natural fibre reinforced biocomposites.

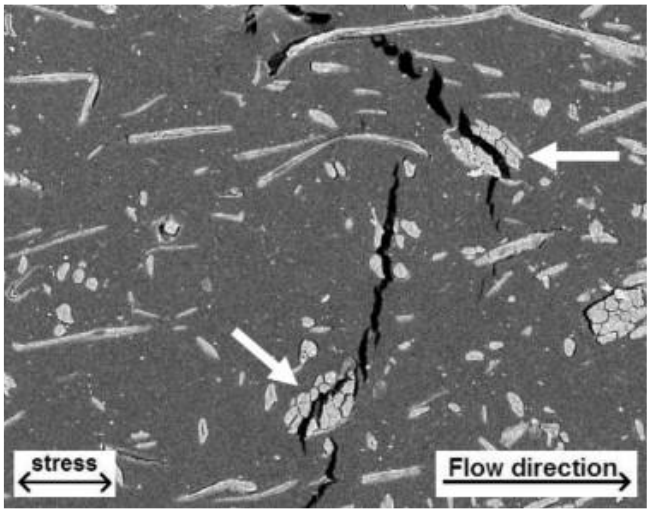

Figure I-28: SEM image in the core of PP / flax sample under loading (reprinted with permission from Bourmaud *et al.* 2013 [133]).

The following part will focus on the interphase zone between natural fibres and polymeric matrix explaining the key role of this region in composites with a detail of the different occurring phenomena.

I. 2. 3. Key role of the natural fibre / matrix interphase

First, the terms "**interface**" and "**interphase**" can be differentiated by the only two dimensions of the interface between fibre and matrix against an interphase (or interfacial zone) in three dimensions with complex occurring phenomena. This interphase corresponds to a transition region between fibre and matrix with a thickness from several hundred nanometers to a few micrometers and more rarely a hundred micrometers for some thermoset biocomposites. This zone is extending between both interfaces bulk matrix and bulk fibre and brings into play several phenomena including intrinsic properties of fibres (roughness, specific surface area,…) and also synergistic effects between fibre and matrix (transcrystallinity or cross-linking gradient, chemisorption, physisorption, chemical interactions,…), illustrated on **Figure I-29**. The interphase plays a key role in biocomposites because this is the preferential site for stress and load transfer. Indeed, during a mechanical solicitation, fibres will support the applied load while the matrix will transfer and distribute this load among the fibres through the interphase zone. Moreover, the interphase is one of the most common sites of damages inducing failure mechanisms. A weak fibre / matrix interface is characterized by adhesive interfacial failures with debonding of fibres from the matrix and crack propagation between both.

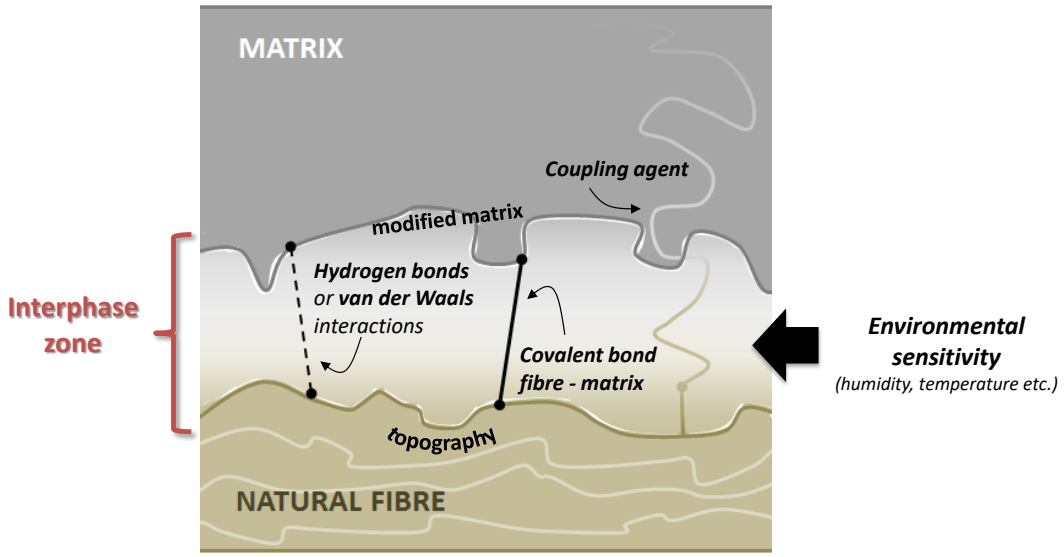

Figure I-29: Schematic of an interphase zone between natural fibre and polymeric matrix including natural or provided physical, chemical and physico-chemical coupling phenomena.

However, a strong fibre / matrix adherence is recognized by cohesive interfacial failures with the rupture within the matrix or within fibre structure [110]. A higher interfacial adhesion will provide better mechanical properties such as stiffness and strength but will probably also increase the brittleness of the material and so decrease its energy absorption capacity upon impact. Indeed, a compromise between strength and toughness is always needed and implies choosing the adapted strategy of compatibilization for good biocomposite performances.

I. 2. 4. Improvement of the interfacial adhesion in natural fibre reinforced biocomposites

First, a clarification must be done about the terms "**adhesion**" and "**mechanical adhesion / adherence**" which provide differences in fibre / matrix interactions [136]. The adhesion features all the physico-chemical phenomena such as mechanical interlocking, roughness and surface free energy of fibres, surface tension of matrix describing the wettability of fibres within a molten polymeric matrix. The adherence (or mechanical adhesion) is a more general term including the interfacial strength between fibres and matrix within the composite at a solid state during mechanical loading. The interfacial adhesion fibre / matrix is driven by the nature of interactions and the quantity of interface and can be modified by different strategies, represented **Figure I-30**, in order to enhance the interphase and so performance of biocomposites.

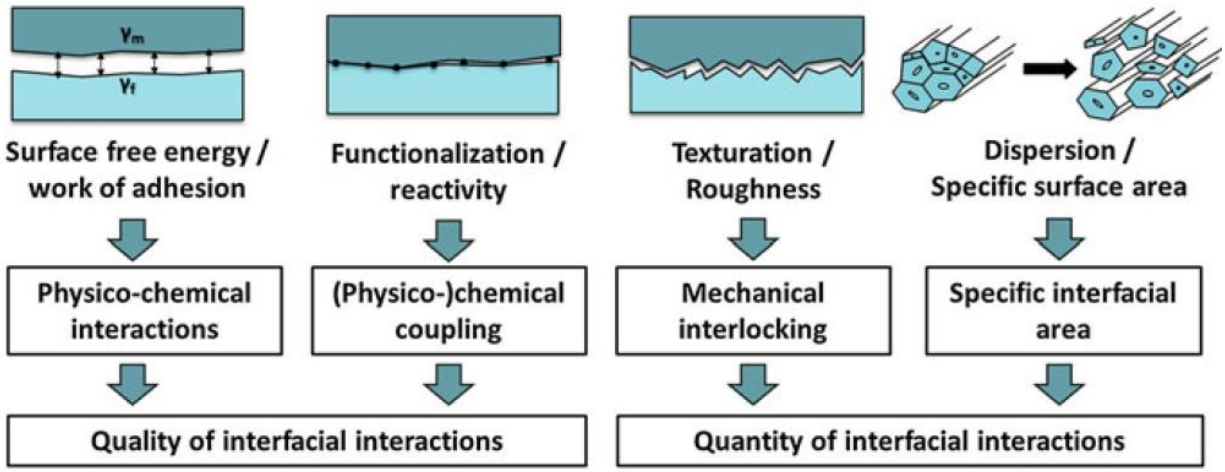

Figure I-30: Different strategies to play on the interfacial adhesion in natural fibre based biocomposites (reprinted with permission from Le Moigne *et al.* (2018) [137]).

The quality of interfacial adhesion fibre / matrix can be modified via the surface free energy of fibres and their polar and dispersive components. This modification will impact directly the work of adhesion with the matrix and so, the wettability and impregnation of the molten or liquid matrix among natural fibres. The (physico-)chemical functionalization of fibres will increase the reactivity of fibres toward the matrix and enhance the coupling with the creation of strong interactions. It can be noticed that this modification is also possible by incorporating a coupling agent inside the matrix which will react with chemical groups present at the surface of natural fibres [138], [139]. Playing on the quantity of interface is another strategy and can be done by changing the topography and/or the specific surface area of the surface of fibres. These supplementary contact points between fibres and matrix will increase the mechanical interlocking with the matrix and so the interfacial adhesion.

The dispersion state of fibres within the matrix must not be neglected and has a strong impact on the macroscopic properties of biocomposites. Indeed, the dispersion state depends on processing parameters (screw speed, rheological behaviour, temperature…) and intrinsic properties of fibres and matrix but can also be changed by the modifications of fibres such as solvent extractions (**Figure I-31**).

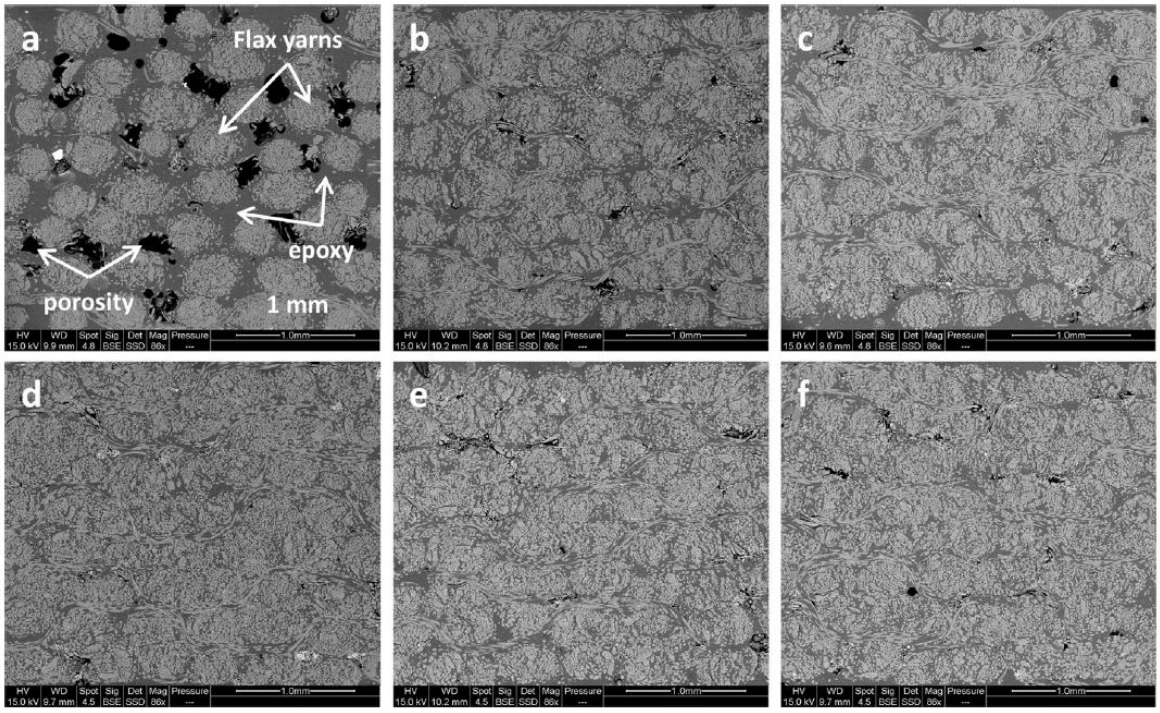

Figure I-31: SEM micrographs of transverse cross section of flax fibre reinforced biocomposites with different fibre treatments: (a) untreated, (b) ethanol, (c) toluene/ethanol, (d) water, (e) surfactants, (f) NaOH 1% (reprinted with permission from Acera Fernández *et al.* (2016) [49]).

Finally, the modification of natural fibres is often performed on industrial products before the processing of biocomposites. In the case of extrusion and injection, it has be found that raw fibres at this step are commonly in bundles shape before the processing, including many untreated surfaces in contact with the molten matrix after their dispersion, estimated at around 90% [140].

The following section will now describe in details the different kind of modifications of fibre / matrix interfaces in natural fibre based biocomposites.

I. 2. 5. Modifications of the interface in natural fibre reinforced biocomposites

As described in the previous section, flax fibres provide many advantages for their use as reinforcement in composites, such as lightness, availability, carbon neutrality, low price but display also drawbacks such as complex structure, hydrophilic and polar characters, thermal sensitivity and poor compatibility with polymeric matrices. It seems necessary to modify

natural fibres to improve their compatibility with the polymeric matrix and so enhance performances of biocomposite materials. Such modifications can be divided in two main categories, i.e. *(i)* **natural fibre pre-treatments** with the main objective of extracting some compounds from middle lamellae and plant cell walls and *(ii)* **natural fibre functionalization** applied directly to raw fibres or after fibre pre-treatments. All these strategies will be detailed below, mainly focusing on flax fibres as natural fibres incorporated in polymeric matrix biocomposites.

I. 2. 5. 1 Pre-treatments

Pre-treatments of natural fibres, mostly originated from textile and wood industries, are used to prepare fibres for their functionalization in order to obtain a better dispersion and compatibilization in the polymeric matrix biocomposite.

Retting processes (dew, water, chemical, enzymatic) partly introduced in the section ***I. 1. 4. 1***, are detailed in **Table I-5**.

Table I-5: Various types of retting processes for the production of natural fibres.

Type of retting	Features	Advantages	Disadvantages
Dew	Plant stems left on the soil → action of **bacterial and fungis**	The most used today Easy removal of pectins	Dependant on the duration and climatic conditions, decrease the fibre tensile strength, low and various quality
Water	Plant stems immersed in water (**microbial action**)	High quality and uniform fibres	Environmental problems and soil pollution from anaerobic bacterial fermentation, high cost, putrid odour, low-grade fibre
Enzymatic	Attack of **specific enzymes** (pectinases, xylanases etc.) on plant stems	Under controlled conditions, selective degradation, fast and clean	Low fibre tensile strength
Chemical	**Boiling and chemicals** (NaOH, H_2O_2, sodium benzoate)	Efficient and clean process in short time, smooth surface	Decrease of the fibre tensile strength (>1% NaOH), high cost

Such processes are used to ease the extraction of bast fibres from the stem by degrading non-cellulosic compounds which act as cement between elementary fibres, represented **Figure I-32**, and prevent afterward the good dispersion of fibres inside the matrix. This retting step is crucial but influences greatly the final biochemical composition, the cleanness and very often

leads to the decrease of the tensile strength of fibres [141], [142]. The main challenge of this pre-treatment is to find a compromise between an efficient separation of fibre bundles to obtain a good dispersion and the keeping of intrinsic mechanical properties of fibres.

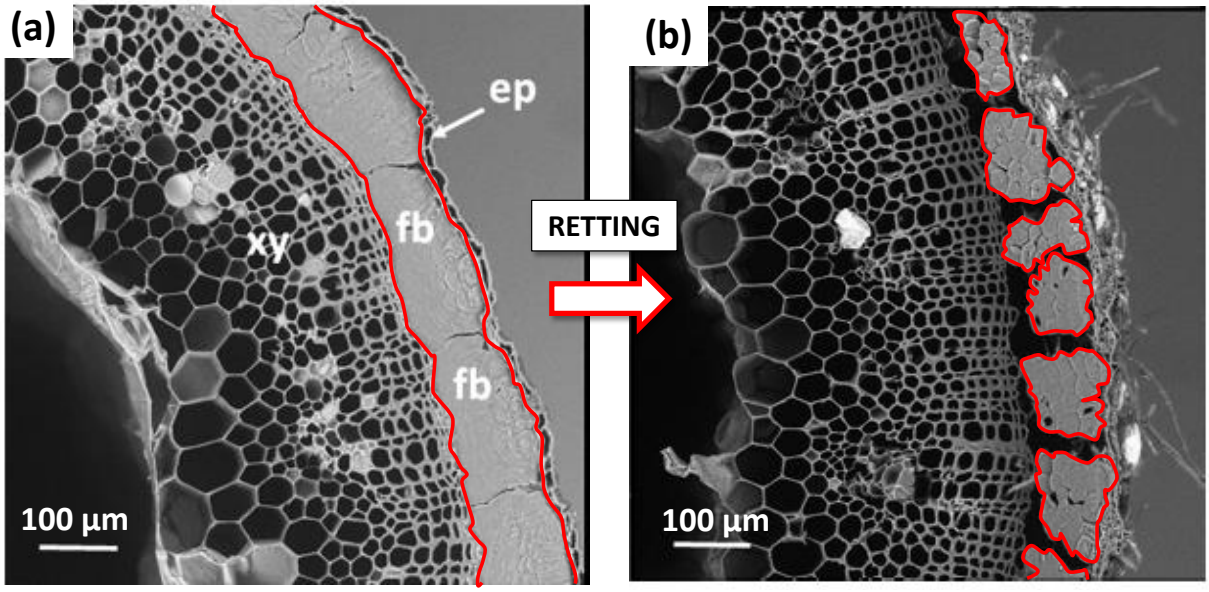

Figure I-32: SEM images of transverse sections of (a) unretted and (b) 8 weeks retted flax stems; xy = xylem, fb = fibre, ep = epidermis (adapted with permission from Chabbert *et al.* 2020 [98]).

Solvent or chemical extraction treatments have also been investigated with partial or total extractions of inter- and intra-cellular compounds, changing the wettability of natural fibres and their dispersion state in the matrix.

The main used flax fibre pre-treatments are water and mercerization, detailed in **Table I-6**, but other pre-treatments have also been investigated in literature such as thermal (mentioned in part ***I. 2. 1. 2. 1***), ethanol, toluene, formic or acetic acid, bleaching, surfactants or HCl [49], [120], [143]. It seems that these pre-treatments on flax fibres are good strategies with a rougher and cleaner fibre surface, a better separation of elementary fibres within bundles and in the matrix, an increase of the available hydroxyl groups on the surface and/or an increase of the interfacial adhesion with the polymeric matrix. However, it is necessary to choose the good one depending on the matrix and natural fibre reinforcing product to study their influence on the physico-chemistry and the intrinsic properties of fibres.

Table I-6: Water and alkali pre-treatments on flax fibres and their influence on the interfacial adhesion in flax fibre reinforced biocomposites.

Solvent	Methods	▲ Advantages ▼ Disadvantages	Interfacial adhesion with polymeric matrix (▲▼)	References
Water	72h at 23°C + drying in air for 8 days (23°C; RH = 50%)	▲ **cleaner, smoother fibre surface** with removal of weakly bonded components ▼ – 14 % fibre failure stress, increase in **fibre peeling** failures (weak cohesion between primary cell walls)	▲ + 15 % interfacial shear strength (IFSS) and + 30 % friction stress with **PLA** matrix	Le Duigou *et al.* (2012) [110]
	72h at 23°C + drying 24h at 40°C	▲ **cleaner surface**, **better separation of fibres**, removal of some pectins and non-cellulosic polysaccharides, **+ 20.5 % fibre Young's modulus** ▼ hydrolysing pectin chains with **boiling water (drastic conditions)**		Bourmaud *et al.* (2010) [144]
NaOH / Mercerization	dipping in NaOH solution of different concentrations (1,2 or 3 %) 20min at room temp. + washing in cold water and then in acidified water (20 drops HCl 0.1 M in 1L water) to remove remaining NaOH + washing in cold water + drying 8h at 80°C		▲ Flexural properties of flax/**epoxy** composites: + 30 % longitudinal strength and stiffness (3 % NaOH); + 150 % and + 510 % resp. transverse strength and stiffness (1 % NaOH)	Van de Weyenberg *et al.* (2003) [142]
	3 fresh water washes + drying 48h at room temp. + 5 wt% NaOH solution for 30min + 10 fresh water washes and 3 distilled water washes (to remove remaining NaOH) + drying 24h at 80°C	▲ **cleaner and rougher fibre surface**, remove of surface impurities (waxes and oils) + some hemicellulose, pectin and lignin ▼ **– 19 % and – 16 %** of respectively tensile failure stress and Young's modulus of yarn	▲ Tensile properties of flax/**epoxy** composites: + 24 % strength and + 12 % Young's modulus	Yan *et al.* (2012) [145]
	Immersion in NaOH (10g/L)/ethanol solution at 78°C for 2h + rinsing by absolute ethanol and drying at 20°C	▲ Best results with the **combination of NaOH + acetic anhydride** with + 13 % of IFSS with polyester resin ▼ visible orientation of microfibrils on fibre surface inducing the **attack of primary cell walls**	▼ – 56 % of IFSS with polyester resin; slight decrease of the work of adhesion	Baley *et al.* (2006) [120]
	2 g/kg of flax of NaOH (purity ≥ 98%) in a 5L round bottomed flask for 1 hour at boiling temperature	▲ **High extraction yield**: 8.4 % of non-cellulosic components removed from fabric with 36.1 %, 53.1 % and 47.7 % of respectively extracted hemicellulose, lignin and lipophilic extractives amounts; ▼ **limited selectivity** with contrasted behaviour; **– 38 %** of longitudinal and transverse fibre modulus	▲ **High dispersion of yarns** in epoxy matrix ▼ Transverse tensile properties of epoxy/flax composite : – 5 % Young's modulus and – 26 % ultimate stress	Acera Fernández *et al.* (2016) [49] *See also* Lacasse and Baumann (2012) [146]

I. 2. 5. 2 Natural fibre functionalization

The functionalization of natural fibres is often performed after pre-treatments and achieves a chemical and/or physical coupling between fibres (-OH, -COOH or phenolic groups, *see paragraph* ***I. 2. 1. 2. 2***) and the considered matrix with grafted polymers and/or reactive molecules on the surface of fibres.

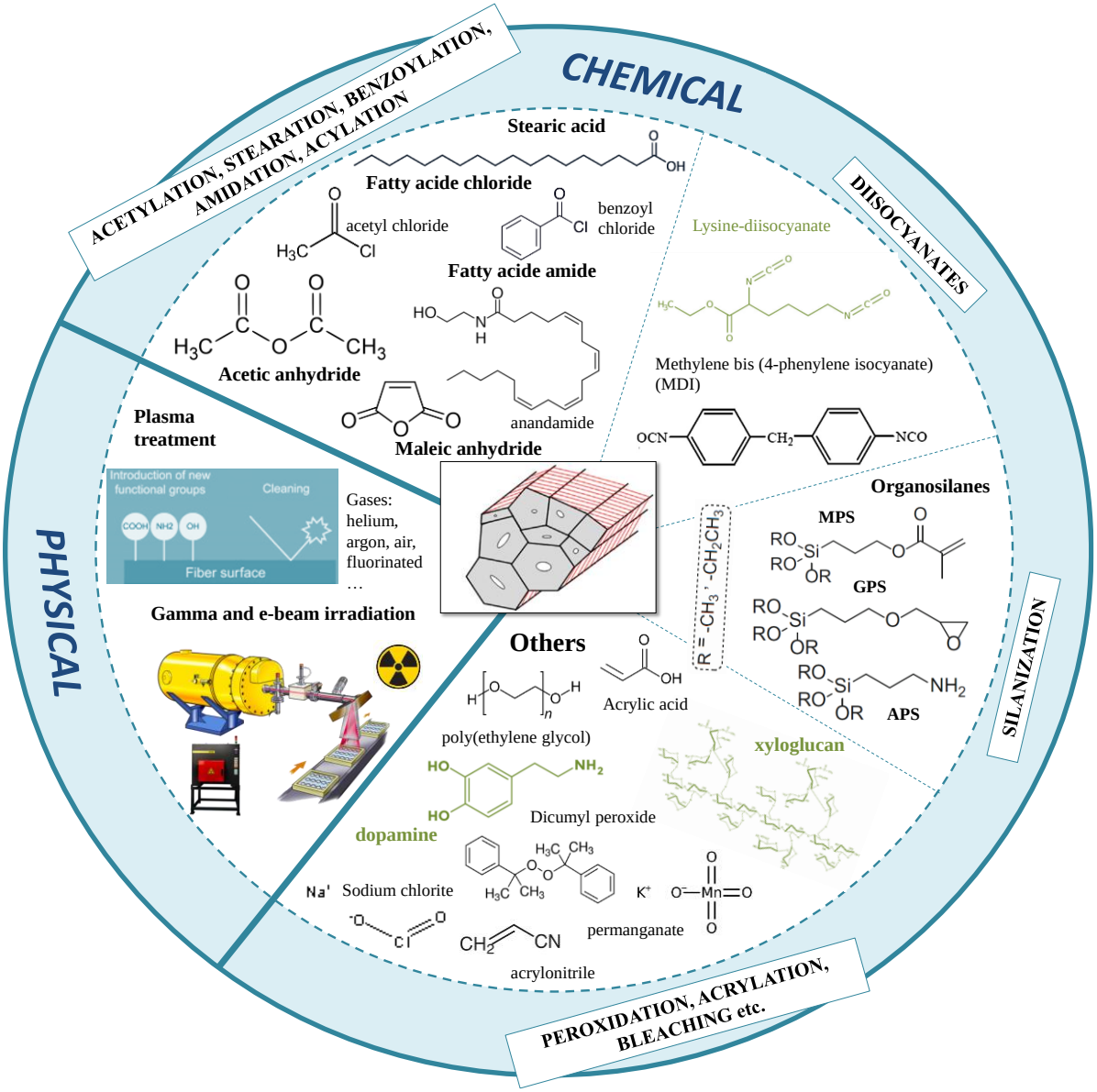

Figure I-33: Various physical treatment technologies and functionalizing molecules and polymers used in chemical modifications of natural fibres in biocomposite materials ([119], [147]–[152]). This schematic is not exhaustive. Green colored molecules/polymers induce "green chemistry".

The functionalizing molecules are selected for their good affinity and/or reactivity towards the matrix and the surface chemistry of considered natural fibres, i.e. fatty acids, anhydride

acids, diisocyanates, organosilanes etc. [153]–[155]. Moreover, physical treatments such as plasma and irradiation treatments have been also investigated in the literature to confer a better interfacial adhesion and compatibilization fibre / matrix inside natural fibre reinforced biocomposites. All these chemical and physical treatments are illustrated in **Figure I-33**.

This modification of the surface chemistry of fibres occurs before biocomposite processing or during their manufacturing with the incorporation of additives such as coupling agents within the matrix. The example of maleic anhydride grafted polypropylene (MAPP) or polyethylene (MAPE) are coupling agents used in polyolefin matrices by reactive extrusion process for the preparation of natural fibre based composites [138], [147], [156]. The coupling agent chains are able to migrate at the fibre / matrix interface during compounding to create a covalent bond with hydroxyl groups of natural fibres. Moreover, these chains are entangled in the polyolefin matrix enhancing the compatibilization.

I. 2. 5. 3 Thermal treatments

Thermal treatments have also been investigated to play on the physico-chemical and morphological properties of flax fibres with a potential increase of composite performances.

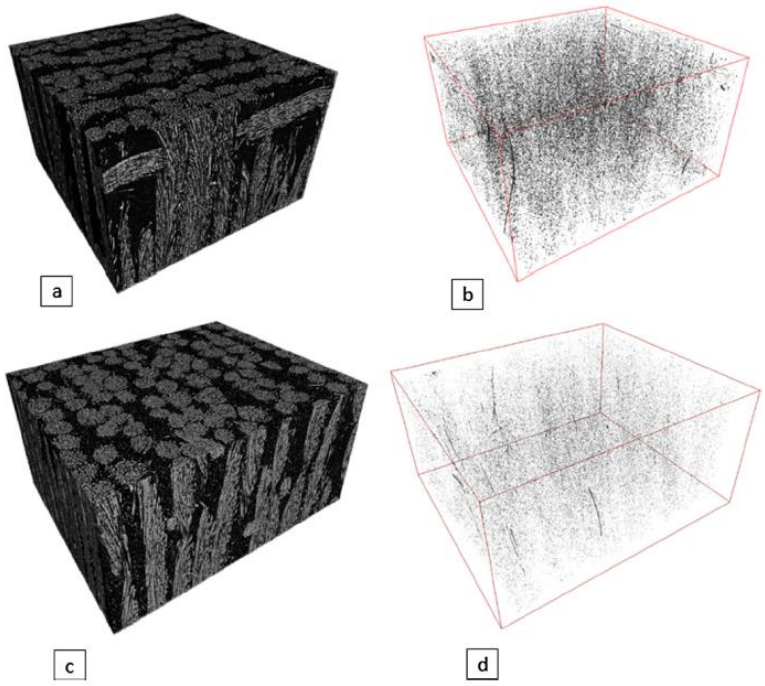

Figure I-34: Three dimensional reconstructions and 3D visualisations of micropores for (a and b) untreated and (c and d) thermal treated quasi-UD flax reinforced composites (reprinted with permission from Pucci *et al.* 2017 [109]).

High temperatures applied to natural fibres provide an elimination of hygroscopic or weakly bonded to the cell wall components. Pucci *et al.* (2017) reported a better dimensional stability of thermal treated flax fibres (220°C, 2 hours) with more hydrophobic fibres and less sensitive to liquid sorption and swelling, conducting to less voids within the quasi-UD flax / epoxy composite [109] (**Figure I-34**).

However, the same team highlighted that this thermal treatment decreased drastically the tensile strength of elementary fibres from 1009 MPa to 447 MPa, and the overall surface energy of fibres from 64.0 mN/m to 56.6 mN.m, decreasing the final mechanical properties of the composite [109], [157]. Gourier *et al.* (2014) reported also the negative effect of thermal cycles on flax fibre mechanical properties, especially on fibre tensile strength [158].

To summarize, natural fibre pre-treatments and functionalization give good results for most of the scientific papers with higher mechanical interlocking, higher interfacial properties and wetting between fibres and matrix and higher mechanical properties for biocomposites. However, they both show some limitations such as the decrease of the fibre structure and properties. Advantages and limitations of these natural fibre modifications are detailed in **Table I-7**.

Table I-7: Advantages and limitations observed in pre-treatments and chemical/physical functionalization strategies for the modification of natural fibre surfaces applied to composite application.

	Advantages	**Limitations**
Pre-treatments	• Individualization of fibre bundles into elementary fibres: higher **L/d** and **specific surface area** • **Removal** of weakly bonded intercellular components: higher surface roughness and cleanness • → better **mechanical interlocking + dispersion state** → increase of **interfacial adhesion** between fibres and matrix and so **mechanical properties** of natural fibre reinforced composites → increase of **surface reactivity** of fibres prior their functionalization	**Degradation or removal** of biopolymers constituting the cell wall; decrease sometimes of the cellulose crystallinity → decrease of the **intrinsic properties of fibres**: tensile ultimate strength and Young's modulus, toughness, defects such as dislocations, kink-bands or knees.

Chemical and Physical functionalization	• Decrease of **waxy components** amount • Decrease of **moisture absorption capacity** • **Physical treatments**: no solvents so considered as **"eco-friendly" processes; high reactivity** of fibre treated surfaces → increase of the **interfacial adhesion** with the formation of an interphase → higher **interfacial shear strength** (IFSS) → better **mechanical interlocking** (entanglements, hydrogen bonds, covalent bonds) → better **wetting** of fibres by matrix during composite processing	• Use of **strong chemical products** (bases, catalysts etc.); **eco-toxicity** for isocyanates with formation of carcinogenic substances such as heterocyclic diamines; • Necessity to control strictly the degree of substitution (DS) for fatty acid chains; • Decrease of fibre microstructure: **tensile strength** and **tenacity;** • **Possible diffusion of functionalizing agents** within the matrix (cross-linking gradient, transcrystallization, chemisorption, physisorption)

Figure I- 35 represents the variations in modulus versus variations in tensile strength of flax fibre reinforced composites and highlights limitations in the enhancement of mechanical properties with these strategies.

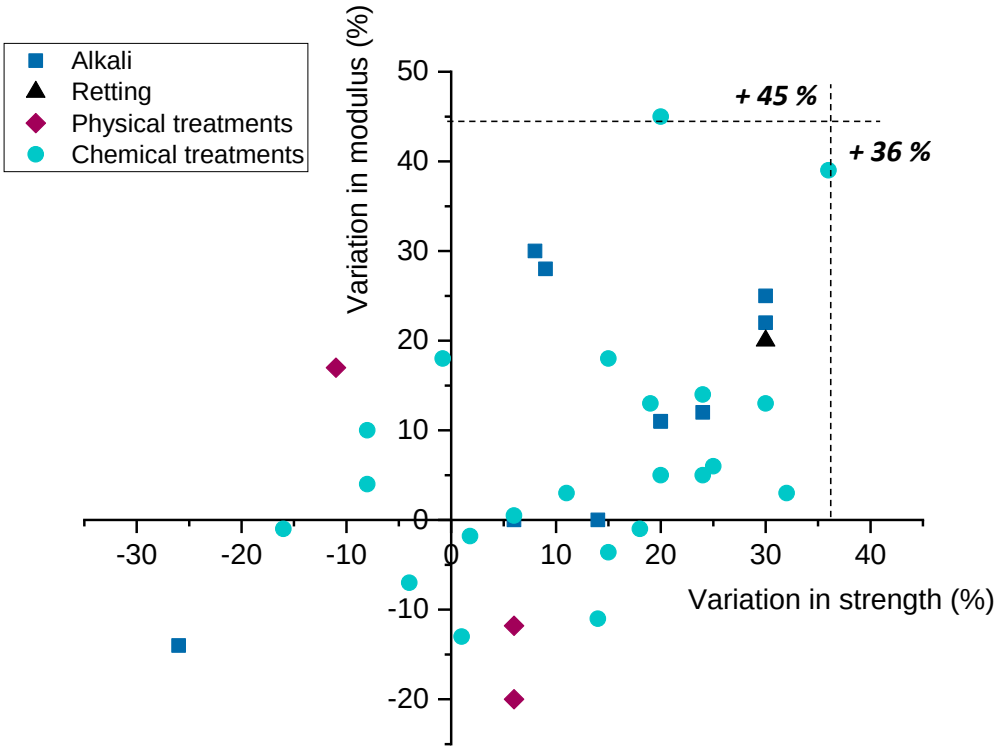

Figure I- 35: Ashby plot – variations in modulus versus variations in strength (flexural and tensile) of flax fibre reinforced composites after pre-treatments (alkali, retting) and/or functionalization (chemical, physical) of flax fibres. Non-exhaustive set of data taken from literature for different matrices (PP, PLA, epoxy resin…) with short or long flax fibres [49], [54], [140], [142], [145], [159]–[169].

It seems crucial to find an appropriate strategy of compatibilization providing a good dispersion of fibres in the polymeric matrix, and simultaneously prevent the alteration of intrinsic properties of natural fibres and also polymeric matrix.

In this way, the bio-inspired strategy consisting on the creation of hierarchically structured fibres with the nanostructuration of fibre surfaces seems to be a good path, combining the improvement of tensile strength and toughness of hierarchical fibre reinforced composites. The following section will present this concept, going from the biological materials (bone, nacre, wood) to the manufacturing of (bio)composites.

I. 3. Development of bio-inspired hierarchical fibres to tailor the fibre/matrix interphase in (bio)composites

The section I.3. is adapted from Doineau E., Cathala B., Bénézet J-C., Bras J., Le Moigne N. "Development of bio-inspired hierarchical fibres to tailor the fibre/matrix interphase in (bio)composites", Polymers, 13(5), p. 804, march 2021.

By combining biopolymers and minerals into hierarchical nanoscaled structures, nature succeeds in developing hybrid materials with amazing mechanical performances such as high toughness and strength adapted to the specific needs of biological system [170]. In this respect, complex biological architectures, displaying self-assembly processes and implying the key role of nanostructuration and nano-objects intrigue researchers and inspire them for the development of innovative engineering materials [171]–[176]. Elaboration of bio-inspired materials has already been investigated in a plethora of engineering materials, mimicking natural systems such as nacre, tooth, bone, or wood [177]–[181]. Practically, it seems that these architectures modify stress transfer mechanisms within the material and boost their strength and fracture toughness thanks to nanostructuration and the development of a "hierarchical architecture" [182]–[186]. The hierarchical architecture of a system can be defined as the deployment of structures exhibiting specific organizations at different length scales, going from the macro- to the nanoscale, and ensuring interesting properties to the entire material. This concept has notably been used in composite materials with the implementation of hierarchical fibres via the deposition of nano-objects on fibre surfaces. As an example, the whiskerization of carbon fibres with carbon nanotubes (CNTs) has been developed for the manufacturing of carbon fibre reinforced composites [187]–[189]. The developed nanostructured composites displayed enhanced mechanical properties due to increased mechanical interlocking and lower local stress concentrations at the fibre / matrix interface, hence resulting in higher strength and toughness [190]–[194].

Besides, current environmental issues push towards the implementation of eco-friendly and high-performance composite materials on the market, either hybrid, that is, synthetic/bio-based, or fully bio-based and reinforced with natural fibres and/or bio-based nano-objects [195], [196]. In this regard, the development of hierarchical fibres at the interphase zone in (bio)composites is at its very early stage and could be an interesting strategy to tackle current and future challenges raised

by the implementation of fully bio-based natural fibre reinforced biocomposites in industrial applications [197]–[199].

The aim of this section is to highlight the potential of hierarchical fibres for the modification of fibre / matrix interfacial adhesion in (bio)composite materials. First, several biological systems will be described to understand the role of nano-objects in naturally occurring hierarchical architectures. Then, current studies on hierarchical fibre reinforced composites will be discussed and divided into three main categories: (i) fully synthetic hierarchical composites, (ii) hybrid hierarchical composites either reinforced with bio-based nanoparticle modified synthetic fibres, or with synthetic or mineral nanoparticle modified natural fibres, and (iii) hierarchical biocomposites reinforced with bio-based nanoparticle modified natural fibres, the matrix being oil-based or bio-based.

I. 3. 1. Naturally occurring hierarchical structures: towards the conception of bio-inspired structures for composite materials

I. 3. 1. 1 Hierarchical structures in biological systems

The complex architectures found in natural biological systems are the result of billions of years of evolution with a continuous refining of their structure to face different challenges and adapt in an ever-changing environment. They are made of hierarchical micro/nanostructures with soft and organic interfaces (or matrices) and small stiff building blocks. In general, these hierarchical structures include nano-objects, enhancing drastically the mechanical properties, as for instance in bones [200], [201], nacre of seashells [202], [203] or wood [204].

The bone is structured by mineral crystals, i.e. hydroxyapatite nanocrystals (thickness 2-4 nm; length up to 100 nm), embedded in a (collagen-rich) protein matrix [205], [206], as illustrated in **Figure I- 36**. The specific three-dimensional network of hydroxyapatite nanocrystals embedded into collagen fibrils shows peculiar deformation mechanisms that impact positively the mechanical properties of bones [182], [183]. Indeed, collagen fibrils are assembled into collagen fibres, forming macroscopic structures such as osteons and lamellae. This hierarchical structure developed over the entire system induces crack deflection and crack bridging mechanisms with impressive properties such as self-healing and adaptation to local stress [207]–[209].

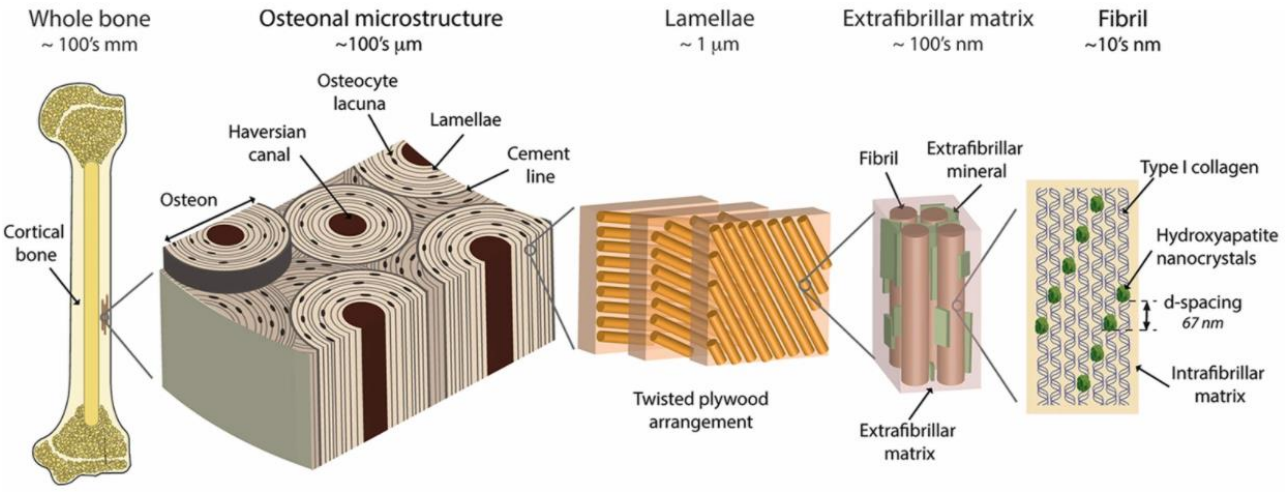

Figure I- 36: Hierarchical structure of human cortical bone with the presence of hydroxyapatite mineral nanocrystals (reprinted from Zimmermann *et al.* 2016 [210]).

The nanostructuration plays a central role in the mechanical behaviour of bones. Gao *et al.* (2003) reported that mineral nanocrystals in natural materials have an optimum size to ensure optimum fracture strength and maximum tolerance of flaws for toughness [211]. Indeed, according to the Griffith criterion, when the mineral size exceeds a critical length of about 30 nm, the fracture strength is sensitive to crack-like flaws and fails by stress concentration. As the mineral platelets size drops below this critical length, the mineral behave similarly to perfect crystals whatever the type of pre-existing flaws due to accidental soft protein matrix incorporation or defective crystal structure. Considering the bone material, the nanometric dimensions of hydroxyapatite crystals and their hierarchical structure thus appear as an optimization for better reinforcement.

Nacre can be found in the inner layer of mollusc shells (mussels, oysters, etc.) and is made of aragonite plate-like crystals (thickness 200-500 nm; length few micrometres) and a soft matrix of proteins and polysaccharides present in very small amounts [212]. These mineral platelets are structured in a three-dimensional brick wall fashion, as illustrated in **Figure I- 37 a**. The interfaces between each platelet are soft and very thin (30-40 nm) but seem to play a key role in the toughening mechanisms of mollusc shells. In fact, nacre has a fracture toughness around 3,000 times higher than its main component, the aragonite $CaCO_3$ [203], due to its high deformation capacity when submitted to stress along the direction of the platelets (**Figure I- 37 b**). A sliding of platelets relative to each other occurs under stress, this phenomenon being driven by the

nanostructured interfaces, strengthened by the nano-asperities of the platelets surface and controlled by the hydration rate [213], [214]. Moreover, the crack propagation in nacre is deflected along the interfaces (**Figure I- 37 c**), which strongly increases the fracture toughness of the material [170].

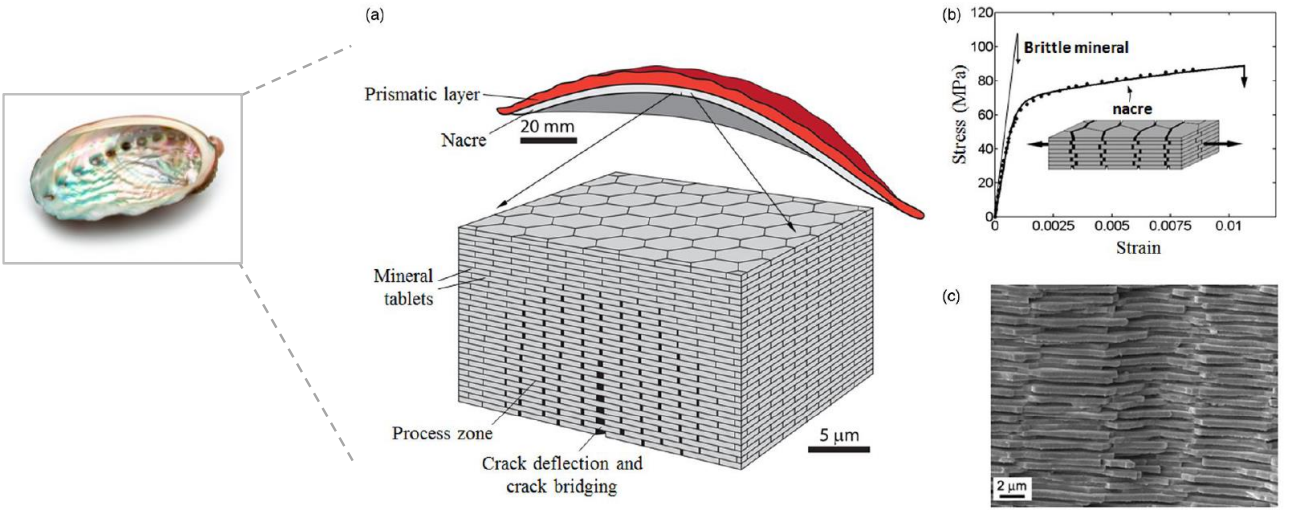

Figure I- 37: Nacre from mollusc shell (a) three-dimensional nanostructure of nacre organized in brick wall fashion, (b) tensile stress-strain curves for pure aragonite and nacre, (c) SEM image of fracture surface of nacre with crack propagation deflected along the interfaces (reprinted with permission from Barthelat *et al.* 2015 [173]).

Plant cell walls are the main components of plant stems and wood ensuring structural, conducting functions and protection against pathogens. They are complex composite materials with a hierarchical structure starting from the stem or branch down to the cellulose elementary fibrils/crystallites (thickness 3-5 nm; length 100-1000 nm) associated with various biopolymers as hemicelluloses, lignin and pectins in various amount depending on the species [63]. Müller *et al.* studied the macroscopic biological interface branch-stem of a Norway spruce in terms of microstructure, and mechanical and self-healing mechanisms [184]. As illustrated in **Figure I-38**, they observed during the bending and breakage of the branch, the occurrence of a zig-zag crack propagation path with crack bridging at the branch-stem interface. This zig-zag shape of cracks has also been observed in natural materials like nacre and bone and requires much more energy for the formation and extension of cracks [215]. This crack pattern is the consequence of the complex and optimized hierarchical interface branch-stem with multiple length scales. At the nanometric scale, the cell orientation and the microfibrillar angle (MFA) of cellulose microfibrils

within plant cell walls are perfectly adjusted in tissues of the branch and stem to ensure high flexibility and strength. Moreover, the distribution of cells appears to be adapted to the local damages that could occur at the branch-stem interface, by limiting local stress concentrations.

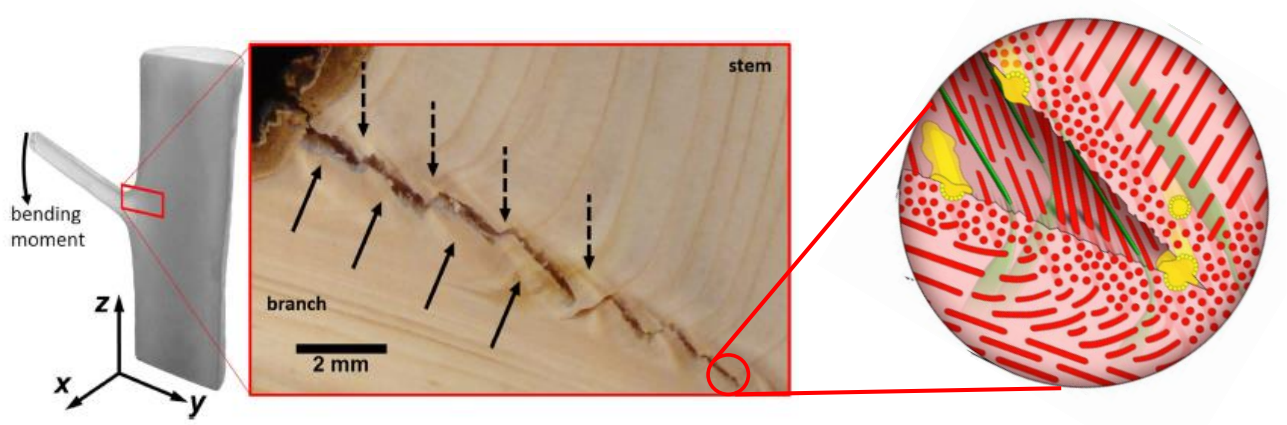

Figure I-38: Zig-zag cracking at branch-stem interface with the model (insert) of the crack propagation in the sacrificial tissue (adapted from Müller *et al*. 2015 [184]). Wood rays (green) reinforced tracheids (red) form tissue bundles responsible for crack bridging. High concentration of activated resin ducts (yellow) after the cracking ensures antimicrobial and hydrophobic protection.

The description of naturally occurring hierarchical architectures and their behaviour under stress can thus be a model for the structuration of interfaces in man-made composite materials based on hierarchical structure concepts using nano-objects. The next section will focus on the conception of hierarchical fibre reinforced composite materials implying the use of nano-objects, as observed in the biological systems presented previously. The creation of such hierarchical composites targets the enhancement of the fibre / matrix interfacial adhesion, a key parameter for stress transfer in composite materials.

I. 3. 1. 2 Towards the conception of hierarchical composite materials using nano-objects

Fibre-reinforced polymer composites are commonly used in many daily life applications and consist of at least three phases: the polymeric matrix (thermoplastic, thermoset), the reinforcing fibres (glass, carbon, natural fibres, etc.) and an interfacial zone in between. The matrix protects reinforcing fibres, transfers and achieves the distribution of loads to the fibres and among fibres [119], [187]. The mechanical properties of the composite such as strength and stiffness are primarily determined by the reinforcement characteristics (intrinsic mechanical properties, volume fraction, orientation, L/d aspect ratio), but the characteristics of the interphases also appear as a

key. Indeed, this interphase between the fibres and the matrix allows the stress transfer from the matrix to the fibre, provided that the fibre / matrix interfacial adhesion is good enough. The bonding strength at the interface largely influences the final properties of the composite, and the role of the interfacial adhesion on their structural integrity is now commonly accepted.

One of the main challenges when developing composite materials is precisely to combine strength and toughness [216]. In general, a strong fibre / matrix interfacial adhesion will achieve high strength and stiffness, while a weaker interfacial adhesion or flexible interphase could enhance toughness performance. Interestingly, structural natural materials such as bones, shells and plants seem to succeed in gathering these mechanical properties often antagonistic. It appears that the combination of soft and stiff components inside the systems, in optimized architectures and concentrations, could be the key to obtain good mechanical properties [173], [217]. Moreover, considering the three examples of biological systems described above, the presence of nano-objects within the structures seems to reinforce the most vulnerable parts of the system undergoing higher stress levels [211]. By now, if we transpose all these observations of natural materials to synthetic and man-made composite materials, it seems that the concept of hierarchical architecture appears as an attractive strategy to tailor the fibre / matrix interphase zone, and so increase the strength and toughness and hamper crack propagation within composites.

The following sections will focus on the different hierarchically nanostructured fibre reinforced composites as schematized in **Figure I-39**, the matrix being either oil-based or bio-based.

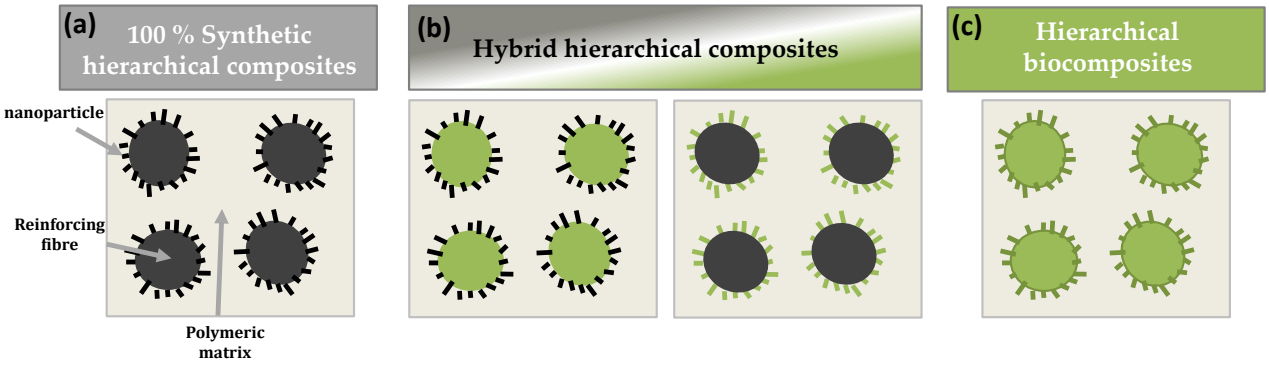

Figure I-39: Schematic of different hierarchically nanostructured fibre-based composites with (a) fully synthetic hierarchical composites, (b) hybrid hierarchical composites either reinforced with bio-based nanoparticle modified synthetic fibres, or with synthetic or mineral nanoparticle modified natural fibres; and (c) hierarchical biocomposites reinforced with bio-based nanoparticle modified natural fibres. Green colour stands for bio-based (nano-)reinforcements and black colour stands for oil-based (nano-)reinforcements.

I. 3. 2. Hierarchical interphase in fully synthetic and hybrid fibre reinforced composites

I. 3. 2. 1 Fully synthetic hierarchical fibre reinforced composites

This concept of developing hierarchically nanostructured fibres has been well studied in synthetic fibre reinforced composites, especially in carbon and glass fibre composites with the deposition of nanofillers such as nanoclays (layered silicate), carbon nanotubes (CNTs, single, double and multi-walled), graphene, zinc oxide (ZnO) nanowires [185], [187], [188], [190], [218]–[220].

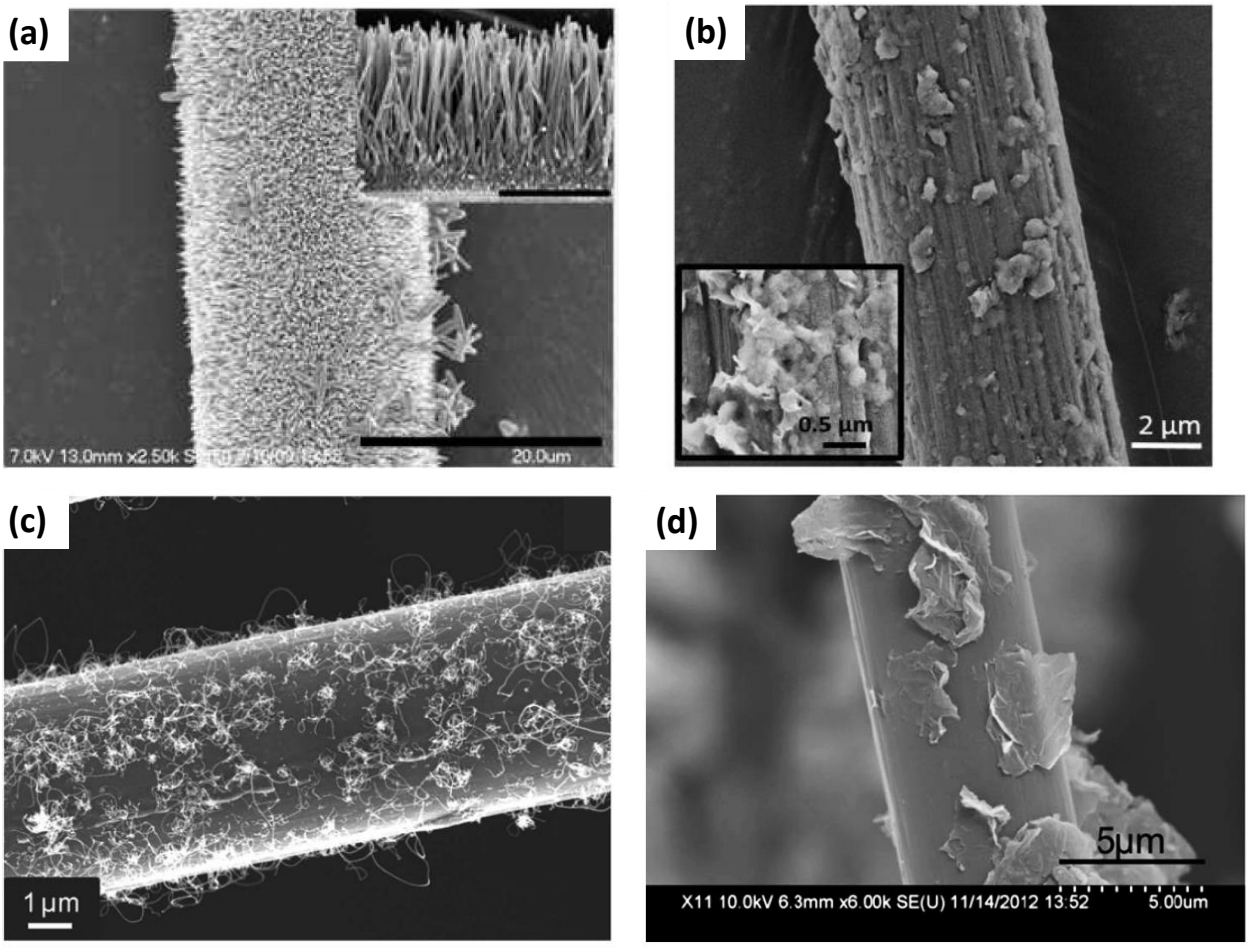

Figure I-40: SEM images of hierarchical synthetic fibres (a) aligned ZnO nanowires grown on aramid fibres (functionalized with carboxylic acid groups) ; (b) Si-nanoclays (nanoclays functionalized with APTES) grafted on N-CF (Carbon Fibre modified with GTMAC) ; (c) growth of CNTs on oxidized IM7 carbon fibres using CVD method; (d) graphene nanosheets deposited on carbon fibre at a content of 1wt% (reprinted with permission from Ehlert *et al.* 2009 [221], Zabihi *et al.* 2017 [218], Qian *et al.* 2010 [222] and Chen *et al.* 2015 [191]).

The anchoring of carbon nanofillers on carbon fibre surface can be achieved by two main pathways [187], [188]: (i) chemical reaction between nanofillers and fibres (sizing, electrospraying, electrostatic and electrophoretic deposition, chemical grafting,…) [223], [224] or (ii) direct growth of nanofillers on fibre surface also called "whiskerization" with various Chemical Vapour Deposition (CVD) methods (thermal, injection,…) [225]. Besides, ZnO nanowires were grown on the surface of aramid and carbon fibres thanks to the strong interactions between ZnO and carboxylic acid functional groups added on fibre surfaces [185], [186], [221]. Some examples of such synthetic hierarchical fibres are presented in **Figure I-40**.

First, the creation of hierarchical fibres by the growth or deposition/grafting of nanofillers at their surface induces modifications in the fibre surface topography. Zabihi *et al.* (2017) studied the grafting of (3-aminopropyl)triethoxysilane (APTES) functionalized nanoclays on glycidyltrimethylammonium chloride (GTMAC) modified carbon fibres [218]. They obtained hierarchical carbon fibres, as shown in **Figure I-40 b**, with increased surface root mean square roughness from ~64 nm to ~103 nm as measured by atomic force microscopy (AFM) on 1 x 1 µm area, due to the pits and debris on the surface. Moreover, the specific surface area measured by Inverse Gas Chromatography (IGC) increased by 5 % and the coefficient of friction by 11 %. Qian *et al.* (2010) also observed an enhancement of the nitrogen BET surface area of the fibres, from 0.71 m^2/g for oxidised IM7 carbon fibres to 1.71 m^2/g after CNT grafting (**Figure I-40 c**) [222]. Fibre surface roughness was qualitatively increased in the work of Hu *et al.* (2019) studying the spray coating of CNTs on carbon fibres (**Figure I-41 a**) for their incorporation in high-density polyethylene (HDPE) composites [226]. This change of fibre surface topography greatly enhanced the mechanical interlocking at the fibre / matrix interface, as shown on SEM images of fracture surfaces (**Figure I-41 c**). Indeed, the presence of CNTs coated on the surface of carbon fibres (**Figure I-41 c**) seems to increase the interfacial bonding between the HDPE matrix and the fibres, and also decrease voids in between, compared to pristine carbon fibres (**Figure I-41 b**).

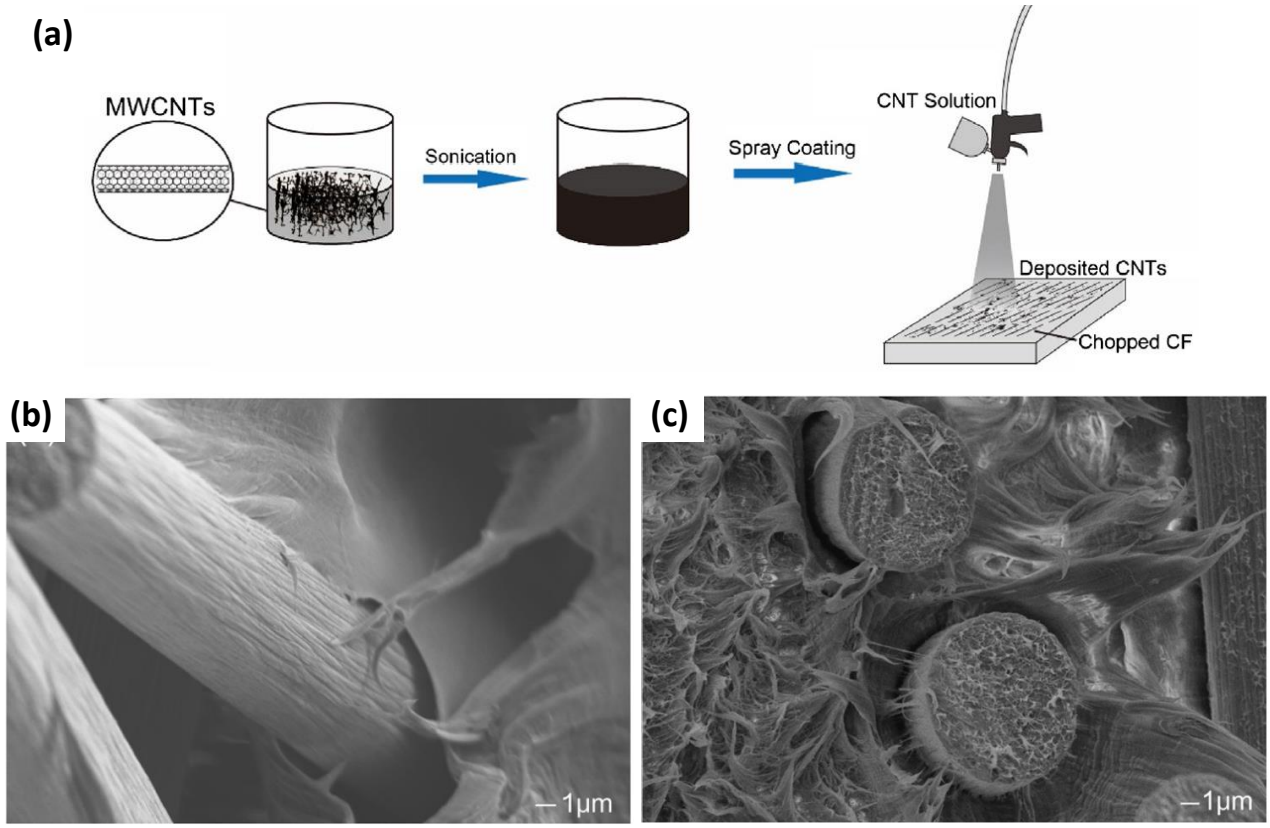

Figure I-41: (a) schematic for the spraying coating of CNT onto carbon fibres, Fracture surfaces for (b) pristine carbon fibre/HDPE composites and (c) CNT coated carbon fibre/HDPE composites (reprinted with permission from Hu *et al.* 2019 [226]).

The deposition of nano-objects on fibre surfaces can also modify their wettability, and hence ease their processing in composite materials. Zabihi *et al.* observed a better wettability towards epoxy resin for carbon fibres modified with APTES functionalized nanoclays. Indeed, contact angles between epoxy and carbon fibres measured by the drop-on-fibre technique decreased from ~42° to ~25° with functionalized nanoclays [218]. Using the same technique, Qian *et al.* found a similar trend with a decrease of the contact angle with poly(methyl methacrylate) (PMMA) matrix from 27.4° to 21.6° after the growth of CNTs on carbon fibre surfaces, indicating a better wettability of CNTs-carbon fibres towards the PMMA matrix [222].

The enhancement of the interfacial adhesion related to the presence of nano-objects on fibre surfaces can be determined by measuring the interfacial shear strength (IFSS) via different techniques. Single fibre fragmentation tests (SFFT) were conducted on hierarchically nanostrctured carbon fibre / PMMA composites [222]. A positive impact of the CNTs deposition onto carbon fibres was highlighted with an increase of the IFSS from 12.5 MPa ± 0.2 to 15.8 MPa ± 0.4 compared

to pristine carbon fibres. However, it should be noticed that the strength of CNTs modified carbon fibres dropped by ~ 15-17 %, probably due, according to the authors, to the CVD reaction temperature of 750°C used for CNTs deposition inducing the dissolution of iron catalyst in carbon fibres and lowering their mechanical properties [222]. On the other hand, Ehlert and Sodano (2009) measured an IFSS improvement of 51 % by SFFT, thanks to the functionalization o aramid fibres with ZNO nanowires imaged in **Figure I-40 a,** compared to the aramid fibre/epoxy composite, without any degradation of the fibre tensile strength [221]. Finally, the deposition of nanoclays on carbon fibres also increased by 32 % the IFSS with epoxy matrix [218]. Note that nanoclays were chemically functionalized by APTES, ensuring better chemical compatibility between the modified fibres and the matrix.

Besides, it is important to point out that the deposition of nano-objects on fibre surfaces is likely to increase the local modulus of interphase regions and thus modify the load transfer from the matrix to the fibres and among fibres within composite structure. Chen *et al.* (2015) studied the deposition of graphene nanosheets on carbon fibres by liquid phase deposition (**Figure I-40 d**) for reinforcing epoxy based composites [191]. Based on AFM measurements in force modulation mode (**Figure I-42 a and b**), the authors evidenced a gradual variation of the relative stiffness from the matrix to the fibres thanks to the presence of graphene nanosheets on carbon fibre surfaces.

The stiffness distribution, illustrated in **Figure I-42 c**, is split in two distinct zones corresponding to the carbon fibre and the epoxy matrix. This is completely modified by the presence of graphene on fibre surfaces with the appearance of a transition phase with local stiffening (**Figure I-42 d**). This gradient interface layer of about 1.5 µm was not observed with pristine carbon fibres (**Figure I-42 e and f**). A smoother transition in the interphase region, from the macroscale (carbon fibres) down to the nanoscale (macromolecular structure of the matrix), contributes to the reduction of local stress concentrations within the composite structure, allowing much more efficient stress transfer when the composite structure is under load. It should be noted that such AFM measurements require a meticulous preparation of the samples with a smooth and clean surface.

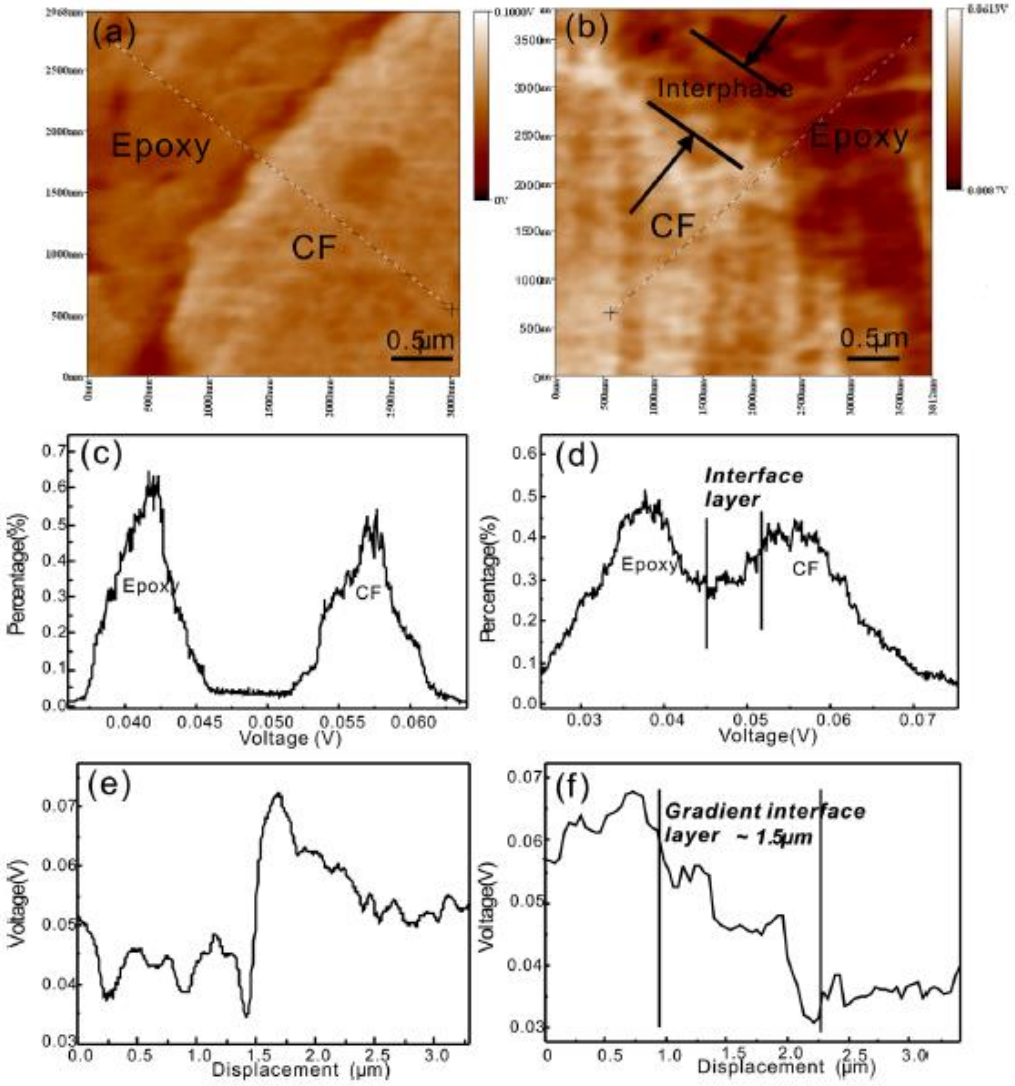

Figure I-42: (a and b) Relative stiffness in the interphase region obtained by force modulation AFM, (c and d) probability histograms of relative stiffness and (e and f) stiffness change tendency with the appearance of a gradient interface layer between carbon fibres and epoxy resin for hierarchical carbon fibres modified with 1wt% graphene nanosheets (d and f) (reprinted with permission from Chen *et al.* 2015 [191]).

Finally, as observed in biological systems, nanoparticles can hinder crack propagation within the composite structure, which then follow a zig-zag path preferentially at interfaces hence inducing crack deflections [188]. In this regard, Zabihi *et al.* [218] observed that the deposition of nanoclays on carbon fibres favoured the deviation of cracks at the fibre / matrix interfaces. Indeed, failure surfaces revealed the presence of big debris of epoxy resin attached to the hierarchical carbon fibres modified with nanoclays, indicating a more tortuous crack propagation favouring energy dissipation during composite failure. This change in failure mechanism enhanced fracture toughness of composite materials.

The hierarchical structuration of fibres can thus modify their surface topography and wettability towards polymeric matrices, and is likely to enhance interfacial adhesion, stress transfer and distribution within the composite structure while also modifying failure mechanisms. As a result, increased strength and fracture toughness can be achieved. Based on this concept, several research works focused on the development of hybrid hierarchical composites (**Figure I-39 b**) reinforced with either synthetic or natural fibres modified by synthetic/mineral nanoparticles such as ZnO, CNTs, or bio-based nanoparticles such as nanocelluloses (cellulose nanocrystals, bacterial cellulose).

I. 3. 2. 2 Hybrid hierarchical fibre reinforced composites

Idumah and Hassan (2016) published a review on the development of hybrid assemblies in polymeric nano-biocomposites [195]. The reviewed works were mainly focused on hybrid composite systems incorporating nanofillers within the bulk of the polymer matrix [227]–[229], and only few examples dealt with the implementation of hierarchical fibres to tailor the interphase in composites. This section will be focused on the development of hierarchical composites modified by nanoparticles located on fibre surfaces, hence following the concept of composites reinforced with hierarchical fibres.

- **Hierarchical natural fibres modified by synthetic/mineral nanoparticles**

Different systems of synthetic or mineral nanoparticles deposited on natural fibres were developed in the literature, primarily to enhance the mechanical properties of composites. The morphologies of some of these hierarchical natural fibres are illustrated **Figure I-43.**

Han *et al.* (2012) studied the coating of kenaf fibre bundles by exfoliated graphite nanoplatelets (xGnP) to reinforce poly (lactic acid) (PLA) based composites [230]. This coating was achieved by simple physical adsorption into acetone solvent with no chemical bonding between xGnP and kenaf bundles (**Figure I-43 a**). The authors tested different amounts of xGnP (0, 1, 3 and 5 wt%) dispersed in solution and observed, via thermogravimetric analysis, a saturation effect (no data values) of coated xGnP on fibres, inducing the dispersion of the xGnP in excess within the PLA matrix during the compounding process. A decrease of the composite flexural strength was observed with the addition of xGnP, suggesting a weaker interface in the xGnP kenaf fibres / PLA

composite. The authors explained this result by the hydrophobic character of xGnP nanoparticles, hence less compatible with the more hydrophilic PLA matrix, implying a decrease of the interfacial adhesion. However, still according to the authors, xGnP deposited on kenaf fibre surfaces could provide better fibre dispersion within PLA by reducing attractive interactions among kenaf fibres. Besides, the flexural modulus of the composite was increased by more than 165 % for PLA composite reinforced with 40 wt% kenaf fibres modified with 5 wt% of xGnP. The authors explained this result by the synergistic effect of both reinforcements (kenaf fibres and xGnP). Indeed, they measured an enhancement of PLA modulus by ~25 % with the addition of 5 wt% xGnP and by ~110 % with the addition of 40 wt% kenaf fibres.

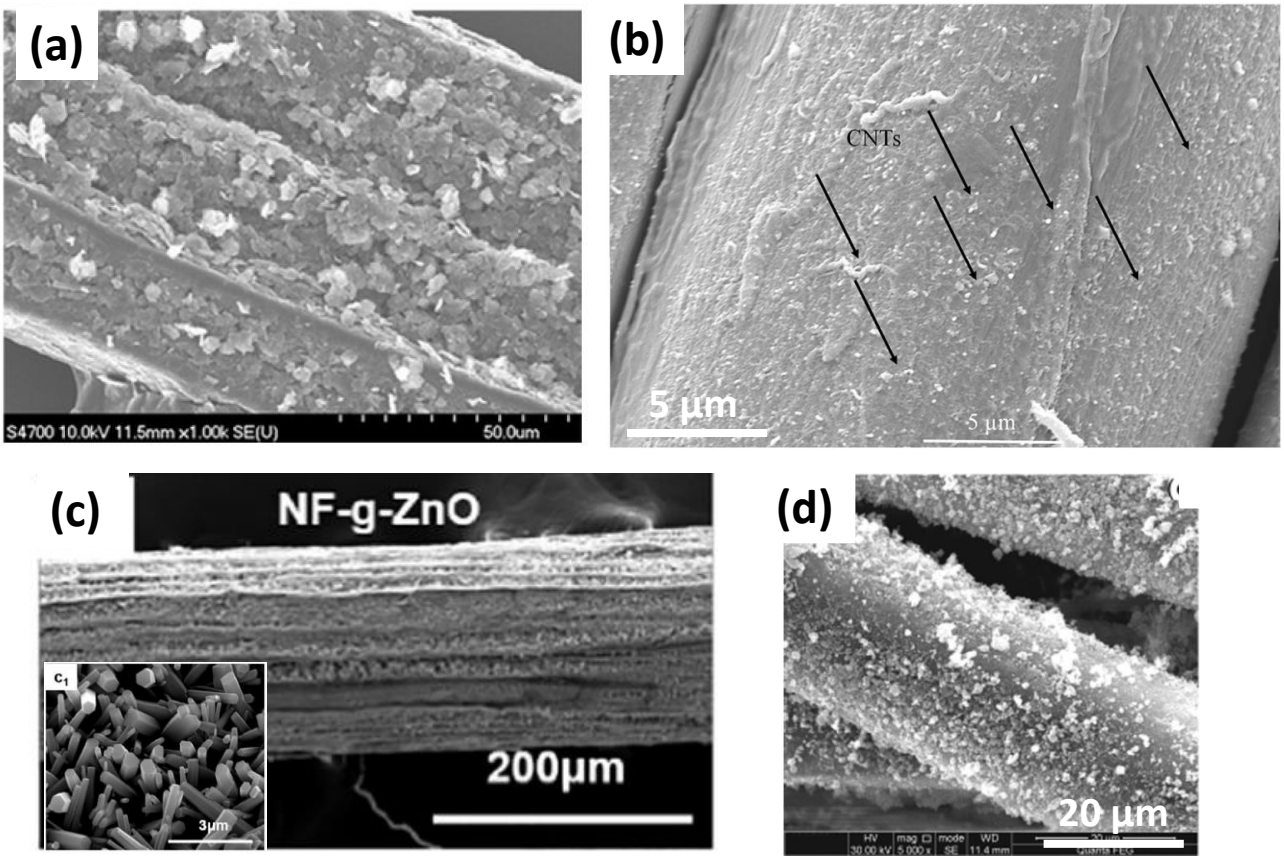

Figure I-43: SEM images of hierarchical natural fibres (a) 5 wt% of graphite nanoplatelets coated on kenaf fibres, (b) 1 wt% carboxyl-functionalized CNTs (COOH-CNTs) coated on flax fibre yarns, (c) laterally-grown ZnO nanowires on sisal fibres, (d) 2.34 wt% grafted nano-TiO_2 on flax fibres of yarns (reprinted with permission from Han *et al.* 2012 [230], Li *et al.* 2015 [231], Yang *et al.* 2020 [232] and Wang *et al.* 2015 [233]).

Li *et al.* (2015) studied the coating of carboxyl-functionalized CNTs (COOH-CNTs) on the surface of flax yarns by the spray-drying process (0.5, 1, and 2 wt% COOH-CNTs suspension concentrations; drying 120°C for 8h) and its effect on mechanical properties of flax fibre reinforced

epoxy composites [231]. The flax yarn coated with 1 wt% COOH-CNTs (**Figure I-43 b**) shows uniformly dispersed and randomly oriented COOH-CNTs on the fibre surfaces, linked by hydrogen bonds with available hydroxyl groups of flax fibres. They observed an increase of the IFSS between flax yarns and epoxy resin by 26 % thanks to the coating of 1 wt% COOH-CNTs on fibres. The interlaminar shear strength (ILSS) of the prepared composites was also increased by 20 % for the coating of 1wt% COOH-CNT. The complex interfacial region, illustrated **Figure I-44 a**, shows COOH-CNT coated on flax yarns by hydrogen bonds but also COOH-CNT located between elementary fibres inside the yarn. According to the authors, several types of interfaces must be considered in COOH-CNTs-coated flax yarn / epoxy composites such as fibre/matrix interfaces but also those between cell walls within elementary flax fibres. **Figure I-44 b** illustrates the interlocking mechanism with the epoxy resin brought by the presence of COOH-CNTs coated on flax fibres, which induces an enhancement of the load transfer in the interphase zone.

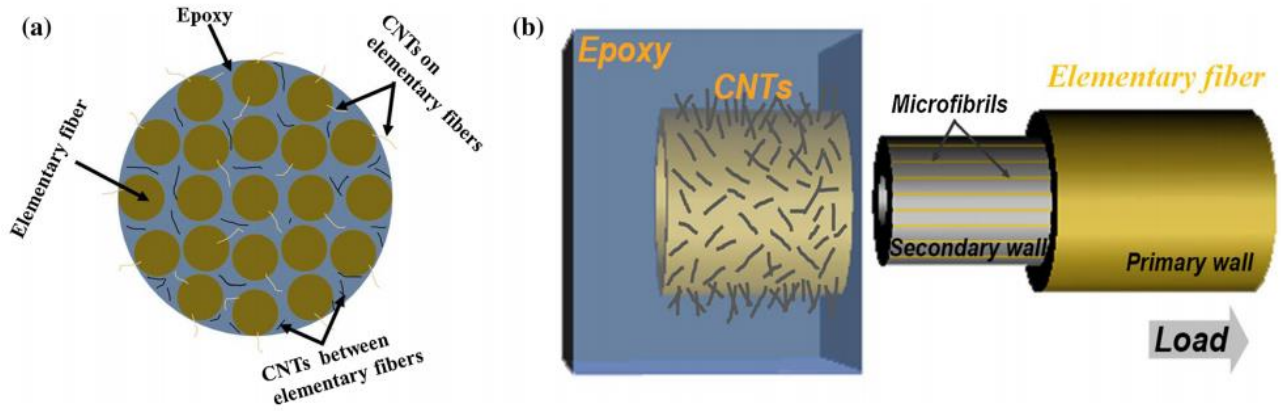

Figure I-44: (a) Distribution of CNTs in flax yarn reinforced epoxy composites and (b) interlocking mechanism and failure process of composites (reprinted with permission from Li *et al.* 2015 [231]).

The deposition or growth of ZnO nanowires on natural fibres has been investigated in some studies. Yang *et al.* (2020) modified sisal fibres with laterally-grown ZnO nanowires to enhance the interface in poly (lactic acid) (PLA) / sisal biocomposites [232]. The deposition method was based on a two-step hydrothermal method with (i) dip-coating or immersion of sisal fibres in a seed suspension of ZnO colloidal particles and (ii) growth of unidirectional ZnO crystals from the seeded surface of sisal fibres (**Figure I-43 c**). The estimated amounts of coated ZnO nanowires on sisal fibres were 1.8 wt%, 8.4 wt% and 16.7 wt% for respectively 1, 2 and 6 dip-coating cycles. The ZnO nanowires modified sisal fibres provided excellent interfacial adhesion with the PLA

matrix, attested by an increase of IFSS and debonding energy of 157 % and 400 %, respectively, for the PLA / sisal fibre modified with 6 dip-coating cycles as compared to the PLA / pristine sisal fibre biocomposites. This hierarchical structure at the surface of sisal fibres improved the mechanical interlocking fibre / matrix, suggesting a more efficient load transfer at the interface. As shown in **Figure I-45**, the authors modelled the stress distribution along the fibre / matrix interface during a single-fibre pull-out test with or without ZnO nanowires on sisal fibres.

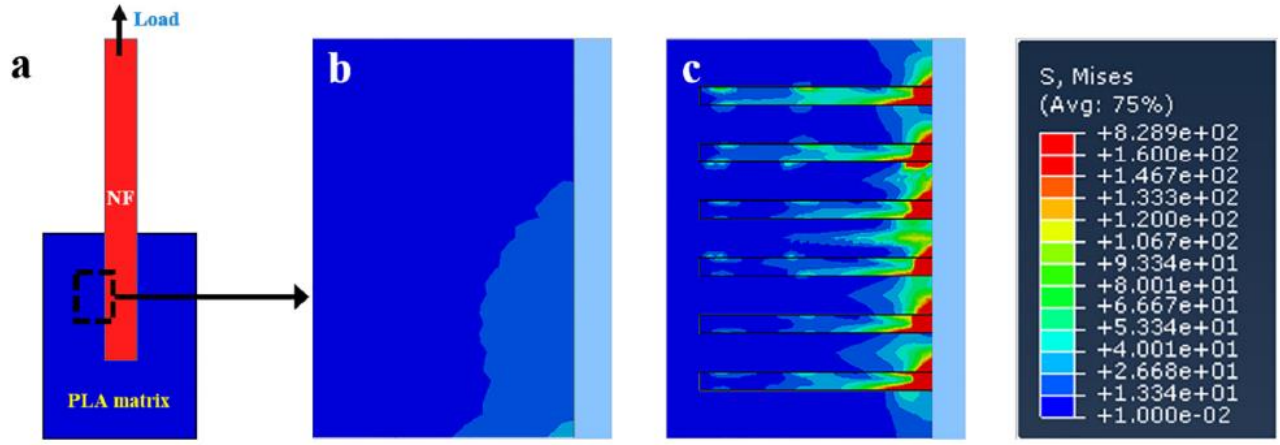

Figure I-45: schematic illustration of the single-fibre pull-out test (a) with the stress distribution analysed during the test of (b) PLA / pristine sisal fibre and (c) PLA / ZnO-modified sisal fibre (reprinted from Yang *et al.* 2020 [232]).

The stress generated at the interface was small and only a part of the interface worked efficiently because of the weak interfacial cohesion between pristine sisal fibre and PLA matrix (**Figure I-45 b**). In contrast, the laterally-grown ZnO nanowires on sisal fibres contributed to the anchoring of nanowires in the PLA matrix with a high mechanical interlocking. Consequently, ZnO coated sisal fibres resulted in enhanced interfacial adhesion with a more efficient transfer of loads within the composite (**Figure I-45 c**).

Wang *et al.* (2015) modified flax fibre yarns by the grafting of nano-TiO_2 particles (**Figure I-43 d**) and studied the effects on tensile and bonding properties of elementary fibres and unidirectional fabric reinforced epoxy composite plates [233]. They cleaned (ultrasonic bath 80W, 20°C, 6h) and dried (20°C, 24h) flax fibres before their dipping in nano-TiO_2/KH560 during 15min under sonication and then washed grafted fibres with ethanol and distilled water for 1h. They also performed NaOH and silane coupling agent treatments to compare different types of flax fibre modifications. They tested different suspension concentrations and succeeded to graft from

0.89 wt% up to 7.14 wt% nano-TiO_2 on flax fibres (estimations based on XPS measurements). **Figure I-46 b** shows the presence of nano-TiO_2 particles at the surface of flax fibres compared to pristine flax fibres **Figure I-46 a**. However, nano-TiO_2 particles are not uniformly distributed on flax fibres' surfaces with the presence of aggregates (150 nm to 300 nm).

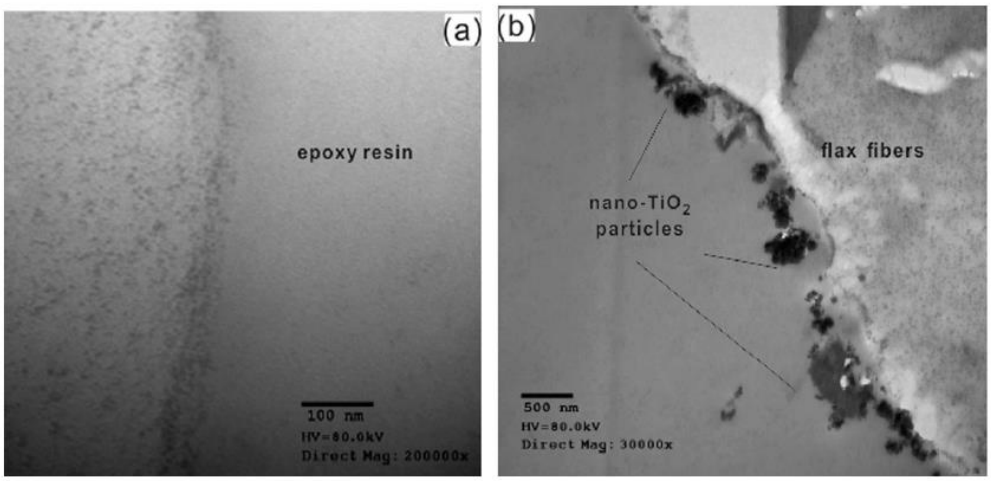

Figure I-46: Transmission electron microscopes images of flax fibres cross sections: (a) untreated flax fibres, (b) flax fibre grafted nano-TiO_2 (reprinted with permission from Wang *et al.* 2015 [233]).

The optimum nano-TiO2 grafting content on flax fabrics was 2.34 wt% and contributed to the increase of tensile strength of flax fibres by 23.1 %. Moreover, the IFSS between flax fibres and the epoxy resin was improved by 40.5 %. In comparison, the modification of flax fibres with a silane coupling agent (KH-560) showed a lower increase of the IFSS with 23.4 %. Flexural strength of flax fibre reinforced epoxy composite plates was increased by 31.4 % when grafting 2.34 wt% of nano-TiO2, by 19 % for the silane treatment and by 9.5 % for NaOH treatment, compared to the untreated flax fabric / epoxy composite. These results suggest that the creation of hierarchical flax fibres with the presence of nano-TiO_2 induces a more significant improvement of the ultimate mechanical properties of flax / epoxy composites (tensile and flexural tests) than chemical treatments such as NaOH or the functionalization with a silane coupling agent.

- **Hierarchical synthetic fibres modified by bio-based nanoparticles**

An important difference with nanocellulose extracted from lignocellulosic biomass such as CNC and CNF, *see details in section* ***I.1.5.1.***, is that Bacterial cellulose (BC) is devoid of hemicellulose and lignin. BC is produced by the bacteria *Acetobacter xylinum*, which synthetizes cellulose nanofibrils

from low molecular weight compounds (sugars, alcohol, ...) [234]. This fermentation process requires the accurate control of different parameters such as culture medium, temperature, incubation time, pH. The resulting bacterial cellulose nanofibers display a lateral dimension around 25 – 100 nm and a length of several micrometres [235]. These nanofibres display high crystallinity (up to 84 – 89 %) and Young's modulus of roughly 78 GPa [236], [237].

The following examples of hybrid hierarchically nanostructured fibre reinforced composites are composed of synthetic fibres, more especially glass fibres, coated with bio-based nanoparticles such as BC or CNC (**Figure I-47**).

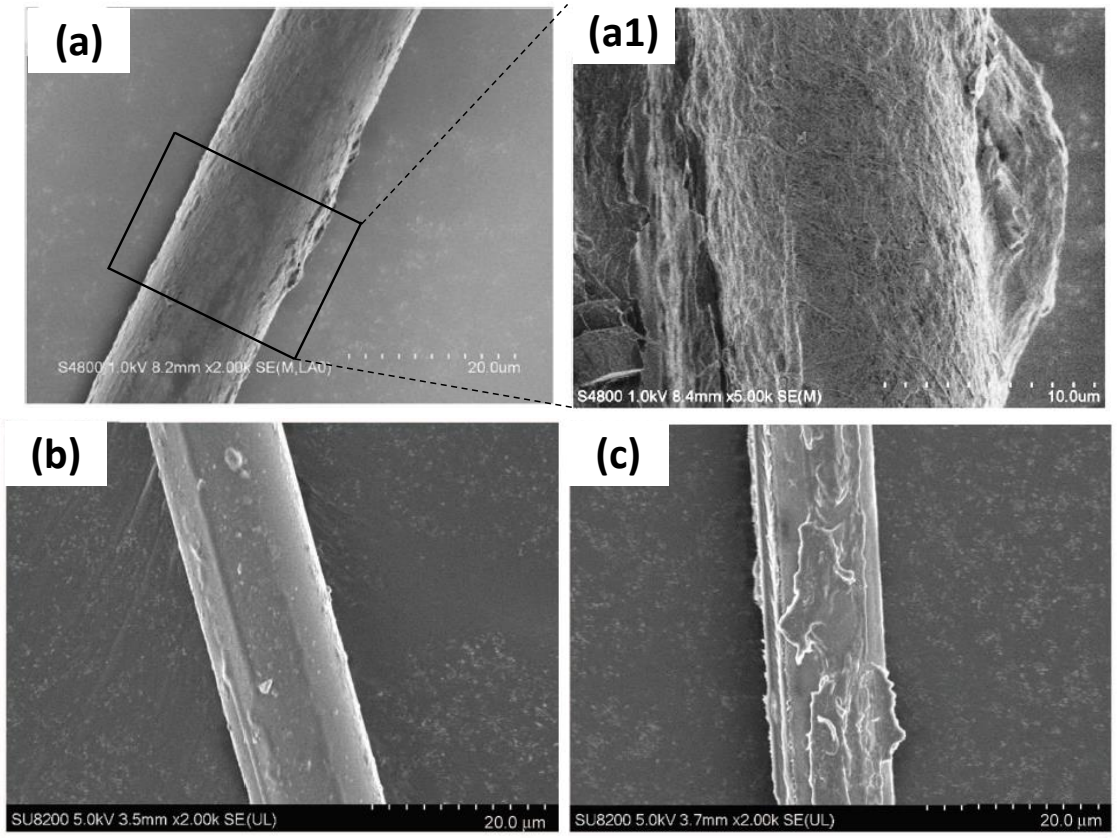

Figure I-47: SEM images of hierarchical glass fibres (a & a1) BC grown on glass fibres, (b) and (c) CNC coated glass fibres with respectively 1 wt% and 5 wt% CNC content in suspensions (reprinted with permission from Chen *et al.* 2014 [238] and Asadi *et al.* 2016 [239]).

Chen *et al.* (2014) studied the influence of the dipping time of glass fibres in the BC culture medium and the effect of heating post-treatment of BC deposited fibres on the final interfacial properties between glass fibres and epoxy resin [238]. BC was deposited on glass fibres by fermentation at 30°C for several hours in a culture medium (**Figure I-47 a and a1**). First, they

obtained by microbond test the optimum IFSS value for 1 h dipping time with an increase from 14.1 MPa ± 1.9 to 21.5 MPa ± 2.2 compared to the untreated glass fibre / epoxy system. Moreover, it appears that the heating post-treatment of BC-glass fibres at 140°C during 24 h increased slightly the IFSS by 3 %. The authors explained that this heating post-treatment could enhance adhesion between BC and glass surfaces. Indeed, they conducted XPS measurements on the surface of unheated and heat-treated BC-glass slides (140°C, 24h). The surface chemical composition of both samples was shown in high-resolution Si 2p XP spectra. After heating of BC-glass slide, Si-C bonds increased from 15.8 % to 30.4 % formed by the reaction between Si-OH of glass fibres and C-OH of BC and so contributing to better BC/glass adhesion. The optimization of treatment parameters increased the BC-glass fibre adhesion with the creation of hydrogen bonds after 1 hour dipping and led to stronger bonding between glass fibres and BC, i.e. C-Si and C-O-Si covalent bonds, after heating post-treatment at 140°C during 24 h, as illustrated in **Figure I-48**.

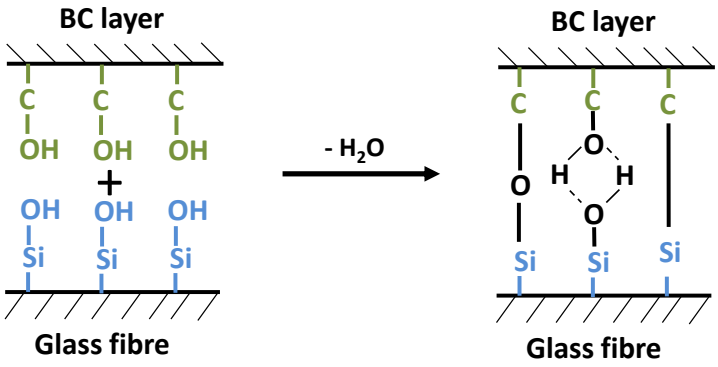

Figure I-48: schematic representation of chemical bonding between hydroxyl groups of bacterial cellulose (BC) and glass fibres and possible formation of C-Si and C-O-Si covalent bonds (adapted with permission from Chen *et al.* 2014 [238]).

Asadi *et al.* (2016) prepared short glass fibre / epoxy composites with pristine and CNC-treated glass fibres (**Figure I-47 b and c**) by the immersion/dipping of chopped glass fibre roving (around 25 mm length) in CNC aqueous suspensions between 0 and 5 wt% CNC contents [239]. First, they observed that the favourable interactions between hydroxyl groups of CNC and glass fibres promote physical adsorption at the surface of the roving but also the partial penetration of CNC within the roving, resulting in heterogeneous coating of individual glass fibres. The interfacial shear strength (IFSS) measured by SFFT showed an optimum value for 1wt% CNC in suspension with an increase of ~69 % compared to the untreated glass fibre / epoxy composite (**Figure I-49 a**). The authors assumed that too much CNC on fibre surfaces could induce slippages between CNC

layers, decreasing the load transfer efficiency across the interphase. Moreover, the composite reinforced with CNC-modified glass fibres prepared in 2 wt% suspension showed a decrease of the tensile strength of ~12 %, while the IFSS measured on the same system was higher than for pristine glass fibres. The authors attributed this antagonism to various mechanisms and in particular to the incomplete impregnation of the epoxy resin around and within the glass roving coated by a thick CNC layer, possibly resulting in the formation of voids that could decrease the composite's strength. SEM images of failure surfaces are presented **Figure I-49 b and c**. The fibre / matrix interfacial adhesion appears very weak for the untreated glass fibre / epoxy composite, with mainly interfacial debonding and fibre pull-outs, characteristic of an adhesive interfacial failure. In contrast, the presence of CNC on the surface of glass fibres results in matrix cracking and fibre breakage, and hence more cohesive interfacial failure.

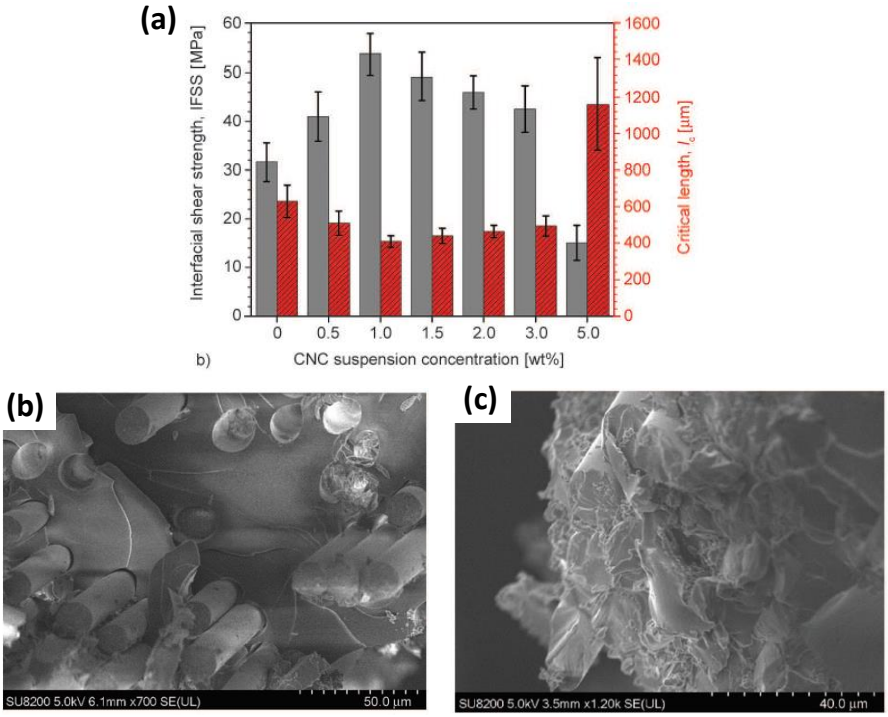

Figure I-49: (a) SFFT results with the IFSS (solid grey bars) and critical fragmentation length (striped red bars) for short glass fibres / epoxy composites as a function of CNC concentration in suspension, (b) failure surfaces observed for 30 wt% uncoated glass fibre (on the left) and 30 wt% CNC-coated glass fibre (1 wt% CNC in suspension) reinforced epoxy composites (reprinted from Asadi *et al.* 2016 [239]).

Combination of nanoparticles was also tested with the deposition of both cellulose nanocrystals and carbon nanotubes on the surface of carbon fibres, in order to enhance the interlaminar shear strength (ILSS) in composite laminates [240], [241]. In this hybrid treatment, CNCs are used as a dispersing and stabilizing agent of CNTs in water before the treatment of carbon fibres by dipping.

The results obtained concerning the mechanical properties of composites are promising with an increase of the flexural strength and the ILSS by 33 % and 35 %, respectively, when treating carbon fibres with 0.2 wt% CNC 0.2 wt% CNT in suspensions.

Most of these works on synthetic and hybrid hierarchical composites evidenced a reinforcement of the interphase zone thanks to hierarchical fibres, with improved interfacial adhesion measured by different techniques such as IFSS, ILSS or flexural tensile tests. The next challenge is to transpose this bio-inspired concept of hierarchical interphase to fully bio-based reinforcements, i.e. natural fibres modified by bio-based nanoparticles. The following section will focus on hierarchical biocomposites as schematized in **Figure I-39 c**, in particular the deposition of cellulose-based nanoparticles on various natural fibres.

All these examples on hybrid hierarchically nanostructured fibre reinforced composites highlight the challenge of depositing nano-objects that can have no physico-chemical affinities with the reinforcing fibres used. Indeed, the deposition or growth of CNT, ZnO or graphene requires in some cases very high temperatures, not compatible with natural fibres. While the preparation of hierarchical synthetic fibres such as carbon fibres is often carried out by the CVD method (750°C for 1 hour, C_2H_2 carrier gas [222]), the deposition of synthetic nano-objects for the creation of hierarchical natural fibres requires gentler techniques such as hydrothermal deposition, spray-drying or dipping in suspension. It should also be noted that the growth of synthetic nano-objects on the surface of fibres has been transposed to biobased nano-objects by the use of bacterial cellulose, growing directly on the fibres by incubation.

Most of the works on the development of synthetic and hybrid hierarchical fibre reinforced composites evidenced a reinforcement of the interphase zone thanks to hierarchical fibres, with improved interfacial adhesion measured by different techniques such as IFSS, ILSS or flexural tensile tests. The next challenge is to transpose this bio-inspired concept of hierarchical interphase to fully bio-based reinforcements, i.e. natural fibres modified by bio-based nanoparticles. The following section will focus on hierarchical biocomposites as schematized in **Figure I-39**, in particular the deposition of cellulose-based nanoparticles on various natural fibres.

I. 3. 3. Hierarchical interphase in natural fibre reinforced biocomposites

The main advantage when treating natural fibres with cellulose-based nanoparticles (i.e. BC, CNC, CNF) is their spontaneous adsorption on fibre surfaces. Indeed, they have a mutual affinity brought by hydrogen bonding and van der Waals interactions. Moreover, surface modification can be performed directly in water without the use of organic solvents or prior fibre pre-treatments that would be less eco-friendly and could induce fibre degradation [242].

I. 3. 3. 1 Hierarchical natural fibres modified by bacterial cellulose

Several works report on the deposition of BC on natural fibres to create hierarchical fibres with the aim of enhancing the fibre / matrix interface in biocomposites. For example, BC was grown on the surface of sisal and hemp fibre bundles (7 days, 30°C) for their further incorporation in bio-based matrices, i.e. PLA and cellulose acetate butyrate (CAB) [198], [243], [244]. The authors performed SEM observations of BC grafted-hemp fibres, **Figure I-50 a**, and BC grafted-sisal fibres, **Figure I-50 b**, and found that BC nanofibres were randomly oriented and covered fibre surfaces almost completely.

The biocomposite showing the most promising results was PLA / BC-grafted sisal fibres with an increase of longitudinal and transverse tensile strengths by 44 % and 68 %, respectively, compared to the untreated sisal fibre reinforced PLA biocomposite. The IFSS measurements showed a positive effect of the BC treatment on the sisal / PLA matrix interfacial adhesion with an improvement from 12.1 ± 0.5 MPa to 14.6 ± 1.2 MPa. In the case of BC modified hemp fibres, the authors observed "glued" elementary fibres forming bundles, which could hamper good impregnation with the matrix during manufacturing, and create defects and voids within the biocomposite microstructure. This is likely to be at the origin of the bad or unchanged results observed for hemp fibre reinforced biocomposites with both PLA CAB matrices. Moreover, the better mechanical properties (strength and stiffness) obtained for PLA based biocomposites compared to CAB based ones could be explained, according to the authors, by the polar functional groups of PLA likely to form hydrogen bonds with BC hydroxyl groups present at fibre surface, hence providing a better fibre / matrix interfacial adhesion.

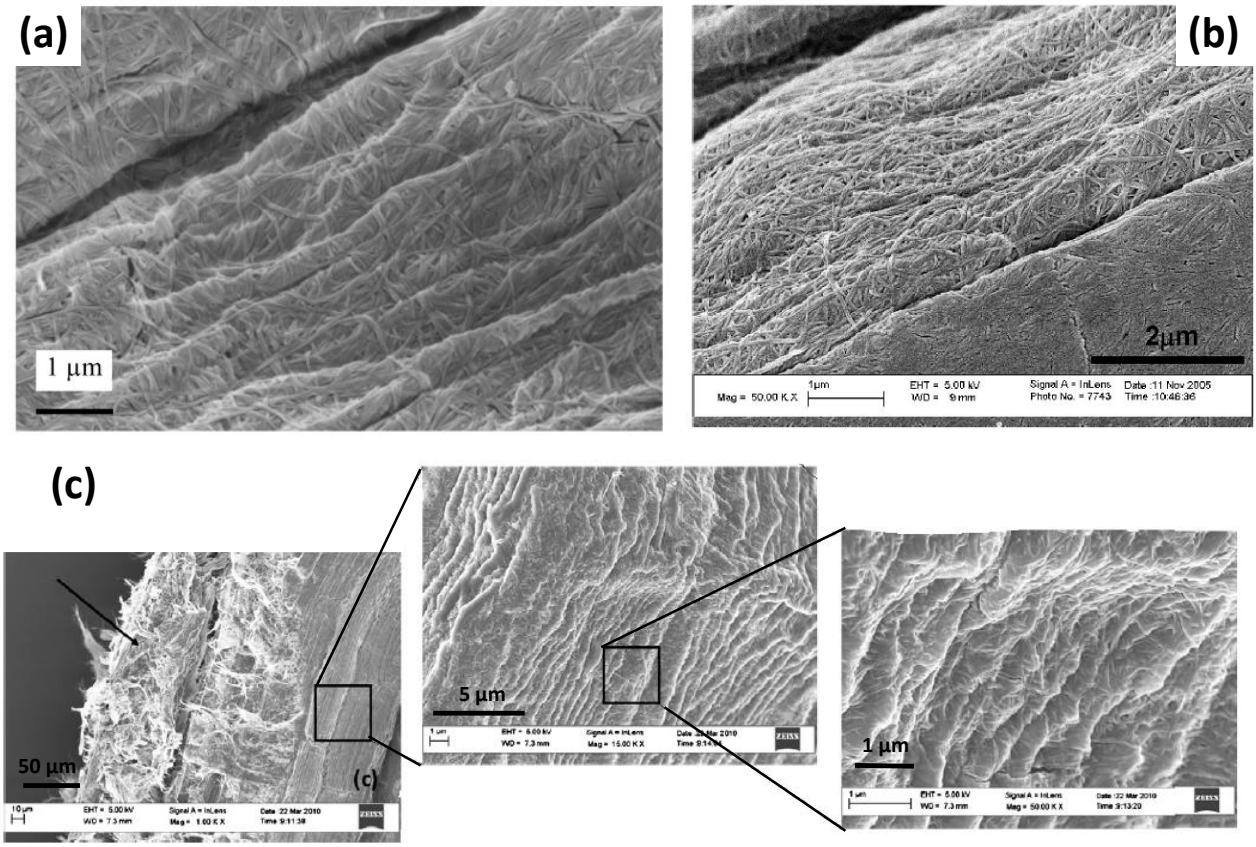

Figure I-50: SEM images of (a) hemp fibres coated by BC, (b) sisal fibres coated by BC and (c) "hairy" short sisal fibres coated by BC, (reprinted with permission from Pommet *et al.* 2008 [198] and Juntaro *et al.* 2007 [243] and Lee *et al.* 2012 [245]).

Lee *et al.* also prepared BC-coated sisal fibres by dipping the sisal fibres in an aqueous dispersion of freeze-dried BC (3 days, room temperature) [245]. Based on two different drying processes, they obtained "dense" and "hairy" BC coated sisal fibres. The resulting "hairy" BC fibres are illustrated in **Figure I-50 c** with BC nanofibres oriented perpendicular to the fibre surface. The loading content of BC on sisal fibre was around 10 ± 1 wt%. The specific surface area of sisal fibres, measured by nitrogen adsorption/desorption isotherms, was slightly increased from 0.10 m^2/g ± 0.01 to 0.77 m^2/g ± 0.03 and 0.49 m^2/g ± 0.03 for respectively "dense" and "hairy" BC coated sisal fibres. According to the authors, the lower specific surface area of "hairy" BC – sisal fibres might be due to the agglomeration of BC nanofibrils on the fibres when they are pressed between filter papers, reducing the accessible area for the nitrogen adsorption. Then, sisal fibre / PLA biocomposites were prepared with untreated and BC-coated sisal fibres but also with the dispersion of freeze-dried BC in the bulk of PLA matrix. The different BC / sisal fibres / PLA systems are shown in **Figure I-51**.

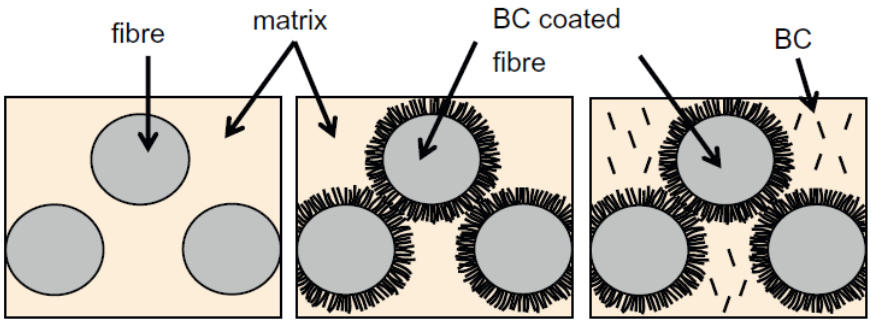

Figure I-51: Illustration of the different hierarchical sisal fibres / PLA biocomposites with or without the addition of bacterial cellulose (BC). (Left) with untreated sisal fibres; (middle) with BC coated sisal fibres and (right) with BC coated sisal fibres and BC in the matrix bulk (reprinted from Lee *et al.* 2012 [245]).

Considering the tensile performances of the different sisal fibre / PLA biocomposites, the combination of BC-coated sisal fibres with also BC dispersed in PLA and seems to give the best results whatever the drying process. Indeed, tensile tests highlighted an increase in Young's modulus and tensile strength by 27 % and 16 % respectively, for PLA / "dense" BC-coated sisal fibres and by 24 % and 18 % respectively, for PLA / "hairy" BC-coated sisal fibres, both containing BC in the PLA matrix, compared to PLA / untreated sisal fibre biocomposite without added BC. According to the authors, these results can be explained by a possible stiffening of the PLA matrix with the presence of BC and additional interactions such as hydrogen bonds and van der Waals interactions between BC dispersed in the matrix and BC coated on the surface of sisal fibres. Indeed, SEM images of fractured surfaces of biocomposites (**Figure I-52**) highlighted a more cohesive interface between sisal fibres and PLA matrix for "hairy" BC coated fibres. This was even more obvious with "hairy" BC coated fibres and BC dispersed in the matrix. Indeed, bonded PLA matrix was observed on sisal fibres (**Figure I-52 c**), hence favouring matrix and fibre breakage rather than fibre debonding.

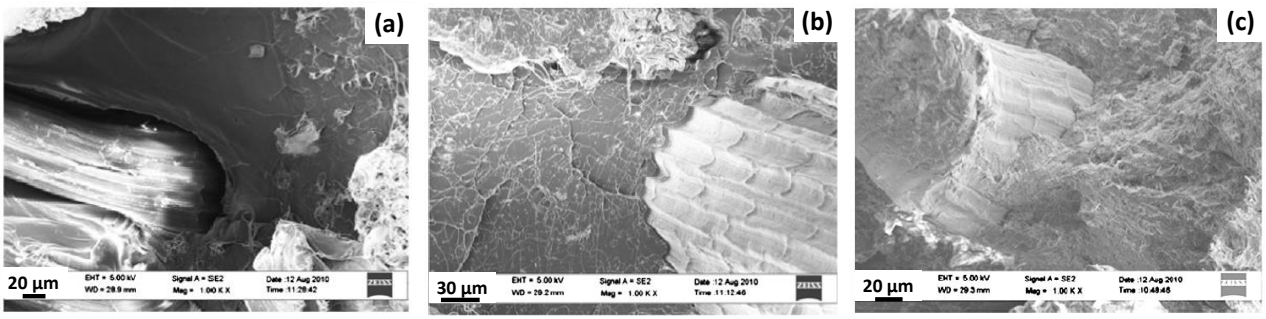

Figure I-52: Fractured surfaces of hierarchical BC / sisal fibres reinforced PLA biocomposites, (a) untreated sisal fibres, (b) "hairy" BC-coated sisal fibres and (c) "hairy" BC-coated sisal fibres with BC dispersed in PLA matrix (reprinted from Lee *et al.* 2012 [245]).

Lee *et al.* (2012) also investigated the manufacturing of a non-woven sisal preform treated with bacterial cellulose for reinforcing acrylated epoxidised soybean oil (AESO) resin [246]. Sisal fibre bundles (10 mm length) were dipped in a suspension of BC overnight and pressed to obtain the non-woven sisal preform bound by BC as illustrated in **Figure I-53 A**. The resulting sisal preform strongly increased both the tensile and flexural Young's modulus of AESO based biocomposite, by 75 % and 142 % respectively, and tensile and flexural strength by 71 % and 116 % respectively, compared to the untreated sisal preform / AESO biocomposite. Dynamic mechanical thermal analysis (DMTA) was performed on biocomposites and results are represented in **Figure I-53 B**. The damping factor *tan δ* ($\tan\delta = E''/E'$) is likely to be affected by the molecular mobility of macromolecular chains within the matrix and at the fibre / matrix interphase [247], [248]. For sisal preform / AESO biocomposites [246], the DMTA curves showed a decrease of the damping factor from 0.09 to 0.07 due to the presence of BC on sisal fibres, characteristic of improved fibre / matrix interactions and restricted molecular motions at the interface. The fibre / matrix interfacial strength indicator *b* was calculated (see relationship in **Figure I-53 B**, with $tan\ \delta_c$ and $tan\ \delta_m$ the damping factors of the composite and the neat matrix respectively; V_f the fibre volume fraction). A higher *b* value was obtained for the BC-sisal preform / AESO biocomposite, highlighting an increase of the interfacial adhesion, and possibly better wetting of the AESO resin.

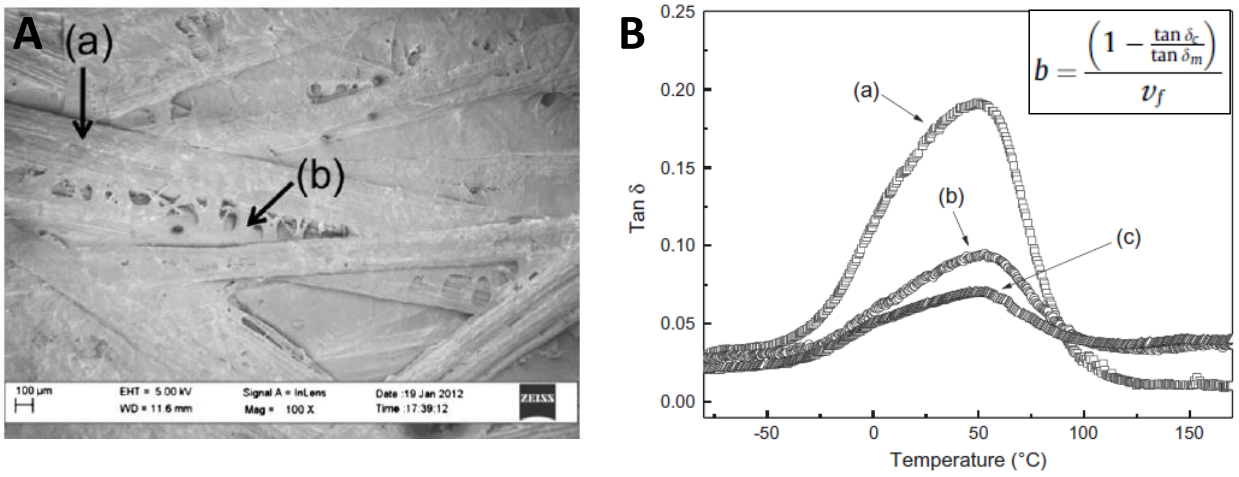

Figure I-53: A. SEM micrograph of sisal fibre (a) preform using (b) BC as binder ; B. results of DMTA tests with tan δ as a function of temperature for (a) neat polyAESAO, (b) sisal-polyAESO and (c) BC-sisal-polyAESO biocomposites (reprinted from Lee *et al.* 2012 [246]).

I. 3. 3. 2 Hierarchical natural fibres modified by cellulose nanocrystals (CNC) or cellulose nanofibrils (CNF)

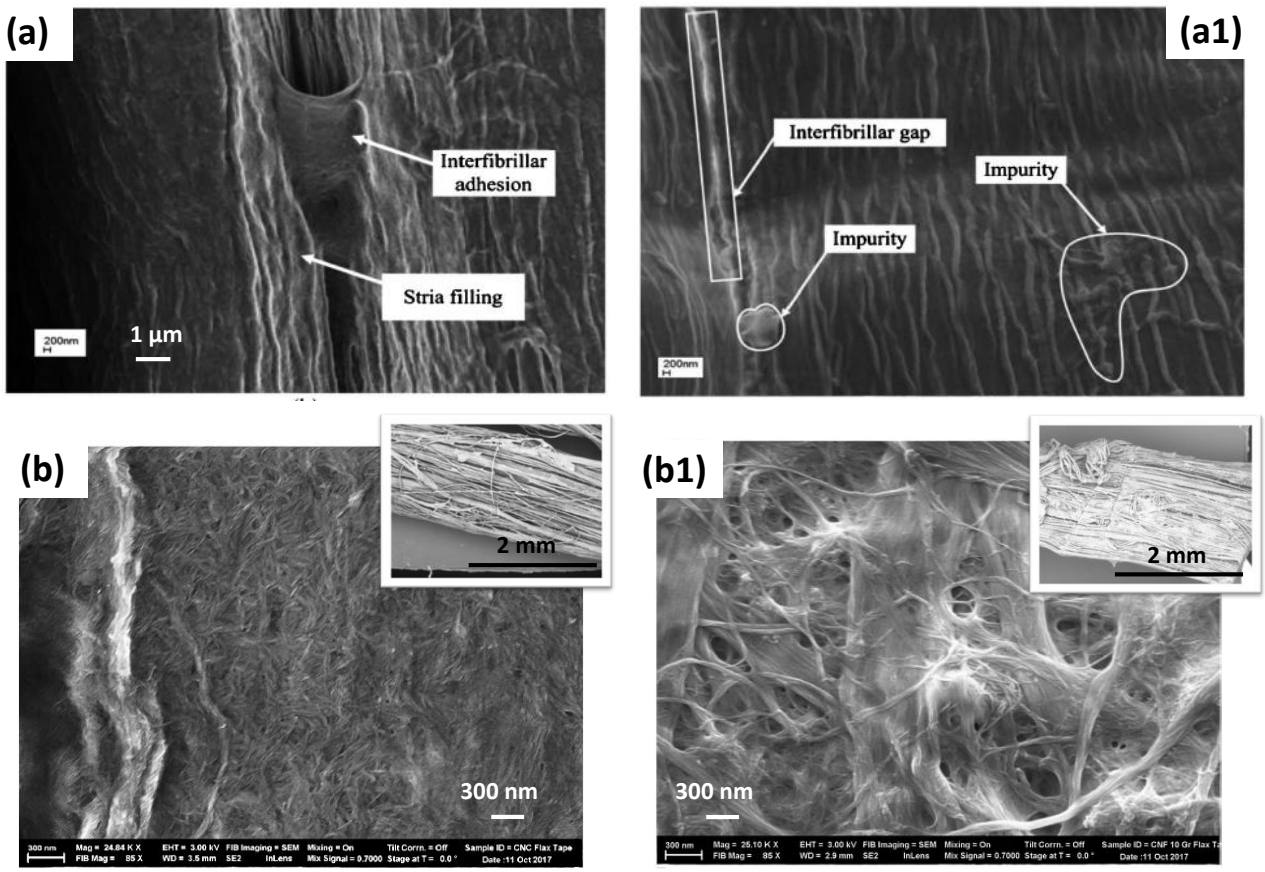

Figure I-54: SEM Images of (a & a1) nanocellulose treated hemp fibres, (b & b1) respectively CNC and CNF 100G treated flax tapes (reprinted with permission from Dai and Fan 2013 [199] and Ghasemi *et al.* 2018 [249]).

Dai and Fan (2013) studied the modification of hemp yarns with the deposition of cellulose nanocrystals (CNC) at the surface of fibres [199] (**Figure I-54 a & a1**). They performed a two-step modification: (1) pre-treatment of yarns in an ultrasonic bath (60°C, 1 h) containing a solution of cationic surfactant_dodecyltrimethylammonium bromide (DTAB) at different concentrations (0.05, 0.10 or 0.15 % the weight of dried fibres) and pH (10, 11 or 12); (2) dipping of DTAB pre-treated hemp fibres in a suspension of nanocellulose at 2 wt% (25°C, 10 min). The pre-treatment at pH = 11 and DTAB 0.10 % prior to the coating of hemp fibres with CNC gave the best results with an increase of elementary fibre Young's modulus and tensile strength of 36.1 % and 72.8 % respectively. Moreover, the addition of 0.10 % of DTAB resulted in much more adsorption of anionic CNC at the surface of hemp fibres. SEM images highlighted the "repairing" capacity of

CNC towards hemp fibre bundles with the filling of stria at their surface and interfibrillar adhesion (**Figure I-54 a & a1**).

Ghasemi *et al.* (2018) studied the produced modified natural fibre yarns (twisted or untwisted gathered elementary fibres) and tapes (aligned elementary fibres without any twist) with CNC and different types of CNF targeting textile and composite applications [249] (**Figure I-54 b & b1**). As Dai and Fan [199], the authors observed the filling of gaps and the binding effect of CNC and CNF on the elementary fibres constituting the yarns / tapes. Moreover, it seems that the substrate structure, i.e. yarns or tapes, induces on the distribution of CNC and CNF with a more heterogeneous deposition and a larger amount of trapped nanocellulose for tapes compared to yarns. **Figure I-54 b & b1** show surfaces of two different manufactured tapes modified by the deposition of CNC and CNF 100G ("100G" stands for "ground for 100 min with an average particle diameter of 2.84 μm"), respectively. CNF and CNC cover the entire tape surface forming a three-dimensional network with many bridges between the fibres. Lower magnification SEM images, inserted in **Figure I-54 b & b1,** taken at the scale of tapes and yarns show more uniform adsorption of CNC through the structure of yarns and tapes due to its smaller size compared to CNF 100G. Finally, the release of water appeared to be easier and more efficient with the presence of CNC in the structure of flax yarns / tapes. Indeed, the drying rate was almost two times faster compared to untreated yarns / tapes. However, the authors did not use these treated natural fibre yarns and tapes to manufacture flax reinforcement-based biocomposite materials.

To conclude, it appears that hierarchical biocomposites reinforced with natural fibres modified by the deposition and/or growth of BC on their surfaces, provide promising results at the microscopic scale with an increase of the IFSS. On the other hand, mechanical tests conducted at the macroscopic scale revealed more contrasting results in terms of tensile and flexural strength. This suggests that the preparation of such hierarchical biocomposites requires an optimization of the different processing steps to guarantee the efficiency of the nanostructurated interphase from the micro-scale, that is, local interfacial adhesion, up to the composite material, that is, the resulting structural performance. Moreover, the treatment procedure appears as a key, especially when considering its scale-up for composite manufacturing. The BC growth technique gives interesting results but its implementation in composite materials could be difficult due to the specific conditions required to control the fermentation bio-process, that is, the culture medium, pH, temperature, and especially the incubation time that can last for several days. In this regard,

the spontaneous adsorption of CNC or CNF on fibre surfaces appears as an interesting approach more suitable for an industrial scale-up in composite or textile applications. However, research works focused on the deposition of CNC and/or CNF on natural fibres [199], [249] did not consider their application to composite materials by conducting wettability or (micro-)mechanical tests with polymer matrices.

I. 3. 4. Conclusion

This section highlighted the key role of nano-objects in hierarchical architectures observed in biological systems such as bones, nacre and wood. These nanoscaled-hierarchical structures increase significantly the tensile strength and toughness of biological systems by modifying the load transfer within their microstructure and the failure mechanisms in interfacial regions. Based on these findings, the bio-inspired concept of hierarchical fibres modified by nano-objects has been considered to enhance the fibre / matrix interphase in man-made composite materials. The coating of synthetic and natural fibres with nano-objects (CNTs, graphene, ZnO nanowires, nano-TiO_2, nanoclay, BC, CNC, CNF) changes their surface properties with higher roughness and specific surface area. Moreover, nano-objects localized at the interface allow a smoother transition between the fibres and the matrix in terms of microstructure and mechanical properties of the interphase, hence improving the load transfer within the composite. Hierarchically nanostructured fibres also ensure a better mechanical interlocking with the matrix and prevent fibre debonding. Finally, nano-objects can hinder crack propagation, which follow a zig-zag path preferentially at interfaces. As a result, the incorporation of hierarchical fibres in composite materials greatly modifies their mechanical behaviour. The interfacial shear strength (IFSS) between fibres and polymer matrix is enhanced, contributing to better mechanical performance of the composites, especially their strength and toughness. Based on this concept, fully bio-based hierarchical composites have been developed. In particular, the deposition and/or growth of various nanocelluloses on natural fibres showed promising results with more cohesive interphases resulting in higher IFSS, tensile and flexural strength as well as modified thermomechanical behaviour. A “repairing” or binding effect between elementary fibres has also been pointed out for natural fibre bundles, yarns or tapes. Nevertheless, increased voids and worst impregnation have been observed in some cases due to thick CNC layers, resulting in a loss of mechanical properties of biocomposites. Concluding, the

bio-inspired concept of hierarchical structures appears as an interesting strategy for the development of sustainable fibre reinforced composite materials with enhanced structural properties and need to be further investigated. Developing new processes to build-up such hierarchically nanostructured fibre reinforced composite with long-scale interphases as those observed in biological systems could be the key.

I. 4. References

[1] E. Kvavadze *et al.*, '30,000-Year-Old Wild Flax Fibers', *Science*, vol. 325, no. 5946, pp. 1359–1359, Sep. 2009, doi: 10.1126/science.1175404.

[2] R. M. Kozłowski, M. Mackiewicz-Talarczyk, K. Wielgusz, M. Praczyk, and A. M. Allam, '5A - Bast fibres: flax', in *Handbook of Natural Fibres (Second Edition)*, R. M. Kozłowski and M. Mackiewicz-Talarczyk, Eds. Woodhead Publishing, 2020, pp. 93–162.

[3] L. Quillien, 'Flax and Linen in the First Millennium Babylonia BC: the Origins, Craft Industry and Uses of a Remarkable Textile', *Prehistoric, Ancient Near Eastern & Aegean Textiles and Dress*, pp. 271–296, 2014.

[4] CELC European Scientific Commitee, *Flax and Hemp fibres: a natural solution for the composite industry*, JEC Composites. 2012.

[5] C. Sultana, 'Growing and harvesting of flax', 1992, [Online]. Available: http://agris.fao.org/agris-search/search.do?recordID=GB9135765.

[6] C. Meirhaeghe, 'Evaluation de la disponibilité et de l'accessibilité de fibres végétales à usages matériaux en France'. ADEME & FRD, Mar. 2011, [Online]. Available: https://www.ademe.fr/sites/default/files/assets/documents/76290_12_evaluation_dispo_accessibilite_fibres_veg_usages_materiaux.pdf.

[7] S. Guyomard, 'Une récolte 2018 rassurante pour la filière', *Terre-net*, p. https://www.terre-net.fr/observatoire-technique-culturale/strategie-technique-culturale/article/une-recolte-2018-rassurante-pour-la-filiere-217-142111.html, Oct. 12, 2018.

[8] USRTL, 'http://www.usrtl-ifl.fr/spip.php?article41'. Accessed: May 19, 2020. [Online].

[9] T. A. Gorshkova *et al.*, 'Cell-Wall Polysaccharides of Developing Flax Plants', *Plant Physiology*, vol. 110, no. 3, pp. 721–729, Mar. 1996, doi: 10.1104/pp.110.3.721.

[10] C. Baley and A. Bourmaud, 'Average tensile properties of French elementary flax fibers', *Materials Letters*, vol. 122, pp. 159–161, May 2014, doi: 10.1016/j.matlet.2014.02.030.

[11] C. Gauberti, 'https://france3-regions.francetvinfo.fr/normandie/normandie-leader-mondial-production-lin-on-vous-explique-1651200.html'. Apr. 24, 2019, Accessed: May 19, 2020. [Online].

[12] FRD, Sinfoni, bpiFrance, 'Panorama des Marchés "Fibres végétales techniques matériaux (Hors bois)"'. 2016.

[13] C. Goudenhooft, A. Bourmaud, and C. Baley, 'Flax (Linum usitatissimum L.) Fibers for Composite Reinforcement: Exploring the Link Between Plant Growth, Cell Walls Development, and Fiber Properties', *Front. Plant Sci.*, vol. 10, 2019, doi: 10.3389/fpls.2019.00411.

[14] A. Razukas, Z. Jankauskiene, J. Jundulas, and R. Asakaviciute, 'Research of technical crops (potato and flax) genetic resources in Lithuania', p. 15.

[15] C. Goudenhooft, A. Bourmaud, and C. Baley, 'Varietal selection of flax over time: Evolution of plant architecture related to influence on the mechanical properties of fibers', *Industrial Crops and Products*, vol. 97, pp. 56–64, Mar. 2017, doi: 10.1016/j.indcrop.2016.11.062.

[16] L. Yan, N. Chouw, and K. Jayaraman, 'Flax fibre and its composites – A review', *Composites Part B: Engineering*, vol. 56, pp. 296–317, Jan. 2014, doi: 10.1016/j.compositesb.2013.08.014.

[17] W. Woigk *et al.*, 'Interface properties and their effect on the mechanical performance of flax fibre thermoplastic composites', *Composites Part A: Applied Science and Manufacturing*, vol. 122, pp. 8–17, Jul. 2019, doi: 10.1016/j.compositesa.2019.04.015.

[18] C. Sultana, 'The cultivation of fibre flax', *Outlook Agric*, vol. 12, no. 3, pp. 104–110, Sep. 1983, doi: 10.1177/003072708301200301.

[19] H. L. Bos and A. M. Donald, 'In situ ESEM study of the deformation of elementary flax fibres', *Journal of Materials Science*, vol. 34, no. 13, pp. 3029–3034, Jul. 1999, doi: 10.1023/A:1004650126890.

[20] A. Bourmaud, M. Gibaud, A. Lefeuvre, C. Morvan, and C. Baley, 'Influence of the morphology characters of the stem on the lodging resistance of Marylin flax', *Industrial Crops and Products*, vol. 66, pp. 27–37, Apr. 2015, doi: 10.1016/j.indcrop.2014.11.047.
[21] M. Gibaud, A. Bourmaud, and C. Baley, 'Understanding the lodging stability of green flax stems; The importance of morphology and fibre stiffness', *Biosystems Engineering*, vol. 137, pp. 9–21, Sep. 2015, doi: 10.1016/j.biosystemseng.2015.06.005.
[22] K. Charlet and A. Béakou, 'Mechanical properties of interfaces within a flax bundle – Part I: Experimental analysis', *International Journal of Adhesion and Adhesives*, vol. 31, no. 8, pp. 875–881, Dec. 2011, doi: 10.1016/j.ijadhadh.2011.08.008.
[23] C. Morvan, C. Andème-Onzighi, R. Girault, D. S. Himmelsbach, A. Driouich, and D. E. Akin, 'Building flax fibres: more than one brick in the walls', *Plant Physiology and Biochemistry*, vol. 41, no. 11, pp. 935–944, Nov. 2003, doi: 10.1016/j.plaphy.2003.07.001.
[24] M. V. Ageeva *et al.*, 'Intrusive growth of flax phloem fibers is of intercalary type', *Planta*, vol. 222, no. 4, pp. 565–574, Nov. 2005, doi: 10.1007/s00425-005-1536-2.
[25] Bourmaud, J. Beaugrand, D. U. Shah, V. Placet, and C. Baley, 'Towards the design of high-performance plant fibre composites', *Progress in Materials Science*, vol. 97, pp. 347–408, Aug. 2018, doi: 10.1016/j.pmatsci.2018.05.005.
[26] J. Beaugrand, B. Chabbert, and B. Kurek, 'Chapitre 1 - Production, transformation et critères de qualité des fibres de lin et de chanvre pour un usage dans les matériaux composites', in *Composites polymères et fibres lignocellulosiques*, 2017.
[27] J.-C. Roland, M. Mosiniak, and D. Roland, 'Dynamique du positionnement de la cellulose dans les parois des fibres textiles du lin (*Linum usitatissimum*)', *Acta Botanica Gallica*, vol. 142, no. 5, pp. 463–484, Jan. 1995, doi: 10.1080/12538078.1995.10515271.
[28] N. Le Moigne, B. Otazaghine, S. Corn, H. Angellier-Coussy, and A. Bergeret, 'Introduction on Natural Fibre Structure: From the Molecular to the Macrostructural Level', in *Surfaces and Interfaces in Natural Fibre Reinforced Composites: Fundamentals, Modifications and Characterization*, N. Le Moigne, B. Otazaghine, S. Corn, H. Angellier-Coussy, and A. Bergeret, Eds. Cham: Springer International Publishing, 2018, pp. 1–22.
[29] C. W. Hock, 'Microscopic structure of flax and related bast fibers', *J. RES. NATL. BUR. STAN.*, vol. 29, no. 1, p. 41, Jul. 1942, doi: 10.6028/jres.029.024.
[30] R. J. Moon, C. R. Frihart, and T. Wegner, 'Nanotechnology applications in the forest products industry', *Forest products journal. Vol. 56, no. 5 (May 2006): pages 4-10.*, 2006, Accessed: May 07, 2020. [Online]. Available: https://www.fs.usda.gov/treesearch/pubs/24445.
[31] C. Baley, 'Fibres naturelles de renfort pour matériaux composites', *Techniques de l'Ingénieur*, no. AM5130v3, 2020, [Online]. Available: https://www.techniques-ingenieur.fr/res/pdf/encyclopedia/42142210-am5130.pdf.
[32] D. N.-S. Hon, 'Cellulose: a random walk along its historical path', *Cellulose*, vol. 1, no. 1, pp. 1–25, Mar. 1994, doi: 10.1007/BF00818796.
[33] O. Nechyporchuk, M. N. Belgacem, and J. Bras, 'Production of cellulose nanofibrils: A review of recent advances', *Industrial Crops and Products*, vol. 93, pp. 2–25, Dec. 2016, doi: 10.1016/j.indcrop.2016.02.016.
[34] D. Klemm, B. Heublein, H.-P. Fink, and A. Bohn, 'Cellulose: Fascinating Biopolymer and Sustainable Raw Material', *Angewandte Chemie International Edition*, vol. 44, no. 22, pp. 3358–3393, 2005, doi: 10.1002/anie.200460587.
[35] G. Banvillet, 'Industrial application of pretreatments for obtaining high quality cellulose nanofibrils', Université Grenoble Alpes, 2021.
[36] P. M. Bonatti, C. Ferrari, B. Focher, C. Grippo, G. Torri, and C. Cosentino, 'Histochemical and supramolecular studies in determining quality of hemp fibres for textile applications', *Euphytica*, vol. 140, no. 1, pp. 55–64, Jan. 2004, doi: 10.1007/s10681-004-4755-x.
[37] J. F. Kennedy and R. J. S. Pons, 'Cellulose: Structure, accessibility and reactivity', *Carbohydrate Polymers*, vol. 26, no. 4, pp. 313–314, Jan. 1995, doi: 10.1016/0144-8617(95)90061-6.

[38] S. Dumitriu, *Polysaccharides: Structural Diversity and Functional Versatility, Second Edition*. CRC Press, 2004.
[39] W. T. Y. Tze, S. Wang, T. G. Rials, G. M. Pharr, and S. S. Kelley, 'Nanoindentation of wood cell walls: Continuous stiffness and hardness measurements', *Composites Part A: Applied Science and Manufacturing*, vol. 38, no. 3, pp. 945–953, Mar. 2007, doi: 10.1016/j.compositesa.2006.06.018.
[40] A. Dufresne, 'Nanocellulose: a new ageless bionanomaterial', *Materials Today*, vol. 16, no. 6, pp. 220–227, Jun. 2013, doi: 10.1016/j.mattod.2013.06.004.
[41] O. Lerouxel, D. M. Cavalier, A. H. Liepman, and K. Keegstra, 'Biosynthesis of plant cell wall polysaccharides — a complex process', *Current Opinion in Plant Biology*, vol. 9, no. 6, pp. 621–630, Dec. 2006, doi: 10.1016/j.pbi.2006.09.009.
[42] M. Ek, G. Gellerstedt, and G. Henriksson, *Wood Chemistry and Biotechnology*. Walter de Gruyter, 2009.
[43] W. J. Cousins, 'Young's modulus of hemicellulose as related to moisture content', *Wood Sci.Technol.*, vol. 12, no. 3, pp. 161–167, Sep. 1978, doi: 10.1007/BF00372862.
[44] Y. B. Park and D. J. Cosgrove, 'Xyloglucan and its Interactions with Other Components of the Growing Cell Wall', *Plant and Cell Physiology*, vol. 56, no. 2, pp. 180–194, Feb. 2015, doi: 10.1093/pcp/pcu204.
[45] D. Mohnen, 'Pectin structure and biosynthesis', *Current Opinion in Plant Biology*, vol. 11, no. 3, pp. 266–277, Jun. 2008, doi: 10.1016/j.pbi.2008.03.006.
[46] H. V. Scheller, J. K. Jensen, S. O. Sørensen, J. Harholt, and N. Geshi, 'Biosynthesis of pectin', *Physiologia Plantarum*, vol. 129, no. 2, pp. 283–295, 2007, doi: 10.1111/j.1399-3054.2006.00834.x.
[47] T. Gorshkova and C. Morvan, 'Secondary cell-wall assembly in flax phloem fibres: role of galactans', *Planta*, vol. 223, no. 2, pp. 149–158, Jan. 2006, doi: 10.1007/s00425-005-0118-7.
[48] G. Marques, J. C. del Río, and A. Gutiérrez, 'Lipophilic extractives from several nonwoody lignocellulosic crops (flax, hemp, sisal, abaca) and their fate during alkaline pulping and TCF/ECF bleaching', *Bioresource Technology*, vol. 101, no. 1, pp. 260–267, Jan. 2010, doi: 10.1016/j.biortech.2009.08.036.
[49] J. Acera Fernández *et al.*, 'Role of flax cell wall components on the microstructure and transverse mechanical behaviour of flax fabrics reinforced epoxy biocomposites', *Industrial Crops and Products*, vol. 85, pp. 93–108, Jul. 2016, doi: 10.1016/j.indcrop.2016.02.047.
[50] J. Barros, H. Serk, I. Granlund, and E. Pesquet, 'The cell biology of lignification in higher plants', *Ann Bot*, vol. 115, no. 7, pp. 1053–1074, Jun. 2015, doi: 10.1093/aob/mcv046.
[51] A. Day *et al.*, 'Lignification in the flax stem: evidence for an unusual lignin in bast fibers', *Planta*, vol. 222, no. 2, pp. 234–245, Oct. 2005, doi: 10.1007/s00425-005-1537-1.
[52] A. Barbulée, 'Compréhension des effets du défibrage sur la morphologie, les propriétés et le comportement mécanique des faisceaux de fibres de lin : étude d'un composite dérivé lin/époxyde', These de doctorat, Caen, 2015.
[53] L. Marrot, A. Lefeuvre, B. Pontoire, A. Bourmaud, and C. Baley, 'Analysis of the hemp fiber mechanical properties and their scattering (Fedora 17)', *Industrial Crops and Products*, vol. 51, pp. 317–327, Nov. 2013, doi: 10.1016/j.indcrop.2013.09.026.
[54] N. Martin, N. Mouret, P. Davies, and C. Baley, 'Influence of the degree of retting of flax fibers on the tensile properties of single fibers and short fiber/polypropylene composites', *Industrial Crops and Products*, vol. 49, pp. 755–767, Aug. 2013, doi: 10.1016/j.indcrop.2013.06.012.
[55] J. Leboucher, 'Valorisation des anas de lin sous forme de nanocelluloses', phdthesis, Normandie Université, 2019.
[56] X. Liu, Q. Lin, Y. Yan, F. Peng, R. Sun, and J. Ren, 'Hemicellulose from Plant Biomass in Medical and Pharmaceutical Application: A Critical Review', *Current Medicinal Chemistry*, vol. 26, no. 14, pp. 2430–2455, Apr. 2019, doi: 10.2174/0929867324666170705113657.

[57] L. da Cruz Cabral, V. Fernández Pinto, and A. Patriarca, 'Application of plant derived compounds to control fungal spoilage and mycotoxin production in foods', *International Journal of Food Microbiology*, vol. 166, no. 1, pp. 1–14, Aug. 2013, doi: 10.1016/j.ijfoodmicro.2013.05.026.
[58] C. Fritsch *et al.*, 'Processing, Valorization and Application of Bio-Waste Derived Compounds from Potato, Tomato, Olive and Cereals: A Review', *Sustainability*, vol. 9, no. 8, Art. no. 8, Aug. 2017, doi: 10.3390/su9081492.
[59] A. M. Pisoschi, A. Pop, C. Cimpeanu, and G. Predoi, 'Antioxidant Capacity Determination in Plants and Plant-Derived Products: A Review', *Oxidative Medicine and Cellular Longevity*, Dec. 04, 2016. https://www.hindawi.com/journals/omcl/2016/9130976/ (accessed Jul. 23, 2020).
[60] H. S. Kambo and A. Dutta, 'A comparative review of biochar and hydrochar in terms of production, physico-chemical properties and applications', *Renewable and Sustainable Energy Reviews*, vol. 45, pp. 359–378, May 2015, doi: 10.1016/j.rser.2015.01.050.
[61] S. A. Jambo, R. Abdulla, S. H. Mohd Azhar, H. Marbawi, J. A. Gansau, and P. Ravindra, 'A review on third generation bioethanol feedstock', *Renewable and Sustainable Energy Reviews*, vol. 65, pp. 756–769, Nov. 2016, doi: 10.1016/j.rser.2016.07.064.
[62] S. Salimi, R. Sotudeh-Gharebagh, R. Zarghami, S. Y. Chan, and K. H. Yuen, 'Production of Nanocellulose and Its Applications in Drug Delivery: A Critical Review', *ACS Sustainable Chem. Eng.*, vol. 7, no. 19, pp. 15800–15827, Oct. 2019, doi: 10.1021/acssuschemeng.9b02744.
[63] A. Dufresne, *Nanocellulose: From Nature to High Performance Tailored Materials*. Walter de Gruyter GmbH & Co KG, 2017.
[64] M. M. de S. Lima and R. Borsali, 'Rodlike Cellulose Microcrystals: Structure, Properties, and Applications', *Macromolecular Rapid Communications*, vol. 25, no. 7, pp. 771–787, 2004, doi: 10.1002/marc.200300268.
[65] M. Roman, 'Toxicity of Cellulose Nanocrystals: A Review', *Industrial Biotechnology*, vol. 11, no. 1, pp. 25–33, Feb. 2015, doi: 10.1089/ind.2014.0024.
[66] N. Lin and A. Dufresne, 'Nanocellulose in biomedicine: Current status and future prospect', *European Polymer Journal*, vol. 59, pp. 302–325, Oct. 2014, doi: 10.1016/j.eurpolymj.2014.07.025.
[67] E. J. Foster *et al.*, 'Current characterization methods for cellulose nanomaterials', *Chemical Society Reviews*, vol. 47, no. 8, pp. 2609–2679, 2018, doi: 10.1039/C6CS00895J.
[68] Y. Habibi, L. A. Lucia, and O. J. Rojas, 'Cellulose Nanocrystals: Chemistry, Self-Assembly, and Applications', *Chemical Reviews*, vol. 110, no. 6, pp. 3479–3500, Jun. 2010, doi: 10.1021/cr900339w.
[69] D.-Y. Kim, Y. Nishiyama, M. Wada, and S. Kuga, 'High-yield Carbonization of Cellulose by Sulfuric Acid Impregnation', *Cellulose*, vol. 8, no. 1, pp. 29–33, Mar. 2001, doi: 10.1023/A:1016621103245.
[70] S. Julien, E. Chornet, and R. P. Overend, 'Influence of acid pretreatment (H2SO4, HCl, HNO3) on reaction selectivity in the vacuum pyrolysis of cellulose', *Journal of Analytical and Applied Pyrolysis*, vol. 27, no. 1, pp. 25–43, Oct. 1993, doi: 10.1016/0165-2370(93)80020-Z.
[71] J. Tang, J. Sisler, N. Grishkewich, and K. C. Tam, 'Functionalization of cellulose nanocrystals for advanced applications', *Journal of Colloid and Interface Science*, vol. 494, pp. 397–409, May 2017, doi: 10.1016/j.jcis.2017.01.077.
[72] A. Dufresne, 'Nanomatériaux cellulosiques', p. 23, 2015.
[73] D. Klemm *et al.*, 'Nanocelluloses: A New Family of Nature-Based Materials', *Angewandte Chemie International Edition*, vol. 50, no. 24, pp. 5438–5466, Jun. 2011, doi: 10.1002/anie.201001273.
[74] R. J. Moon, A. Martini, J. Nairn, J. Simonsen, and J. Youngblood, 'Cellulose nanomaterials review: structure, properties and nanocomposites', *Chem. Soc. Rev.*, vol. 40, no. 7, pp. 3941–3994, Jun. 2011, doi: 10.1039/C0CS00108B.
[75] K. Nishinari, M. Takemasa, K. Yamatoya, and M. Shirakawa, '19 - Xyloglucan', in *Handbook of Hydrocolloids (Second Edition)*, G. O. Phillips and P. A. Williams, Eds. Woodhead Publishing, 2009, pp. 535–566.

[76] Z. Zhao, V. H. Crespi, J. D. Kubicki, D. J. Cosgrove, and L. Zhong, 'Molecular dynamics simulation study of xyloglucan adsorption on cellulose surfaces: effects of surface hydrophobicity and side-chain variation', *Cellulose*, vol. 21, no. 2, pp. 1025–1039, Apr. 2014, doi: 10.1007/s10570-013-0041-1.

[77] S. C. Fry, 'The Structure and Functions of Xyloglucan', *Journal of experimental botany*, vol. 40, no. 210, pp. 1–11, 1989.

[78] T. Hayashi, 'Xyloglucans in the Primary Cell Wall', *Annual Review of Plant Physiology and Plant Molecular Biology*, vol. 40, no. 1, pp. 139–168, 1989, doi: 10.1146/annurev.pp.40.060189.001035.

[79] F. Muller *et al.*, 'SANS Measurements of Semiflexible Xyloglucan Polysaccharide Chains in Water Reveal Their Self-Avoiding Statistics', *Biomacromolecules*, vol. 12, no. 9, pp. 3330–3336, Sep. 2011, doi: 10.1021/bm200881x.

[80] T. Hayashi, K. Ogawa, and Y. Mitsuishi, 'Characterization of the adsorption of Xyloglucan to Cellulose', *Plant and Cell Physiology*, vol. 35, no. 8, pp. 1199–1205, 1994, doi: 10.1093/oxfordjournals.pcp.a078714.

[81] D. U. Lima, W. Loh, and M. S. Buckeridge, 'Xyloglucan–cellulose interaction depends on the sidechains and molecular weight of xyloglucan', *Plant Physiology and Biochemistry*, vol. 42, no. 5, pp. 389–394, May 2004, doi: 10.1016/j.plaphy.2004.03.003.

[82] J.-P. Vincken, A. de Keizer, G. Beldman, and A. Gerard Joseph Voragen, 'Fractionation of xyloglucan fragments and their interaction with cellulose', *Plant Physiol*, vol. 108, pp. 1579–1585, 1995.

[83] Y. B. Park and D. J. Cosgrove, 'A Revised Architecture of Primary Cell Walls Based on Biomechanical Changes Induced by Substrate-Specific Endoglucanases', *Plant Physiology*, vol. 158, pp. 1933–1943, 2012.

[84] T. Benselfelt *et al.*, 'Adsorption of Xyloglucan onto Cellulose Surfaces of Different Morphologies: An Entropy-Driven Process', *Biomacromolecules*, vol. 17, no. 9, pp. 2801–2811, Sep. 2016, doi: 10.1021/acs.biomac.6b00561.

[85] A. Villares, C. Moreau, A. Dammak, I. Capron, and B. Cathala, 'Kinetic aspects of the adsorption of xyloglucan onto cellulose nanocrystals', *Soft Matter*, vol. 11, no. 32, pp. 6472–6481, 2015, doi: 10.1039/C5SM01413A.

[86] A. Dammak *et al.*, 'Exploring Architecture of Xyloglucan Cellulose Nanocrystal Complexes through Enzyme Susceptibility at Different Adsorption Regimes', *Biomacromolecules*, vol. 16, no. 2, pp. 589–596, Feb. 2015, doi: 10.1021/bm5016317.

[87] J. Hanus and K. Mazeau, 'The xyloglucan–cellulose assembly at the atomic scale', *Biopolymers*, vol. 82, no. 1, pp. 59–73, May 2006, doi: 10.1002/bip.20460.

[88] M. Lopez *et al.*, 'Enthalpic Studies of Xyloglucan−Cellulose Interactions', *Biomacromolecules*, vol. 11, no. 6, pp. 1417–1428, Jun. 2010, doi: 10.1021/bm1002762.

[89] J. Stiernstedt, H. Brumer, Q. Zhou, T. T. Teeri, and M. W. Rutland, 'Friction between Cellulose Surfaces and Effect of Xyloglucan Adsorption', *Biomacromolecules*, vol. 7, no. 7, pp. 2147–2153, Jul. 2006, doi: 10.1021/bm060100i.

[90] J. Stiernstedt, N. Nordgren, L. Wågberg, H. Brumer, D. G. Gray, and M. W. Rutland, 'Friction and forces between cellulose model surfaces: A comparison', *Journal of Colloid and Interface Science*, vol. 303, no. 1, pp. 117–123, Nov. 2006, doi: 10.1016/j.jcis.2006.06.070.

[91] A. Oksanen, R. Timo, E. Retulainen, K. Salminen, and H. Brumer, 'Improving Wet Web Runnability and Paper Quality by an Uncharged Polysaccharide', *Journal of Biobased Materials and Bioenergy*, vol. 5, no. 2, pp. 187–191, Jun. 2011, doi: 10.1166/jbmb.2011.1144.

[92] M. Christiernin *et al.*, 'The effects of xyloglucan on the properties of paper made from bleached kraft pulp', *Nordic Pulp & Paper Research Journal*, vol. 18, no. 2, pp. 182–187, 2003, doi: 10.3183/npprj-2003-18-02-p182-187.

[93] H. Yan, T. Lindström, and M. Christiernin, 'Some ways to decrease fibre suspension flocculation and improve sheet formation', *Nordic Pulp & Paper Research Journal*, vol. 21, no. 1, pp. 36–43, Jan. 2006, doi: 10.3183/npprj-2006-21-01-p036-043.

[94] H. Sehaqui, L. A. Berglund, and Q. Zhou, 'Nanofibrillated cellulose for enhancement of strength in high-density paper structures', *Nordic Pulp & Paper Research Journal*, vol. 28, no. 2, pp. 182–189, May 2013, doi: 10.3183/npprj-2013-28-02-p182-189.
[95] F. Vilaseca, A. Serra, and J. J. Kochumalayil, 'Xyloglucan coating for enhanced strength and toughness in wood fibre networks', *Carbohydrate Polymers*, vol. 229, p. 115540, Feb. 2020, doi: 10.1016/j.carbpol.2019.115540.
[96] Z. Jaafar *et al.*, 'Plant cell wall inspired xyloglucan/cellulose nanocrystals aerogels produced by freeze-casting', *Carbohydrate Polymers*, vol. 247, p. 116642, Nov. 2020, doi: 10.1016/j.carbpol.2020.116642.
[97] A. Bourmaud, M. Gibaud, and C. Baley, 'Impact of the seeding rate on flax stem stability and the mechanical properties of elementary fibres', *Industrial Crops and Products*, vol. 80, pp. 17–25, Feb. 2016, doi: 10.1016/j.indcrop.2015.10.053.
[98] B. Chabbert *et al.*, 'Multimodal assessment of flax dew retting and its functional impact on fibers and natural fiber composites', *Industrial Crops and Products*, vol. 148, p. 112255, Jun. 2020, doi: 10.1016/j.indcrop.2020.112255.
[99] C. Goudenhooft *et al.*, 'Investigation of the Mechanical Properties of Flax Cell Walls during Plant Development: The Relation between Performance and Cell Wall Structure', *Fibers*, vol. 6, no. 1, Art. no. 1, Mar. 2018, doi: 10.3390/fib6010006.
[100] W. Garat, S. Corn, N. Le Moigne, J. Beaugrand, and A. Bergeret, 'Analysis of the morphometric variations in natural fibres by automated laser scanning: Towards an efficient and reliable assessment of the cross-sectional area', *Composites Part A: Applied Science and Manufacturing*, vol. 108, pp. 114–123, May 2018, doi: 10.1016/j.compositesa.2018.02.018.
[101] C. Baley, M. Gomina, J. Breard, A. Bourmaud, and P. Davies, 'Variability of mechanical properties of flax fibres for composite reinforcement. A review', *Industrial Crops and Products*, vol. 145, p. 111984, Mar. 2020, doi: 10.1016/j.indcrop.2019.111984.
[102] C. Baley, 'Analysis of the flax fibres tensile behaviour and analysis of the tensile stiffness increase', *Composites Part A: Applied Science and Manufacturing*, vol. 33, no. 7, pp. 939–948, Jul. 2002, doi: 10.1016/S1359-835X(02)00040-4.
[103] O. Faruk, A. K. Bledzki, H.-P. Fink, and M. Sain, 'Biocomposites reinforced with natural fibers: 2000–2010', *Progress in Polymer Science*, vol. 37, no. 11, pp. 1552–1596, Nov. 2012, doi: 10.1016/j.progpolymsci.2012.04.003.
[104] R. M. Rowell, '1 - Natural fibres: types and properties', in *Properties and Performance of Natural-Fibre Composites*, K. L. Pickering, Ed. Woodhead Publishing, 2008, pp. 3–66.
[105] W. Garat, N. Le Moigne, S. Corn, J. Beaugrand, and A. Bergeret, 'Swelling of natural fibre bundles under hygro- and hydrothermal conditions: Determination of hydric expansion coefficients by automated laser scanning', *Composites Part A: Applied Science and Manufacturing*, vol. 131, p. 105803, Apr. 2020, doi: 10.1016/j.compositesa.2020.105803.
[106] C. Baley, A. Le Duigou, A. Bourmaud, and P. Davies, 'Influence of drying on the mechanical behaviour of flax fibres and their unidirectional composites', *Composites Part A: Applied Science and Manufacturing*, vol. 43, no. 8, pp. 1226–1233, Aug. 2012, doi: 10.1016/j.compositesa.2012.03.005.
[107] M. F. Pucci, P.-J. Liotier, and S. Drapier, 'Capillary effects on flax fibers – Modification and characterization of the wetting dynamics', *Composites Part A: Applied Science and Manufacturing*, vol. 77, pp. 257–265, Oct. 2015, doi: 10.1016/j.compositesa.2015.03.010.
[108] M. F. Pucci, P.-J. Liotier, and S. Drapier, 'Capillary wicking in flax fabrics – Effects of swelling in water', *Colloids and Surfaces A: Physicochemical and Engineering Aspects*, vol. 498, pp. 176–184, Jun. 2016, doi: 10.1016/j.colsurfa.2016.03.050.
[109] M. F. Pucci, P.-J. Liotier, D. Seveno, C. Fuentes, A. Van Vuure, and S. Drapier, 'Wetting and swelling property modifications of elementary flax fibres and their effects on the Liquid Composite Molding process', *Composites Part A: Applied Science and Manufacturing*, vol. 97, pp. 31–40, Jun. 2017, doi: 10.1016/j.compositesa.2017.02.028.

[110] A. Le Duigou, A. Bourmaud, E. Balnois, P. Davies, and C. Baley, 'Improving the interfacial properties between flax fibres and PLLA by a water fibre treatment and drying cycle', *Industrial Crops and Products*, vol. 39, pp. 31–39, Sep. 2012, doi: 10.1016/j.indcrop.2012.02.001.
[111] M. M. Lu and A. W. Van Vuure, 'Improving moisture durability of flax fibre composites by using non-dry fibres', *Composites Part A: Applied Science and Manufacturing*, vol. 123, pp. 301–309, Aug. 2019, doi: 10.1016/j.compositesa.2019.05.029.
[112] J. Andersons, E. Poriķe, and E. Spārniņš, 'The effect of mechanical defects on the strength distribution of elementary flax fibres', *Composites Science and Technology*, vol. 69, no. 13, pp. 2152–2157, Oct. 2009, doi: 10.1016/j.compscitech.2009.05.010.
[113] T. Hänninen, A. Thygesen, S. Mehmood, B. Madsen, and M. Hughes, 'Mechanical processing of bast fibres: The occurrence of damage and its effect on fibre structure', *Industrial Crops and Products*, vol. 39, pp. 7–11, Sep. 2012, doi: 10.1016/j.indcrop.2012.01.025.
[114] G. C. Davies and D. M. Bruce, 'Effect of Environmental Relative Humidity and Damage on the Tensile Properties of Flax and Nettle Fibers':, *Textile Research Journal*, 1998, doi: 10.1177/004051759806800901.
[115] A. Thygesen, B. Madsen, A. B. Bjerre, and H. Lilholt, 'Cellulosic Fibers: Effect of Processing on Fiber Bundle Strength', *Journal of Natural Fibers*, vol. 8, no. 3, pp. 161–175, Jul. 2011, doi: 10.1080/15440478.2011.602236.
[116] M. Aslan, S. Mehmood, B. Madsen, and S. Goutianos, 'The effect of processing on defects and tensile strength of single flax fibres', presented at the 14th European Conference on Composite Materials, 2010, Accessed: May 14, 2020. [Online]. Available: https://orbit.dtu.dk/en/publications/the-effect-of-processing-on-defects-and-tensile-strength-of-singl.
[117] M. Hughes, G. Sèbe, J. Hague, C. Hill, M. Spear, and L. Mott, 'An investigation into the effects of micro-compressive defects on interphase behaviour in hemp-epoxy composites using half-fringe photoelasticity', *Composite Interfaces*, vol. 7, no. 1, pp. 13–29, Jan. 2000, doi: 10.1163/156855400300183551.
[118] C. Baley, 'Influence of kink bands on the tensile strength of flax fibers', *Journal of Materials Science*, vol. 39, no. 1, pp. 331–334, Jan. 2004, doi: 10.1023/B:JMSC.0000007768.63055.ae.
[119] N. Le Moigne, B. Otazaghine, S. Corn, H. Angellier-Coussy, and A. Bergeret, *Surfaces and Interfaces in Natural Fibre Reinforced Composites*. Cham: Springer International Publishing, 2018.
[120] C. Baley, F. Busnel, Y. Grohens, and O. Sire, 'Influence of chemical treatments on surface properties and adhesion of flax fibre–polyester resin', *Composites Part A: Applied Science and Manufacturing*, vol. 37, no. 10, pp. 1626–1637, Oct. 2006, doi: 10.1016/j.compositesa.2005.10.014.
[121] J. M. van Hazendonk, J. C. van der Putten, J. T. F. Keurentjes, and A. Prins, 'A simple experimental method for the measurement of the surface tension of cellulosic fibres and its relation with chemical composition', *Colloids and Surfaces A: Physicochemical and Engineering Aspects*, vol. 81, pp. 251–261, Dec. 1993, doi: 10.1016/0927-7757(93)80252-A.
[122] N. E. Zafeiropoulos, P. E. Vickers, C. A. Baillie, and J. F. Watts, 'An experimental investigation of modified and unmodified flax fibres with XPS, ToF-SIMS and ATR-FTIR', *Journal of Materials Science*, vol. 38, no. 19, pp. 3903–3914, Oct. 2003, doi: 10.1023/A:1026133826672.
[123] A. Le Duigou, A. Kervoelen, A. Le Grand, M. Nardin, and C. Baley, 'Interfacial properties of flax fibre–epoxy resin systems: Existence of a complex interphase', *Composites Science and Technology*, vol. 100, pp. 152–157, Aug. 2014, doi: 10.1016/j.compscitech.2014.06.009.
[124] N. Sgriccia, M. C. Hawley, and M. Misra, 'Characterization of natural fiber surfaces and natural fiber composites', *Composites Part A: Applied Science and Manufacturing*, vol. 39, no. 10, pp. 1632–1637, Oct. 2008, doi: 10.1016/j.compositesa.2008.07.007.
[125] D. Klemm, B. Philpp, T. Heinze, U. Heinze, and W. Wagenknecht, 'Comprehensive cellulose chemistry. Volume 1: Fundamentals and analytical methods.', *Comprehensive cellulose chemistry*.

Volume 1: Fundamentals and analytical methods., 1998, Accessed: May 20, 2020. [Online]. Available: https://www.cabdirect.org/cabdirect/abstract/20000609594.

[126] K. Charlet, 'Contribution to the study of flax fibre reinforced unidirectional composites: relationships between the fibre microstructure and its mechanical properties', Theses, Université de Caen / Basse-Normandie, 2008.

[127] A. Thuault, 'Approche multi-échelle de la structure et du comportement mécanique d'une fibre de lin', These de doctorat, Caen, 2011.

[128] A. Bismarck *et al.*, 'Surface characterization of flax, hemp and cellulose fibers; Surface properties and the water uptake behavior', *Polymer Composites*, vol. 23, no. 5, pp. 872–894, 2002, doi: 10.1002/pc.10485.

[129] A. Legras, A. Kondor, M. T. Heitzmann, and R. W. Truss, 'Inverse gas chromatography for natural fibre characterisation: Identification of the critical parameters to determine the Brunauer–Emmett–Teller specific surface area', *Journal of Chromatography A*, vol. 1425, pp. 273–279, Dec. 2015, doi: 10.1016/j.chroma.2015.11.033.

[130] J. Müssig, H. Fischer, N. Graupner, and A. Drieling, 'Testing Methods for Measuring Physical and Mechanical Fibre Properties (Plant and Animal Fibres)', in *Industrial Applications of Natural Fibres*, John Wiley & Sons, Ltd, 2010, pp. 267–309.

[131] K. Oksman, A. P. Mathew, R. Långström, B. Nyström, and K. Joseph, 'The influence of fibre microstructure on fibre breakage and mechanical properties of natural fibre reinforced polypropylene', *Composites Science and Technology*, vol. 69, no. 11, pp. 1847–1853, Sep. 2009, doi: 10.1016/j.compscitech.2009.03.020.

[132] N. Le Moigne, M. van den Oever, and T. Budtova, 'A statistical analysis of fibre size and shape distribution after compounding in composites reinforced by natural fibres', *Composites Part A: Applied Science and Manufacturing*, vol. 42, no. 10, pp. 1542–1550, Oct. 2011, doi: 10.1016/j.compositesa.2011.07.012.

[133] A. Bourmaud, G. Ausias, G. Lebrun, M.-L. Tachon, and C. Baley, 'Observation of the structure of a composite polypropylene/flax and damage mechanisms under stress', *Industrial Crops and Products*, vol. 43, no. Supplement C, pp. 225–236, May 2013, doi: 10.1016/j.indcrop.2012.07.030.

[134] A. Le Duigou, P. Davies, and C. Baley, 'Exploring durability of interfaces in flax fibre/epoxy micro-composites', *Composites Part A: Applied Science and Manufacturing*, vol. 48, pp. 121–128, May 2013, doi: 10.1016/j.compositesa.2013.01.010.

[135] R. Castellani *et al.*, 'Lignocellulosic fiber breakage in a molten polymer. Part 1. Qualitative analysis using rheo-optical observations', *Composites Part A: Applied Science and Manufacturing*, vol. 91, pp. 229–237, Dec. 2016, doi: 10.1016/j.compositesa.2016.10.015.

[136] E. Darque-Ceretti and E. Felder, *Adhésion et Adhérence*, vol. Sciences et Techniques de l'ingénieur. CNRS Editions, 2003.

[137] N. Le Moigne, B. Otazaghine, S. Corn, H. Angellier-Coussy, and A. Bergeret, 'Interfaces in Natural Fibre Reinforced Composites: Definitions and Roles', in *Surfaces and Interfaces in Natural Fibre Reinforced Composites: Fundamentals, Modifications and Characterization*, N. Le Moigne, B. Otazaghine, S. Corn, H. Angellier-Coussy, and A. Bergeret, Eds. Cham: Springer International Publishing, 2018, pp. 23–34.

[138] S. Mohanty, S. K. Nayak, S. K. Verma, and S. S. Tripathy, 'Effect of MAPP as a Coupling Agent on the Performance of Jute–PP Composites':, *Journal of Reinforced Plastics and Composites*, Aug. 2016, doi: 10.1177/0731684404032868.

[139] A. Elsabbagh, L. Steuernagel, and G. Ziegmann, 'Effect of fiber/matrix chemical modification on the mechanical properties and water absorption of extruded flax/polypropylene composite', *Journal of Applied Polymer Science*, vol. 111, no. 5, pp. 2279–2289, Mar. 2009, doi: 10.1002/app.29272.

[140] N. Le Moigne, M. Longerey, J.-M. Taulemesse, J.-C. Bénézet, and A. Bergeret, 'Study of the interface in natural fibres reinforced poly(lactic acid) biocomposites modified by optimized organosilane treatments', *Industrial Crops and Products*, vol. 52, pp. 481–494, Jan. 2014, doi: 10.1016/j.indcrop.2013.11.022.

[141] M. T. Paridah, A. B. Basher, S. SaifulAzry, and Z. Ahmed, 'RETTING PROCESS OF SOME BAST PLANT FIBRES AND ITS EFFECT ON FIBRE QUALITY: A REVIEW', *BioResources*, vol. 6, no. 4, Art. no. 4, Sep. 2011.
[142] I. Van de Weyenberg, J. Ivens, A. De Coster, B. Kino, E. Baetens, and I. Verpoest, 'Influence of processing and chemical treatment of flax fibres on their composites', *Composites Science and Technology*, vol. 63, no. 9, pp. 1241–1246, Jul. 2003, doi: 10.1016/S0266-3538(03)00093-9.
[143] A. Lefeuvre, A. L. Duigou, A. Bourmaud, A. Kervoelen, C. Morvan, and C. Baley, 'Analysis of the role of the main constitutive polysaccharides in the flax fibre mechanical behaviour', *Industrial Crops and Products*, vol. 76, pp. 1039–1048, Dec. 2015, doi: 10.1016/j.indcrop.2015.07.062.
[144] A. Bourmaud, C. Morvan, and C. Baley, 'Importance of fiber preparation to optimize the surface and mechanical properties of unitary flax fiber', *Industrial Crops and Products*, vol. 32, no. 3, pp. 662–667, Nov. 2010, doi: 10.1016/j.indcrop.2010.08.002.
[145] L. Yan, N. Chouw, and X. Yuan, 'Improving the mechanical properties of natural fibre fabric reinforced epoxy composites by alkali treatment', *Journal of Reinforced Plastics and Composites*, vol. 31, no. 6, pp. 425–437, Mar. 2012, doi: 10.1177/0731684412439494.
[146] K. Lacasse and W. Baumann, *Textile Chemicals: Environmental Data and Facts*. Springer Science & Business Media, 2012.
[147] J. Z. Lu, 'Chemical coupling in wood fiber and polymer composites: A review of coupling agents and treatments', *Wood and Fiber Science*, vol. 32, no. 1, pp. 88–104, 2000.
[148] J. George, M. S. Sreekala, and S. Thomas, 'A review on interface modification and characterization of natural fiber reinforced plastic composites', *Polymer Engineering & Science*, vol. 41, no. 9, pp. 1471–1485, 2001, doi: 10.1002/pen.10846.
[149] A. Gholampour and T. Ozbakkaloglu, 'A review of natural fiber composites: properties, modification and processing techniques, characterization, applications', *J Mater Sci*, vol. 55, no. 3, pp. 829–892, Jan. 2020, doi: 10.1007/s10853-019-03990-y.
[150] N. E. Zafeiropoulos, C. A. Baillie, and J. M. Hodgkinson, 'Engineering and characterisation of the interface in flax fibre/polypropylene composite materials. Part II. The effect of surface treatments on the interface', *Composites Part A: Applied Science and Manufacturing*, vol. 33, no. 9, pp. 1185–1190, Sep. 2002, doi: 10.1016/S1359-835X(02)00088-X.
[151] X. Li, L. G. Tabil, and S. Panigrahi, 'Chemical Treatments of Natural Fiber for Use in Natural Fiber-Reinforced Composites: A Review', *J Polym Environ*, vol. 15, no. 1, pp. 25–33, Jan. 2007, doi: 10.1007/s10924-006-0042-3.
[152] Bourmaud, J. Riviere, A. Le Duigou, G. Raj, and C. Baley, 'Investigations of the use of a mussel-inspired compatibilizer to improve the matrix-fiber adhesion of a biocomposite', *Polymer Testing*, vol. 28, no. 6, pp. 668–672, Sep. 2009, doi: 10.1016/j.polymertesting.2009.04.006.
[153] N. E. Zafeiropoulos, *Interface Engineering of Natural Fibre Composites for Maximum Performance*. Elsevier, 2011.
[154] K. L. Pickering, M. G. A. Efendy, and T. M. Le, 'A review of recent developments in natural fibre composites and their mechanical performance', *Composites Part A: Applied Science and Manufacturing*, vol. 83, pp. 98–112, Apr. 2016, doi: 10.1016/j.compositesa.2015.08.038.
[155] Mohanty, M. Misra, and L. T. Drzal, 'Surface modifications of natural fibers and performance of the resulting biocomposites: An overview', *Composite Interfaces*, vol. 8, no. 5, pp. 313–343, Jan. 2001, doi: 10.1163/156855401753255422.
[156] J.-M. Park, S. T. Quang, B.-S. Hwang, and K. L. DeVries, 'Interfacial evaluation of modified Jute and Hemp fibers/polypropylene (PP)-maleic anhydride polypropylene copolymers (PP-MAPP) composites using micromechanical technique and nondestructive acoustic emission', *Composites Science and Technology*, vol. 66, no. 15, pp. 2686–2699, Dec. 2006, doi: 10.1016/j.compscitech.2006.03.014.
[157] P.-J. Liotier *et al.*, 'Role of interface formation versus fibres properties in the mechanical behaviour of bio-based composites manufactured by Liquid Composite Molding processes', *Composites Part B: Engineering*, pp. 86–95, Apr. 2019.

[158] C. Gourier, A. Le Duigou, A. Bourmaud, and C. Baley, 'Mechanical analysis of elementary flax fibre tensile properties after different thermal cycles', *Composites Part A: Applied Science and Manufacturing*, vol. 64, pp. 159–166, Sep. 2014, doi: 10.1016/j.compositesa.2014.05.006.
[159] E. Zini, M. Baiardo, L. Armelao, and M. Scandola, 'Biodegradable Polyesters Reinforced with Surface-Modified Vegetable Fibers', *Macromolecular Bioscience*, vol. 4, no. 3, pp. 286–295, 2004, doi: 10.1002/mabi.200300120.
[160] E. Zini, M. L. Focarete, I. Noda, and M. Scandola, 'Bio-composite of bacterial poly(3-hydroxybutyrate-co-3-hydroxyhexanoate) reinforced with vegetable fibers', *Composites Science and Technology*, vol. 67, no. 10, pp. 2085–2094, Aug. 2007, doi: 10.1016/j.compscitech.2006.11.015.
[161] M. Baiardo, E. Zini, and M. Scandola, 'Flax fibre–polyester composites', *Composites Part A: Applied Science and Manufacturing*, vol. 35, no. 6, pp. 703–710, Jun. 2004, doi: 10.1016/j.compositesa.2004.02.004.
[162] G. Cantero, A. Arbelaiz, R. Llano-Ponte, and I. Mondragon, 'Effects of fibre treatment on wettability and mechanical behaviour of flax/polypropylene composites', *Composites Science and Technology*, vol. 63, no. 9, pp. 1247–1254, Jul. 2003, doi: 10.1016/S0266-3538(03)00094-0.
[163] Y. El Moussi, B. Otazaghine, A.-S. Caro-Bretelle, R. Sonnier, A. Taguet, and N. L. Moigne, 'Controlling interfacial interactions in LDPE/flax fibre biocomposites by a combined chemical and radiation-induced grafting approach', *Cellulose*, 2020, Accessed: Jun. 05, 2020. [Online]. Available: https://hal.mines-ales.fr/hal-02632185.
[164] V. Fiore, T. Scalici, and A. Valenza, 'Effect of sodium bicarbonate treatment on mechanical properties of flax-reinforced epoxy composite materials':, *Journal of Composite Materials*, Jul. 2017, doi: 10.1177/0021998317720009.
[165] M. Kodal, Z. D. Topuk, and G. Ozkoc, 'Dual effect of chemical modification and polymer precoating of flax fibers on the properties of short flax fiber/poly(lactic acid) composites', *Journal of Applied Polymer Science*, vol. 132, no. 48, 2015, doi: 10.1002/app.42564.
[166] Q. Hu, X. Yan, C. Dong, and W. Hu, 'Chemical modifications on linen for unsaturated polyester composites', *Chem. Res. Chin. Univ.*, vol. 32, no. 6, pp. 1057–1062, Dec. 2016, doi: 10.1007/s40242-016-6101-y.
[167] I. Van de Weyenberg, T. Chi Truong, B. Vangrimde, and I. Verpoest, 'Improving the properties of UD flax fibre reinforced composites by applying an alkaline fibre treatment', *Composites Part A: Applied Science and Manufacturing*, vol. 37, no. 9, pp. 1368–1376, Sep. 2006, doi: 10.1016/j.compositesa.2005.08.016.
[168] S. Marais *et al.*, 'Unsaturated polyester composites reinforced with flax fibers: effect of cold plasma and autoclave treatments on mechanical and permeation properties', *Composites Part A: Applied Science and Manufacturing*, vol. 36, no. 7, pp. 975–986, Jul. 2005, doi: 10.1016/j.compositesa.2004.11.008.
[169] A. Arbelaiz, B. Fernández, J. A. Ramos, A. Retegi, R. Llano-Ponte, and I. Mondragon, 'Mechanical properties of short flax fibre bundle/polypropylene composites: Influence of matrix/fibre modification, fibre content, water uptake and recycling', *Composites Science and Technology*, vol. 65, no. 10, pp. 1582–1592, Aug. 2005, doi: 10.1016/j.compscitech.2005.01.008.
[170] F. Barthelat, R. Rabiei, and A. K. Dastjerdi, 'Multiscale toughness amplification in natural composites', *MRS Online Proceedings Library Archive*, vol. 1420, ed 2012, doi: 10.1557/opl.2012.714.
[171] F. Libonati and M. J. Buehler, 'Advanced Structural Materials by Bioinspiration', *Advanced Engineering Materials*, vol. 19, no. 5, p. 1600787, 2017, doi: 10.1002/adem.201600787.
[172] M. H. Malakooti, Z. Zhou, J. H. Spears, T. J. Shankwitz, and H. A. Sodano, 'Biomimetic Nanostructured Interfaces for Hierarchical Composites', *Advanced Materials Interfaces*, vol. 3, no. 2, p. 1500404, 2016, doi: 10.1002/admi.201500404.

[173] F. Barthelat, 'Architectured materials in engineering and biology: fabrication, structure, mechanics and performance', *International Materials Reviews*, vol. 60, no. 8, pp. 413–430, Nov. 2015, doi: 10.1179/1743280415Y.0000000008.
[174] U. G. K. Wegst, H. Bai, E. Saiz, A. P. Tomsia, and R. O. Ritchie, 'Bioinspired structural materials', *Nature Materials*, vol. 14, no. 1, Art. no. 1, Jan. 2015, doi: 10.1038/nmat4089.
[175] A. R. Studart, 'Biological and Bioinspired Composites with Spatially Tunable Heterogeneous Architectures', *Advanced Functional Materials*, vol. 23, no. 36, pp. 4423–4436, 2013, doi: 10.1002/adfm.201300340.
[176] C. Sanchez, H. Arribart, and M. M. Giraud Guille, 'Biomimetism and bioinspiration as tools for the design of innovative materials and systems', *Nature Materials*, vol. 4, no. 4, pp. 277–288, Apr. 2005, doi: 10.1038/nmat1339.
[177] M. Li *et al.*, 'Preparation of and research on bioinspired graphene oxide/nanocellulose/polydopamine ternary artificial nacre', *Materials & Design*, vol. 181, p. 107961, Nov. 2019, doi: 10.1016/j.matdes.2019.107961.
[178] J. Duan, S. Gong, Y. Gao, X. Xie, L. Jiang, and Q. Cheng, 'Bioinspired Ternary Artificial Nacre Nanocomposites Based on Reduced Graphene Oxide and Nanofibrillar Cellulose', *ACS Appl. Mater. Interfaces*, vol. 8, no. 16, pp. 10545–10550, Apr. 2016, doi: 10.1021/acsami.6b02156.
[179] L. S. Dimas and M. J. Buehler, 'Influence of geometry on mechanical properties of bio-inspired silica-based hierarchical materials', *Bioinspir. Biomim.*, vol. 7, no. 3, p. 036024, Jun. 2012, doi: 10.1088/1748-3182/7/3/036024.
[180] J. Du, X. Niu, N. Rahbar, and W. Soboyejo, 'Bio-inspired dental multilayers: Effects of layer architecture on the contact-induced deformation', *Acta Biomaterialia*, vol. 9, no. 2, pp. 5273–5279, Feb. 2013, doi: 10.1016/j.actbio.2012.08.034.
[181] D. V. Opdenbosch, G. Fritz-Popovski, O. Paris, and C. Zollfrank, 'Silica replication of the hierarchical structure of wood with nanometer precision', *Journal of Materials Research*, vol. 26, no. 10, pp. 1193–1202, May 2011, doi: 10.1557/jmr.2011.98.
[182] H. S. Gupta, J. Seto, W. Wagermaier, P. Zaslansky, P. Boesecke, and P. Fratzl, 'Cooperative deformation of mineral and collagen in bone at the nanoscale', *Proceedings of the National Academy of Sciences*, vol. 103, no. 47, pp. 17741–17746, Nov. 2006, doi: 10.1073/pnas.0604237103.
[183] S. Weiner and H. D. Wagner, 'THE MATERIAL BONE: Structure-Mechanical Function Relations', *Annual Review of Materials Science*, vol. 28, no. 1, pp. 271–298, 1998, doi: 10.1146/annurev.matsci.28.1.271.
[184] U. Müller, W. Gindl-Altmutter, J. Konnerth, G. A. Maier, and J. Keckes, 'Synergy of multi-scale toughening and protective mechanisms at hierarchical branch-stem interfaces', *Scientific Reports*, vol. 5, no. 1, Nov. 2015, doi: 10.1038/srep14522.
[185] G. J. Ehlert, U. Galan, and H. A. Sodano, 'Role of Surface Chemistry in Adhesion between ZnO Nanowires and Carbon Fibers in Hybrid Composites', *ACS Appl. Mater. Interfaces*, vol. 5, no. 3, pp. 635–645, Feb. 2013, doi: 10.1021/am302060v.
[186] U. Galan, Y. Lin, G. J. Ehlert, and H. A. Sodano, 'Effect of ZnO nanowire morphology on the interfacial strength of nanowire coated carbon fibers', *Composites Science and Technology*, vol. 71, no. 7, pp. 946–954, May 2011, doi: 10.1016/j.compscitech.2011.02.010.
[187] J. Karger-Kocsis, H. Mahmood, and A. Pegoretti, 'Recent advances in fiber/matrix interphase engineering for polymer composites', *Progress in Materials Science*, vol. 73, pp. 1–43, Aug. 2015, doi: 10.1016/j.pmatsci.2015.02.003.
[188] J. Karger-Kocsis, H. Mahmood, and A. Pegoretti, 'All-carbon multi-scale and hierarchical fibers and related structural composites: A review', *Composites Science and Technology*, vol. 186, p. 107932, Jan. 2020, doi: 10.1016/j.compscitech.2019.107932.
[189] J. J. Vargis and C. Vargis, 'Surface Whiskerization Of Carbon Fibers With Carbon Nanotubes', 2007.

[190] M. Sharma, S. Gao, E. Mäder, H. Sharma, L. Y. Wei, and J. Bijwe, 'Carbon fiber surfaces and composite interphases', *Composites Science and Technology*, vol. 102, pp. 35–50, Oct. 2014, doi: 10.1016/j.compscitech.2014.07.005.
[191] L. Chen *et al.*, 'Role of a gradient interface layer in interfacial enhancement of carbon fiber/epoxy hierarchical composites', *J Mater Sci*, vol. 50, no. 1, pp. 112–121, Jan. 2015, doi: 10.1007/s10853-014-8571-y.
[192] E. J. Garcia, B. L. Wardle, A. John Hart, and N. Yamamoto, 'Fabrication and multifunctional properties of a hybrid laminate with aligned carbon nanotubes grown In Situ', *Composites Science and Technology*, vol. 68, no. 9, pp. 2034–2041, Jul. 2008, doi: 10.1016/j.compscitech.2008.02.028.
[193] K. L. Kepple, G. P. Sanborn, P. A. Lacasse, K. M. Gruenberg, and W. J. Ready, 'Improved fracture toughness of carbon fiber composite functionalized with multi walled carbon nanotubes', *Carbon*, vol. 46, no. 15, pp. 2026–2033, Dec. 2008, doi: 10.1016/j.carbon.2008.08.010.
[194] W. X. Wang, Y. Takao, T. Matsubara, and H. S. Kim, 'Improvement of the interlaminar fracture toughness of composite laminates by whisker reinforced interlamination', *Composites Science and Technology*, vol. 62, no. 6, pp. 767–774, May 2002, doi: 10.1016/S0266-3538(02)00052-0.
[195] C. I. Idumah and A. Hassan, 'Emerging trends in eco-compliant, synergistic, and hybrid assembling of multifunctional polymeric bionanocomposites', *Reviews in Chemical Engineering*, vol. 32, no. 3, pp. 305–361, Jun. 2016, doi: 10.1515/revce-2015-0046.
[196] N. Saba, M. Jawaid, and M. Asim, 'Recent Advances in Nanoclay/Natural Fibers Hybrid Composites', in *Nanoclay Reinforced Polymer Composites: Natural Fibre/Nanoclay Hybrid Composites*, M. Jawaid, A. el K. Qaiss, and R. Bouhfid, Eds. Singapore: Springer, 2016, pp. 1–28.
[197] K.-Y. Lee, A. Delille, and A. Bismarck, 'Greener Surface Treatments of Natural Fibres for the Production of Renewable Composite Materials', in *Cellulose Fibers: Bio- and Nano-Polymer Composites*, S. Kalia, B. S. Kaith, and I. Kaur, Eds. Berlin, Heidelberg: Springer Berlin Heidelberg, 2011, pp. 155–178.
[198] M. Pommet *et al.*, 'Surface Modification of Natural Fibers Using Bacteria: Depositing Bacterial Cellulose onto Natural Fibers To Create Hierarchical Fiber Reinforced Nanocomposites', *Biomacromolecules*, vol. 9, no. 6, pp. 1643–1651, Jun. 2008, doi: 10.1021/bm800169g.
[199] D. Dai and M. Fan, 'Green modification of natural fibres with nanocellulose', *RSC Advances*, vol. 3, no. 14, p. 4659, 2013, doi: 10.1039/c3ra22196b.
[200] J.-Y. Rho, L. Kuhn-Spearing, and P. Zioupos, 'Mechanical properties and the hierarchical structure of bone', *Medical Engineering & Physics*, vol. 20, no. 2, pp. 92–102, Mar. 1998, doi: 10.1016/S1350-4533(98)00007-1.
[201] S. Weiner, W. Traub, and H. D. Wagner, 'Lamellar Bone: Structure–Function Relations', *Journal of Structural Biology*, vol. 126, no. 3, pp. 241–255, Jun. 1999, doi: 10.1006/jsbi.1999.4107.
[202] S. Kamat, X. Su, R. Ballarini, and A. H. Heuer, 'Structural basis for the fracture toughness of the shell of the conch Strombus gigas', *Nature*, vol. 405, no. 6790, pp. 1036–1040, Jun. 2000, doi: 10.1038/35016535.
[203] A. P. Jackson, J. F. V. Vincent, R. M. Turner, and R. M. Alexander, 'The mechanical design of nacre', *Proceedings of the Royal Society of London. Series B. Biological Sciences*, vol. 234, no. 1277, pp. 415–440, Sep. 1988, doi: 10.1098/rspb.1988.0056.
[204] A. L. Gershon, H. A. Bruck, S. Xu, M. A. Sutton, and V. Tiwari, 'Multiscale mechanical and structural characterizations of Palmetto wood for bio-inspired hierarchically structured polymer composites', *Materials Science and Engineering: C*, vol. 30, no. 2, pp. 235–244, Jan. 2010, doi: 10.1016/j.msec.2009.10.004.
[205] W. J. Landis, 'The strength of a calcified tissue depends in part on the molecular structure and organization of its constituent mineral crystals in their organic matrix', *Bone*, vol. 16, no. 5, pp. 533–544, May 1995, doi: 10.1016/8756-3282(95)00076-P.
[206] P. Roschger *et al.*, 'Structural Development of the Mineralized Tissue in the Human L4 Vertebral Body', *Journal of Structural Biology*, vol. 136, no. 2, pp. 126–136, Nov. 2001, doi: 10.1006/jsbi.2001.4427.

[207] M. E. Launey, M. J. Buehler, and R. O. Ritchie, 'On the Mechanistic Origins of Toughness in Bone', *Annual Review of Materials Research*, vol. 40, no. 1, pp. 25–53, 2010, doi: 10.1146/annurev-matsci-070909-104427.
[208] H. Peterlik, P. Roschger, K. Klaushofer, and P. Fratzl, 'From brittle to ductile fracture of bone', *Nature Materials*, vol. 5, no. 1, Art. no. 1, Jan. 2006, doi: 10.1038/nmat1545.
[209] R. K. Nalla, J. J. Kruzic, J. H. Kinney, and R. O. Ritchie, 'Mechanistic aspects of fracture and R-curve behavior in human cortical bone', *Biomaterials*, vol. 26, no. 2, pp. 217–231, Jan. 2005, doi: 10.1016/j.biomaterials.2004.02.017.
[210] E. A. Zimmermann *et al.*, 'Intrinsic mechanical behavior of femoral cortical bone in young, osteoporotic and bisphosphonate-treated individuals in low- and high energy fracture conditions', *Scientific Reports*, vol. 6, no. 1, Art. no. 1, Feb. 2016, doi: 10.1038/srep21072.
[211] H. Gao, B. Ji, I. L. Jager, E. Arzt, and P. Fratzl, 'Materials become insensitive to flaws at nanoscale: Lessons from nature', *Proceedings of the National Academy of Sciences*, vol. 100, no. 10, pp. 5597–5600, May 2003, doi: 10.1073/pnas.0631609100.
[212] R. Menig, M. H. Meyers, M. A. Meyers, and K. S. Vecchio, 'Quasi-static and dynamic mechanical response of Haliotis rufescens (abalone) shells', *Acta Materialia*, vol. 48, no. 9, pp. 2383–2398, May 2000, doi: 10.1016/S1359-6454(99)00443-7.
[213] R. Z. Wang, Z. Suo, A. G. Evans, N. Yao, and I. A. Aksay, 'Deformation mechanisms in nacre', *Journal of Materials Research*, vol. 16, no. 9, pp. 2485–2493, Sep. 2001, doi: 10.1557/JMR.2001.0340.
[214] F. Song and Y. L. Bai, 'Effects of nanostructures on the fracture strength of the interfaces in nacre', *Journal of Materials Research*, vol. 18, no. 8, pp. 1741–1744, Aug. 2003, doi: 10.1557/JMR.2003.0239.
[215] M. A. Meyers, P.-Y. Chen, A. Y.-M. Lin, and Y. Seki, 'Biological materials: Structure and mechanical properties', *Progress in Materials Science*, vol. 53, no. 1, pp. 1–206, Jan. 2008, doi: 10.1016/j.pmatsci.2007.05.002.
[216] R. O. Ritchie, 'The conflicts between strength and toughness', *Nature Materials*, vol. 10, no. 11, Art. no. 11, Nov. 2011, doi: 10.1038/nmat3115.
[217] S. Mann, *Biomineralization: Principles and Concepts in Bioinorganic Materials Chemistry*. Oxford University Press, 2001.
[218] O. Zabihi, M. Ahmadi, Q. Li, S. Shafei, M. G. Huson, and M. Naebe, 'Carbon fibre surface modification using functionalized nanoclay: A hierarchical interphase for fibre-reinforced polymer composites', *Composites Science and Technology*, vol. 148, pp. 49–58, Aug. 2017, doi: 10.1016/j.compscitech.2017.05.013.
[219] A. K. Subramaniyan and C. T. Sun, 'Interlaminar Fracture Behavior of Nanoclay Reinforced Glass Fiber Composites', *Journal of Composite Materials*, vol. 42, no. 20, pp. 2111–2122, Oct. 2008, doi: 10.1177/0021998308094550.
[220] S. Gao, R.-C. Zhuang, J. Zhang, J.-W. Liu, and E. Mäder, 'Glass Fibers with Carbon Nanotube Networks as Multifunctional Sensors', *Advanced Functional Materials*, vol. 20, no. 12, pp. 1885–1893, Jun. 2010, doi: 10.1002/adfm.201000283.
[221] G. J. Ehlert and H. A. Sodano, 'Zinc Oxide Nanowire Interphase for Enhanced Interfacial Strength in Lightweight Polymer Fiber Composites', *ACS Appl. Mater. Interfaces*, vol. 1, no. 8, pp. 1827–1833, Aug. 2009, doi: 10.1021/am900376t.
[222] H. Qian, A. Bismarck, E. S. Greenhalgh, and M. S. P. Shaffer, 'Carbon nanotube grafted carbon fibres: A study of wetting and fibre fragmentation', *Composites Part A: Applied Science and Manufacturing*, vol. 41, no. 9, pp. 1107–1114, Sep. 2010, doi: 10.1016/j.compositesa.2010.04.004.
[223] M. Tansan, 'Tailoring interfacial interactions in fiber reinforced polymeric composites by the electrospray deposition of waterborne carbon nanotubes', 2019.
[224] M. R. Zakaria, 'Woven Carbon Fiber Epoxy Composite Laminates Reinforced With Carbon Nanotube Interlayer Using Electrospray Deposition Method', 2020.

[225] S. Mayela Garcia Montes, 'Synthesis of carbon nanotubes on surface of recovered carbon fibers by chemical vapor deposition, as a sizing process to obtain a hybrid material', 2017.
[226] C. Hu, X. Liao, Q.-H. Qin, and G. Wang, 'The fabrication and characterization of high density polyethylene composites reinforced by carbon nanotube coated carbon fibers', *Composites Part A: Applied Science and Manufacturing*, vol. 121, pp. 149–156, Jun. 2019, doi: 10.1016/j.compositesa.2019.03.027.
[227] G. Han, Y. Lei, Q. Wu, Y. Kojima, and S. Suzuki, 'Bamboo–Fiber Filled High Density Polyethylene Composites: Effect of Coupling Treatment and Nanoclay', *J Polym Environ*, vol. 16, no. 2, pp. 123–130, Apr. 2008, doi: 10.1007/s10924-008-0094-7.
[228] A. Najafi, B. Kord, A. Abdi, and S. Ranaee, 'The impact of the nature of nanoclay on physical and mechanical properties of polypropylene/reed flour nanocomposites':, *Journal of Thermoplastic Composite Materials*, Sep. 2011, doi: 10.1177/0892705711412813.
[229] A. R. Rozyanty, H. D. Rozman, and G. S. Tay, 'Ultra-Violet Radiationcured Composites Based on Unsaturated Polyester Resin Filled with MMT and Kenaf Bast Fiber', *Advanced Materials Research*, vol. 264–265, pp. 712–718, Jun. 2011, doi: 10.4028/www.scientific.net/AMR.264-265.712.
[230] S. O. Han, M. Karevan, M. A. Bhuiyan, J. H. Park, and K. Kalaitzidou, 'Effect of exfoliated graphite nanoplatelets on the mechanical and viscoelastic properties of poly(lactic acid) biocomposites reinforced with kenaf fibers', *J Mater Sci*, vol. 47, no. 8, pp. 3535–3543, Apr. 2012, doi: 10.1007/s10853-011-6199-8.
[231] Y. Li, C. Chen, J. Xu, Z. Zhang, B. Yuan, and X. Huang, 'Improved mechanical properties of carbon nanotubes-coated flax fiber reinforced composites', *J Mater Sci*, vol. 50, no. 3, pp. 1117–1128, Feb. 2015, doi: 10.1007/s10853-014-8668-3.
[232] C. Yang, R. Han, M. Nie, and Q. Wang, 'Interfacial reinforcement mechanism in poly(lactic acid)/natural fiber biocomposites featuring ZnO nanowires at the interface', *Materials & Design*, vol. 186, p. 108332, Jan. 2020, doi: 10.1016/j.matdes.2019.108332.
[233] H. Wang, G. Xian, and H. Li, 'Grafting of nano-TiO2 onto flax fibers and the enhancement of the mechanical properties of the flax fiber and flax fiber/epoxy composite', *Composites Part A: Applied Science and Manufacturing*, vol. 76, pp. 172–180, Sep. 2015, doi: 10.1016/j.compositesa.2015.05.027.
[234] K.-Y. Lee, G. Buldum, A. Mantalaris, and A. Bismarck, 'More Than Meets the Eye in Bacterial Cellulose: Biosynthesis, Bioprocessing, and Applications in Advanced Fiber Composites', *Macromolecular Bioscience*, vol. 14, no. 1, pp. 10–32, 2014, doi: 10.1002/mabi.201300298.
[235] M. Iguchi, S. Yamanaka, and A. Budhiono, 'Review Bacterial cellulose—a masterpiece of nature's arts', *Journal of Materials Science*, vol. 35, pp. 261–270, 2000.
[236] W. Czaja, D. Romanovicz, and R. malcolm Brown, 'Structural investigations of microbial cellulose produced in stationary and agitated culture', *Cellulose*, vol. 11, no. 3/4, pp. 403–411, Sep. 2004, doi: 10.1023/B:CELL.0000046412.11983.61.
[237] G. Guhados, W. Wan, and J. L. Hutter, 'Measurement of the Elastic Modulus of Single Bacterial Cellulose Fibers Using Atomic Force Microscopy', *Langmuir*, vol. 21, no. 14, pp. 6642–6646, Jul. 2005, doi: 10.1021/la0504311.
[238] Y. Chen, X. Zhou, X. Yin, Q. Lin, and M. Zhu, 'A Novel Route to Modify the Interface of Glass Fiber-Reinforced Epoxy Resin Composite via Bacterial Cellulose', *International Journal of Polymeric Materials and Polymeric Biomaterials*, vol. 63, no. 4, pp. 221–227, Mar. 2014, doi: 10.1080/00914037.2013.830250.
[239] A. Asadi, M. Miller, R. J. Moon, and K. Kalaitzidou, 'Improving the interfacial and mechanical properties of short glass fiber/epoxy composites by coating the glass fibers with cellulose nanocrystals', *Express Polymer Letters*, vol. 10, no. 7, pp. 587–597, 2016, doi: 10.3144/expresspolymlett.2016.54.

[240] S. Shariatnia, A. V. Kumar, O. Kaynan, and A. Asadi, 'Hybrid Cellulose Nanocrystal-Bonded Carbon Nanotubes/Carbon Fiber Polymer Composites for Structural Applications', *ACS Appl. Nano Mater.*, vol. 3, no. 6, pp. 5421–5436, Jun. 2020, doi: 10.1021/acsanm.0c00785.
[241] A. Kumar, S. Shariatnia, and A. Asadi, 'Cellulose Nanocrystals Assisted Process to Integrate Carbon Nanotubes in CFRP Composites', in *AIAA Scitech 2020 Forum*, American Institute of Aeronautics and Astronautics, 2020.
[242] J. A. Fernandez, 'Modification of flax fibres for the development of epoxy-based biocomposites', IMT Mines Alès, 2016.
[243] J. Juntaro, M. Pommet, A. Mantalaris, M. Shaffer, and A. Bismarck, 'Nanocellulose enhanced interfaces in truly green unidirectional fibre reinforced composites', *Composite Interfaces*, vol. 14, no. 7–9, pp. 753–762, Jan. 2007, doi: 10.1163/156855407782106573.
[244] J. Juntaro, M. Pommet, G. Kalinka, A. Mantalaris, M. S. P. Shaffer, and A. Bismarck, 'Creating Hierarchical Structures in Renewable Composites by Attaching Bacterial Cellulose onto Sisal Fibers', *Advanced Materials*, vol. 20, no. 16, pp. 3122–3126, 2008, doi: 10.1002/adma.200703176.
[245] K.-Y. Lee, P. Bharadia, J. J. Blaker, and A. Bismarck, 'Short sisal fibre reinforced bacterial cellulose polylactide nanocomposites using hairy sisal fibres as reinforcement', *Composites Part A: Applied Science and Manufacturing*, vol. 43, no. 11, pp. 2065–2074, Nov. 2012, doi: 10.1016/j.compositesa.2012.06.013.
[246] K.-Y. Lee, K. K. C. Ho, K. Schlufter, and A. Bismarck, 'Hierarchical composites reinforced with robust short sisal fibre preforms utilising bacterial cellulose as binder', *Composites Science and Technology*, vol. 72, no. 13, pp. 1479–1486, Aug. 2012, doi: 10.1016/j.compscitech.2012.06.014.
[247] S. Dong and R. Gauvin, 'Application of dynamic mechanical analysis for the study of the interfacial region in carbon fiber/epoxy composite materials', *Polymer Composites*, vol. 14, no. 5, pp. 414–420, 1993, doi: 10.1002/pc.750140508.
[248] N. Le Moigne, 'Study of the interface in natural fibres reinforced poly(lactic acid) biocomposites modified by optimized organosilane treatments', 2014. https://ac-els-cdn-com.gaelnomade-1.grenet.fr/S0926669013006481/1-s2.0-S0926669013006481-main.pdf?_tid=e3c134a0-b88e-11e7-b1ba-00000aacb361&acdnat=1508831130_e27b5e60e2ad05855251cc3a8979f342 (accessed Oct. 24, 2017).
[249] S. Ghasemi, M. Tajvidi, D. W. Bousfield, and D. J. Gardner, 'Reinforcement of natural fiber yarns by cellulose nanomaterials: A multi-scale study', *Industrial Crops and Products*, vol. 111, pp. 471–481, Jan. 2018, doi: 10.1016/j.indcrop.2017.11.016.

CHAPTER II

Adsorption of xyloglucan and cellulose nanocrystals on flax fibres for the creation of hierarchical fibres

Table of contents - Chapter II

This Chapter is adapted from Doineau E., Bauer G., Ensenlaz L., Novales B., Sillard C., Bénézet J-C., Bras J., Cathala B., Le Moigne N. « Adsorption of xyloglucan and cellulose nanocrystals on natural fibres for the creation of hierarchically structured fibres », Carbohydrate Polymers, vol. 248, p. 116713, nov. 2020.

II. 1. Introduction

Surface treatments of natural fibres (chemical, physical, enzymatic...) are commonly used in a wide range of industrial sectors like textile, paper or biocomposites to bring them specific properties according to the targeted applications [1]. For instance, in textile applications, surface treatments primarily concern the dyeing and the finishing while in paper industry, surface treatments target functional properties such as printability, bleaching, hydrophobicity, gas barrier, softness, strong mechanical properties. In the more recently developed field of biocomposites, most of the natural fibres surface treatments are developed to improve wettability and compatibility with polymeric matrices. In all these applications, environmental concerns prompt the search and the development of environmental friendly surface treatments procedures in order to decrease the use of polluting chemical products [2]–[8].

In the search of innovative and greener surface modifications of natural fibres, functionalization with nanoparticules or biopolymers knows a growing interest [9]–[16]. With this long term goal, this work proposes to combine adsorption capacity of xyloglucan (XG) on cellulosic substrates with the outstanding properties of cellulose nanocrystals (CNC) to develop hierarchically structured assemblies at the surface of flax woven fabrics. XG is an hemicellulose found in the primary cell wall of plants, which is involved in the wall extensibility and its integrity, through its strong affinity with cellulose microfibrils [17]–[22]. On the other hand, CNC are used in many applications thanks to their amazing properties [23]. They have outstanding mechanical properties, i.e high Young's Modulus estimated between 100 and 150 GPa, a high specific surface area [24]–[28] and can be chemically functionalized through substitution of their hydroxyl groups. Xyloglucan interactions with cellulosic surfaces have been intensively studied in vitro and in vivo [29], [30], [20], [31]–[33], and are known to be an entropy driven process [34].

XG and cellulose interact through hydrogen, van der Waals and polar bonds. The hydroxyl groups, in majority on the glucan chains, will interact each other and create physicochemical interactions. The final architecture of the cellulose/xyloglucan assemblies is related to concentrations of the building blocks, the molar mass and other adsorption processing parameters [34], [35], [19], [36], [30], [37]–[40], [33]. In particular, the strong affinity of XG for cellulose surfaces has attracted researchers for the elaboration of cellulose-based materials as natural cross-linker. For instance, XG and CNC have been already used for the implementation of thin films displaying structural colors or for the reinforcement of nanocellulose aerogels [41]–[48].

Lignocellulosic fibres properties have also been improved by the adsorption of either XG or nanocellulose. For example, addition of XG by spraying on a bleached birch kraft pulp increases its wet web strength, tension holding, drying tension and also its smoothness [14]. Similarly, when XG is used as a wet end additives in paper making process, paper formation is facilitated and final paper strength is increased [49], [50]. Nanocellulose, and more especially bacterial cellulose, has also demonstrated its capacity to increase the strength of the interfacial adhesion between natural fibres and polymeric matrices as reported by Bismarck's group [12], [51]–[54], *detailed in* ***Chapter I – section I.3***. However, up to our knowledge there is no report of combined adsorption of XG and nanocellulose on (ligno-)cellulosic substrates. In this work, the challenge addressed is to characterize the adsorption of XG and CNC on flax fibres and the potential synergistic effect of the combination of the two biobased building blocks. Indeed, similarly to the plant wall architecture, combination of XG and CNC adsorption may yield different to final organization to achieve hierarchical materials combining microscale fibers displaying nanostructured surfaces. Moreover, this study has been achieved on substrates of industrial interest, i.e. flax woven fabrics that present additional levels of complexity when compared to model substrates or unitary natural fibres.

The adsorption of XG and CNC on flax woven fabrics is investigated in terms of localization by confocal and scanning electron microscopy. In order to quantify the adsorbed amount of XG and CNC on flax woven fabrics, adsorption isotherms are established by an UV spectroscopy method. Different adsorption sequences on flax woven fabrics are evaluated: (i) adsorption of

XG or CNC (ii) successive adsorption of XG then CNC, (iii) successive adsorption of CNC then XG. Finally, Atomic Force Microscopy (AFM) with XG and CNC modified tips was used to analyze the adhesion between XG, CNC and flax fibres.

II. 2. Materials and methods

II. 2. 1. Materials

A twill 2x2 flax woven fabric 200 g/m² was provided by SF Composites (France). Cellulose nanocrystals (CNC) were produced by acid hydrolysis of wood pulp and purchased in spray-dried powder from CelluForce (Quebec, Canada). CNC surface charge density : 0.023 mmol/g; Crystalline fraction : 0.88; CNC lateral dimensions : 2-5 nm; CNC length : 50-110 nm. Xyloglucan Glyloid 6 C was obtained from tamarind seed gum and purchased from DSP Gokyo Food & Chemical. Mw = 840 000 g/mol; Mw/Mn = 1.24, Rg 72 nm; monosaccharide composition: Glucose 50.7%; Xylose : 31.7%; Galactose 16.0%; Arabinose 1.6%. Fluorescent agents RBITC (Rhodamine B isothiocyanate) and FITC (Fluoresceine isothiocyanate) were purchased from Sigma-Aldrich.

II. 2. 2. Labelling of XG and CNC with RBITC and FITC

The fluorescent labelling of XG and CNC were performed according to the method reported by Belder A & Granath K [55]. The reaction occurring is the formation of covalent bonds between hydroxyl groups of polysaccharides and isothiocyanate groups of the fluorescent agents [56]. First, 1 g of CNC or XG was solubilized in 40 mL of DMSO under stirring and heated at 65°C. After 15 minutes, few drops of pyridine, 50 µL of dibutyltin dilaurate and 7.5 mg of RBITC (Rhodamine B Isothiocyanate) or FITC (Fluoresceine isothiocyanate) were added. The reaction was heated under stirring at 65°C during 2 hours. XG-RBITC and CNC-RBITC (or CNC-FITC) were recovered by precipitation in ethanol/acetone mixture for XG and NaCl 1M solution for CNC followed by centrifugation (10 min; 10000 g). Three dispersion/centrifugation cycles were

achieved and final precipitates were dissolved / dispersed in deionized water at average concentration of 1wt% and dialyzed (12-14000 MWCO) during one week against ultrapure water.

II. 2. 3. Adsorption experiments on flax woven fabrics

The different steps of adsorption experiments have been illustrated in **Figure II-1** and detailed below.

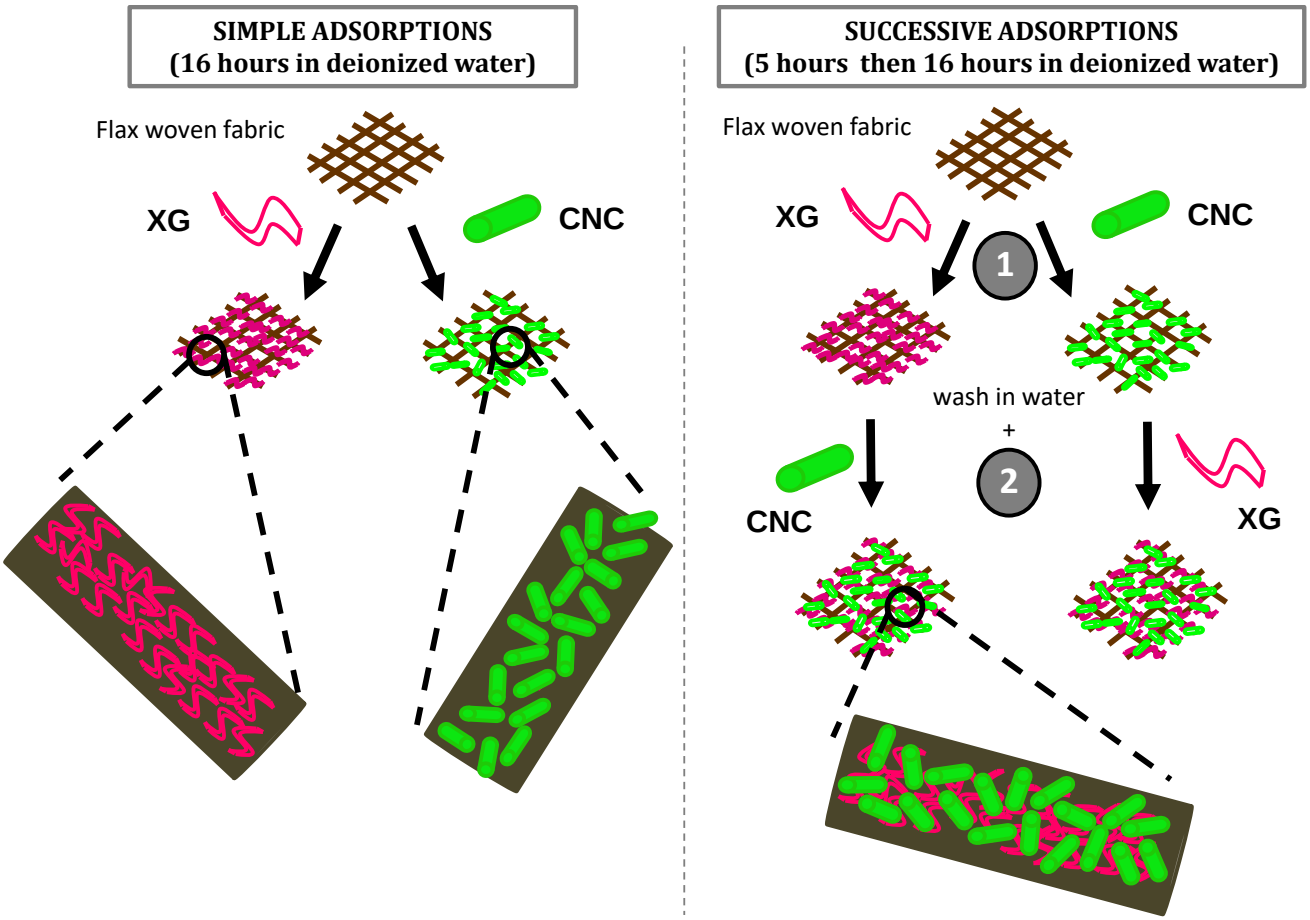

Figure II-1: Illustration of the different steps of the adsorption processes of the flax woven fabric with labeled cellulose nanocrystals (CNC) and xyloglucan (XG)

II. 2. 3. 1 Simple adsorptions

Small pieces of flax fabrics between 8 to 12 mg were cut and put in test tubes. To avoid the quenching of RBITC or FITC, all samples need to be in the dark (tubes were wrapped in aluminium film). XG-RBITC or CNC-RBITC solutions of 0.5 g/L were diluted with water in test tubes (final volume 5 mL) to obtain final concentrations ranging between 0.05 g/L and 0.45 g/L. Each adsorption experiment was duplicated. Reference samples were prepared in the same way without flax woven fabrics. Test tubes were gently shaken during 16 hours. Other samples were prepared with CNC-FITC in the same conditions for confocal microscopic observations. At least triplicate was performed.

II. 2. 3. 2 Successive adsorptions

For successive adsorptions of XG / CNC-RBITC and CNC / XG-RBITC on flax woven fabrics, similar protocol as for labeled-CNC or -XG adsorption was used preceded by adsorption of XG or CNC. A solution of non-labeled XG or CNC at 0.4 g/L was added in test tubes. After 5 hours, the flax woven fabrics were washed with deionized water. Labeled CNC or XG were added at concentrations ranging between 0.05 g/L and 0.45 g/L, during 16 hours. Other samples were prepared with both XG-RBITC and CNC-FITC in the same conditions for confocal microscopic observations. At least triplicate was performed.

After adsorption experiments, the supernatant was collected and the absorbance of Rhodamine at 558 nm for XG-RBITC or CNC-RBITC was measured by UV spectroscopy. The amount of adsorbed XG-RBITC and CNC-RBITC on the fibres was calculated by the difference between measured absorbance in test tubes with flax woven and the absorbance of reference tubes (without flax woven).

II. 2. 4. Scanning Electron Microscopy (SEM)

Elementary flax fibres extracted from the raw and treated flax woven fabrics were observed with an Environmental Scanning Electron Microscope (ESEM, FEI Quanta 200 FEG, Netherlands).

The samples were pasted on an adhesive wafer and metallized in high vacuum by depositing a thin layer of carbon on their surface using a BALZERS CED 030. SEM micrographs were obtained under high vacuum at an acceleration voltage of 3 keV, a working distance of 9 mm and magnification up to 50 000 X. At least 10 micrographs per sample were performed and the most representative pictures were conserved for the discussion.

II. 2. 5. Confocal microscopy

The confocal microscopy images were obtained using an inverted Nikon A1 laser scanning confocal microscope. Several pieces of yarns (raw or treated) were deposited between slide and slip cover with one spacer and deionized water, avoiding the prolonged light contact. The samples were viewed with a Plan Fluor 4× or with a Plan Apo 20× Nikon objective by scanning using a laser beam at a wavelength of 488 nm and 561 nm, for imaging FITC and RBITC fluorescences respectively. The emissions of fluorescence were recorded via a photomultiplier through 500–530 nm and 570–620 nm band-pass filters, respectively. Images were processed using the NIS-Element software (Nikon). At least triplicate was performed.

II. 2. 6. Atomic Force Microscopy (AFM)

AFM force curves (Bruker Icon dimension) between the tip and the substrate have been performed in the air to study the adhesion between xyloglucan (XG), cellulose nanocrystals (CNC) and flax fibres. Shortly, during the adhesive force measurements, the cantilever tip approached the surface of the substrate at a speed of 1.4 μm/s until contact, and then separated. Before all these measurements, calibrations have to be performed on the cantilever Sharp Nitride Lever (SNL-10, Bruker) with a tip radius below 10 nm. First, the stiffness of the cantilever was determined by the thermal tune method and gave a spring constant of 0.098 N/m. Secondly, the sensitivity of the cantilever has to be measured. To achieve this calibration, force curves have been performed on a sapphire in contact mode. By measuring the yield of the curve, made possible by a functionality of the AFM device, the sensitivity of the cantilever can be

determined. Then, the different force curves between cantilever tips and substrates were measured [57], [58]. The raw data were converted by a calculation algorithm detailed in **Figure II-2**.

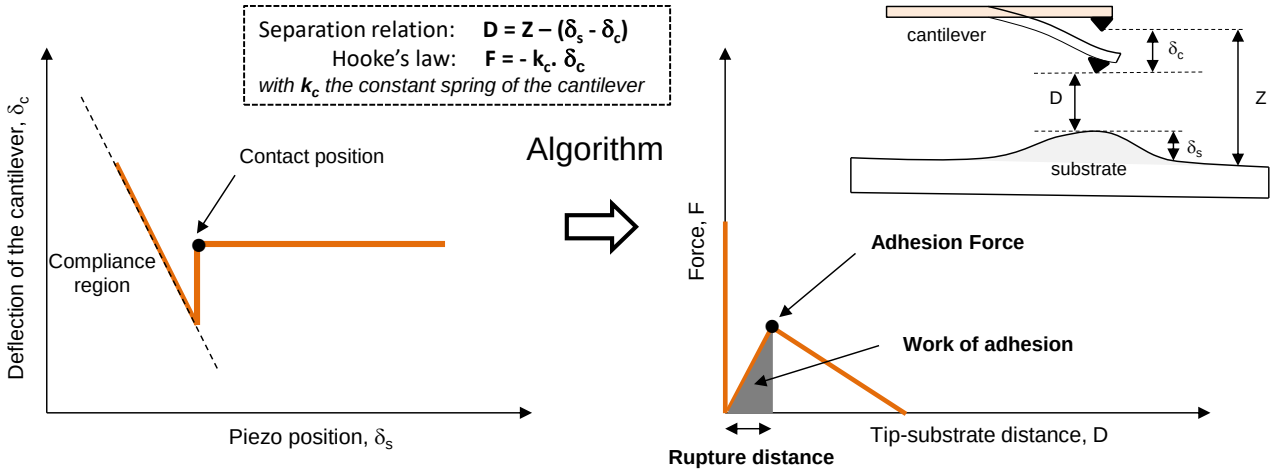

Figure II-2: Algorithm employed to convert the raw data graph of the force measurements obtained by AFM to the force-distance curve.

The method is based on the conversion of the raw data graph (deflection of the cantilever vs piezo position) into a force-distance curve representing the force vs the tip-substrate distance (D). The baseline was done and the zero separation was obtained from the gradient of the constant compliance region. Different parameters are required like the cantilever rest position (Z), the deflection of the cantilever (δc), the deformation of the surface of the substrate (δs) and the constant spring of the cantilever (kc).

In order to perform the experiments, two different tips functionalization have been done. First, one consisted on the dipping of the SNL-10 cantilever tip in a drop of XG solution at 20 g/L during 1 min and then a rinsing in water during 1 min before a drying at 60°C during 30 min. This functionalized tip is named XG-tip within this article. The second one consisted on a tip's functionalization with CNC. The pre-coating of the tip by polycations poly(ethylene imine) (PEI, Mw = 750 000, Sigma Aldrich) was made to decrease the time of dipping and obtain a uniform coating of CNC [59], [60]. The different steps of the dipping are described in the study of Jean *et al.* (2008). This functionalized tip is named CNC-tip within this article. Finally, a mica substrate

was also spin coated (POLO SPIN150i, SPS-Europe) by PEI and CNC following the protocol of Aulin *et al.* (2009), and is named CNC-surface throughout the article. Adhesion measurements were taken in contact mode at three localizations, 35 on each, i.e. 105 measurements in total for each configuration. No obvious irreversible deformation or damaging of the substrates or the tip was detected during the measurements.

II. 3. Results and discussions

II. 3. 1. Adsorption behaviour of XG and CNC on flax woven fabrics

In order to assess XG and CNC adsorption behaviors qualitatively and quantitatively, CNC and XG were labeled with fluorescent dies. In a first approach, confocal microscopy was used to study the localization and homogeneity of XG and CNC adsorption on flax fibres. Using the UV absorbance of the dies, the amount of XG and CNC adsorbed on flax fabrics were then used to determine adsorption isotherms.

II. 3. 1. 1 Microscopic observations

Confocal microscopy images in **Figure II-3** present two different views of XG-RBITC (**Figure II-3 a**) and CNC-FITC (**Figure II-3 b**) adsorbed on flax woven fabrics, at the scale of a yarn and an elementary fibre.

Both adsorption of XG-RBITC and CNC-FITC is homogeneous with no aggregates on the surface of yarns and elementary fibres. Some microfibrils functionalized by XG-RBITC or CNC-FITC were also observed at the surface of elementary fibres. These microfibrils probably originate from the peeling of fibre cell walls and/or the presence of impurities and residues at the surface of flax fibres generated during the manufacturing process of flax woven fabrics [63]. Some elementary flax fibres were extracted from the yarns of treated flax woven fabrics to compare qualitatively the homogeneity of XG-RBITC (**Figure II-3 c**) and CNC-FTIC (**Figure II-3 d**) adsorption across flax yarns diameter.

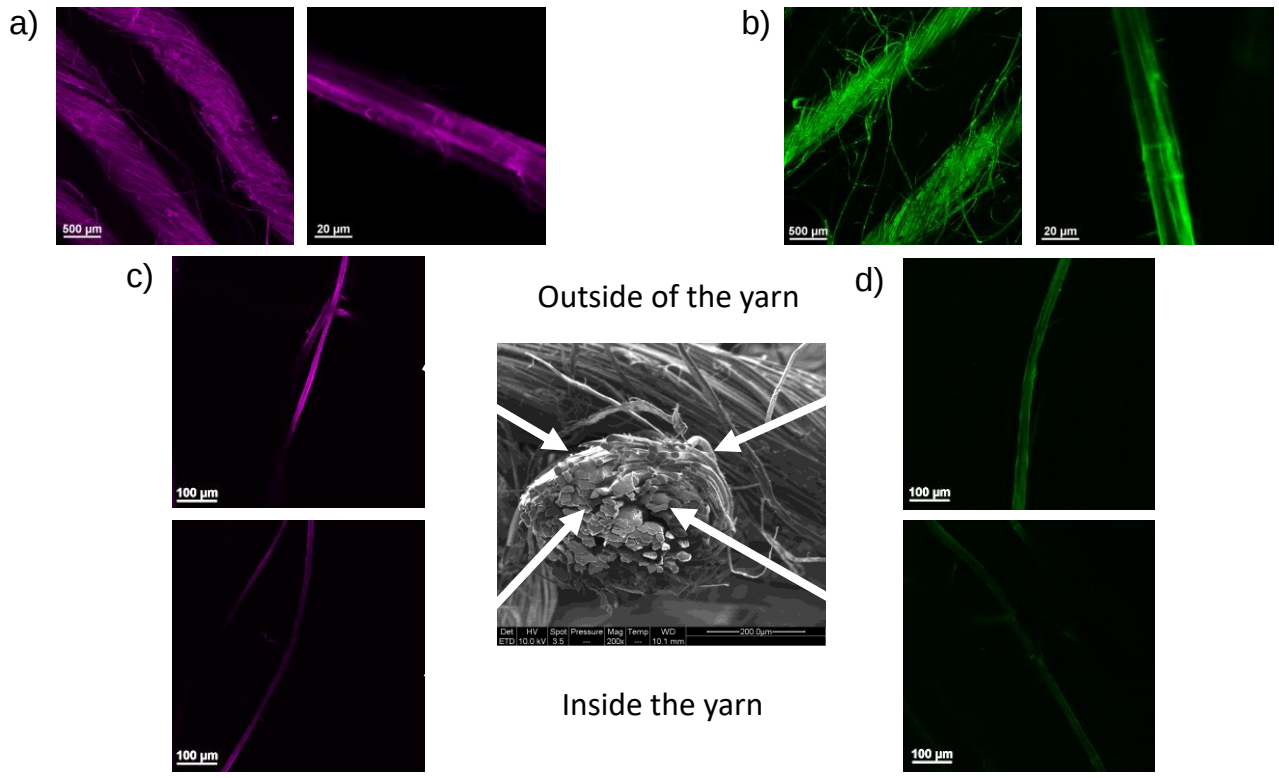

Figure II-3: Confocal microscopy images of (a) XG-RBITC and (b) CNC-FITC adsorption on flax yarns and elementary fibres; and of (c) XG-RBITC and (d) CNC-FITC adsorbed on elementary flax fibres extracted from different positions across the diameter of flax yarns.

The elementary fibres collected at the outer part of flax yarns show higher intensities for both CNC-FTIC and XG-RBITC, compared to fibres extracted within the yarns. These results highlight differences in penetration of CNC-FTIC and XG-RBITC within the complex and multi-scale architecture of flax woven fabrics. Indeed the elementary fibres are twisted together to form flax yarns that are then woven to form the fabric. This puts forwards the issues related to the homogeneous treatment of industrial ligno-cellulosic substrates as natural woven fabrics having complex architectures and possibly impurities.

The surface of flax fibres treated with CNC was imaged by SEM. Cellulose nanocrystals at the surface of treated flax fibres are clearly visible in **Figure II-4 b** (see also insert), compared to raw flax fibres (**Figure II-4 a**) with no visible rod-like shaped nanoparticles at their surface.

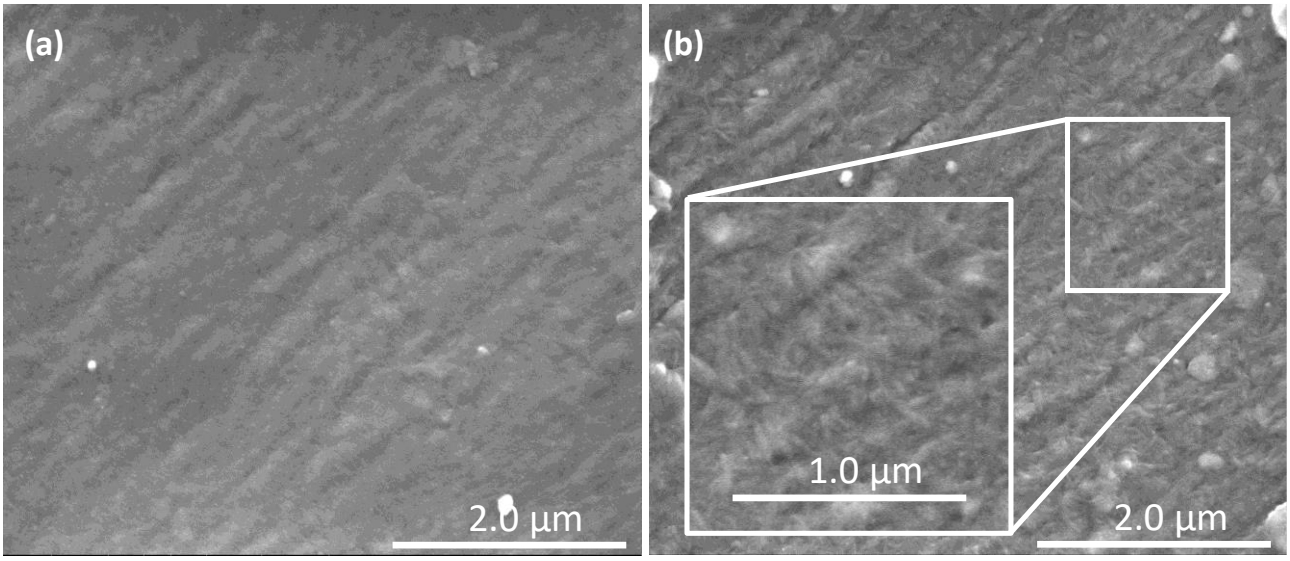

Figure II-4: SEM images of elementary flax fibres surface extracted from (a) raw flax woven fabrics; (b) CNC treated flax woven fabrics. (X 50 000).

Adsorbed CNC appear homogeneously distributed and randomly oriented at the surface of flax fibres. This clearly demonstrated the creation of hierarchical structuration at the surface of the fibres by the formation of a nanostructured layer. This microscale structuration echoes the organization of the cellulosic elements of the flax fibers. It should be noticed that CNC were not present on all elementary fibre surfaces. This has to be related to the accessibility of fibre surfaces during adsorption treatments. Indeed, the twisted structure of flax yarns and physical contacts between elementary fibres likely limit the exposure of flax surface upon adsorption. As observed by confocal microscopy (**Figure II-3**), flax fibres from the inside of the yarns are less accessible and hence likely treated to a lower extent.

II. 3. 1. 2 Adsorption isotherms

Xyloglucan (XG) and cellulose nanocrystals (CNC) adsorption processes are complex phenomena, and the final adsorbed amount and conformation over substrate's surface are related to several parameters such as the molar mass, concentrations, solubility, etc. [64], [65]. Additionally, flax woven fabrics are industrial materials and as such are far from being model substrates. For instance, flax fibres swelling and destructuration of the fabrics occurring during treatment might influence the adsorption kinetics. Indeed it changes the available surfaces for

adsorption and their accessibility, as well as the particular microstructure of natural fibres with its porosities and the lumen. Based on preliminary adsorption trials, an adsorption time of 16 hours was chosen. These trials also highlighted that further investigations on the adsorption kinetics of XG and CNC on flax fibres would be of interest.

The obtained adsorption isotherms are displayed in **Figure II-5**, for XG and CNC on flax woven fabrics.

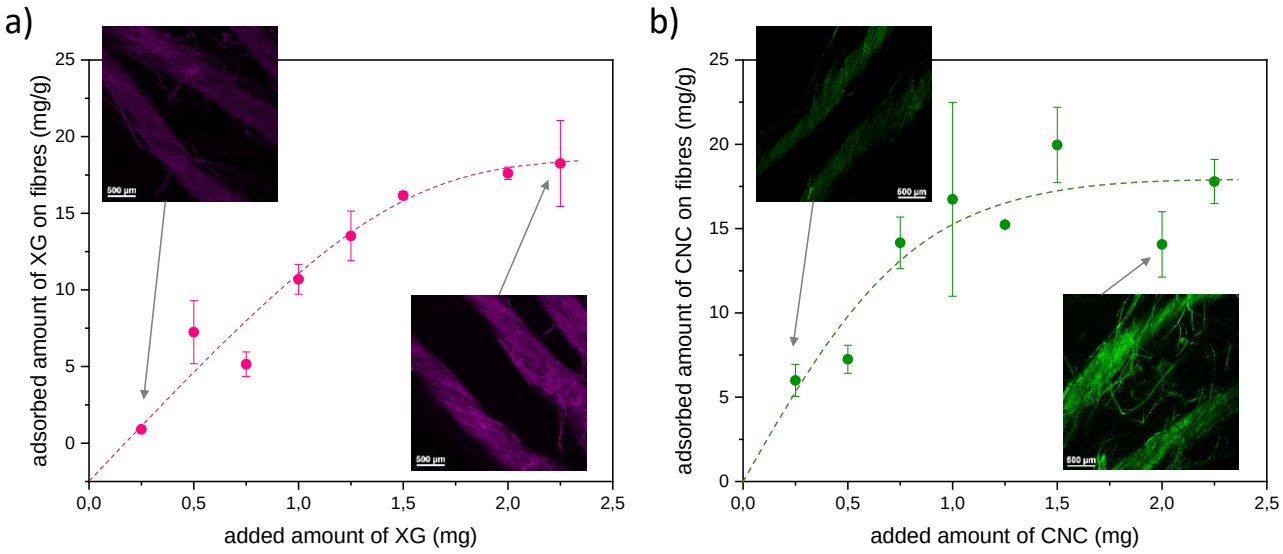

Figure II-5: Adsorption isotherms of (a) XG and (b) CNC on flax woven fabric and associated confocal images of XG-RBITC and CNC-FITC at low and high adsorption ratios.

Adsorption was determined by comparing the UV absorbance of reference labeled CNC-RBITC or XG-RBITC solution to those incubated with flax woven fabrics. First, the Figure 5a represents the adsorption isotherm of XG on flax woven fabrics. The insert shows the related confocal images of the yarns at low and high adsorption ratios. The difference in intensity of XG-RBITC on confocal images is nicely correlated with the increase of adsorbed amount of XG on flax fibres depending on initial concentrations of XG in solutions. A plateau is observed at average 15-20 mg/g. In literature, the adsorption of xyloglucan has already been studied on different substrates.

For example, paper fibres like bleached softwood kraft pulp (BSKP) [66] or chemical and mechanical pulp [15]. For BSKP fibres, the amount of adsorbed XG was between 4 and 12 mg/g pulp depending on the refining time. In the case of thermomechanical pulp (TMP) and chemi-thermomechanical pulp (CTMP), refined or unrefined pine/spruce and birch pulp, an adsorption of XG from 15 to 30 mg/g pulp was reached. In our study, the adsorbed amount of XG on flax woven fabrics seems to be in the same range as TMP and CTMP pulps. Previous studies also reported the adsorption of xyloglucan on cellulose nanocrystals [35], [67], [38] with a maximal adsorption between 98 to 333 mgXG/gcellulose. The higher amount of adsorbed XG on cellulose nanocrystals as substrates is due to the much higher specific surface area of CNC that range from 150 to 800 m^2/g [68], [69], as compared to that of flax fibres, roughly 1 m^2/g [70]–[73], even if fibre swelling could contribute to improve specific surface area. Figure 5b represents the adsorption isotherm of CNC on flax woven fabrics. As for XG adsorption, the difference in intensity of CNC-FITC on confocal images is well correlated with the increase amount of adsorbed CNC on flax fibres depending on initial concentrations of CNC in suspensions. A plateau is reached at average 15-20 mg/g. Plateau values of the amount of adsorbed XG and CNC are thus similar for the studied flax woven fabric. This points out that both XG and CNC can be adsorbed in similar quantities on flax woven fabrics, and suggests that the surface availability of the substrate has more influence on the amount of adsorbed polymers/particles than its nature and physico-chemical characteristics. It should be noticed that the adsorbed amounts of XG and CNC are rather high when considering the low specific surface area of flax woven fabric. It might be suggested that adsorption occurs in multilayered structure and not only in monolayer as usually proposed in adsorption studies based on model substrates. Other parameters than adsorption mechanisms cannot be ruled out to explain our findings. As discussed above, other processes such as the swelling of flax yarns and fibres with an increase of the available surface for adsorption, the complex and heterogeneous surface chemistry of flax fibres as well as a significant fibrillation rate due to flax processing (retting, scutching, weaving etc.) should also be considered.

II. 3. 2. Successive XG and CNC adsorptions on flax woven fabrics

Two different successive adsorption procedures of XG and CNC have been tested on flax woven fabrics, i.e. adsorption of XG then CNC (XG-CNC) and vice versa (CNC-XG). Both had the aim to observe a possible synergy between XG and CNC during their adsorption on flax woven fabrics.

II. 3. 2. 1 Microscopic observations

Figure II- 6 shows confocal microscopy images of XG-RBITC (**Figure II- 6 a**) and CNC-FITC (**Figure II- 6 b**) on the same elementary flax fibre.

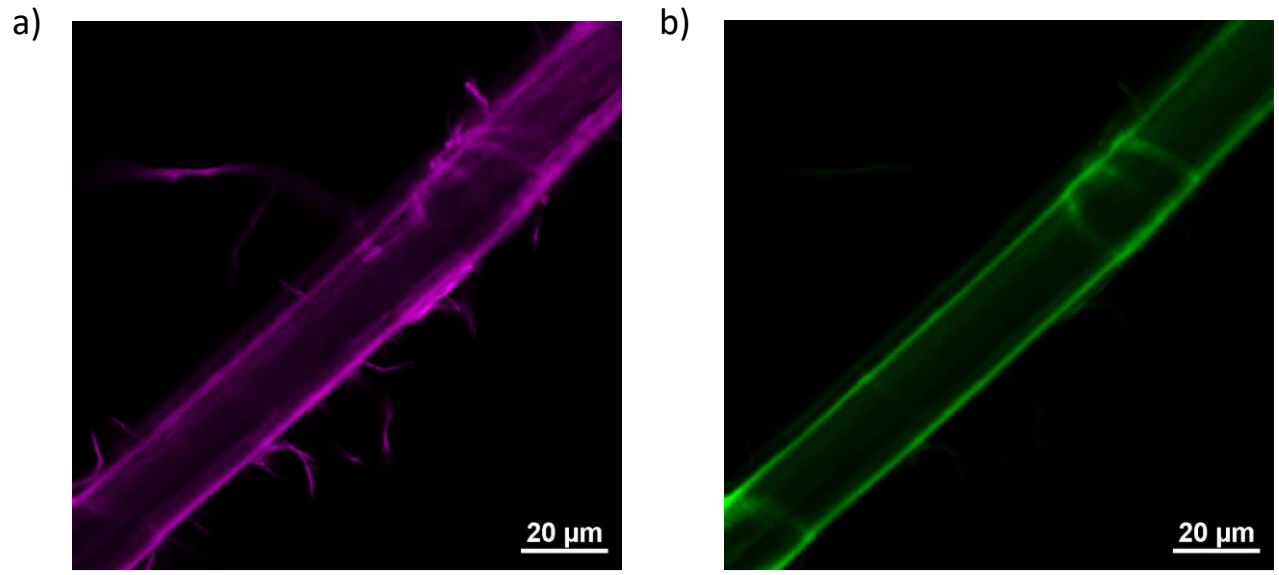

Figure II- 6: Confocal microscopy images of successive adsorption of XG-CNC on an elementary flax fibre with (a) XG-RBITC (b) CNC-FITC.

RBITC and FTIC were successively imaged to investigate their potential co-localization. Globally XG and CNC are homogeneously adsorbed on flax fibres, recovering the entire surface of the fibre on both **Figure II- 6 a** and **Figure II- 6 b**, even if some difference can be seen between the two images. As for the simple adsorptions of XG or CNC on flax woven fabrics, some microfibrils around the flax fibre are visible and are likely originated from the peeling of fibre cell walls and/or residues produced during the manufacturing process of the industrial flax

woven fabric. These residues display RBTIC labeling and seem thus to have a preferential adsorption of xyloglucan (**Figure II- 6 a**) than cellulose nanocrystals (**Figure II- 6 b**). The confocal plan used allows also the imaging of the inner part of the fibre. It has to be noticed that any fluorescence can be detected in the bulk of the fibres indicating that the adsorption of both XG and CNC remain located at the surface of the fibres.

Surface of XG-CNC treated flax fibres were imaged by SEM. As for simple CNC adsorption (**Figure II-4**), cellulose nanocrystals are clearly visible at the surface of treated flax fibres in **Figure II-7 b** (see also insert). Adsorbed CNC appear homogeneously distributed and randomly oriented at the surface of flax fibres. As mentioned above, CNC were not present on all elementary fibre surfaces which could be explained by differences in fibre surfaces accessibility and chemistry during adsorption treatments.

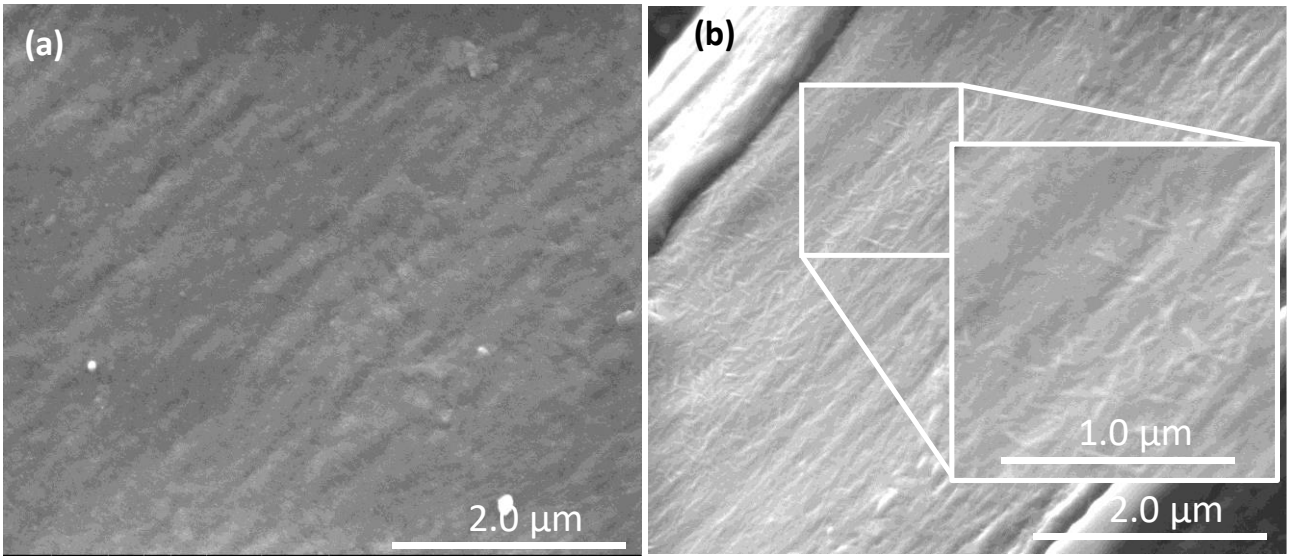

Figure II-7: SEM images of elementary flax fibres surface extracted from (a) raw flax woven fabrics; (b) XG-CNC treated flax woven fabrics. (X 50 000).

II. 3. 2. 2 Adsorption isotherms of successive XG and CNC

Adsorption isotherms of the successive adsorptions CNC-XG and XG-CNC have been plotted in **Figure II-8**. The goal was to investigate if the pre-treatment of flax woven fabric by CNC or XG had an influence on the adsorbed amount of the second compound (**Figure II-8 a**; **Figure II-8 b**).

It seems that the pre-adsorption of CNC on flax fibres, **Figure II-8 a**, has no influence on the adsorption behavior of XG. Indeed, the two adsorption isotherms are very similar with the same plateau around 15-20 mg/g. However, it should be noticed that the plateau seems to be reached at lower initial concentrations of XG in solution with the presence of CNC on flax woven fabric. The pre-adsorption of XG on flax fibres, **Figure II-8 b**, appears to have a slight influence on the amount of adsorbed CNC. In fact, the adsorption isotherm for XG-CNC reaches a plateau at around 25-30 mg/g for against 15-20 mg/g for simple CNC adsorption. These results demonstrate that CNC have a good affinity for flax fibres surface, the pre-adsorption of XG increasing the amount of adsorbed CNC at high initial concentration of CNC in the suspension.

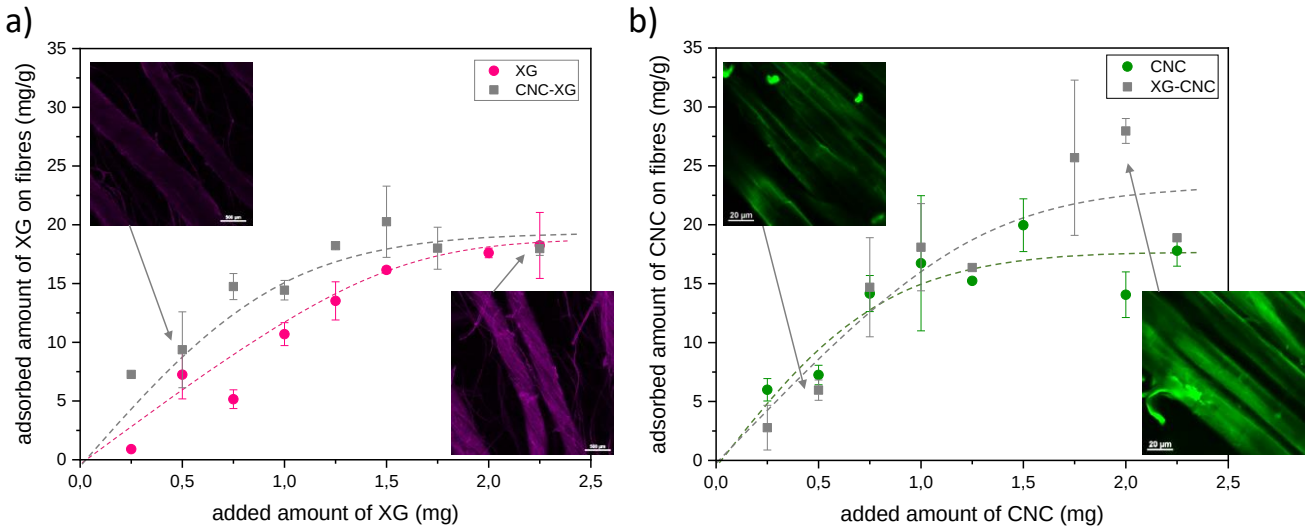

Figure II-8: Adsorption isotherms of (a) XG and (b) CNC for simple and successive adsorptions (XG-CNC and CNC-XG) on flax woven fabrics and associated confocal images of XG-RBITC and CNC-FITC at low and high adsorption ratios.

II. 3. 3. Adhesive force measurements by Atomic Force Microscopy

In order to get a deeper understanding of the affinity between xyloglucan (XG), cellulose nanocrystals (CNC) and flax woven fabric, we performed different adhesive force measurements by the atomic force microscopy (AFM). All of these results are detailed in **Figure II-9**. Different configurations tip / substrate were analyzed:

(a) neat-tip or XG-tip / CNC-surface obtained by deposition of CNC on PEI pre-coated mica substrate by spin-coating.

(b) XG-tip / flax-CNC or XG-tip / raw flax, where flax-CNC corresponds to a flax fibre surface adsorbed with CNC,

(c) CNC-tip / flax-XG or CNC-tip / raw flax, where flax-XG corresponds to a flax fibre surface adsorbed with XG.

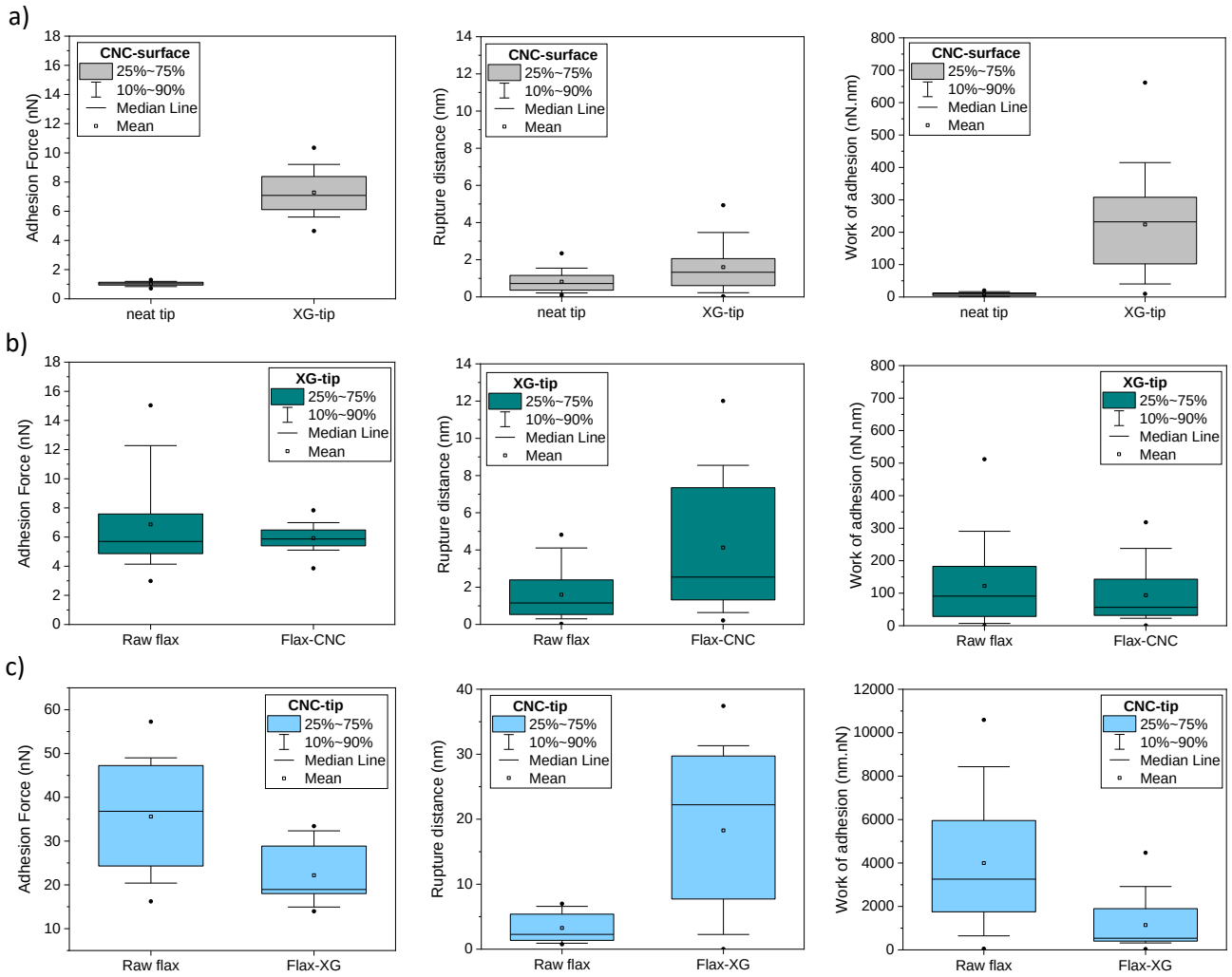

Figure II-9: Adhesion force, rupture distance and work of adhesion obtained with force measurements by AFM in different tip / substrate configurations (a) neat-tip or XG-tip / CNC-surface, (b) XG-tip / raw flax or flax-CNC, (c) CNC-tip / raw flax or flax-XG.

The adhesion between the tip and the substrate is due to the chemical interactions between the two surfaces into contact. The force curves measurements allow the quantification of these interactions. The rupture distance corresponds to the distance tip-substrate needed to completely separate the tip and the substrate. Finally, the work of adhesion is the energy required to separate the tip from the substrate. All the results in **Figure II-9** show high standard deviations, probably due to differences in surface roughness and chemistry between the different surfaces.

First, the configuration (a) with the neat-tip or the XG-tip approaching the CNC-surface, was used as a supplementary control of the dipping of the XG-tip. The adhesion force and the work of adhesion between the XG-tip and the CNC-substrate are respectively 7 times and 25 times higher than the measurements with the untreated nitride tip. In this configuration, the rupture distance is unchanged. These results show that the XG-tip has a high adhesion force with the CNC-substrate, which is correlated with the high affinity between XG and CNC with strong hydrogen and van der Waals bonds.

Then force curves measurements were performed with the configuration (b), XG-tip in contact with the raw flax or the flax-CNC and results are detailed in **Figure II-9 b**. We can observe that the adhesive force is the same, around 6 nN for both, with more heterogeneous measurements for the raw flax substrate (between 3 and 15 nN). The work of adhesion is also in the same range with 60-90 nN.nm. However the rupture distance seems to be slightly increased with the presence of CNC on the flax woven fabric with a maximum of 12 nm against 5 nm for the raw flax. This result shows a possible increase of the interactions zone between biopolymers XG and adsorbed CNC with the creation of an extended network. The configuration (c) is the opposite of the configuration (b), with the flax-XG as substrate and CNC coated on the AFM tip. The adhesion force and the work of adhesion are higher between the CNC-tip and the raw flax than the flax-XG substrate with respectively 35 nN against 20 nN and 750 nN.nm against 3100 nN.nm. It means that CNC seem to have very good interactions with the flax woven fabrics, without the presence of adsorbed XG on the surface.

On the other side, the rupture distance is strongly improved between the CNC-tip and the flax-XG with a median around 23 nm against 5 nm for the raw flax. That means, like the configuration (b), that the interactions between CNC and adsorbed XG create specific bonds and entanglements with an extensible network, illustrated in **Figure II- 10**.

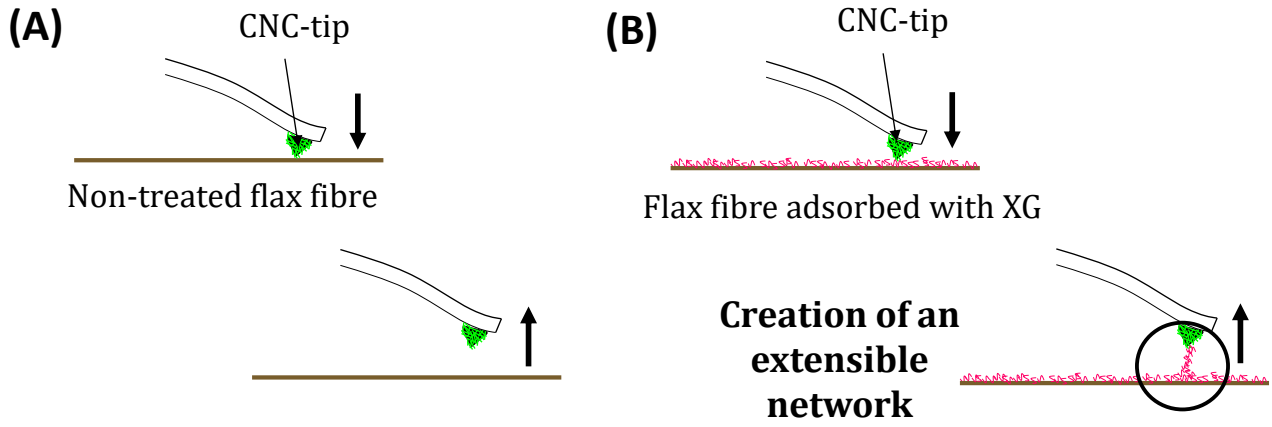

Figure II- 10: Illustration of the adhesive force measurements by AFM with the CNC-tip comparing (A) a non-treated flax fibre and (B) treated flax fibre with XG as substrates.

Despite the similar adsorbed amounts are similar for CNC and XG whatever the adsorption process, the AFM results suggest that a change in the sequence of adsorption and the combination of the two biobased building blocks can be a mean to vary the structuration of the surface organization. Accordingly, future studies will focus on the impact of hierarchically structured surfaces obtained by varying the adsorption sequence on the macroscopic properties of flax fibres based materials.

II. 4. Conclusions

Adsorption isotherms, confocal microscopy and force measurements by Atomic Force Microscopy (AFM) have been used to characterize different architectures of xyloglucan (XG) and cellulose nanocrystals (CNC) adsorptions on an industrial flax woven fabric. This industrial fabric has a complex architecture with twisted yarns composed of several hundred elementary flax fibres. Moreover, some residues provided probably during the manufacturing process of the fabric are present at the surface and seems to have affinities mainly with xyloglucan and also cellulose nanocrystals. The confocal images show the homogeneous distribution of XG and CNC on the flax fabric for the simple and successive adsorptions with no aggregates. However, SEM images show non-treated surfaces, which can be explained by the complex architecture of the fabric with porosities, entanglements etc. Moreover, phenomena such as swelling and destructuration occur during the dipping in water suspension and can influence the adsorption. The adsorption isotherms of XG and CNC on the flax woven fabric are very similar for the simple and successive adsorptions with a plateau around 20 mg/gfibres. The pre-adsorption with XG on flax woven fabrics increases the adsorbed amount of CNC in the high concentrations and seems to change the architecture of the biopolymers network. In fact the AFM adhesive force measurements show first a good affinity between CNC and XG and also higher adhesive force and work of adhesion between CNC and the neat flax woven fabric. However, it seems that the pre-adsorption of XG on the fabric increases the rupture distance with the CNC-tip. The combined XG and CNC, adsorbed with strong interactions on the flax woven fabric, create an extensible network. These results open perspectives in the treatment of natural fabrics and the possibility to change the surface and the architecture with the adsorption of biopolymers like xyloglucan and cellulose nanocrystals. However, we have to keep in mind the complexity of the hierarchical architecture of the industrial flax woven fabric for such treatments in terms of homogeneity, residual components and swelling.

II. 5. References

[1] S. Kalia, K. Thakur, A. Celli, M. A. Kiechel, et C. L. Schauer, « Surface modification of plant fibers using environment friendly methods for their application in polymer composites, textile industry and antimicrobial activities: A review », *Journal of Environmental Chemical Engineering*, vol. 1, nº 3, p. 97‑112, sept. 2013, doi: 10.1016/j.jece.2013.04.009.

[2] R. Araújo, M. Casal, et A. Cavaco-Paulo, « Application of enzymes for textile fibres processing », *Biocatalysis and Biotransformation*, vol. 26, nº 5, p. 332‑349, janv. 2008.

[3] O. Faruk, A. K. Bledzki, H.-P. Fink, et M. Sain, « Biocomposites reinforced with natural fibers: 2000–2010 », *Progress in Polymer Science*, vol. 37, nº 11, p. 1552‑1596, nov. 2012, doi: 10.1016/j.progpolymsci.2012.04.003.

[4] Z. Haider, H. Cho, G. Moon, et H. Kim, « Minireview: Selective production of hydrogen peroxide as a clean oxidant over structurally tailored carbon nitride photocatalysts », *Catalysis Today*, vol. 335, p. 55‑64, sept. 2019, doi: 10.1016/j.cattod.2018.11.067.

[5] N. Le Moigne, B. Otazaghine, S. Corn, H. Angellier-Coussy, et A. Bergeret, *Surfaces and Interfaces in Natural Fibre Reinforced Composites*. Cham: Springer International Publishing, 2018.

[6] V. K. Rastogi et P. Samyn, « Bio-based coatings for paper applications », *Coatings*, vol. 5, p. 887‑930, 2015.

[7] D. Sun, « Surface Modification of Natural Fibers Using Plasma Treatment », *Biodegradable Green Composites*, p. 18‑39, mars 2016, doi: 10.1002/9781118911068.ch2.

[8] Q. Wei, « 14 - Emerging approaches to the surface modification of textiles », in *Surface Modification of Textiles*, Q. Wei, Éd. Woodhead Publishing, 2009, p. 318‑323.

[9] D. Dai et M. Fan, « Green modification of natural fibres with nanocellulose », *RSC Advances*, vol. 3, nº 14, p. 4659, 2013, doi: 10.1039/c3ra22196b.

[10] A. Hajlane, R. Joffe, et H. Kaddami, « Cellulose nanocrystal deposition onto regenerated cellulose fibres: effect on moisture absorption and fibre–matrix adhesion », *Cellulose*, vol. 25, nº 3, p. 1783‑1793, mars 2018, doi: 10.1007/s10570-018-1680-z.

[11] C. I. Idumah, J. E. Ogbu, J. U. Ndem, et V. Obiana, « Infuence of chemical modification of kenaf fiber on xGNP‑PP nano‑biocomposites », *SN Applied Sciences*, vol. 1, nº 1261, 2019, [En ligne]. Disponible sur: https://link.springer.com/content/pdf/10.1007%2Fs42452-019-1319-1.pdf.

[12] K.-Y. Lee, P. Bharadia, J. J. Blaker, et A. Bismarck, « Short sisal fibre reinforced bacterial cellulose polylactide nanocomposites using hairy sisal fibres as reinforcement », *Composites Part A: Applied Science and Manufacturing*, vol. 43, nº 11, p. 2065‑2074, nov. 2012, doi: 10.1016/j.compositesa.2012.06.013.

[13] N. Malik, P. Kumar, S. B. Ghosh, et S. Shrivastava, « Organically modified nanoclay and aluminium hydroxide incorporated bionanocomposites towards enhancement of physico-mechanical and thermal properties of lignocellulosic structural reinforcement », *Journal of Polymers and the Environment*, vol. 26, nº 8, p. 3243‑3249, 2018.

[14] A. Oksanen, R. Timo, E. Retulainen, K. Salminen, et H. Brumer, « Improving Wet Web Runnability and Paper Quality by an Uncharged Polysaccharide », *Journal of Biobased*

Materials and Bioenergy, vol. 5, nº 2, p. 187‑191, juin 2011, doi: 10.1166/jbmb.2011.1144.
[15] Q. Zhou, M. Baumann, H. Brumer, et T. Teeri, « The influence of surface chemical composition on the adsorption of xyloglucan to chemical and mechanical pulps », *Carbohydrate Polymers*, vol. 63, nº 4, p. 449‑458, mars 2006, doi: 10.1016/j.carbpol.2005.09.015.
[16] R.-C. Zhuang, T. T. L. Doan, J.-W. Liu, J. Zhang, S.-L. Gao, et E. Mäder, « Multi-functional multi-walled carbon nanotube-jute fibres and composites », *Carbon*, vol. 49, nº 8, p. 2683‑2692, juill. 2011, doi: 10.1016/j.carbon.2011.02.057.
[17] S. C. Fry, « The Structure and Functions of Xyloglucan », *Journal of experimental botany*, vol. 40, nº 210, p. 1‑11, 1989.
[18] S. C. Fry *et al.*, « An unambiguous nomenclature for xyloglucan-derived oligosaccharides », *Physiologia Plantarum*, vol. 89, nº 1, p. 1‑3, sept. 1993, doi: 10.1111/j.1399-3054.1993.tb01778.x.
[19] J. Hanus et K. Mazeau, « The xyloglucan–cellulose assembly at the atomic scale », *Biopolymers*, vol. 82, nº 1, p. 59‑73, mai 2006, doi: 10.1002/bip.20460.
[20] T. Hayashi, K. Ogawa, et Y. Mitsuishi, « Characterization of the adsorption of Xyloglucan to Cellulose », *Plant and Cell Physiology*, vol. 35, nº 8, p. 1199‑1205, 1994, doi: 10.1093/oxfordjournals.pcp.a078714.
[21] Y. B. Park et D. J. Cosgrove, « Xyloglucan and its Interactions with Other Components of the Growing Cell Wall », *Plant and Cell Physiology*, vol. 56, nº 2, p. 180‑194, févr. 2015, doi: 10.1093/pcp/pcu204.
[22] M. Pauly, P. Albersheim, A. Darvill, et W. S. York, « Molecular domains of the cellulose/xyloglucan network in the cell walls of higher plants », *The Plant Journal*, vol. 20, nº 6, p. 629‑639, déc. 1999, doi: 10.1046/j.1365-313X.1999.00630.x.
[23] Y. Habibi, L. A. Lucia, et O. J. Rojas, « Cellulose Nanocrystals: Chemistry, Self-Assembly, and Applications », *Chemical Reviews*, vol. 110, nº 6, p. 3479‑3500, juin 2010, doi: 10.1021/cr900339w.
[24] A. Dufresne, *Nanocellulose: From Nature to High Performance Tailored Materials*. Walter de Gruyter GmbH & Co KG, 2017.
[25] Y. Habibi, H. Chanzy, et M. R. Vignon, « TEMPO-mediated surface oxidation of cellulose whiskers », *Cellulose*, vol. 13, p. 679‑687, 2006.
[26] M. Nagalakshmaiah, N. El Kissi, et A. Dufresne, « Ionic Compatibilization of Cellulose Nanocrystals with Quaternary Ammonium Salt and Their Melt Extrusion with Polypropylene », *ACS Applied Materials & Interfaces*, vol. 8, nº 13, p. 8755‑8764, avr. 2016, doi: 10.1021/acsami.6b01650.
[27] R. Rusli et S. J. Eichhorn, « Determination of the stiffness of cellulose nanowhiskers and the fiber-matrix interface in a nanocomposite using Raman spectroscopy », *Applied Physics Letters*, vol. 93, nº 3, p. 033111, juill. 2008, doi: 10.1063/1.2963491.
[28] L. Yue *et al.*, « Surface-modified cellulose nanocrystals for biobased epoxy nanocomposites », *Polymer*, vol. 134, p. 155‑162, janv. 2018, doi: 10.1016/j.polymer.2017.11.051.
[29] M. Dick-Pérez, Y. Zhang, J. Hayes, A. Salazar, O. A. Zabotina, et M. Hong, « Structure and interactions of Plant Cell-Wall Polysaccharides by Two- and Three-Dimensional Magic-Angle-Spinning Solid-State NMR », *Biochemistry*, vol. 50, p. 989‑1000, 2011.

[30] T. Hayashi, M. P. F. Marsden, et D. P. Delmer, « Pea xyloglucan and cellulose V: xyloglucan-cellulose interactions in vitro and in vivo », *Plant Physiol*, vol. 83, p. 384‑389, 1987.
[31] S. Morris, S. Hanna, et M. J. Miles, « The self-assembly of plant cell wall components by single-molecule force spectroscopy and Monte Carlo modelling », *Nanotechnology*, vol. 15, nº 9, 2004, Consulté le: sept. 11, 2019. [En ligne]. Disponible sur: https://iopscience-iop-org.gaelnomade-1.grenet.fr/article/10.1088/0957-4484/15/9/031/meta.
[32] Y. B. Park et D. J. Cosgrove, « A Revised Architecture of Primary Cell Walls Based on Biomechanical Changes Induced by Substrate-Specific Endoglucanases », *Plant Physiology*, vol. 158, p. 1933‑1943, 2012.
[33] J.-P. Vincken, A. de Keizer, G. Beldman, et A. Gerard Joseph Voragen, « Fractionation of xyloglucan fragments and their interaction with cellulose », *Plant Physiol*, vol. 108, p. 1579‑1585, 1995.
[34] T. Benselfelt *et al.*, « Adsorption of Xyloglucan onto Cellulose Surfaces of Different Morphologies: An Entropy-Driven Process », *Biomacromolecules*, vol. 17, nº 9, p. 2801‑2811, sept. 2016, doi: 10.1021/acs.biomac.6b00561.
[35] A. Dammak *et al.*, « Exploring Architecture of Xyloglucan Cellulose Nanocrystal Complexes through Enzyme Susceptibility at Different Adsorption Regimes », *Biomacromolecules*, vol. 16, nº 2, p. 589‑596, févr. 2015, doi: 10.1021/bm5016317.
[36] T. Hayashi et G. A. Maclachlan, « Pea xyloglucan and cellulose: I. Macromolecular organization », *Plant Physiology*, vol. 75, p. 596‑604, 1984.
[37] D. U. Lima, W. Loh, et M. S. Buckeridge, « Xyloglucan–cellulose interaction depends on the sidechains and molecular weight of xyloglucan », *Plant Physiology and Biochemistry*, vol. 42, nº 5, p. 389‑394, mai 2004, doi: 10.1016/j.plaphy.2004.03.003.
[38] M. Lopez *et al.*, « Enthalpic Studies of Xyloglucan−Cellulose Interactions », *Biomacromolecules*, vol. 11, nº 6, p. 1417‑1428, juin 2010, doi: 10.1021/bm1002762.
[39] J. Stiernstedt, H. Brumer, Q. Zhou, T. T. Teeri, et M. W. Rutland, « Friction between Cellulose Surfaces and Effect of Xyloglucan Adsorption », *Biomacromolecules*, vol. 7, nº 7, p. 2147‑2153, juill. 2006, doi: 10.1021/bm060100i.
[40] J. Stiernstedt, N. Nordgren, L. Wågberg, H. Brumer, D. G. Gray, et M. W. Rutland, « Friction and forces between cellulose model surfaces: A comparison », *Journal of Colloid and Interface Science*, vol. 303, nº 1, p. 117‑123, nov. 2006, doi: 10.1016/j.jcis.2006.06.070.
[41] C. Cerclier, F. Cousin, H. Bizot, C. Moreau, et B. Cathala, « Elaboration of Spin-Coated Cellulose-Xyloglucan Multilayered Thin Films », *Langmuir*, vol. 26, nº 22, p. 17248‑17255, nov. 2010, doi: 10.1021/la102614b.
[42] C. Cerclier *et al.*, « Coloured Semi-reflective Thin Films for Biomass-hydrolyzing Enzyme Detection », *Advanced Materials*, vol. 23, nº 33, p. 3791‑3795, 2011, doi: 10.1002/adma.201101971.
[43] C. V. Cerclier *et al.*, « Xyloglucan-cellulose nanocrystal multilayered films: Effect of film architecture on enzymatic hydrolysis », *Biomacromolecules*, vol. 14, p. 3599‑3609, 2013.
[44] Z. Jaafar *et al.*, « Plant cell wall inspired xyloglucan/cellulose nanocrystals aerogels produced by freeze-casting », *Carbohydrate Polymers*, vol. 247, p. 116642, nov. 2020, doi: 10.1016/j.carbpol.2020.116642.

[45] A. Dammak, C. Moreau, F. Azzam, B. Jean, F. Cousin, et B. Cathala, « Influence of cellulose nanocrystals concentration and ionic strength on the elaboration of cellulose nanocrystals–xyloglucan multilayered thin films », *Journal of Colloid and Interface Science*, vol. 460, nº Supplement C, p. 214‑220, déc. 2015, doi: 10.1016/j.jcis.2015.08.048.
[46] B. Jean, L. Heux, F. Dubreuil, G. Chambat, et F. Cousin, « Non-Electrostatic Building of Biomimetic Cellulose−Xyloglucan Multilayers », *Langmuir*, vol. 25, nº 7, p. 3920‑3923, avr. 2009, doi: 10.1021/la802801q.
[47] H. Sehaqui, Q. Zhou, et L. A. Berglund, « High-porosity aerogels of high specific surface area prepared from nanofibrillated cellulose (NFC) », *Composites Science and Technology*, vol. 71, nº 13, p. 1593‑1599, sept. 2011, doi: 10.1016/j.compscitech.2011.07.003.
[48] H. Sehaqui, Q. Zhou, O. Ikkala, et L. A. Berglund, « Strong and Tough Cellulose Nanopaper with High Specific Surface Area and Porosity », *Biomacromolecules*, vol. 12, nº 10, p. 3638‑3644, oct. 2011, doi: 10.1021/bm2008907.
[49] M. Christiernin *et al.*, « The effects of xyloglucan on the properties of paper made from bleached kraft pulp », *Nordic Pulp & Paper Research Journal*, vol. 18, nº 2, p. 182‑187, 2003, doi: 10.3183/npprj-2003-18-02-p182-187.
[50] H. Yan, T. Lindström, et M. Christiernin, « Some ways to decrease fibre suspension flocculation and improve sheet formation », *Nordic Pulp & Paper Research Journal*, vol. 21, nº 1, p. 36‑43, janv. 2006, doi: 10.3183/npprj-2006-21-01-p036-043.
[51] M. Fortea-Verdejo, K.-Y. Lee, T. Zimmermann, et A. Bismarck, « Upgrading flax nonwovens: Nanocellulose as binder to produce rigid and robust flax fibre preforms », *Composites Part A: Applied Science and Manufacturing*, vol. 83, nº Supplement C, p. 63‑71, avr. 2016, doi: 10.1016/j.compositesa.2015.11.021.
[52] J. Juntaro, M. Pommet, A. Mantalaris, M. Shaffer, et A. Bismarck, « Nanocellulose enhanced interfaces in truly green unidirectional fibre reinforced composites », *Composite Interfaces*, vol. 14, nº 7‑9, p. 753‑762, janv. 2007, doi: 10.1163/156855407782106573.
[53] K.-Y. Lee, K. K. C. Ho, K. Schlufter, et A. Bismarck, « Hierarchical composites reinforced with robust short sisal fibre preforms utilising bacterial cellulose as binder », *Composites Science and Technology*, vol. 72, nº 13, p. 1479‑1486, août 2012, doi: 10.1016/j.compscitech.2012.06.014.
[54] M. Pommet *et al.*, « Surface Modification of Natural Fibers Using Bacteria: Depositing Bacterial Cellulose onto Natural Fibers To Create Hierarchical Fiber Reinforced Nanocomposites », *Biomacromolecules*, vol. 9, nº 6, p. 1643‑1651, juin 2008, doi: 10.1021/bm800169g.
[55] A. N. de Belder et K. Granath, « Preparation and properties of fluorescein-labelled dextrans », *Carbohydrate Research*, vol. 30, nº 2, p. 375‑378, oct. 1973, doi: 10.1016/S0008-6215(00)81824-8.
[56] Y. Iwakura et H. Okada, « The kinetics of the reaction of organic isothiocyanates with 1-octanol in o-Dichlorobenzene », *Canadian Journal of Chemistry*, vol. 40, p. 2369‑2375, 1962.
[57] B. Cappella et G. Dietler, « Force-distance curves by atomic force microscopy », *Surface Science Reports*, vol. 34, nº 1‑3, p. 1‑104, janv. 1999, doi: 10.1016/S0167-5729(99)00003-5.

[58] J. Ralston, I. Larson, M. W. Rutland, A. A. Feiler, et M. Kleijn, « Atomic force microscopy and direct surface force measurements (IUPAC Technical Report) », *Pure and Applied Chemistry*, vol. 77, nº 12, p. 2149‑2170, janv. 2005, doi: 10.1351/pac200577122149.
[59] M. Kolasinska et P. Warszynski, « The effect of nature of polyions and treatment after deposition on wetting characteristics of polyelectrolyte multilayers », *Applied Surface Science*, vol. 252, nº 3, p. 759‑765, 2005.
[60] P. Podsiadlo *et al.*, « Layer-by-Layer assembled films of cellulose nanowires with antireflective properties », *Langmuir*, vol. 23, nº 15, p. 7901‑7906, 2007, doi: 10.1021/la700772a.
[61] B. Jean, F. Dubreuil, L. Heux, et F. Cousin, « Structural details of cellulose nanocrystals/polyelectrolytes multilayers probed by neutron reflectivity and AFM », *Langmuir*, p. 3452‑3458, 2008.
[62] C. Aulin *et al.*, « Nanoscale Cellulose Films with Different Crystallinities and Mesostructures—Their Surface Properties and Interaction with Water », *Langmuir*, vol. 25, nº 13, p. 7675‑7685, juill. 2009, doi: 10.1021/la900323n.
[63] A. Barbulée, « Compréhension des effets du défibrage sur la morphologie, les propriétés et le comportement mécanique des faisceaux de fibres de lin : étude d'un composite dérivé lin/époxyde », These de doctorat, Caen, 2015.
[64] A. Villares, C. Moreau, A. Dammak, I. Capron, et B. Cathala, « Kinetic aspects of the adsorption of xyloglucan onto cellulose nanocrystals », *Soft Matter*, vol. 11, nº 32, p. 6472‑6481, 2015, doi: 10.1039/C5SM01413A.
[65] S. Ahola, P. Myllytie, M. Österberg, T. Teerinen, et J. Laine, « Effect of polymer adsorption on cellulose nanofibril water binding capacity and aggregation », *BioResources*, vol. 3, nº 4, p. 1315‑1328, oct. 2008.
[66] C. Moser, H. Backlund, M. Lindström, et G. Henriksson, « Xyloglucan for estimating the surface area of cellulose fibers », *Nordic Pulp & Paper Research Journal*, vol. 33, nº 2, p. 194‑198, 2018.
[67] J. Gu et J. M. Catchmark, « The impact of cellulose structure on binding interactions with hemicellulose and pectin », *Cellulose*, vol. 20, p. 1613‑1627, 2013.
[68] A. Brinkmann, M. Chen, M. Couillard, Z. J. Jakubek, T. Leng, et L. J. Johnston, « Correlating Cellulose Nanocrystal Particle Size and Surface Area », *Langmuir*, vol. 32, nº 24, p. 6105‑6114, juin 2016, doi: 10.1021/acs.langmuir.6b01376.
[69] Y. Habibi, « Key advances in the chemical modification of nanocelluloses », *Chem. Soc. Rev.*, vol. 43, nº 5, p. 1519‑1542, févr. 2014, doi: 10.1039/C3CS60204D.
[70] A. Bismarck *et al.*, « Surface characterization of flax, hemp and cellulose fibers; Surface properties and the water uptake behavior », *Polymer Composites*, vol. 23, nº 5, p. 872‑894, 2002, doi: 10.1002/pc.10485.
[71] A. Le Duigou, A. Bourmaud, E. Balnois, P. Davies, et C. Baley, « Improving the interfacial properties between flax fibres and PLLA by a water fibre treatment and drying cycle », *Industrial Crops and Products*, vol. 39, p. 31‑39, sept. 2012, doi: 10.1016/j.indcrop.2012.02.001.
[72] A. Legras, A. Kondor, M. T. Heitzmann, et R. W. Truss, « Inverse gas chromatography for natural fibre characterisation: Identification of the critical parameters to determine the

Brunauer–Emmett–Teller specific surface area », *Journal of Chromatography A*, vol. 1425, p. 273‑279, déc. 2015, doi: 10.1016/j.chroma.2015.11.033.

[73] J. Müssig, H. Fischer, N. Graupner, et A. Drieling, « Testing Methods for Measuring Physical and Mechanical Fibre Properties (Plant and Animal Fibres) », in *Industrial Applications of Natural Fibres*, John Wiley & Sons, Ltd, 2010, p. 267‑309.

CHAPTER III

Hierarchical thermoplastic biocomposites reinforced with short flax fibres modified by XG and CNC

Table of contents - Chapter III

This Chapter is adapted from Doineau E., Coqueugniot G., Pucci M. F., Caro A-S., Cathala B., Bénézet J-C., Bras J. and Le Moigne N. « Hierarchical thermoplastic biocomposites reinforced with flax fibres modified by xyloglucan and cellulose nanocrystals", Carbohydrate Polymers, vol. 254, p. 117403, feb. 2021.

III. 1. Introduction

Considering the current environmental concerns towards the creation of eco-friendly materials entirely or partially biobased, the use of natural fibres as reinforcements in biocomposites in sectors like automotive, building and constructive or sports is a great opportunity and has been the subject of various recent scientific reviews [1]–[7]. Natural fibres have many advantages compared to synthetic fibres, such as their renewability, biodegradability, wide availability associated with low density, low cost and high specific mechanical properties. However, the implementation of these materials in industrial applications is limited by low thermal and dimensional stability of natural fibres, especially in humid conditions, as well as interfacial adhesion with several polymer matrices [8]–[12]. The fibre / matrix interface plays a key role in the stress transfer within the biocomposite materials and their resulting mechanical performances. The main difficulty comes from the polar and hydrophilic character of lignocellulosic fibres considering their global biochemical composition, whereas the thermoplastic polymer matrices display a very often hydrophobic and apolar character [13], [14].

To tackle these compatibility issues, a wide panel of chemical and physical modification strategies of natural fibre surfaces have been reported in literature [15]–[18]. For example, coupling agents such as MAPP or MAPE were used in biocomposites to create chemical bonds between natural fibres and polyolefins [19]–[22]. Another strategy consists in the deposition of nanoparticles on fibre surfaces. This concept is directly inspired from naturally occurring composites such as bones, shells and wood which show nanoscaled structures inducing amazing mechanical behaviour [23], [24], *detailed in* ***Chapter I, section I.3***. The purpose is to use nanomaterials at the interphase to create local reinforcement and increase the mechanical interlocking between fibres and matrix [25], [26].

Following this concept, the goal of this work is to modify raw short flax fibre surfaces by nanostructuration with bio-based reinforcements as CNC so as to reinforce polypropylene (PP) matrix. It has been shown in literature that the strength of the interfacial adhesion is mainly governed by the polymer surface tension, the fibre surface free energy and also to the surface chemistry and topography of the fibres [27], [28]. Nanostructuration with CNC appears interesting as they display a high specific surface area of 150 – 800 m²/g and a high Young's modulus of 100 – 130 GPa [29]–[32]. Moreover, Khoshkava and Kamal found a total surface free energy of CNC γ_{CNC}= 68.9 mJ/m², being characterized by a predominant dispersive component, i.e. γ_{CNC}^{d} = 40.9 mJ/m² against γ_{CNC}^{p} = 28.0 mJ/m² for the polar component [33], due to its highly crystalline and (almost pure) cellulosic structure. This characteristic could be very interesting to enhance the interfacial adhesion with apolar polymer matrices such as PP. The previous work described in the ***Chapter II*** highlighted the creation of an extensible network XG/CNC on the surface of fibres [34]. The deposition of such XG/CNC complex on natural fibres could provide in composite applications an expended interphase region with enhanced interfacial adhesion.

In this context, this work will focus on the surface modification of short flax fibres by the adsorption of cellulose nanocrystals (CNC) and xyloglucan (XG), and the resulting interfacial adhesion and mechanical behaviour of PP / flax biocomposites prepared by extrusion and injection moulding. The coupling agent maleic anhydride grafted polypropylene (MAPP) was also incorporated in some biocomposites to provide chemical interactions and improve the compatibility between the PP matrix and (modified) flax fibres [21], [22]. Wettability tests on CNC and XG/CNC modified flax fibres, and mechanical tests on biocomposites at macro- and microscopic length scales were performed. In addition, possible changes in microstructure such as crystallinity, fibre size and shape distribution, which could also influence the final mechanical performances of the materials, were analysed.

III. 2. Materials and methods

III. 2. 1. Materials

Flax fibre bundles of average length 2.24 mm and width 110 µm (initial aspect ratio around 20) were supplied by Fibres Recherche Développement (Troyes, France). Their biochemical composition was characterized according to van Soest method (standards NF EN ISO 13,906 and NF V18-122): cellulose (79.7 ± 1.7 wt%), hemicelluloses (5.6 ± 1.0 wt%), lignin (2.8 ± 0.3 wt%), solubles (11.2 ± 0.5 wt%) and ashes (0.7 ± 0.3 wt%). Polypropylene (PP), grade PPH 9020, homopolymer, was purchased from Total Petrochemicals (Melting point = 165°C; Density 0.905 g/cm^3). Maleic anhydride-grafted polypropylene (MAPP) OREVAC CA100 was purchased from Arkema (MA content = 1 %; Melting point = 167°C). Cellulose nanocrystals (CNC) were obtained by acid hydrolysis of wood pulp and provided in spray-dried powder by CelluForce (Quebec, Canada). CNC lateral dimensions: 2-5 nm; CNC length: 50-110 nm; CNC surface charge density: 0.023 mmol/g; Crystalline fraction: 0.88. Xyloglucan (XG) Glyloid 6 C was obtained from tamarind seed gum and purchased from DSP Gokyo Food & Chemical. M_w = 840 000 g/mol; M_w/M_n = 1.24; R_g = 72 nm. Monosaccharide composition: Glucose 50.7 %; Xylose: 31.7 %; Galactose 16.0 %; Arabinose 1.6 %.

III. 2. 2. Flax fibres modification by CNC and XG

Cellulose nanocrystals (CNC) and xyloglucan (XG) were adsorbed on short flax fibre bundles. At first, flax fibres were modified only with CNC. A CNC suspension was prepared under stirring during 2 hours (10 g of CNC in 1L deionized water) followed by sonication (cycle 5; amplitude 50%; 2 x 1min) to break residual CNC agglomerates. Then, 10 g of flax fibres were added in the CNC suspension and gently stirred during 5 min to obtain a good dispersion of flax fibres within the suspension. The resulting mixture was stored at 4°C during 24 hours. The CNC modified fibres were then filtered with a Büchner system and dried at 105°C during 2 hours.

Same procedure was followed for the modification of flax fibres with both XG and CNC. In this case, XG was firstly adsorbed onto flax fibres as follows: XG suspension was prepared, i.e. 10 g of XG added gradually in 1L deionized water with a vortex, at 50 – 60 °C during few hours. Then, 10 g of flax fibres were added in the XG solution and gently stirred during 5 min to obtain a good dispersion of flax fibres within the solution. The resulting mixture was stored at 4°C during 24 hours. The XG modified fibres were then filtered with a Büchner system and dried at 105°C during 2 hours. These fibres were then modified with CNC following the procedure described above.

The resulting CNC and XG/CNC modified flax fibres, named flax_CNC and flax_XG/CNC respectively, were stored in a conditioning room at 23°C and 50% relative humidity. Based on the ***Chapter II***, the amount of XG and CNC on flax fibres was estimated around 2 %.

III. 2. 3. Surface free energy of flax fibres

As flax fibre bundles are dispersed and individualized in the matrix during composite processing, elementary flax fibres extracted from an unidirectional flax woven fabric 300 g / m² (FRD, France) were used for these experiments, and modified with CNC and XG/CNC following the same procedure described *in* ***section 2.2***. The tensiometer K100SF (Krüss, GmbH) was used to perform wettability tests in different reference liquids following the Wilhelmy method (**Equation III-1**):

$$F = m.g = \gamma_L^{tot}.p.\cos\theta_e \quad \text{(III-1)}$$

With F the capillary force (mN) measured by the tensiometer when a single fibre is immersed in the test liquid, m (g) corresponding to the mass of the liquid meniscus formed around the immersed elementary fibre, γ_L^{tot} (mJ/m²) the liquid surface tension, p (µm) the fibre wetted length or perimeter and θ_e (°) the static advancing contact angle between the fibre and the liquid [35].

Due to the heterogeneity of elementary flax fibre diameters, the perimeter p was determined beforehand for each tested fibre by using *n*-hexan (Sodipro) which has a surface tension γ_L^{tot} = 18.4 mJ/m², and is a totally wetting liquid, implying that $\cos\theta_e = 1$. Then, the tested fibres were dried (16 hours, 60°C) to remove any residual *n*-hexan before being tested in the two other reference liquids, i.e. water, diiodomethane (Sodipro).

The contact angle between the elementary flax fibre and the reference liquids was determined as follows. The elementary flax fibres (modified or not) were dipped at a velocity of 1 mm/min in a vessel containing the test liquid. The vessel was approached manually close to the fibre extremity and a fixed depth immersion was set in order to have at least 3-4 mm immersion depth. During immersion (advancing mode), the mass m is measured to obtain the contact angle. When immersion is completed, the fibre is maintained in contact with the liquid in a static position during 60 seconds in order to reach an "equilibrium state". At equilibrium, the capillary force is measured and the corresponding static advancing contact angle θ_e is derived from the **Equation (III-1)**. Then, the fibre is withdrawn from the liquid (receding mode). Tensiometric tests were carried out on eight samples for each type of fibre, i.e. raw flax fibres, CNC and XG/CNC modified flax fibres. Results were reproducible and gave low standard deviations.

III. 2. 4. Biocomposites processing

Blends of PP or PP / MAPP loaded at 5, 20 and 30 wt% of raw, flax_CNC or flax_XG/CNC modified fibres were compounded in a co-rotating twin-screw DSM Micro 15 extruder. The amount of MAPP was fixed at a ratio of flax fibres / MAPP (w / w) = 10. This ratio was shown to give the most efficient compatibilization between PP matrix and flax fibres [36]. The composition of the different biocomposites is detailed in **Table III-1**.

Flax fibres were dried before compounding in an oven at 80°C during 2 hours. The PP matrix or PP / MAPP pre-mix were introduced simultaneously with raw and modified flax fibres in the mixing chamber. Processing temperature was roughly 185-190°C (setpoint temperature) with a screw speed of 50 rpm and a processing time of 10 min. The resulting biocomposite compounds were collected and pelletized to around 4 mm diameter. Then, pelletized compounds were shaped by injection moulding with the HAAKE Minijet Inject press (Thermofisher), into dumbbells type 5A specimens (ISO 157-2) for the measurement of mechanical properties. Injection conditions were T_{inject} = 180°C, P_{inject} = 650 bar during 15 s and T_{mold} = 50°C. Biocomposite specimens were stored in a conditioning room at 23°C and 50% relative humidity during at least 48 hours, prior to mechanical tests.

Table III-1: Composition of the different extruded and injected biocomposites.

Designations	Fibre content (wt%)		
	5 %	20 %	30 %
	Matrix composition (wt%)		
PP_flax **PP_flax_CNC**	95 % PP	80 % PP	70 % PP
PP_MAPP_flax **PP_MAPP_flax_CNC**	94.5 % PP + 0.5 % MAPP	78 % PP + 2 % MAPP	67 % PP + 3 % MAPP
PP_MAPP_flax_XG/CNC	/	78 % PP + 2 % MAPP	/

III. 2. 5. Differential scanning calorimetry (DSC)

Differential Scanning Calorimetry (DSC) tests were carried out using Perkin-Elmer Pyris Diamond DSC, equipped with an Intracooler II using nitrogen as purge gas. Samples of 10 mg were cut from the injection moulded specimens and placed in aluminium pans. The thermal cycle was a first heating from 10 to 200°C, then cooling down to 10°C and a second heating up to 200°C with heating/cooling rates of 10°C/min and holding times of 2 min between each step. Two samples were tested per materials. Results were highly reproducible and gave low standard deviations. Melting enthalpies ΔH_m (J/g) were determined between 143 and 175°C on the first heating ramp. The degree of crystallinity X_c (%) was calculated according to the following **Equation (III-2)**:

$$X_c = \left(\frac{|\Delta H_m|}{\chi_{matrix} \text{ x } |\Delta H_m^0|} \right) \text{x } 100 \qquad \text{(III-2)}$$

Where ΔH_m^0 is the melting enthalpy of 100% crystalline PP (207 J/g) [37], ΔH_m is the melting enthalpy of the sample (J/g) and χ_{matrix} is the weight fraction of PP or PP / MAPP within the sample.

III. 2. 6. Microstructural analysis by SEM

Microstructural analysis of the biocomposites was conducted on tensile specimens polished in the central zone down to 300 μm below the surface, ensuring that samples were observed in the shell/core zone [38], [39]. These polished samples were observed by Scanning Electron Microscopy SEM (FEI Quanta 200) and cartographies of 4 mm x 4 mm consisting of 16 SEM images were built using the software Aztec® (Oxford Instruments). All the SEM observations were made on sputter coated samples with carbon using a BALZERS CED 030 in order to avoid any degradation. Micrographs were obtained under high vacuum at acceleration voltage 12.5 keV. Based on cartographies, fibre size and shape distributions were analysed with the software AphelionTM V.4.3.2 (ADCIS and Amerinex Applied Imaging Inc.), which automatically detects the outlines of the fibres present on the pictures. Fibre length (L) and width (W) were determined as the maximum and minimum Feret's diameters with roughly 1300 fibres per cartography. The fibre shape is defined by its aspect ratio (L / W), i.e. the ratio between the maximum and the minimum Feret's diameter. Overlapped fibres were excluded from the counts. Because of the pictures resolution (0.67 μm/pixel), the particles with the maximum size smaller than 335 μm^2 (corresponding to cell wall fragments) were not considered in the fibre size and shape distributions.

III. 2. 7. Tensile properties

Tensile properties of the biocomposites were measured with a Zwick TH 010 testing machine equipped with an extensometer Zwick "clip-on" for the determination of the Young's modulus (ISO 527 standard). The displacement speed of the crosshead was 1 mm/min for the determination of the Young's modulus and 10 mm/min for the determination of the ultimate tensile properties (ultimate strength, elongation at break and work of rupture). Five samples per materials were tested and showed good reproducibility.

III. 2. 8. *In situ* micro-mechanical tensile SEM experiments

The SEM was equipped with a tensile stage (DEBEN microtest, maximum load 5 kN) to analyse interfacial failure mechanisms. Direct observations of the crack propagation were conducted at a displacement speed of 0.1 mm/min on notched specimens with dimensions of 20 mm × 5 mm × 2 mm and a notch of 1 mm depth and 45 ± 1° opening. Before testing, notched samples were polished to remove the 100 µm thick polymer layer from the surface and better observe failure mechanisms between the fibres and the matrix. Experiments were performed twice per materials.

III. 3. Results and discussions

III. 3. 1. Surface free energy of flax fibres and work of adhesion

Total surface free energy γ_s^{tot} of elementary flax fibre and its polar and dispersive components γ_s^p and γ_s^d (mJ/m²) were determined by the Owens, Wendt, Rabel and Kaelble (OWRK) approach [40] (valid only at small temperature variations), knowing the respective polar and dispersive surface tensions of the testing liquid γ_L^p and γ_L^d (mJ/m²), **Equation (III-3)**:

$$\frac{\gamma_L^{tot}(1+\cos\theta_e)}{2\sqrt{\gamma_L^d}} = \sqrt{\boldsymbol{\gamma_S^p}} \times \sqrt{\frac{\gamma_L^p}{\gamma_L^d}} + \sqrt{\boldsymbol{\gamma_S^d}} \qquad \text{(III-3)}$$

Polar and dispersive surface tensions values of water ($\gamma_L^p = 51.0$ mJ/m²; $\gamma_L^d = 21.8$ mJ/m²), *n*-hexan ($\gamma_L^p = 0$ mJ/m²; $\gamma_L^d = 18.4$ mJ/m²), diiodomethane ($\gamma_L^p = 2.3$ mJ/m²; $\gamma_L^d = 48.5$ mJ/m²) have been used. The resulting surface free energy and its dispersive and polar components values are reported in **Table III-2** for non-treated and treated flax fibres. It was verified that the wetted length did not change after immersion in liquids, meaning that fibre swelling did not occur here and then, this phenomenon has not be considered for surface energy determination [35]. Raw flax fibres have a total surface free energy of 34.3 mJ/m² with polar and dispersive components of 18.2 mJ/m² and 16.1 mJ/m², respectively. First, the presence of cellulose nanocrystals (CNC) at the surface of flax fibres decreases their total surface free energy to 30.9 mJ/m². Its polar component

is greatly decreased from 18.2 mJ/m² to 12.9 mJ/m² while its dispersive component is slightly increased from 16.1 mJ/m² to 18.0 mJ/m².

Table III-2: Measured surface free energies (with their polar and dispersive components) for non-treated and treated flax fibres at 20°C; Surface energies of PP and MAPP matrices at 20°C (data from Fuentes *et al.* 2018) and 190°C (calculated from literature data* obtained between 20°C and 220°C).

Temperature 20°C	γ_S^p (mJ/m²)	γ_S^d (mJ/m²)	γ_S^{tot} (mJ/m²)
PP [41]	0.1	30.5	30.6
MAPP [41]	0.3	31.8	32.1
Flax	18.2 ± 3.0	16.1 ± 0.2	34.3 ± 3.2
Flax_CNC	12.9 ± 0.8	18.0 ± 1.1	30.9 ± 1.9
Flax_XG/CNC	17.5 ± 3.8	16.8 ± 0.4	34.4 ± 4.2
Temperature 190°C	γ_L^p (mJ/m²)	γ_L^d (mJ/m²)	γ_L^{tot} (mJ/m²)
PP *	0.1	21.1	21.2
MAPP *	0.2	22.0	22.2

**calculated from Fuentes et al. (2018), Khoshkava & Kamal (2013), Kwok et al. (1998), Schonhorn et Sharpe (1965), Tran et al. (2013).*

As explained in the introduction section, CNC display a predominant dispersive character due to its crystalline and almost pure cellulosic structure. This characteristic may explain the increase dispersive character of CNC modified flax fibres. Topographical changes at the flax fibre surface due to nanostructuration with CNC might also play a role. In fact, the wettability of a surface is governed by its physico-chemical interactions with test liquids but also by its surface morphology and characteristic (roughness, specific surface area,…) [42]. Qian *et al.* obtained the same trend via the grafting of carbon nanotubes on carbon fibre surface with a pronounced decrease of the total surface energy of the carbon fibre from 54.6 ± 1.4 mN/m to 38.8 ± 2.4 mN/m [43]. The polar part decreased strongly from 29.7 ± 1.0 mN/m to 1.0 ± 0.6 mN/m while an increase of the dispersive part from 24.9 ± 0.4 mN/m to 37.8 ± 1.9 mN/m was observed.

For the XG/CNC modified flax fibres, no changes were observed with total surface free energy and polar and dispersive components similar to the raw flax fibres. It is thus assumed that

xyloglucan has a counterbalancing effect compared to CNC, and increases the polarity of flax fibres. It is known in literature that hemicelluloses as xyloglucan have a pronounced polar character [44].

Based on the respective surface free energy of flax fibres and surface tension of the molten matrices, i.e. PP or MAPP, it is possible to predict the adhesion strength at the fibre / matrix interface. The work of adhesion (W_A) greatly influences the wettability of the fibres towards the matrix during processing and plays a role in the interfacial adhesion within the final biocomposite. The highest the W_A, the better would be the wettability and the quality of adhesion between fibres and matrix. The work of adhesion W_A (mJ/m²) was calculated with **Equation III-4** derived from the OWRK approach [40] based on the geometric mean of dispersive and polar components of the liquid surface tension and solid surface free energy:

$$W_A = 2 \times [\sqrt{\gamma_S^d \times \gamma_L^d} + \sqrt{\gamma_S^p \times \gamma_L^p}] \quad \text{(III-4)}$$

And with the **Equation III-5** derived from the Wu approach [45] based on the harmonic mean of dispersive and polar components of the liquid surface tension and solid surface free energy:

$$W_A = 4 \times (\frac{\gamma_L^d . \gamma_S^d}{\gamma_L^d + \gamma_S^d} + \frac{\gamma_L^p . \gamma_S^p}{\gamma_L^p + \gamma_S^p}) \quad \text{(III-5)}$$

Surface energy / tension values of PP at various temperatures measured either by the sessile drop (low temperature) or the pendant drop (high temperature) techniques [33], [41], [46]–[48] have been used to determine the surface tension of PP at a temperature of 190°C, corresponding to the processing conditions used in the micro-compounder. We assumed that the evolution of the surface tension of PP and MAPP is linear, a constant polarity ratio $\gamma_L^p / \gamma_L^{tot}$ (0.003 for PP and 0.01 for MAPP determined at 20°C from Fuentes et al., 2018) and a constant ratio $\gamma_{PP}^{tot} / \gamma_{MAPP}^{tot}$ (0.953 determined at 20°C from Fuentes et al., 2018) over the temperature range 20 – 220°C. On this basis, we calculated the surface tension and its polar and dispersive components for PP and MAPP at 190°C (see **Table III-2**). Based on our calculation, the increase in temperature decreases the total surface free energy of PP and MAPP with a surface energy thermal coefficient k = - 0.0495 mJ / m²

°C. Note that the variations of polar and dispersive components of these polymers as a function of temperature are not well known but considering the quasi-dispersive character of polyolefin matrices, we assumed that variations should be limited.

The work of adhesion W_A between flax fibres and PP or MAPP was thus determined according to **Equation III-4 and III-5**, and considering the surface tension of PP or MAPP in the molten state at 190°C and the surface energies of raw and flax_CNC or flax_XG/CNC fibres determined by tensiometric tests on single fibres at 20°C given in **Table III-2**. Besides, the values of W_A determined for flax fibres / MAPP suppose a complete migration of MAPP at the fibre / PP matrix interface during the compounding process. The resulting works of adhesion for the different systems are compared in **Figure III-1**.

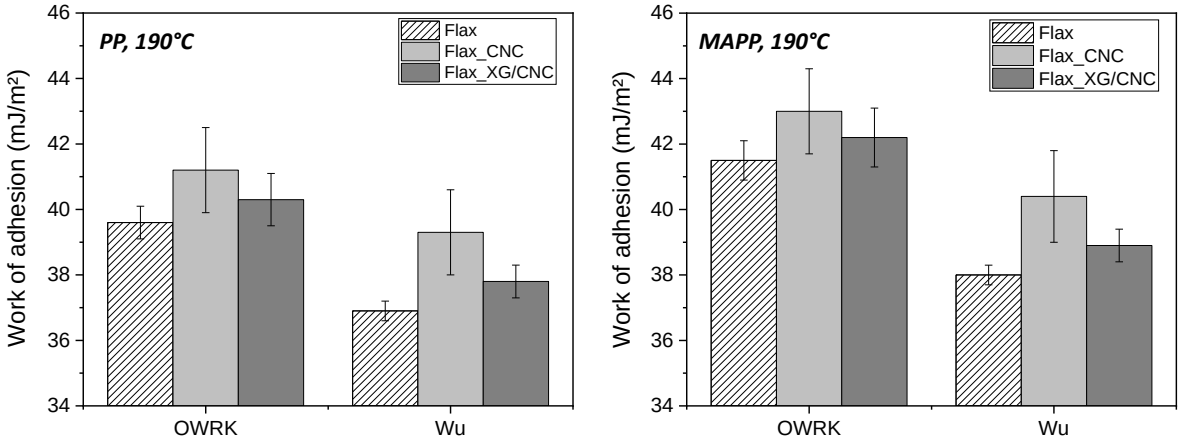

Figure III-1: Work of adhesion between non-treated or treated flax fibres, and PP or MAPP matrices at 190°C calculated by OWRK (**Eq. 4**) and Wu (**Eq. 5**) approaches.

As detailed in the materials and methods, two different approaches were used to calculate W_A (mJ/m²), i.e. the OWRK approach (**Equation III-4**) and the Wu approach (**Equation III-5**). OWRK approach is widely used in literature dealing with interfacial adhesion in composites. However, Wu assumed that the harmonic mean approach gives more consistent results for low energy systems interactions, the geometric mean approach being more suitable to high energy systems like adhesives on metals [45].

As can be seen in **Figure III-1**, the Wu approach gives lower work of adhesion for both PP and MAPP matrices compared to OWRK approach. Taking the example of PP matrix, W_A varies from 36.7 to 38.8 mJ/m² (Wu) against 38.9 mJ/m² to 40.7 mJ/m² (OWRK) for the different flax fibres (raw, flax_CNC or flax_XG/CNC).

Firstly, it is noticeable that the work of adhesion is slightly increased with MAPP whatever the calculation approach and fibre treatment. This suggests a better adhesion and wettability of non-treated and treated flax fibres in the presence of MAPP. This is related to the highest surface tension and polarity of MAPP (versus PP) brought by maleic anhydride functional groups grafted on PP chains [49]. Secondly, an interesting increase of the work of adhesion between CNC treated flax fibres and PP is observed, i.e. from 39.6 mJ/m² to 40.9 mJ/m² (OWRK) and 36.9 mJ/m² to 38.9 mJ/m² (Wu). Similar trend is also observed for CNC treated flax fibres and MAPP, i.e. from 41.5 mJ/m² to 42.7 mJ/m² (OWRK) and 38.0 mJ/m² to 40.0 mJ/m² (Wu). It thus appears that the increase dispersive character of CNC treated fibres promotes the adhesion with mostly apolar polymer matrices such as PP and MAPP.

In contrast, the XG/CNC treated fibres only bring slight improvement of the work of adhesion as their surface free energy and dispersive and polar components are similar to raw flax fibres, the more polar character of XG counterbalancing the increase in dispersive character of the fibres brought by CNC.

Our results suggest that the surface treatment of flax fibres with nano-objects as CNC can improve their work of adhesion with mainly apolar matrices such as PP and MAPP thanks to a better polar / dispersive balance at the fibre surface. The use of PP based coupling agents functionalized with maleic anhydride groups (MAPP) allows a further increase of the work of adhesion due to their higher surface tension and polarity providing that MAPP efficiently migrates at the fibre / PP interfaces.

III. 3. 2. Crystallization and microstructure of biocomposites

III. 3. 2. 1 Crystallization of PP and PP / MAPP

DSC analyses were performed to study the effect of the adsorption of CNC and XG/CNC on flax fibres on the crystallization of PP and PP / MAPP. In fact, the chemical composition as well as the topography of fibre surfaces could play a role on the crystallization behaviour of polymer matrices [50], [51]. Curves of the first heating scan and cooling scan are represented in **Figure III-2** for each prepared biocomposites.

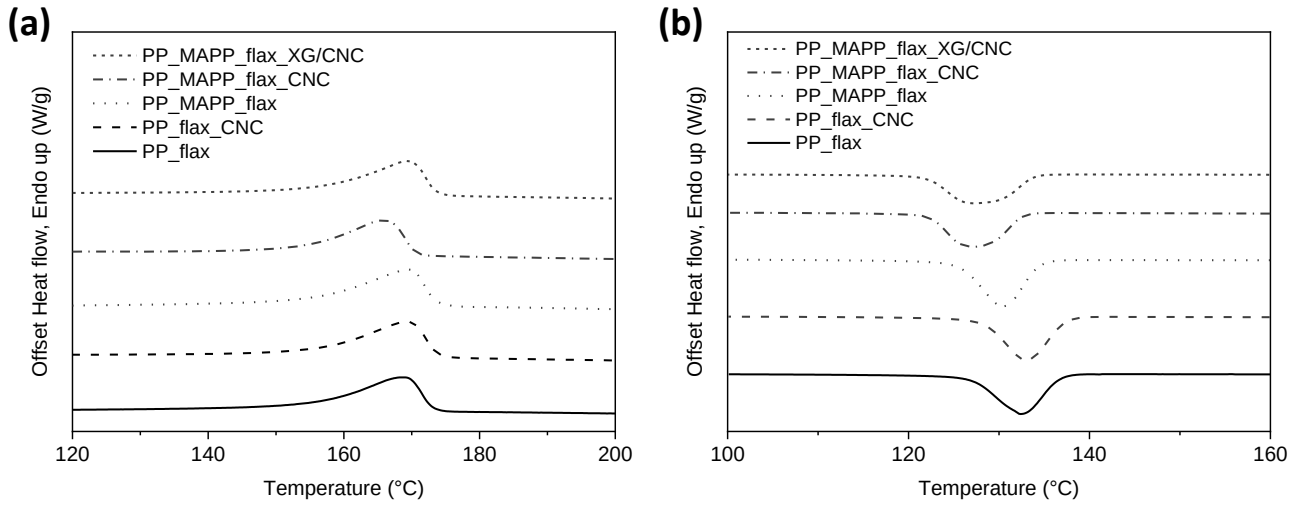

Figure III-2: Thermograms obtained by Differential Scanning Calorimetry of the different prepared biocomposites (a) first heating scan and (b) cooling scan.

First, melting temperatures T_m of the different biocomposites were similar, i.e. roughly 166-170°C, indicating that the thermal stability of the crystals was not significantly affected by the presence of CNC and XG/CNC on flax fibre surface. Then, crystallization temperatures T_c were measured during the cooling step and showed slight differences between biocomposites as shown in **Table III-3**.

Table III-3: Melting temperature T_m and enthalpy ΔH_m, degree of crystallinity X_c and crystallization temperature T_c of the matrix determined from the first heating and cooling scans of DSC thermograms for PP or PP / MAPP based biocomposites reinforced with 20 wt% flax fibres (non-treated, CNC and XG/CNC treated).

	Melting temperature T_m (°C)	**Melting enthalpy ΔH_m (J/g)**	**Degree of crystallinity χ_c (%)**	**Crystallization temperature T_c (°C)**
PP_flax	168.2 ± 1.1	61.9 ± 0.6	37.3 ± 0.4	132.4 ± 0.1
PP_flax_CNC	168.9 ± 0.3	62.1 ± 0.0	37.5 ± 0.0	132.7 ± 0.4
PP_MAPP_flax	170.3 ± 1.3	62.2 ± 1.4	37.6 ± 0.8	131.1 ± 1.0
PP_MAPP_flax_CNC	165.7 ± 0.2	61.2 ± 0.3	37.0 ± 0.2	127.2 ± 0.1
PP_MAPP_flax_XG/CNC	167.8 ± 2.1	58.8 ± 0.1	35.5 ± 0.1	126.8 ± 0.4

PP_flax, PP_flax_CNC and PP_MAPP_flax had T_c = 131 - 132 °C, while PP_MAPP_flax_CNC and PP_MAPP_flax_XG/CNC display lower T_c around 127°C. It seems that the combination of both MAPP and CNC (or XG/CNC) induces a change in the crystallization behaviour of PP with a slight decrease of its crystallization temperature, and hence a possible delayed and/or reduced nucleation. Further isothermal crystallization analysis by DSC and polarized optical microscopy observations would be necessary to better depict the effect of flax fibres and surface modification on the crystallization behaviour of PP.

PP / MAPP based biocomposites reinforced with XG/CNC modified flax fibres also showed a slight decrease in the degree of crystallinity X_c from around 37.5 % to 35.5 % (**Table III-3**). This can be explained by the occurrence of covalent bonds between MAPP and the hydroxyl groups present at the surface of XG/CNC assemblies. This leads to the formation of a covalent bond network of lower molecular mobility at the fibres / matrix interface that could locally hamper the crystallization of PP matrix. This phenomenon is also likely to occur with non-treated flax fibres but the higher specific surface area of CNC implies a higher amount of available hydroxyl groups at the surface of fibres, and hence possibly more covalent bonds with MAPP.

III. 3. 2. 2 Fibre size and shape distribution

The fibre treatments could affect the fibre size and shape distribution within the biocomposites after extrusion and injection processes, so microstructural analysis was performed to investigate this possible effect. In fact, fibre morphology changes influence greatly the mechanical properties of the biocomposite material. The higher the aspect ratio, the most efficient is the load transfer from the matrix to the fibres, and the higher is the stiffness and strength of the composite.

All 4 mm x 4 mm cartographies obtained by SEM of each biocomposite polished surface are shown in **Figure III-3**. A good dispersion and individualization into elementary fibres is observed for a large fraction of flax fibres for all biocomposites with the presence of small particles and also some fibre bundles having a much higher diameter. Results of the fibre aspect ratio distributions are reported in **Figure III-4**. Median aspect ratios are very similar for all biocomposites and range from 2.9 to 3.2 and 3.4 to 3.8 for number and surface weighted distributions, respectively. The morphology of flax fibres after biocomposite processing appears to be unchanged by the different treatments, i.e. addition of MAPP coupling agent and adsorption of CNC or XG/CNC. The obtained mechanical properties of the biocomposites should thus not be influenced by variation in the aspect ratio of the fibres.

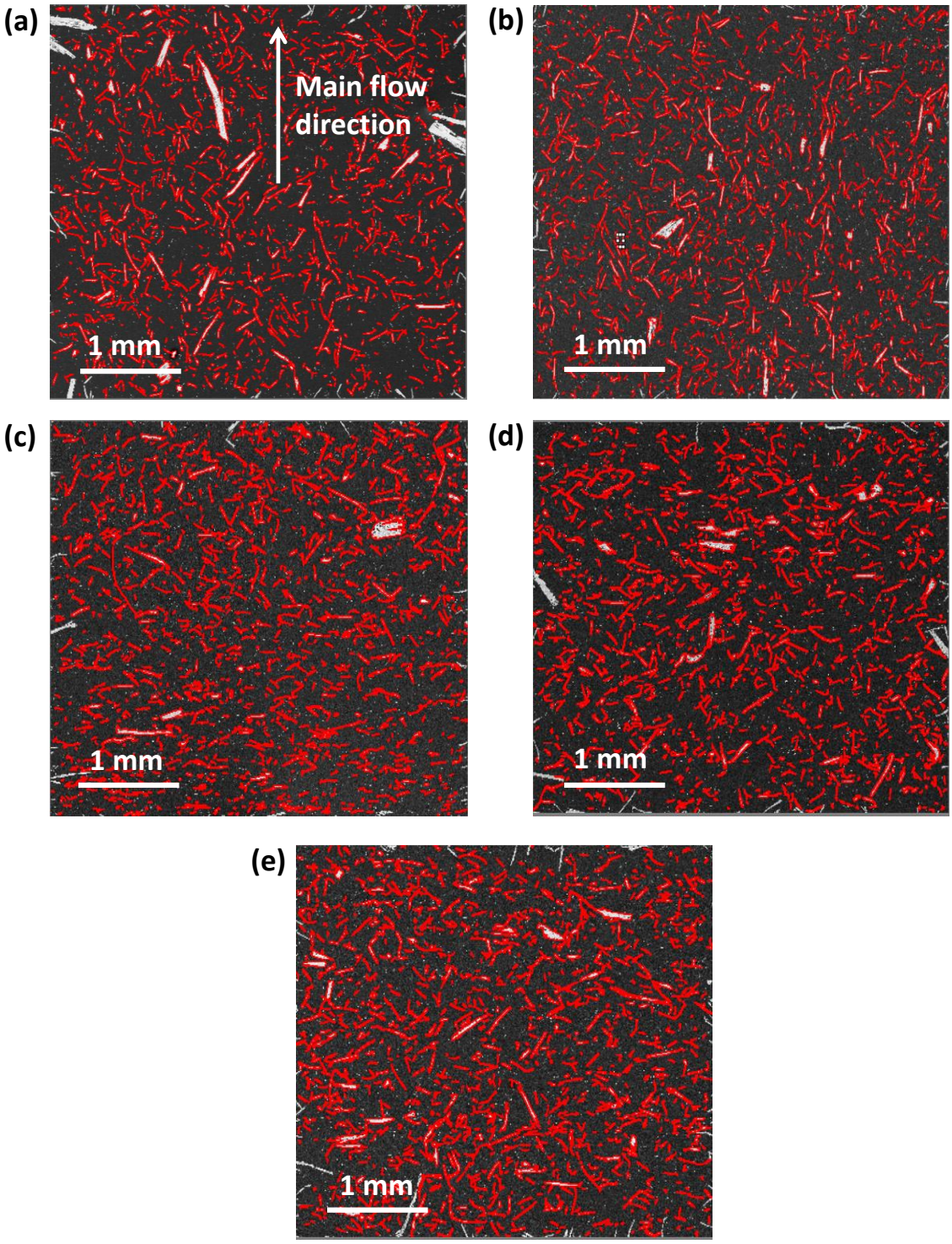

Figure III-3: 4 mm x 4 mm cartography images obtained by SEM for the (a) PP_flax, (b) PP_flax_CNC, (c) PP_MAPP_flax, (d) PP_MAPP_flax_CNC, (e) PP_MAPP_flax_XG/CNC biocomposite. Red lines correspond to automatic detection of the outlines of flax fibres further used for image analysis and calculation of maximum and minimum Feret's diameters.

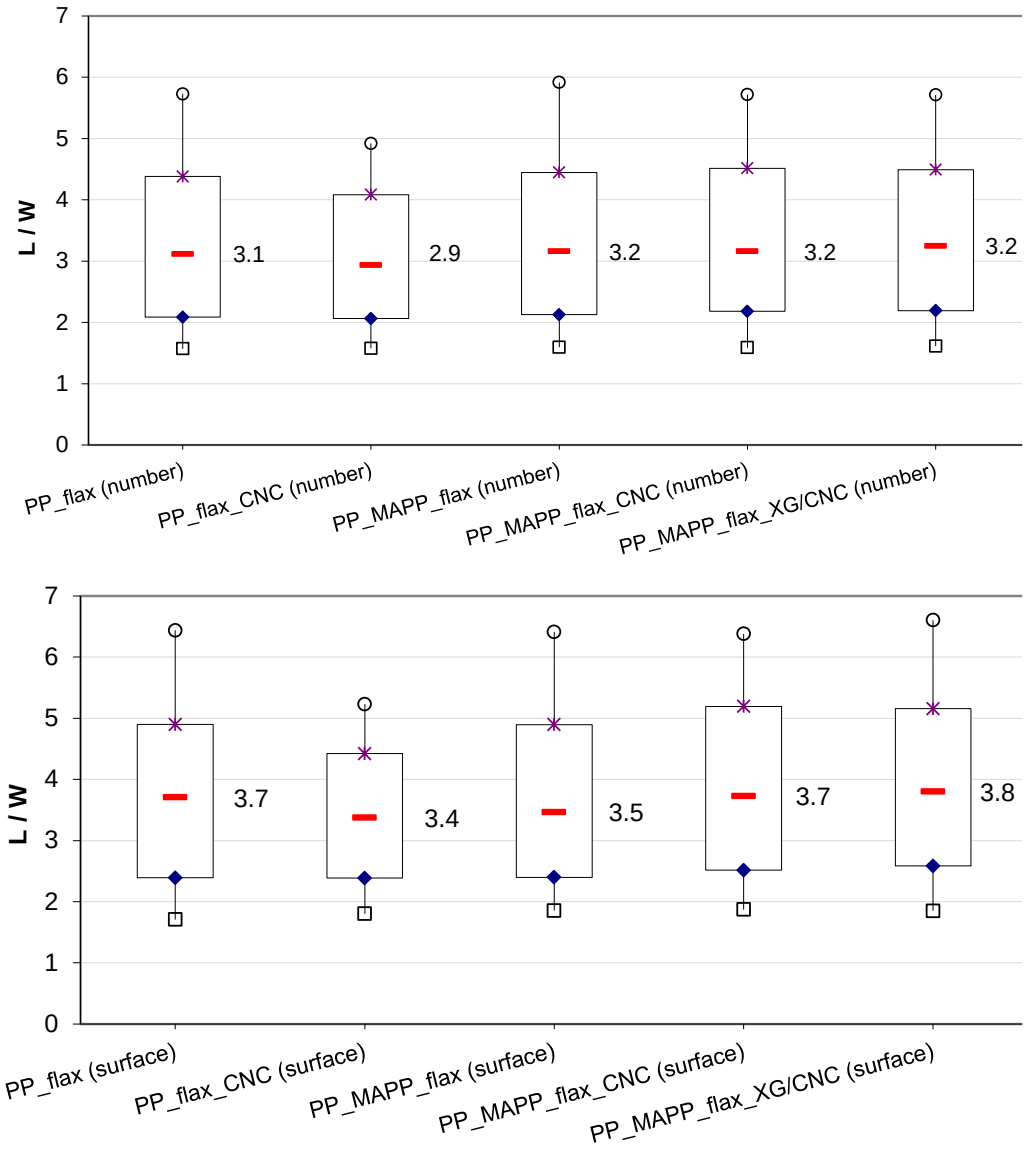

Figure III-4: Resulting box-plots of fibre aspect ratio distributions weighted in surface and in number for the different biocomposites.

Concluding, there are no significant variations in the biocomposites microstructure in terms of fibre size and shape distributions and matrix crystallinity. We thus assume that the mechanical behaviour of the biocomposites should primarily be influenced by variations in the interfacial adhesion brought by the treatments with CNC and XG/CNC on flax fibre surface.

III. 3. 3. Mechanical behaviour and interfacial adhesion of biocomposites

It has been shown previously the positive effect of CNC adsorption onto flax fibres with better work of adhesion with the matrix, this being primarily due to increased dispersive character of fibre surface. Moreover, the MAPP coupling agent also increases the work of adhesion thanks to its higher surface tension and polarity. These results are completed below by macro- and micro-mechanical tests to study the influence of CNC and XG/CNC fibre modifications combined with MAPP coupling agent on the mechanical behaviour of biocomposites and thereby study the practical interfacial adhesion at different length scales.

III. 3. 3. 1 Uniaxial tensile tests

Uniaxial tensile tests were perfomed on biocomposites to determinate their Young's modulus *E* as well as their tensile strength σ_{max} and work of rupture more sensitive to failure mechanisms at the fibre / matrix interface and hence interfacial modifications [15]. The results of the uniaxial tensile tests are presented in **Figure III-5**.

As expected, Young's modulus (**Figure III-5 c**) increases with the amount of flax fibres [52]. No pronounced effect of the CNC and XG/CNC fibre functionalization were observed as the Young's modulus is generally little influenced by the interfacial adhesion, especially for short natural fibres composites for which the quantity of fibre / matrix interfaces developed is limited [15], [53]. We can also observe that the presence of the MAPP coupling agent even slightly decreases the Young's modulus of the biocomposites. It could be explained by a plasticizing effect related to the presence of MAPP within the bulk of the PP matrix that did not migrate at the fibre / matrix interface.

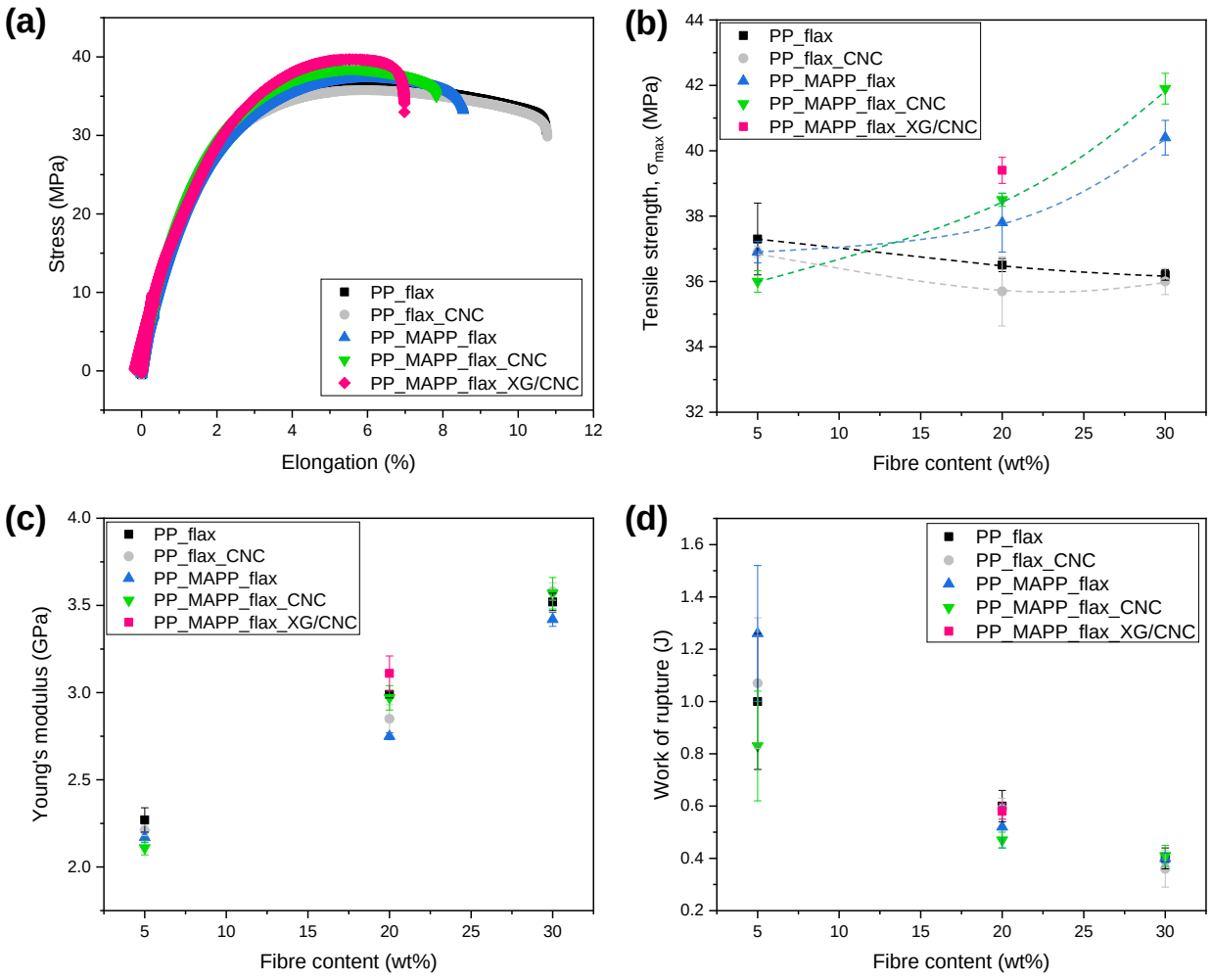

Figure III-5: Typical uniaxial tensile curves at 20wt% fibre content (a), tensile strength (b), Young's modulus (c) and work of rupture (d) for the different biocomposites.

In contrast, pronounced variations in tensile strength (**Figure III-5 b**) are observed for the different biocomposites depending on the interfacial modifications either MAPP coupling agent or CNC, XG/CNC fibre functionalizations. Without the presence of MAPP, it is obvious that the PP / flax interface is not cohesive. The increase in fibre content even results in a slight decrease of the tensile strength because of this weak interfacial adhesion. The same trend is observed for raw flax and flax_CNC fibres. On the other hand, the incorporation of MAPP appears to increase the tensile strength, especially for the highest flax fibre contents. For 30 wt% flax fibres, the tensile strength increases significantly from 36.2 MPa ± 0.2 to 40.4 MPa ± 0.5 for respectively PP_ flax and

PP_MAPP_flax (p-value = 0.0079 based on the statistical Mann & Whitney non-parametric U test). The novelty of our approach is the combination of MAPP with the flax fibres treatment by CNC and XG/CNC. The presence of CNC and XG/CNC on fibre surfaces have a positive effect on the tensile strength of the biocomposite. In fact, the tensile strength increases from 37.4 MPa ± 0.9 to 38.5 MPa ± 0.2 and 39.3 MPa ± 0.3 for respectively PP_MAPP_flax, PP_MAPP_flax_CNC and PP_MAPP_flax_XG/CNC at 20 wt% flax fibres (p-values of 0.19 and 0.015, respectively, based on the statistical Mann & Whitney non-parametric U test). This suggests that the combination of CNC or XG/CNC functionalizations onto flax fibres combined with the incorporation of MAPP coupling agent improves the interfacial adhesion, possibly due to increased interfacial area and preferential chemical interactions between CNC and MAPP.

The work of rupture (**Figure III-5 d**) decreases significantly with increasing fibre contents. In fact, the incorporation of flax fibres makes biocomposite materials less ductile with much lower elongation at break as seen on **Figure III-5 a**. The increase in tensile strength brought by interfacial modifications cannot compensate this loss in ductility, thereby leading to a decreased work of rupture.

III. 3. 3. 2 Micro-mechanical tensile tests

The developed *in situ* micro-mechanical tensile SEM test allows direct observations of crack propagation while recording force-displacement curves (**Figure III-6 a**). This experiment could be assimilated to a pull-out test at a larger scale, i.e. several fibres and bundles are progressively extracted from the matrix during the test. These experiments were performed to better depict the effect of CNC and XG/CNC treatments on interfacial adhesion of flax / PP at the microscale. First, the PP_MAPP_flax composites break at average 233 ± 2 N, while PP_MAPP_flax_CNC and PP_MAPP_flax_XG/CNC break at higher tensile forces, respectively 262 ± 15 N and 260 ± 3 N. The strength improvement related to interfacial adhesion is highlighted by the micro-mechanical tensile test, which is conducted at low tensile speed (0.1 mm/min). PP matrix have more time to dissipate energy and is known to be strain rate dependant [54].

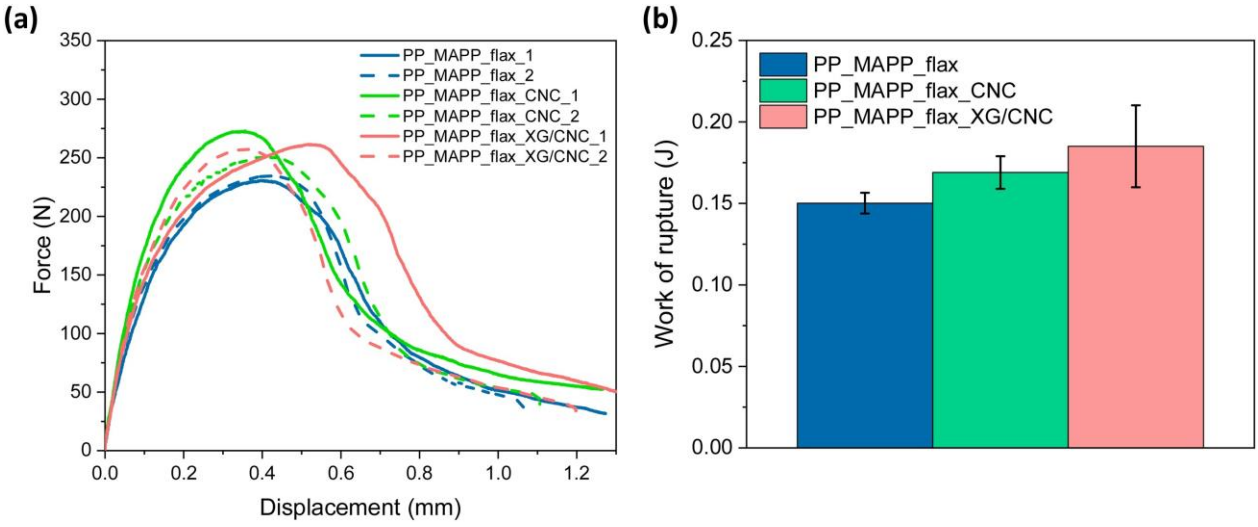

Figure III-6: (a) Force - displacement curves recorded during the micro-tensile test for notched specimens of PP_MAPP_flax, PP_MAPP_flax_CNC and PP_MAPP_flax_XG/CNC with 20 wt% flax fibres and (b) the resulting work of rupture.

Moreover, the work of rupture during crack propagation has also been calculated (**Figure III-6 b**). The biocomposites with CNC and XG/CNC modified flax fibres have better tenacity with an increase of 12.5 % and 21.6 %, respectively. This suggests that the presence of both XG and CNC on the flax fibres modifies the failure mechanisms in the interphase zone between fibres and matrix, leading to higher forces and elongation at break. This hierarchical and extensible XG/CNC network with strong interactions and increasing rupture distance was characterized in our previous work [34] by AFM adhesive force measurements. Our results suggested that such network can have a positive influence in the breaking strength of composite systems.

An analysis of the failure mechanisms by in-situ visualization of the crack propagation has been done for the different biocomposites (**Figure III-7**, the **three videos** are available online on Doineau *et al.* 2021 [55]). As regard the local fibre / matrix interfacial adhesion, behaviours are similar and characteristic of both adhesive and cohesive interfacial failures. Indeed, fibre debonding as well as fibre breakage occurs, the matrix showing mainly ductile behaviour with stretching and tearing. Nevertheless, flax fibres modified by CNC and XG/CNC seem to change the failure pattern of the biocomposites (**Figure III-7**). In the case of PP_MAPP_flax, the failure occurs through the formation of a macro-crack that propagates quasi linearly behind the crack tip.

In the case of PP_MAPP_flax_XG/CNC, the crack propagation is more uneven and occurs through the formation of numerous micro-cracks. These qualitative observations support the higher work of rupture measured for these biocomposites.

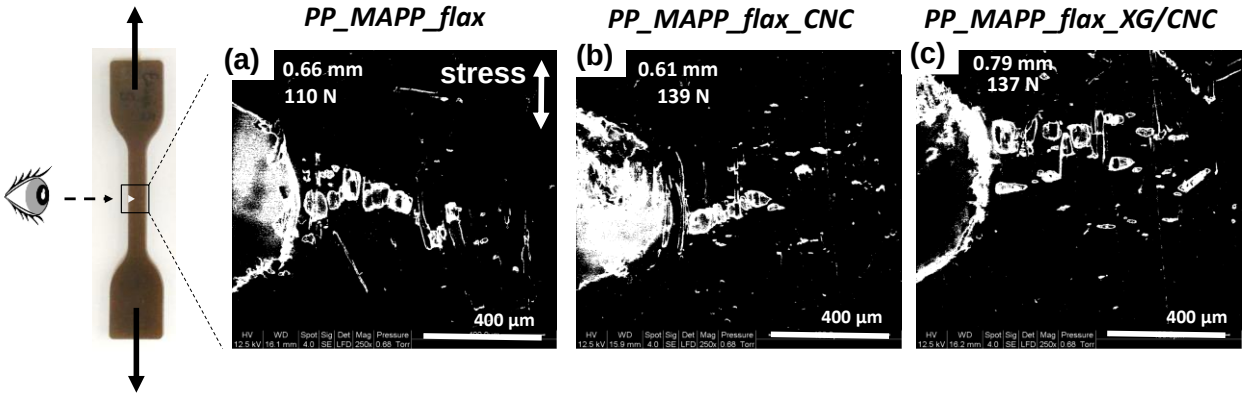

Figure III-7: SEM observations during crack propagation in notched specimens for (a) PP_MAPP_flax, (b) PP_MAPP_flax_CNC and (c) PP_MAPP_flax_XG/CNC with 20 wt% flax fibres. Note that a B&W threshold was applied to the pictures to ease the observation of the described failure phenomena.

The development of hierarchical interphases by the surface modification of natural fibres with biopolymers and nano-reinforcements such as XG/CNC thus appears an interesting strategy to modify failure mechanisms and enhance the strength of biocomposite materials. However, it appears that a chemical coupling between the matrix and modified flax fibres such as MAPP is needed to ensure good interfacial strength and hence better work of rupture.

III. 3. 4. Work of adhesion versus practical adhesion

Figure III-8 shows the correspondence between the work of adhesion that is only governed by physico-chemical interactions between the fibres and the matrix; and the practical adhesion that is related to interfacial strength and influenced by fibre / matrix chemical interactions, mechanical anchorage, transcrystallinity at the interphase and intra and intercellular cohesion within elementary flax fibres and bundles [15].

Both plots evidence that the combination of interfacial modifications with (i) MAPP coupling agent that brought covalent bonds with the fibres and; (ii) hierarchically structured interphases with CNC or XG/CNC assemblies that enhance adhesion and modify the mechanical behaviour in the interfacial zone, could improve the ultimate properties of biocomposites with higher tensile strength and more progressive local failure with higher work of rupture.

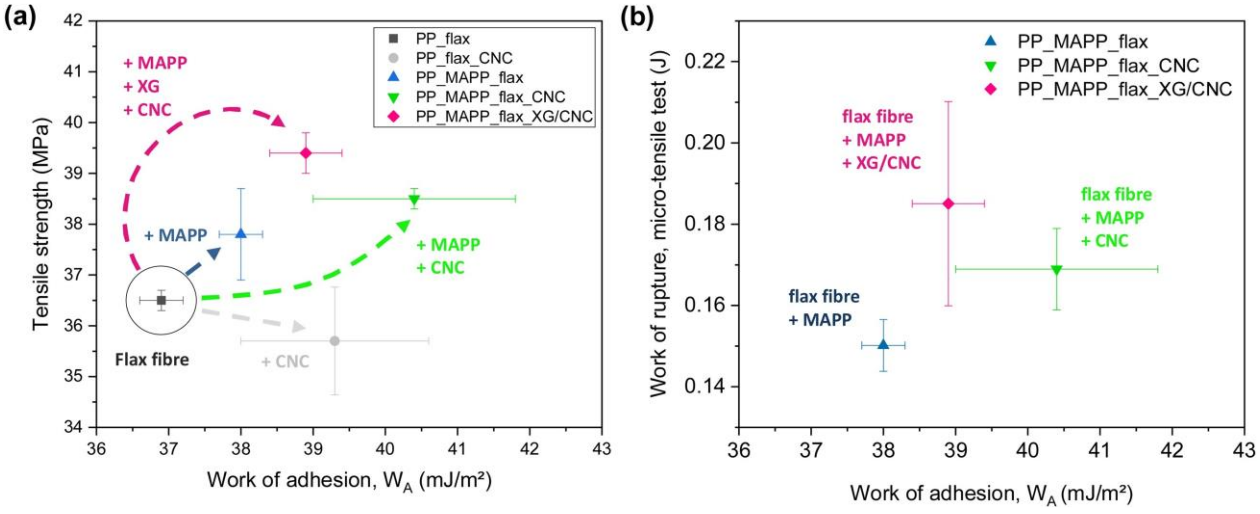

Figure III-8: (a) Tensile strength by uniaxial tensile tests and (b) work of rupture measured by micro-tensile tests for the different biocomposite specimens at 20 wt% flax fibres versus the calculated work of adhesion W_a (Eq. 5) between flax fibres and matrix.

III. 4. Conclusions

The interphase of PP / short flax fibre thermoplastic composites was modified by the combination of two strategies, i.e. (i) chemical coupling by MAPP and (ii) flax fibre nanostructuration with the adsorption of CNC and XG. The resulting fibres and biocomposites were characterized by wettability tests, micro-mechanical tensile tests with *in situ* SEM observations and uniaxial tensile tests. The presence of cellulose nanocrystals on the surface of flax fibres decreased their polar character and improved the work of adhesion with PP / MAPP matrix. Uniaxial tensile tests revealed that combining the incorporation of MAPP coupling agent and the adsorption of CNC or XG/CNC on flax fibres enhanced the strength of PP / flax biocomposites. Furthermore, the work of rupture of the materials measured by micro-mechanical tensile tests was improved by 12.5% and 21.6% for CNC and XG/CNC treatments, respectively. To conclude, the combination of interfacial modifications with nanostructured fibres via the adsorption of CNC and XG/CNC at their surface and the use of coupling agent MAPP that provides covalent bonds with fibres, improves the ultimate properties of biocomposites, giving higher strength and work of rupture, and more progressive local failures. These results open interesting perspectives for the development of bio-based hierarchical composites inspired by naturally occurring structures with enhanced structural properties.

III. 5. References

[1] Bourmaud, J. Beaugrand, D. U. Shah, V. Placet, and C. Baley, 'Towards the design of high-performance plant fibre composites', *Progress in Materials Science*, vol. 97, pp. 347–408, Aug. 2018, doi: 10.1016/j.pmatsci.2018.05.005.

[2] Mohanty, S. Vivekanandhan, J.-M. Pin, and M. Misra, 'Composites from renewable and sustainable resources: Challenges and innovations', *Science*, vol. 362, no. 6414, pp. 536–542, Nov. 2018, doi: 10.1126/science.aat9072.

[3] K. Lau, P. Hung, M.-H. Zhu, and D. Hui, 'Properties of natural fibre composites for structural engineering applications', *Composites Part B: Engineering*, vol. 136, pp. 222–233, Mar. 2018, doi: 10.1016/j.compositesb.2017.10.038.

[4] M. R. Sanjay, P. Madhu, M. Jawaid, P. Senthamaraikannan, S. Senthil, and S. Pradeep, 'Characterization and properties of natural fiber polymer composites: A comprehensive review', *Journal of Cleaner Production*, vol. 172, pp. 566–581, Jan. 2018, doi: 10.1016/j.jclepro.2017.10.101.

[5] K. L. Pickering, M. G. A. Efendy, and T. M. Le, 'A review of recent developments in natural fibre composites and their mechanical performance', *Composites Part A: Applied Science and Manufacturing*, vol. 83, pp. 98–112, Apr. 2016, doi: 10.1016/j.compositesa.2015.08.038.

[6] L. Yan, N. Chouw, and K. Jayaraman, 'Flax fibre and its composites – A review', *Composites Part B: Engineering*, vol. 56, pp. 296–317, Jan. 2014, doi: 10.1016/j.compositesb.2013.08.014.

[7] J. Müssig, *Industrial Applications of Natural Fibres: Structure, Properties and Technical Applications*. John Wiley & Sons, 2010.

[8] W. Garat, N. Le Moigne, S. Corn, J. Beaugrand, and A. Bergeret, 'Swelling of natural fibre bundles under hygro- and hydrothermal conditions: Determination of hydric expansion coefficients by automated laser scanning', *Composites Part A: Applied Science and Manufacturing*, vol. 131, p. 105803, Apr. 2020, doi: 10.1016/j.compositesa.2020.105803.

[9] C. Baley, A. Le Duigou, A. Bourmaud, and P. Davies, 'Influence of drying on the mechanical behaviour of flax fibres and their unidirectional composites', *Composites Part A: Applied Science and Manufacturing*, vol. 43, no. 8, pp. 1226–1233, Aug. 2012, doi: 10.1016/j.compositesa.2012.03.005.

[10] M. Khaldi, M. M. Bouziane, A. Vivet, and H. Bougherara, 'About the influence of temperature and environmental relative humidity on the longitudinal and transverse mechanical properties of elementary alfa fibers', *Journal of Applied Polymer Science*, pp. 1–9, 2019, doi: 10.1002/app.48992.

[11] A. Le Duigou, A. Bourmaud, E. Balnois, P. Davies, and C. Baley, 'Improving the interfacial properties between flax fibres and PLLA by a water fibre treatment and drying cycle', *Industrial Crops and Products*, vol. 39, pp. 31–39, Sep. 2012, doi: 10.1016/j.indcrop.2012.02.001.

[12] A. Le Duigou, J. Merotte, A. Bourmaud, P. Davies, K. Belhouli, and C. Baley, 'Hygroscopic expansion: A key point to describe natural fibre/polymer matrix interface bond strength', *Composites Science and Technology*, vol. 151, pp. 228–233, Oct. 2017, doi: 10.1016/j.compscitech.2017.08.028.

[13] A. Bismarck *et al.*, 'Surface characterization of flax, hemp and cellulose fibers; Surface properties and the water uptake behavior', *Polymer Composites*, vol. 23, no. 5, pp. 872–894, 2002, doi: 10.1002/pc.10485.

[14] O. Faruk, A. K. Bledzki, H.-P. Fink, and M. Sain, 'Biocomposites reinforced with natural fibers: 2000–2010', *Progress in Polymer Science*, vol. 37, no. 11, pp. 1552–1596, Nov. 2012, doi: 10.1016/j.progpolymsci.2012.04.003.

[15] N. Le Moigne, B. Otazaghine, S. Corn, H. Angellier-Coussy, and A. Bergeret, *Surfaces and Interfaces in Natural Fibre Reinforced Composites*. Cham: Springer International Publishing, 2018.

[16] K.-Y. Lee, A. Delille, and A. Bismarck, 'Greener Surface Treatments of Natural Fibres for the Production of Renewable Composite Materials', in *Cellulose Fibers: Bio- and Nano-Polymer*

Composites, S. Kalia, B. S. Kaith, and I. Kaur, Eds. Berlin, Heidelberg: Springer Berlin Heidelberg, 2011, pp. 155–178.
[17] Mohanty, M. Misra, and L. T. Drzal, 'Surface modifications of natural fibers and performance of the resulting biocomposites: An overview', *Composite Interfaces*, vol. 8, no. 5, pp. 313–343, Jan. 2001, doi: 10.1163/156855401753255422.
[18] N. E. Zafeiropoulos, *Interface Engineering of Natural Fibre Composites for Maximum Performance*. Elsevier, 2011.
[19] A. Elsabbagh, L. Steuernagel, and G. Ziegmann, 'Effect of fiber/matrix chemical modification on the mechanical properties and water absorption of extruded flax/polypropylene composite', *Journal of Applied Polymer Science*, vol. 111, no. 5, pp. 2279–2289, Mar. 2009, doi: 10.1002/app.29272.
[20] J. Z. Lu, 'Chemical coupling in wood fiber and polymer composites: A review of coupling agents and treatments', *Wood and Fiber Science*, vol. 32, no. 1, pp. 88–104, 2000.
[21] S. Mohanty, S. K. Nayak, S. K. Verma, and S. S. Tripathy, 'Effect of MAPP as a Coupling Agent on the Performance of Jute–PP Composites':, *Journal of Reinforced Plastics and Composites*, Aug. 2016, doi: 10.1177/0731684404032868.
[22] J.-M. Park, S. T. Quang, B.-S. Hwang, and K. L. DeVries, 'Interfacial evaluation of modified Jute and Hemp fibers/polypropylene (PP)-maleic anhydride polypropylene copolymers (PP-MAPP) composites using micromechanical technique and nondestructive acoustic emission', *Composites Science and Technology*, vol. 66, no. 15, pp. 2686–2699, Dec. 2006, doi: 10.1016/j.compscitech.2006.03.014.
[23] H. Gao, B. Ji, I. L. Jager, E. Arzt, and P. Fratzl, 'Materials become insensitive to flaws at nanoscale: Lessons from nature', *Proceedings of the National Academy of Sciences*, vol. 100, no. 10, pp. 5597–5600, May 2003, doi: 10.1073/pnas.0631609100.
[24] H. S. Gupta, J. Seto, W. Wagermaier, P. Zaslansky, P. Boesecke, and P. Fratzl, 'Cooperative deformation of mineral and collagen in bone at the nanoscale', *Proceedings of the National Academy of Sciences*, vol. 103, no. 47, pp. 17741–17746, Nov. 2006, doi: 10.1073/pnas.0604237103.
[25] H. Daniel Wagner, 'Nanotube–polymer adhesion: a mechanics approach', *Chemical Physics Letters*, vol. 361, no. 1, pp. 57–61, Jul. 2002, doi: 10.1016/S0009-2614(02)00948-X.
[26] J. D. H. Hughes, H. Morley, and E. E. Jackson, 'Aligned carbon fibre composite which approaches theoretical strength', *J. Phys. D: Appl. Phys.*, vol. 13, no. 6, pp. 921–936, Jun. 1980, doi: 10.1088/0022-3727/13/6/005.
[27] A. Le Duigou, A. Kervoelen, A. Le Grand, M. Nardin, and C. Baley, 'Interfacial properties of flax fibre–epoxy resin systems: Existence of a complex interphase', *Composites Science and Technology*, vol. 100, pp. 152–157, Aug. 2014, doi: 10.1016/j.compscitech.2014.06.009.
[28] P.-J. Liotier *et al.*, 'Role of interface formation versus fibres properties in the mechanical behaviour of bio-based composites manufactured by Liquid Composite Molding processes', *Composites Part B: Engineering*, pp. 86–95, Apr. 2019.
[29] A. Dufresne, *Nanocellulose: From Nature to High Performance Tailored Materials*. Walter de Gruyter GmbH & Co KG, 2017.
[30] E. J. Foster *et al.*, 'Current characterization methods for cellulose nanomaterials', *Chemical Society Reviews*, vol. 47, no. 8, pp. 2609–2679, 2018, doi: 10.1039/C6CS00895J.
[31] D. Klemm *et al.*, 'Nanocelluloses: A New Family of Nature-Based Materials', *Angewandte Chemie International Edition*, vol. 50, no. 24, pp. 5438–5466, Jun. 2011, doi: 10.1002/anie.201001273.
[32] R. J. Moon, A. Martini, J. Nairn, J. Simonsen, and J. Youngblood, 'Cellulose nanomaterials review: structure, properties and nanocomposites', *Chem. Soc. Rev.*, vol. 40, no. 7, pp. 3941–3994, Jun. 2011, doi: 10.1039/C0CS00108B.
[33] V. Khoshkava and M. R. Kamal, 'Effect of Surface Energy on Dispersion and Mechanical Properties of Polymer/Nanocrystalline Cellulose Nanocomposites', *Biomacromolecules*, vol. 14, no. 9, pp. 3155–3163, Sep. 2013, doi: 10.1021/bm400784j.

[34] E. Doineau *et al.*, 'Adsorption of xyloglucan and cellulose nanocrystals on natural fibres for the creation of hierarchically structured fibres', *Carbohydrate Polymers*, vol. 248, p. 116713, Nov. 2020, doi: 10.1016/j.carbpol.2020.116713.
[35] M. F. Pucci, P.-J. Liotier, D. Seveno, C. Fuentes, A. Van Vuure, and S. Drapier, 'Wetting and swelling property modifications of elementary flax fibres and their effects on the Liquid Composite Molding process', *Composites Part A: Applied Science and Manufacturing*, vol. 97, pp. 31–40, Jun. 2017, doi: 10.1016/j.compositesa.2017.02.028.
[36] M. H. B. Snijder and H. L. Bos, 'Reinforcement of polypropylene by annual plant fibers: optimisation of the coupling agent efficiency', *Composite Interfaces*, vol. 7, no. 2, pp. 69–75, Jan. 2000, doi: 10.1163/156855400300184235.
[37] RL. Blaine, 'Polymer Heats of fusion'. Therm Appl Note TN048, 2002.
[38] A. Abdennadher, 'Injection Moulding of Natural Fibre Reinforced Polypropylene: Process, Microstructure and Properties', PhD Thesis, Ecole nationale supérieure des Mines de Paris, 2015.
[39] R. S. Bay and C. L. Tucker III, 'Fiber orientation in simple injection moldings. Part I: Theory and numerical methods', *Polymer Composites*, vol. 13, no. 4, pp. 317–331, Aug. 1992, doi: 10.1002/pc.750130409.
[40] D. K. Owens and R. C. Wendt, 'Estimation of the surface free energy of polymers', *Journal of Applied Polymer Science*, vol. 13, no. 8, pp. 1741–1747, 1969, doi: 10.1002/app.1969.070130815.
[41] C. A. Fuentes *et al.*, 'Predicting the adhesion strength of thermoplastic/glass interfaces from wetting measurements', *Colloids and Surfaces A: Physicochemical and Engineering Aspects*, vol. 558, pp. 280–290, Dec. 2018, doi: 10.1016/j.colsurfa.2018.08.052.
[42] S. Li *et al.*, 'Super-Hydrophobicity of Large-Area Honeycomb-Like Aligned Carbon Nanotubes', *J. Phys. Chem. B*, vol. 106, no. 36, pp. 9274–9276, Sep. 2002, doi: 10.1021/jp0209401.
[43] H. Qian, A. Bismarck, E. S. Greenhalgh, G. Kalinka, and M. S. P. Shaffer, 'Hierarchical Composites Reinforced with Carbon Nanotube Grafted Fibers: The Potential Assessed at the Single Fiber Level', *Chem. Mater.*, vol. 20, no. 5, pp. 1862–1869, Mar. 2008, doi: 10.1021/cm702782j.
[44] C. L. Pirich, R. A. de Freitas, M. A. Woehl, G. F. Picheth, D. F. S. Petri, and M. R. Sierakowski, 'Bacterial cellulose nanocrystals: impact of the sulfate content on the interaction with xyloglucan', *Cellulose*, vol. 22, no. 3, pp. 1773–1787, Jun. 2015, doi: 10.1007/s10570-015-0626-y.
[45] S. Wu, 'Calculation of interfacial tension in polymer systems', *Journal of Polymer Science Part C: Polymer Symposia*, vol. 34, no. 1, pp. 19–30, 1971, doi: 10.1002/polc.5070340105.
[46] D. Y. Kwok, L. K. Cheung, C. B. Park, and A. W. Neumann, 'Study on the surface tensions of polymer melts using axisymmetric drop shape analysis', *Polymer Engineering & Science*, vol. 38, no. 5, pp. 757–764, 1998, doi: 10.1002/pen.10241.
[47] H. Schonhorn and L. H. Sharpe, 'Surface tension of molten polypropylene', *Journal of Polymer Science Part B: Polymer Letters*, vol. 3, no. 3, pp. 235–237, 1965, doi: 10.1002/pol.1965.110030316.
[48] L. Q. N. Tran, C. A. Fuentes, C. Dupont-Gillain, A. W. Van Vuure, and I. Verpoest, 'Understanding the interfacial compatibility and adhesion of natural coir fibre thermoplastic composites', *Composites Science and Technology*, vol. 80, pp. 23–30, May 2013, doi: 10.1016/j.compscitech.2013.03.004.
[49] F. Berzin *et al.*, 'Influence of the polarity of the matrix on the breakage mechanisms of lignocellulosic fibers during twin-screw extrusion', *Polymer Composites*, vol. 41, no. 3, pp. 1106–1117, 2020, doi: 10.1002/pc.25442.
[50] J. Girones, L. T. T. Vo, J.-M. Haudin, L. Freire, and P. Navard, 'Crystallization of polypropylene in the presence of biomass-based fillers of different compositions', *Polymer*, vol. 127, pp. 220–231, Oct. 2017, doi: 10.1016/j.polymer.2017.09.006.
[51] Y. Wang, B. Tong, S. Hou, M. Li, and C. Shen, 'Transcrystallization behavior at the poly(lactic acid)/sisal fibre biocomposite interface', *Composites Part A: Applied Science and Manufacturing*, vol. 42, no. 1, pp. 66–74, Jan. 2011, doi: 10.1016/j.compositesa.2010.10.006.

[52] F. Puch and C. Hopmann, ‘Experimental investigation of the influence of the compounding process and the composite composition on the mechanical properties of a short flax fiber–reinforced polypropylene composite’, *Polym. Compos.*, vol. 36, no. 12, pp. 2282–2290, Dec. 2015, doi: 10.1002/pc.23141.
[53] B. D. Agarwal, L. J. Broutman, and K. Chandrashekhara, *Analysis and Performance of Fiber Composites*. John Wiley & Sons, 2017.
[54] A. S. Caro, F. Bernardeau, D. Perrin, R. Leger, J. C. Benezet, and P. Ienny, ‘Computational modelling of void growth in Phenolic Molding Compounds filled PolyPropylene from optical measurements’, *Polymer Testing*, vol. 71, pp. 209–216, Oct. 2018, doi: 10.1016/j.polymertesting.2018.09.008.
[55] E. Doineau *et al.*, ‘Hierarchical thermoplastic biocomposites reinforced with flax fibres modified by xyloglucan and cellulose nanocrystals’, *Carbohydrate Polymers*, vol. 254, p. 117403, Feb. 2021, doi: 10.1016/j.carbpol.2020.117403.

CHAPTER IV

Multi-scale analysis of hierarchical flax fabric reinforced epoxy biocomposites

Table of contents - Chapter IV

Introduction

Unidirectional flax fibre based epoxy laminated composites have already been studied in literature using different processes such as thermocompression, (vacuum-assisted) compression molding, liquid resin infusion or resin transfer molding [1]–[14]. They obtained good mechanical properties with tensile Young's modulus values going from 15 GPa to 39 GPa and tensile strength values from 130 MPa to 415 MPa. Such high variations are strongly due to differences of fibre volume fractions in composites, manufacturing processes and also type of flax reinforcement (directly scutched fibres, unidirectional (UD) or quasi-UD fabrics) [11], [15], [16]. Indeed, as shown in the **Figure IV-1**, performances of fibre based composites are governed by many parameters linked to intrinsic properties of matrix and fibres but also to the manufacturing process and the interphase zone fibre / matrix.

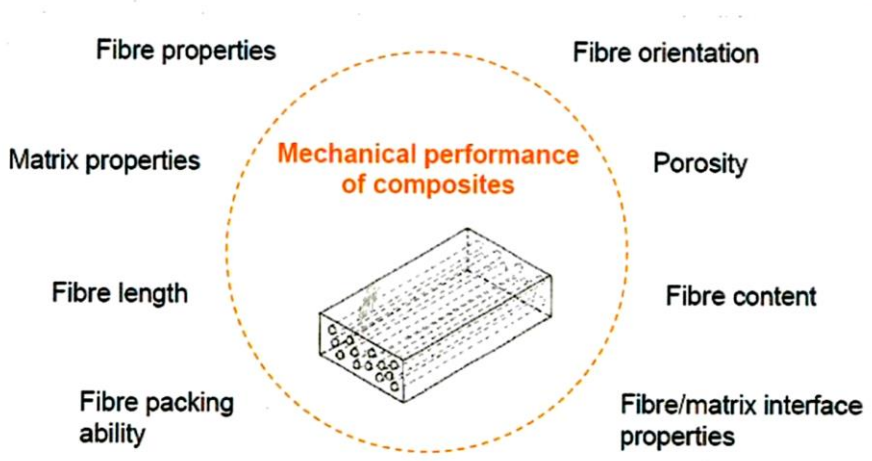

Figure IV-1: A range of parameters influencing the performance of fibre based composites with polymeric matrix (reprinted with permission from CELC & JEC Composites 2012 [15]).

The study of Coroller *et al.* (2013) on the manufacturing of epoxy/glass and epoxy/flax composites with unidirectional reinforcements shows differences in mechanical properties of composites [1]: fibre volume fraction, tensile Young's modulus and strength of 45 %, 34 GPa and 550 MPa for glass fibres respectively, and 51 – 54 %, 26 – 34 GPa and 290 – 410 MPa for flax fibres respectively (according to flax fibre varieties, i.e. Hermès, Andrea or Marylin). This difference is partly due to

differences in intrinsic mechanical properties of reinforcements and also to worse compatibility and interfacial adhesion flax / epoxy. Indeed, glass fibres are systematically submitted to a sizing surface treatment [17], [18], the fruit of several years of development allowing an improvement of fibre / matrix adhesion. This scientific and technological background has not yet been reached for natural fibre reinforced composites. This lower compatibility flax / epoxy is mainly due to hydrophilic and polar flax fibres in contact with apolar and hydrophobic epoxy matrix [19], [20], and induces bad load transfer within the composite at the interphase, a complex zone between flax fibres and epoxy resin [21]. In order to tackle this problem, pre-treatments (retting, defibrillation process, solvent extractions…) [5], [22], chemical functionalization (silanes, NaOH, acid anhydrides…) [13], [14], [23], [24], plasma treatments [25] and/or thermal treatments [26] of flax fibres have been performed to increase the compatibility fibre / matrix and so the interfacial adhesion. However, those strategies did not enhance significantly mechanical properties of flax / epoxy composites. Another strategy based on biological systems (bone, nacre, wood) [27], [28] has also been followed in synthetic/mineral [29]–[32], hybrid [33]–[35] and more recently biobased fibres reinforced epoxy composites [36], ***see Chapter I section I.3***. This strategy of fibre surface modification consists of creating hierarchical fibres via the deposition of nano-objects on their surface (carbon nanotubes, ZnO nanowires, graphene, nanoclay, nano-TiO_2 or nanocellulose). In the paper of Lilli *et al.* (2020), ZnO nanorods coated basalt fibres show a lower surface energy of 23.8 mN/m compared to 32.3 mN/m for commercial sized basalt fibres, with also a strong decrease of the polar component γ_S^p from 14 to 4.2 mN/m [29]. The nanostructuration of fibres show in most of cases an increase of the interfacial shear strength (IFSS) with the epoxy resin, for example an increase of 40.5 % was observed in the work of Wang *et al.* (2015) for nano-TiO2 modified flax fibres (2.34 wt% of particle content) compared to untreated fibres [33]. Finally, the deposition of nano-objects on fibres enhances tensile and flexural mechanical properties. Lee *et al.* (2012) used BC as binder in a sisal preform and obtained huge increases of tensile Young's modulus and strength by 75 % and 71 % respectively for BC – sisal preform / Acrylated Epoxidized Soybean Oil (AESO) biobased composites.

In this context, this work reported the modification of unidirectional flax fabrics by the adsorption of cellulose nanocrystals (CNC) and xyloglucan (XG) and their incorporation in an epoxy resin

matrix to prepare biobased laminates. This study will focus on the multi-scale analysis of hierarchical flax fabric reinforced epoxy biocomposites. The resulting modified flax fabrics, the microstructure and the mechanical behaviour of flax fabric reinforced epoxy laminates are studied. Wettability tests on single CNC and XG/CNC modified flax fibres extracted from fabrics are performed to study the effect of the surface treatments on the surface free energy and its polar and dispersive components as well as the work of adhesion with epoxy matrix. The thermo-mechanical behaviour of the biocomposites is studied by uniaxial tensile tests in the transverse and longitudinal directions and dynamic mechanical thermal analysis. The results are related to the microstructure of the manufactured biocomposite laminates, which are analyzed in terms of volume fractions of the different components and with observations of yarns layout and dispersion within the matrix by scanning electron microscopy (SEM). Finally, the impact of the washing and drying steps applied to flax fabrics during XG/CNC treatments is discussed as regard the biocomposite microstructure and performances.

IV. 2. Materials and methods

IV. 2. 1. Materials

Unidirectional (UD) flax woven fabric 300 g/m² was manufactured by Eyraud (France) and supplied by Fibres Recherche Développement (FRD, France). Cellulose nanocrystals (CNC) were produced by acid hydrolysis of wood pulp and purchased from CelluForce in spray-dried powder (Quebec, Canada). The CNC surface charge density is 0.023 mmol/g; the crystalline fraction: 0.88; the CNC lateral dimensions: 2-5 nm; and the CNC length: 50-110 nm. Xyloglucan Glyloid 6 C was obtained from tamarind seed gum and purchased from DSP Gokyo Food & Chemical (Japan). *Mw* = 840,000 g.mol^{-1}; *Mw*/*Mn* = 1.24, *Rg* 72 nm; monosaccharide composition: Glucose 50.7%; Xylose: 31.7%; Galactose 16.0%; Arabinose 1.6%. Epoxy resin SR Infugreen 810 and hardener SD 4770 were provided by Sicomin (France); ratio 100/29 (g/g); T_g = 97°C; viscosity is 142 mPa.s at 20°C and a maximum bio-based carbon content of 29% for the mix resin/hardener.

IV. 2. 2. Treatment of flax woven fabric with XG and CNC

Cellulose nanocrystals (CNC) and xyloglucan (XG) were adsorbed on UD flax woven fabrics. A CNC suspension was prepared, i.e. 26 g of CNC in 1.8 L deionized water under stirring during 5 hours, corresponding to a ratio *CNC:flax* of *1:6.6*, followed by sonication (cycle 5; amplitude 50%; 2 x 1min) to break residual CNC agglomerates. Then, 8 layers of 25 x 25 cm² flax fabrics were cut from a UD flax woven fabric roll, added in the CNC suspension and stored at 4°C during 16 hours (**Figure IV-2**). The CNC modified flax fabrics, named *flax_CNC*, were then washed carefully with deionized water to remove the non-adsorbed CNC and dried in a heat chamber at 60°C overnight.

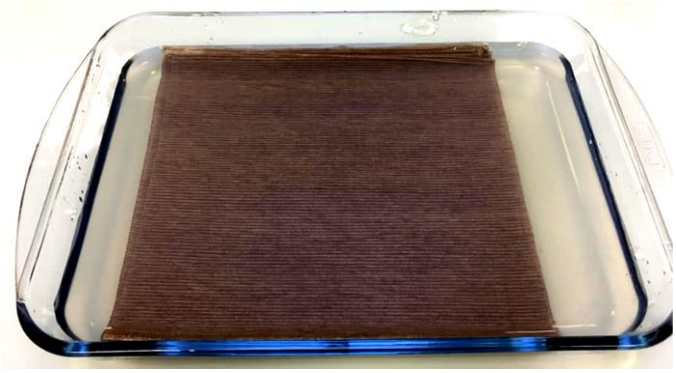

Figure IV-2: Dipping step of flax fabrics in the CNC suspension during 16 hours at 4°C.

Same procedure was followed for the modification of flax fabrics with both XG and CNC. In this case, XG was firstly adsorbed onto flax fabrics as follows: XG suspension was prepared, i.e. 34.8 g of XG added gradually in 2.8 L deionized water with a vortex, at 50 – 60 °C during few hours, corresponding to a ratio *XG:flax* of *1:5*. Then, 8 plies of flax fabrics were put in an adequate container containing the XG suspension and stored at 4°C during 24 hours. The XG modified flax fabrics were then washed carefully with deionized water to remove the non-adsorbed XG, and were then dipped in a suspension of CNC following the previous treatment protocol.

In order to study the possible effect of the water washing/dipping steps on the structure of flax fabrics, a control material has been prepared, i.e. 8 plies of UD flax fabrics were dipped in deionized water (without XG/CNC), stored at 4°C during 24 hours and then dried in a heat chamber at 60°C overnight. Moreover, a different drying method was tested for CNC modified flax fabrics, i.e. 8 plies of CNC modified flax fabrics were dried by contact with hot cylinders (60°C), under strength, to analyse the effect of shrinkage and possible destructuration of the fabric during treatment (**Figure IV-3**).

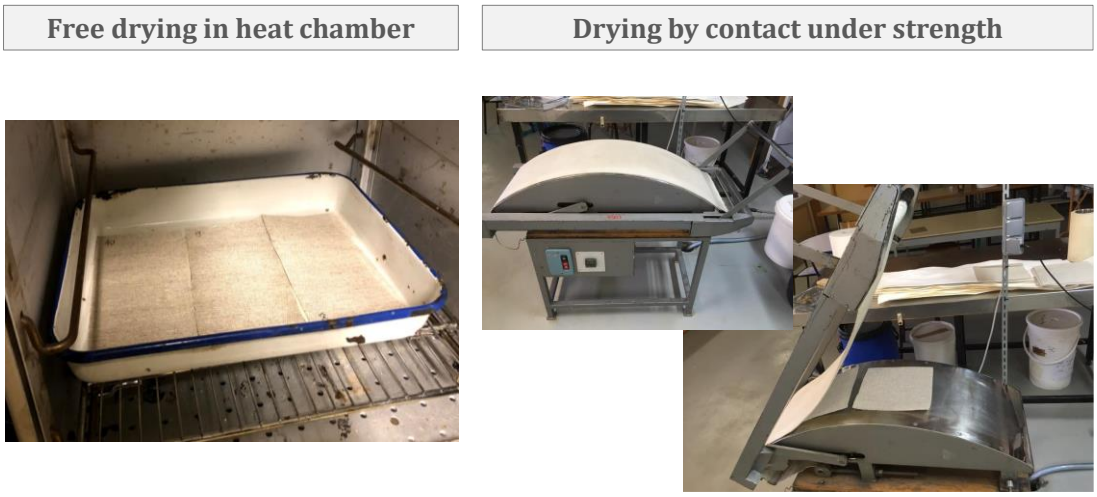

Figure IV-3: Two different dring techniques of the flax fabrics at 60°C with free dring in a heat chamber and drying by contact under strength.

The resulting untreated, control, CNC (free drying or under strength) and XG/CNC modified flax fabrics, named *flax*, *flax_control*, *flax_CNC*, *flax_CNC_under strength* and *flax_XG/CNC* respectively, were stored in a conditioning room at 23°C and 50% relative humidity before being used for composite manufacturing.

IV. 2. 3. Morphology of flax fabrics and yarns

SEM observations were done on flax yarns extracted from raw, CNC and XG/CNC treated UD flax fabrics before their impregnation with epoxy resin, with a Quanta 200 FEG (FEI Company) under high vacuum at acceleration voltage 12.5 keV and magnifications x70 and 2000x (WD = 9.5 mm).

Discs of 25 mm diameter were cut from UD flax fabrics (raw or treated) with a punching machine (CEAST) and placed in an IR-balance (Precisa XM66) to measure their areal density (g/m²) in the dried state at 105°C during 5 minutes (five samples per fabric).

IV. 2. 4. Single fibre tensiometry

As flax yarns are dispersed into individualized flax fibres in the matrix during composite processing, elementary flax fibres extracted from yarns of UD fabrics modified with CNC and XG/CNC were used for these experiments. The tensiometer K100SF (Krüss, GmbH) was used to perform wettability tests in different reference liquids following the Wilhelmy method (**Equation IV-1**):

$$F = m.g = \gamma_L.p.\cos\theta \quad \text{(IV-1)}$$

With F the capillary force (mN) measured by the tensiometer when a single fibre is immersed in the test liquid, m (g) corresponding to the mass of the liquid meniscus formed around the immersed elementary fibre, γ_L (mJ/m²) the liquid surface tension, p (µm) the fibre wetted length or perimeter and θ (°) the static advancing contact angle between the fibre and the liquid [37]. The tensiometry experiments method of this study is based on the one presented in the ***Chapter III, section 2.3.***, with additional experiments consisting in the study of the wettability of flax fibres towards the epoxy resin non-mixed with the hardener. Measurements were done on eight to ten fibres and six were exploited for each.

IV. 2. 5. Manufacturing of biocomposites

The 8 layers of flax fabrics (*flax, flax_control, flax_CNC, flax_CNC_under strength or flax_XG/CNC*) were dried in a heat chamber overnight at 60°C in order to remove any residual water before composite manufacturing. The epoxy system was prepared with a 100 / 29 (g / g) ratio, i.e. 310 g of epoxy resin SR Infugreen 810 and 89.9 g of hardener SD 4770 containing amines, and mixed with a wooden spatula during 5 min to homogenize the mixture. Each flax layer was removed from the heat chamber and directly impregnated by the hand lay-up technique with a silicon basting brush following the longitudinal direction of the yarns (**Figure IV-4**). Between each layer, a spiked roller was used to remove entrapped air bubbles between stacked flax layers. Then, the 8 impregnated and stacked plies were placed in a thermocompression press under various curing pressure and fixed curing temperature (60°C) and time (16 hours). The effect of curing pressure

has been studied to define optimal processing conditions. After processing, the composite laminates were cooled at ambient temperature during 2 hours, demoulded and stored in a conditioning room (23°C; HR = 50%) before subsequent analysis.

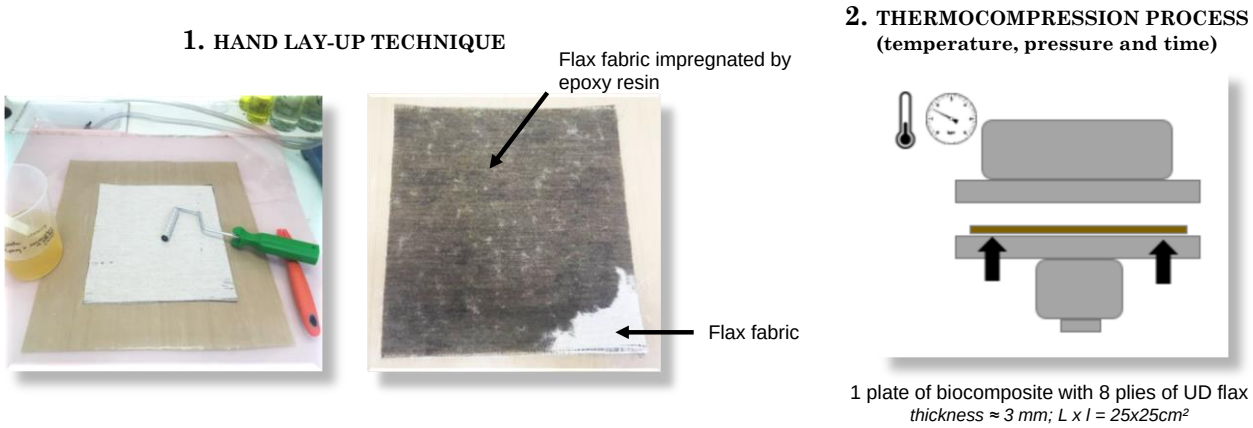

Figure IV-4: Different steps of UD flax / epoxy laminates manufacturing, i.e. hand lay-up technique for the impregnation of epoxy resin on flax plies and thermocompression process.

IV. 2. 6. Microstructural analysis of biocomposites

The fibre ($\%V_f$), matrix ($\%V_m$) and pore ($\%V_p$) volume fractions were calculated using **Equations IV-2, IV-3 and IV-4** [38]:

$$\%V_f = \%m_f \times \frac{\rho_c}{\rho_f} \quad \text{(IV-2)}$$

$$\%V_m = \%m_m \times \frac{\rho_c}{\rho_m} \quad \text{(IV-3)}$$

$$\%V_p = 100 - (\%V_f + \%V_m) \quad \text{(IV-4)}$$

With $\%m_f$ and $\%m_m$ respectively the fibre and matrix mass fractions deduced from the areal densities of the composite plates and the 8 plies of UD flax woven fabric in the dried state (g/m²); ρ_f, ρ_m and ρ_c the bulk densities of respectively flax fibre fabrics, epoxy resin and composite plates. Discs of 25 mm diameter were cut from UD flax / epoxy composite plates with a holesaw and

placed in an IR-balance (Precisa XM66) to measure their areal density (g/m²) in the dried state at 105°C during 5 minutes (three samples per plate). Bulk densities (g/m²) were obtained in dried state (60°C during one night) using a Gas pycnometer (Micromeritics AccuPyc 1330) in helium atmosphere. Densities of flax woven fabrics and epoxy resin were respectively 1.54 and 1.17 g/cm^3 (two samples per material).

In order to analyse the dispersion state and layout of flax yarns within the epoxy matrix in composite laminates, SEM observations were conducted on cross-sections cut in composite plates, perpendicular and parallel to the fibre direction, with a Quanta 200 FEG (FEI Company) under high vacuum at an acceleration voltage of 15 keV. These cross-sections were polished and sputter coated with carbon using a BALZERS CED 030 in order to ensure good surface conductivity and limit flax fibre degradation under the electron beam. For observations parallel to the fibre direction, cartographies of 3.5 mm x 12 mm consisting of 8 SEM images was built using the software Aztec® (Oxford Instruments).

Moreover, the thickness of each composite plate has been measured with a caliper on three different locations.

IV. 2. 7. Uniaxial tensile testing

Tensile mechanical properties were investigated on biocomposite laminates in the longitudinal and transverse directions, i.e. parallel and perpendicular to fibre direction, respectively. Tensile tests were carried out using a MTS machine (Criterion C45.105) equipped with a force sensor of 100 kN and a MTS laser extensometer (LX500). Two reflective stripes were stuck on samples for the determination of the Young's modulus. According to NF EN 2747 standard, composite plates were cut to obtain specimens of 3 mm x 10 mm x 170 mm with a reference length between tensile jaws of 105 mm. The crosshead speed was fixed at 0.5 mm/min until a preload of 20 N and then 2 mm/min until the rupture of the sample. Note that some specimens broke in the crosshead jaws, which could give an underestimation of composites' tensile strength. The tests were performed at 23°C and 50% relative humidity. Minimum of five samples were tested for each biocomposite laminate.

Tensile tests were also performed on the epoxy resin plate prepared with a 100 / 29 (g / g) ratio, i.e. epoxy resin SR Infugreen 810 and hardener SD 4770 containing amines), and mixed with a wooden spatula during 5 min to homogenise the mixture. The epoxy resin modulus E_m = 3.35 GPa, measured following same procedure as flax / epoxy composites, has been used in mixture rules in this article.

IV. 2. 8. Dynamic mechanical thermal analysis (DMTA)

Dynamic mechanical thermal analysis was performed using a VA 815 Metravib RDS in the dual cantilever bending mode in transverse direction to UD composite laminates, i.e. perpendicular to fibre direction. Samples of 80 mm x 10 mm x 3 mm were cut from flax, flax_control, flax_CNC and flax_XG/CNC composites. In order to determine the linear viscoelastic domain of the material, displacement sweeps were tested on raw flax based biocomposite for constant frequency (5 Hz) and temperature (ambient temperature). The optimal displacement amplitude was found to be around 10 µm. Based on this result, samples were heated from 40°C to 120°C with a heating rate of 3°C/min at a frequency of 5 Hz and fixed displacement of 10 µm. The storage modulus (E'), loss modulus (E''), the damping or loss factor (tan δ) and the temperature of the loss factor peak Tα, were recorded. Two samples were tested over two consecutive heating cycles (noted 1st cycle and 2nd cycle) for each biocomposite laminate.

IV. 3. Results and discussions

IV. 3. 1. Effect of treatments on the morphology of flax fabrics and yarns

The dry areal density of the treated flax fabrics was determined (105°C; 5 minutes) and reported in **Table IV-1**. During the treatment with CNC and XG/CNC, UD flax fabrics undergo a dipping step in water and a subsequent drying step at 60°C that could affect their architecture. The sole effect of water dipping has been tested with a flax fabric submitted to same dipping and drying steps but without the functionalizing components (XG and CNC). Moreover, flax fabrics were treated by CNC and dried by contact under strength to analyze eventual shrinkage or destructuration of the fabrics that could occur with a free drying.

Table IV-1: Dry areal density of flax fabrics and adsorbed amount of CNC and XG/CNC on fabrics.

	Flax	**Flax_control**	**Flax_CNC**	**Flax_CNC_under strength**	**Flax_XG/CNC**
Dry areal density of flax fabrics (g/m²)	297.6 ± 7.3	324.1 ± 9.3	334.2 ± 16	342.9 ± 3.8	343.7 ± 5.5
Quantity of adsorbed amount (%)	-	-	3.1	5.8	6.0

First, results highlight a great influence of the treatment steps, i.e. dipping and drying, with an areal density of 324 g/m² for the flax_control fabrics versus 298 g/m² for the raw flax fabrics, which is attributed to shrinkage of the fabrics upon drying. It is also possible to estimate the quantity of XG/CNC adsorbed onto flax fabrics when comparing the areal density of the treated fabrics with the flax_control fabric. Values of adsorbed CNC and XG/CNC vary from 3.1 to 6.0%. Those values are higher than the quantification made in the ***Chapter II*** on twisted yarns based on the UV spectroscopy method via the fluorescent labelling of XG and CNC [39] with an estimated amount of XG/CNC of around 2 %. Variations in the architecture of fabrics during treatments, especially local shrinkage, could explain an overestimation made with the direct gravimetric measurements based on the areal density of the fabrics. On the other hand, the more opened structure of yarns

used in this study could have favoured higher adsorption of XG/CNC than for twisted yarns used in the *Chapter II*.

SEM images of yarns treated with XG/CNC (**Figure IV-5**) show polymeric web- or net-like structures surrounding the fibres (white arrows).

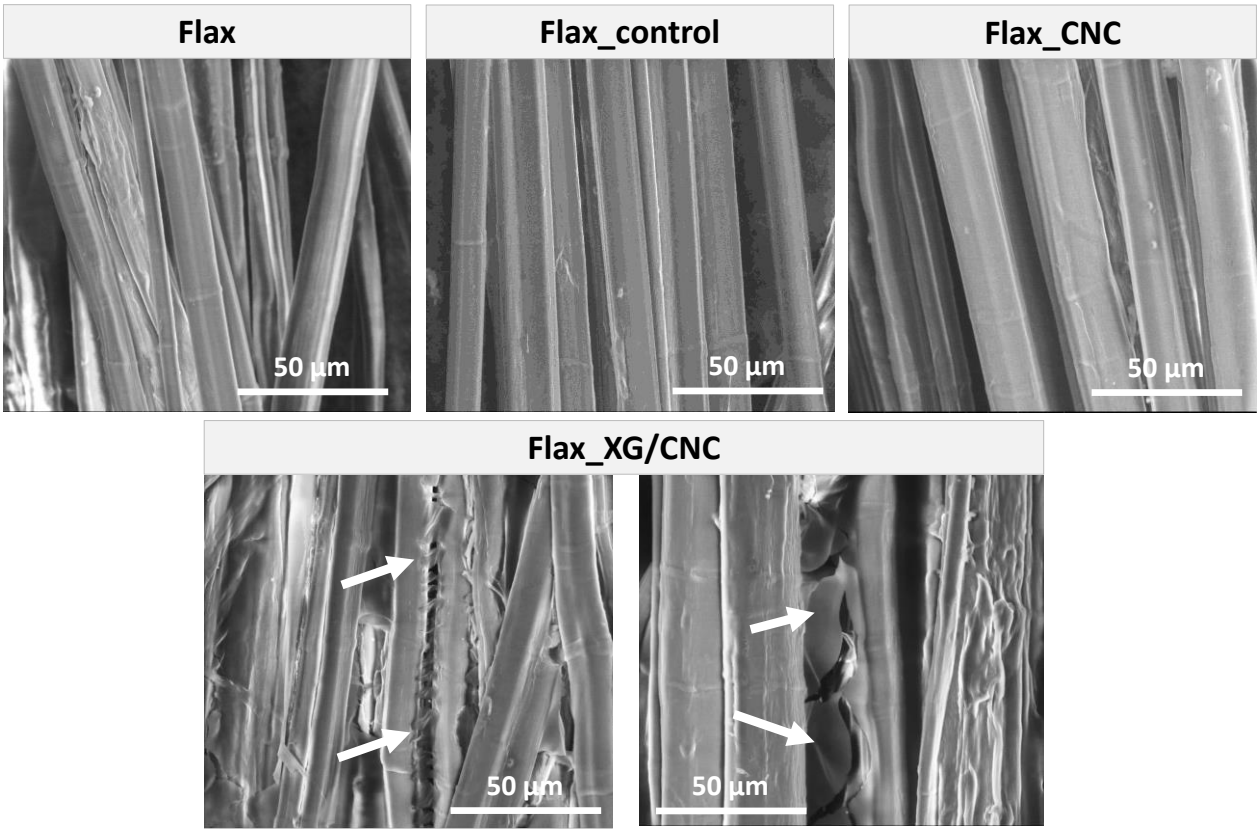

Figure IV-5: SEM images of yarns of raw, control, CNC and XG/CNC treated flax fabrics at magnification x2000.

This was not seen for flax, flax_control and CNC treated flax fabrics, supporting that the presence of XG, possibly in higher amounts in some areas, is responsible for the formation of these polymeric structures.

IV. 3. 2. Surface free energy of flax fibres and work of adhesion

The surface free energy γ_s of elementary flax fibres and its polar and dispersive components γ_s^p and γ_s^d (mJ/m²) were determined by the Owens, Wendt, Rabel and Kaelble (OWRK) approach [40] knowing the respective polar and dispersive surface tensions of the testing liquids γ_L^p and γ_L^d (mJ/m²) (**Equation IV-5**).

$$\frac{\gamma_L(1+\cos\theta)}{2\sqrt{\gamma_L^d}} = \sqrt{\gamma_S^p} \times \sqrt{\frac{\gamma_L^p}{\gamma_L^d}} + \sqrt{\gamma_S^d} \qquad \text{(IV-5)}$$

Surface free energies and its dispersive and polar components have been determined by single-fibre tensiometry and are reported in **Table IV-2** for raw and treated flax fibres (*flax_CNC* and *flax_XG/CNC*). Known surface tensions values of testing liquids are also reported in **Table IV-2** [41]. For the epoxy resin, an overall surface tension of 46.0 mN/m was measured. The polar/dispersive ratio was arbitrarily chosen as such, 44.0 mN/m and 2.0 mN/m for dispersive and polar components, considering the proportions classically observed in the literature [37], [42].

Raw flax fibres have a surface free energy of 34.3 mJ/m² with polar and dispersive components of 18.2 mJ/m² and 16.1 mJ/m², respectively. The treatment of flax fibre surfaces by cellulose nanocrystals (CNC) decreases their surface free energy by roughly 10%. This decrease could be related to the nanostructuration of flax fibre surfaces with the deposition of CNC inducing a possible change in their surface topography such as an increased roughness and an enhancement of their specific surface area [43]. This trend has already been reported for the deposition of carbon nanotubes on carbon fibre surfaces [44]. In contrast, the XG/CNC treatment did not change the surface free energy of flax fibres, which is similar to raw flax fibres. This is probably due to the presence of XG on flax surfaces, modifying their physico-chemistry and possibly smoothing the surfaces and so limiting nanostructuration effects. As discussed in the ***Chapter III, section 3.1***, Khoshkava and Kamal reported concerning CNC a high surface free energy value of 68.9 mJ/m² with a predominant dispersive component, i.e. γ_{CNC}^d = 40.9 mJ/m² and γ_{CNC}^p = 28.0 mJ/m² [45].

Table IV-2: Surface tensions of testing liquids and surface free energies (with their polar and dispersive components) for raw and treated flax fibres at 20°C.

Surface tensions		γ_L^p (mN/m)	γ_L^d (mN/m)	γ_L (mN/m)
Water		51.0	21.8	72.8
n-hexane		0.0	18.4	18.4
Diiodomethane		2.3	48.5	50.8
Epoxy resin		2.0	44.0	46.0
Surface free energies		γ_S^p (mJ/m²)	γ_S^d (mJ/m²)	γ_s (mJ/m²)
Flax		18.2 ± 3.1	16.1 ± 0.2	34.3 ± 3.3
Flax_CNC		13.1 ± 1.3	17.7 ± 0.1	30.8 ± 1.4
Flax_ XG/CNC		17.8 ± 4.4	16.4 ± 0.5	34.2 ± 4.9
Wettability	θ_{epoxy} (°)	W_A (mJ/m²)	W_A' (mJ/m²)	W_A'' (mJ/m²)
Flax	65.2 ± 1.3	65.3 ± 1.1	65.3 ± 1.4	54.4 ± 0.6
Flax_CNC	65.6 ± 1.2	65.0 ± 2.5	66.1 ± 0.7	57.4 ± 0.3
Flax_ XG/CNC	66.9 ± 1.6	64.0 ± 2.5	65.7 ± 2.4	55.0 ± 1.3

Considering their high dispersive character, the adsorption of CNC on flax fibre surfaces appears to decrease strongly the polar character of raw flax fibres by 28%, while the dispersive component is slightly increased from 16.1 mJ/m² to 17.7 mJ/m². In the case of flax_XG/CNC treated fibres, the polar component is almost identical to raw flax fibres, suggesting that the presence of XG counterbalances the dispersive effect of CNC due to its pronounced polar character [46].

The wettability of flax fibres towards epoxy resin was further analyzed by comparing the contact angles between raw and treated flax fibres and the epoxy resin liquid, and by calculating the work of adhesion W_A in between. Values are reported in **Table IV-2**. The lower the contact angle and the highest the W_A, the better would be the wettability and the quality of adhesion between flax fibres and epoxy matrix. Works of adhesion W_A, W_A' and W_A'' (mJ/m²) between flax fibres and the epoxy resin were respectively calculated by three different ways: Young-Dupré equation [47]–[49] (**Equation IV-6**), Owens, Wendt, Rabel and Kaelble (OWRK) approach [40] based on the geometric mean of dispersive and polar components of the liquid surface tension and solid surface

free energy (**Equation IV-7**) and Wu approach [50] based on the harmonic mean of dispersive and polar components of the liquid surface tension and solid surface free energy (**Equation IV-8**):

$$W_A = \gamma_L(1 + \cos\theta) \quad \text{(IV-6)}$$

$$W_A' = 2 \times [\sqrt{\gamma_S^d \times \gamma_L^d} + \sqrt{\gamma_S^p \times \gamma_L^p}] \quad \text{(IV-7)}$$

$$W_A'' = 4 \times (\frac{\gamma_L^d \cdot \gamma_S^d}{\gamma_L^d + \gamma_S^d} + \frac{\gamma_L^p \cdot \gamma_S^p}{\gamma_L^p + \gamma_S^p}) \quad \text{(IV-8)}$$

Where W_A, W_A' and W_A'' refer to the work of adhesion between the epoxy resin and flax fibre surface, θ the contact angle in between, and γ_L the surface tension of the epoxy resin (46 mJ/m²). Note that the spreading pressure was neglected as the contact angle between flax surface and epoxy is higher than 10° [49]. In OWRK and Wu approaches, γ_s^p and γ_s^d (mJ/m²) refer to polar and dispersive components of elementary flax fibres knowing the respective polar and dispersive surface tensions of the testing liquid γ_L^p and γ_L^d (mJ/m²).

Considering the calculated values of work of adhesion, it seems that the treatment of flax fibres with CNC does not change significantly their wettability towards the epoxy resin despite the pronounced dispersive character of CNC that could have favoured a better physico-chemical compatibility with epoxy. However, Wu approach shows a slight increase of the work of adhesion by 5.5 % with the adsorption of CNC on flax fibres with small standard deviations. These results are attributed to the decrease of the surface free energy of CNC treated flax fibres that does not allow a significant enhancement of the wettability, and hence a decrease of the contact angle with epoxy resin. In contrast, the XG/CNC treatment increases slightly the contact angle with the epoxy resin up to 67°, thus implying a slight reduced or unchanged wettability of flax_XG/CNC fibres towards the epoxy resin.

To conclude, our results show that the surface treatment of flax fibres with CNC decreases the polar character of flax fibres but does not increase significantly their wettability and work of adhesion with the epoxy resin. However, the XG/CNC treatment appears to slightly reduce the

wettability towards epoxy resin with a higher contact angle, probably due to the pronounced polar character of adsorbed XG that is less compatible with apolar epoxy resin.

IV. 3. 3. Optimization of thermocompression conditions

An optimization of the thermocompression process was performed on the basis of the highest mechanical performances reached for the raw flax fibre reinforced biocomposite. Indeed, the processing parameters (temperature, pressure and processing time) influence strongly the microstructure of biocomposites, i.e. fibre and matrix volume fractions, pore volume and the arrangement of fibres within the polymeric matrix, but also the eventual degradation of the components [6], [51]. When studying the interfacial zone in (bio)composites, manufacturing should thus be controlled as best as possible to limit materials property variations related to processing conditions.

In this regard, Cadu *et al.* (2018) investigated the manufacturing of flax / epoxy UD laminates (12 or 20 plies) by thermocompression to highlight the key manufacturing parameters to obtain high-grade biocomposites [6]. The most decisive parameters in terms of mechanical properties seem to be the fibre conditioning, the pressure, the cooling speed, the exit temperature and the post-curing duration.

In our study, the curing temperature and time were fixed at 60°C and 16 h according to manufacturer's datasheet. The effect of curing pressure (21, 42 and 70 bars) was studied and had a strong effect on fibre volume fraction and voids as well as on longitudinal tensile modulus and strength (**Figure IV-6**). In general, a higher curing pressure implies an easier extraction of trapped air out of the composite laminate and an efficient impregnation of the resin into flax yarns leading to higher fibre volume and limited voids.

As shown in **Figure IV-6**, curing at 70 bars allowed reaching the highest fibre volume V_f of 55.6% and the highest tensile Young's modulus and strength, 33.0 GPa and 295.5 MPa respectively.

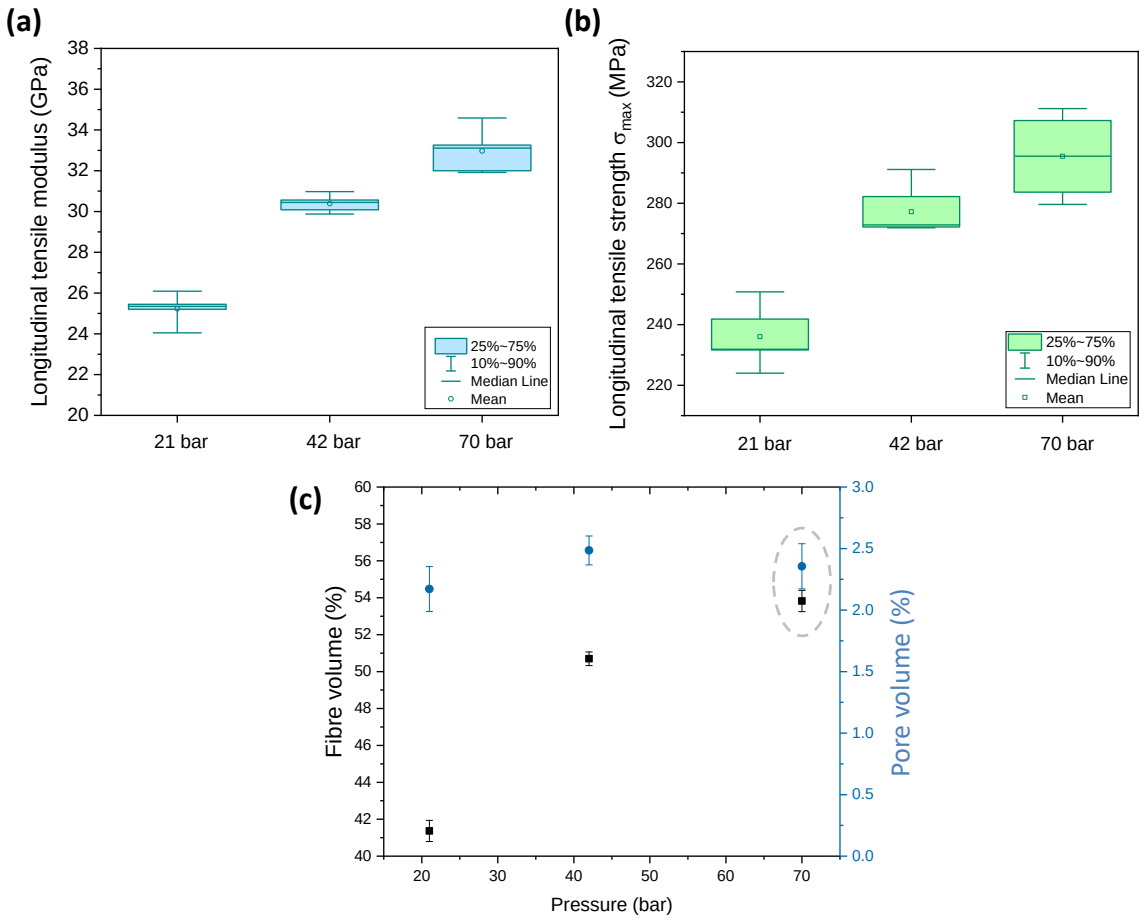

Figure IV-6: Effect of curing pressure during thermocompression process on (a) the longitudinal tensile modulus, (b) the longitudinal tensile strength and (c) fibre and pore volume fractions.

If we compare these results with data from literature for composites UD or quasi-UD flax / epoxy laminates, (**Figure IV-7**), the Young's modulus is in the highest values and the tensile strength in the upper part. Green triangle symbols represented all values found in the work of Cadu *et al.*, very comparable with our study thanks to the use of the thermocompression process [6]. However, it has to be mentioned that they decided to define two different moduli E1 and E2 because of an under-estimation of the Young's modulus due to the inflexion point of the tensile curve. E1 and E2 are moduli defined respectively before and after the inflexion point on the curve. They obtained E1 = 25 – 34 GPa (reported in the **Figure IV-7**) and E2 = 17 – 23 GPa. If we calculate E1 and E2 for the composite at 70 bars, we obtain values of 37 GPa and 24 GPa respectively, higher than those in the work of Cadu *et al.* Moreover, they found hier ultimate tensile strength values

ranged between 260 – 380 MPa, maybe due to the epoxy resin type and viscosity and / or flax fabric properties.

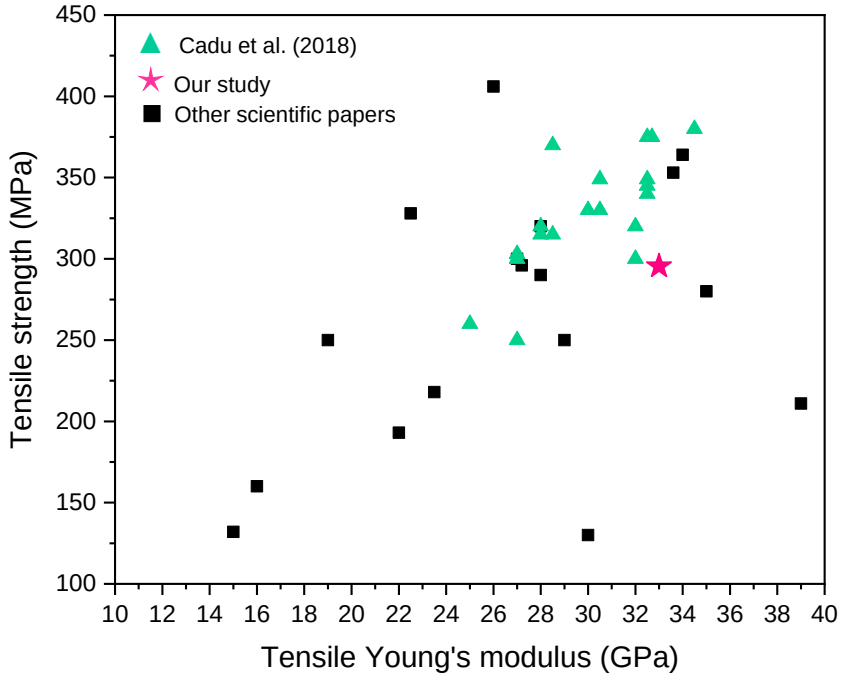

Figure IV-7: Representation of tensile mechanical properties, especially Young's modulus and strength, obtained in the literature for UD or quasi-UD flax / epoxy laminated composites [1]–[14].

Pore volume V_p (2.4 %) was relatively low for such biocomposite systems and not much influenced by the curing pressure with values from 2.2 % to 2.5 %. Compared to the literature, Cadu *et al.* obtained V_p from 2.4 to 3.1 % [6] and Fiore *et al.* manufactured UD flax / epoxy laminates by vacuum-assisted resin infusion technique with V_p from 2.8 % to 4.8 % [14]. Considering the volume fractions V_f (55.6 %), the literature reports a wide range going from 39 % to 65 % strongly depending on the manufacturing process.

Based on these results, biocomposite laminates were thus manufactured at 70 bars, 60°C during 16 h for the further experiments.

IV. 3. 4. Microstructure of biocomposites

The effect of the different flax fabric treatments (XG, CNC, water dipping, drying under strength) on the microstructure of biocomposites was investigated through SEM observations in different localizations within the specimens as well as measurements of fibre and pore volume fractions.

IV. 3. 4. 1 Dispersion state of flax yarns and fibres in epoxy resin

Transverse cross-sections of raw and treated flax fabrics reinforced composites at low (100x) and high (2000x) magnifications are shown in **Figure IV-8**. At low magnification, we can observe distinct oval shaped yarns for the raw flax fabric reinforced epoxy biocomposite. For the CNC treated flax fabrics, the yarns are less distinguishable and fibres appear to be more dispersed and individualized into elementary fibres (also visible at high magnification) and nearly no bundles are observed. In contrast, the XG/CNC treatment induces a more packed structure of the yarns consisting in agglomerated elementary fibres forming bundles. As showed in **Figure IV-5**, SEM observations performed on XG/CNC treated flax fabrics before composite manufacturing revealed polymeric web-like structures between elementary fibres within the yarns that must have favoured the remaining of fibre bundles within the biocomposite microstructure, implying a worse dispersion state of yarns. Fibre bundles can be preferential sites of stress concentrations under mechanical solicitations inducing failures and cracks [52]. If we look at the flax_control composite, few voids are visible and there is a good dispersion of elementary flax fibres, suggesting that water dipping tends to favour the fibre individualization within the yarns. Considering the CNC treated flax fabrics laminates with the drying under strength, several fibre bundles are obvious at high magnification with the presence of cracks/voids along the fibre / matrix interphase zone, and also within the bundles. It seems that this drying process for CNC treated flax fabrics induces a worse dispersion of yarns in the epoxy matrix. The drying under strength could favour the formation of compact structures of elementary flax fibres – CNC within the yarns, preventing their further dispersion during manufacturing of the composite.

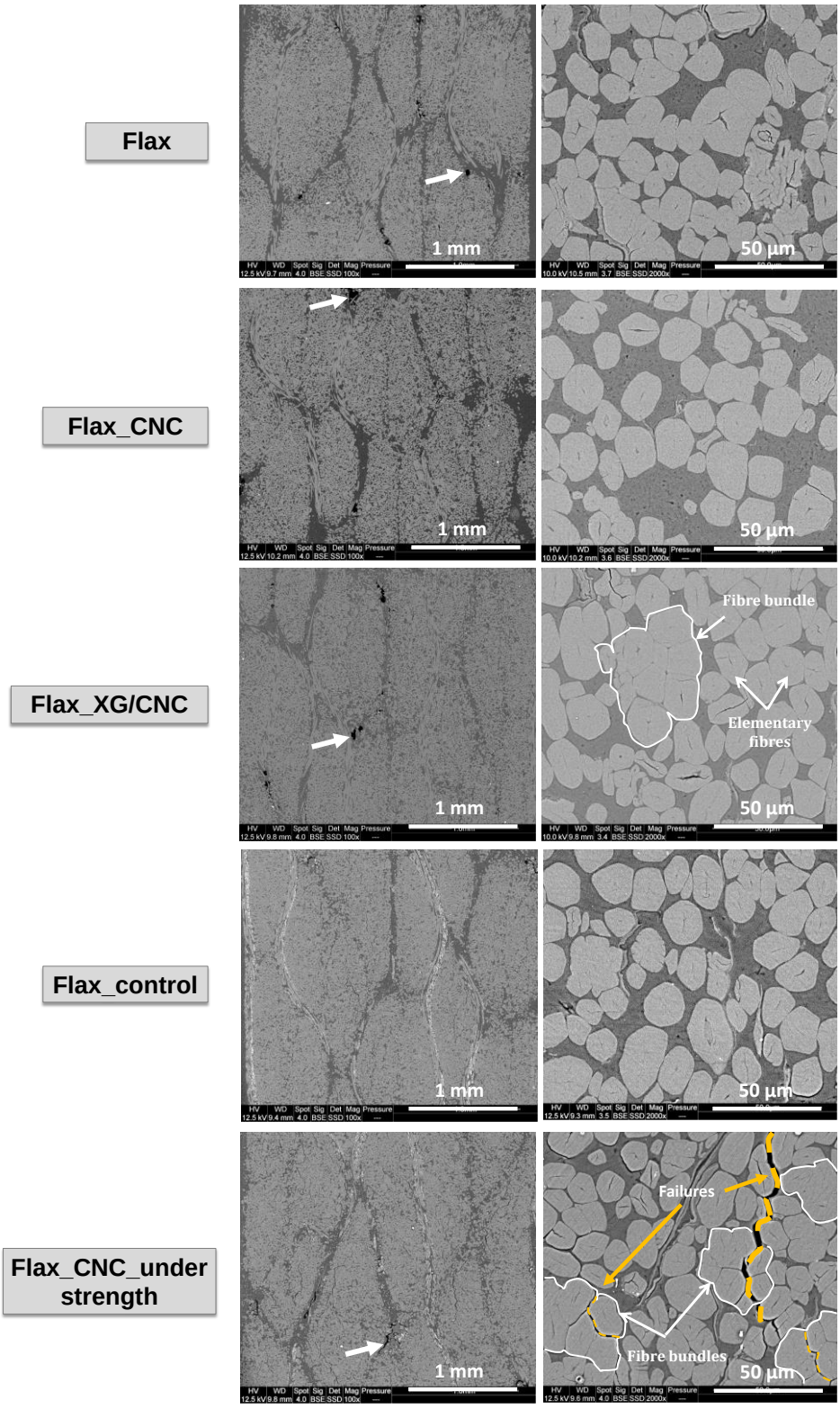

Figure IV-8: SEM images of cross-sections of flax, flax_CNC, flax_XG/CNC, flax_control and flax_CNC_under strength fabric / epoxy laminates composites at low (100x) and high (2000x) magnifications. Flax yarns composed of bundles and elementary fibres appear in light grey, epoxy matrix in dark grey, voids in black (white arrow) and failures in orange (dashes and orange arrow).

In summary, CNC, XG/CNC and treatment processes thus have a strong influence on the dispersion state of flax fibres and yarns within the manufactured biocomposites. The water dipping and free drying (control composite) induce more dispersed microstructures without much influence of adsorbed CNC. However, the adsorption of biopolymers as XG having strong interactions with cellulosic surfaces induces more packed structures with the formation of fibre bundles within the yarns and worse dispersion in epoxy matrix. Finally, the drying under strength seems also to induce a bad dispersion of elementary fibres in the yarns and the epoxy matrix, possibly due to the formation of packed CNC – elementary fibres structures.

IV. 3. 4. 2 Fibre and porosity volume fractions

Fibre V_f and pore V_p volume fractions are strongly related to the quality of impregnation of the fibres by the matrix, and are key microstructural parameters influencing considerably the mechanical performances of composites. Basically, high fibre volume fraction and low pore volume induce better stiffness, strength and toughness [1], [10], [53].

The impregnation of flax fabrics with epoxy resin is a complex process as it involves different length-scale and multiple locations, i.e. around and within flax yarns, but also in between and within elementary fibres via the lumen cavity [54]. The quality of impregnation is driven by many parameters, i.e. *(i)* processing conditions, *(ii)* resin viscosity and its wetting capacity towards flax fibres and *(iii)* packing ability of flax fabrics [15], [54].

The measured V_f and V_p, determined according to **Equations (IV-2 – IV-4)**, are presented in **Figure IV-9** for the different biocomposites. The raw flax fabric reinforced epoxy biocomposite displays V_f= 55.6 % and V_p = 2.4 %. Using the same manufacturing conditions for the biocomposites, it appears that the washing and free drying steps have a positive impact with an increase of the fibre volume fraction up to 61.2% with similar pore volume (V_p = 2.3 %). The treatments of flax fabrics with CNC and XG/CNC also enhance the fibre volume fraction of composite plates, respectively up to 58.2% and 61.5%. However, they also induce increased voids for flax_CNC (V_p = 2.9%) and especially for flax_XG/CNC up to 3.8%.

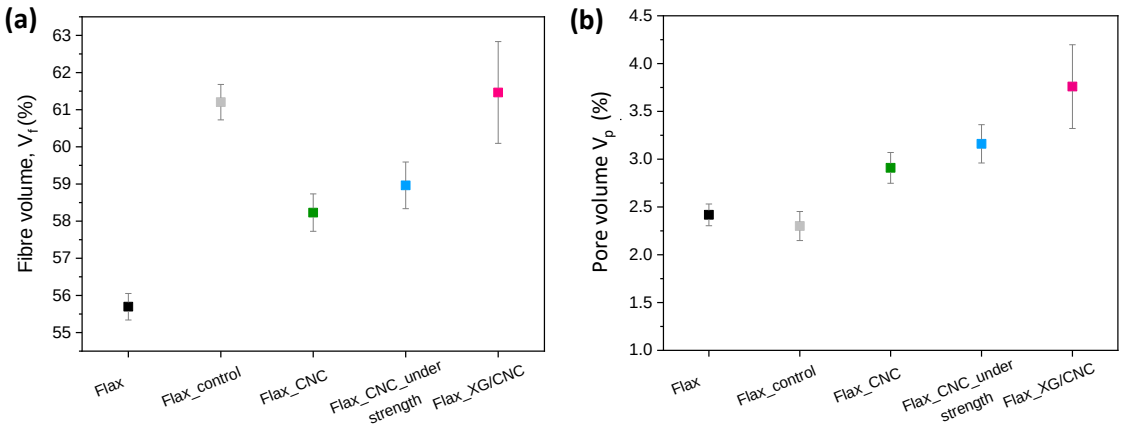

Figure IV-9: (a) Fibre V_f and (b) pore V_p volume fractions of flax, flax_CNC, flax_CNC_dry, flax_XG/CNC and flax_control fabrics reinforced epoxy biocomposites.

Considering that processing conditions and resin viscosity remained unchanged for all biocomposites, the quality of impregnation and resulting V_f and V_p were thus mainly influenced by variations in the wettability and permeability of raw and treated flax fabrics. This will be analysed at different length-scales, i.e. (*i*) the wettability of elementary fibres, (*ii*) the impregnation of flax yarns and (*iii*) the packing ability of flax fabrics.

As supported by tensiometry experiments, the wettability of flax fibres with epoxy resin did not significantly change with the adsorption of CNC, while the presence of XG on flax fabrics appeared to increase slightly the contact angle and hence decrease the wettability with the epoxy matrix. This decreased wettability at the scale of elementary flax fibres by the XG/CNC treatment could explain partly the higher pore volume measured for the corresponding biocomposite plate.

The presence of polymeric web-like structures (**Figure IV-5**) between elementary fibres and consecutive formation of fibre bundles within yarns (**Figure IV-8**) in the case of the XG/CNC treatment should affect the impregnation of yarns by the epoxy resin. Such packed structures are likely to prevent resin diffusion within the yarns and to generate so-called impregnation voids during biocomposites manufacturing [54], thus explaining the higher pore volume in the XG/CNC biocomposite.

Finally, Madsen *et al.* (2007) also pointed out that among other factors (lumen, interfacial compatibility, heterogeneous shape of natural fibres), the low packing ability of natural fibre fabrics [54] is responsible for the creation of voids. In particular, Madsen and Lilholt [15], [55] observed that when increasing fibre weight fractions above an optimum value around 52 wt% for composite polypropylene / flax, lowering of tensile Young's modulus and strength was obtained. The authors assumed that beyond this optimum fibre weight fraction, the fibres/yarns reach their maximum packing ability. Indeed, they explain that the balance between the fibre fraction volume and the presence of (high) structural pore content induces a maximum in physical and mechanical properties. Concretely, at high fibre weight fractions and thus lower matrix weight fraction, there is not enough matrix to fill the open spaces between fibres in the maximally packed fibre arrangement [15]. This induces voids and hence lowers the mechanical properties of the biocomposite. The increased pore volume for CNC and XG/CNC treated biocomposites could thus originate from the higher fibre volume fractions in composite plates, being above the maximum packing ability of flax fabrics, as represented **Figure IV-10**.

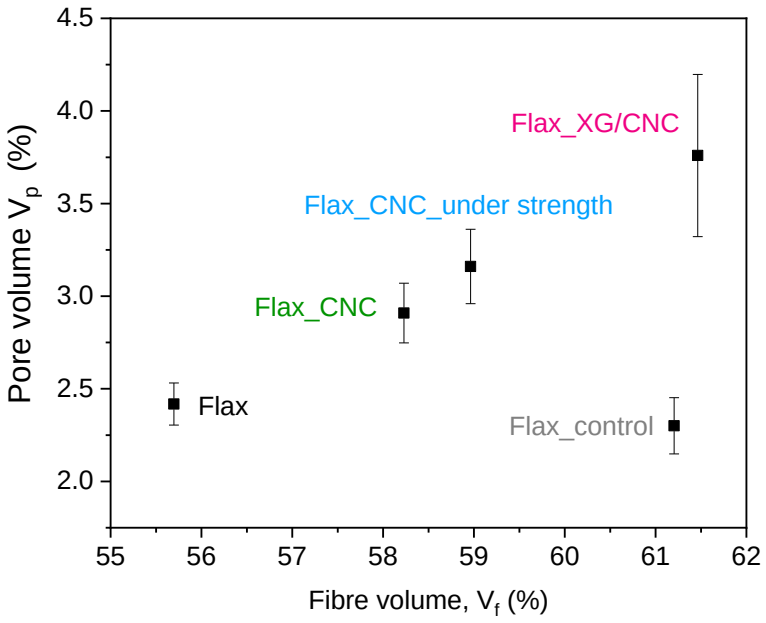

Figure IV-10: Fibre volume V_f (%) versus pore volume V_p (%) for all composite plates.

Interestingly, under the same manufacturing conditions (pressure and temperature), the resulting thickness of the plates (**Table IV-3**) for CNC and XG/CNC treatments are higher (from 6.0 to 9.8 %) than those obtained for raw and flax fabrics, supporting that CNC and XG/CNC treatments decrease the packing ability of flax fabrics. The lower thickness obtained with the control fabric, suggesting higher packing ability, could explain why this composite plate has lower pore volume (V_p = 2.3 %) while having high fibre volume fraction (V_f = 61.2 %). The packing ability thus appears here as a key factor influencing fibre and pore volume fractions.

Table IV-3: Final thickness of the different biocomposite plates after manufacturing.

	Flax	**Flax_control**	**Flax_CNC**	**Flax_CNC_under strength**	**Flax_XG/CNC**
Thickness of the composite plate (mm)	2.85 ± 0.01	2.82 ± 0.07	3.09 ± 0.05	3.13 ± 0.06	3.02 ± 0.06

Concluding, CNC and XG/CNC treatments strongly influence the fibre and pore volume fractions of biocomposites even when manufactured in the same processing conditions. Higher fibre volume fractions up to 61.5% were reached but overall pore volume increased up to 3.8% for the XG/CNC treatment. Beyond some variations in wettability at the scale of elementary fibres, the formation of fibre bundles within yarns due to XG and the decreased packing ability of treated flax fabrics are responsible for worse impregnation and substantial increase in voids. This higher amount of voids is likely to be detrimental for the mechanical properties of composite plates, especially their strength, because it could favour the creation and propagation of micro-cracks.

IV. 3. 4. 3 Layout of flax fabrics and yarns within biocomposites

Mapping of composite laminates (polished surfaces in the longitudinal direction) were done by SEM (**Figure IV-11**). The observation of such cross-sections allows visualizing the stacking of the plies and the alignment of yarns within the laminates. Alignment of yarns is indeed crucial for the mechanical performances of structural composites.

First, it is observed that the yarns are well aligned in the reference composite laminate. In contrast, the composite made of flax_control fabrics (*flax_control_2*) shows a more disordered microstructure with epoxy-rich zones and wavy flax yarns. The dipping in water and the drying of flax fabrics thus alter the layout of UD flax fabrics and alignment of flax yarns. This could be related to the shrinkage of flax fabrics after dipping in water and drying, as evidenced in **Table IV-1**. However, two images of the flax_control composite, i.e. *flax_control_1* and *flax_control_2*, highlight the heterogeneity of such composites depending in the sample localization inside the plate.

The treatments with CNC and XG/CNC appear to restrain this misalignment effect, suggesting that the adsorption of cellulose nanocrystals and xyloglucan allows to better preserve the original structure of flax fabrics during composite manufacturing.

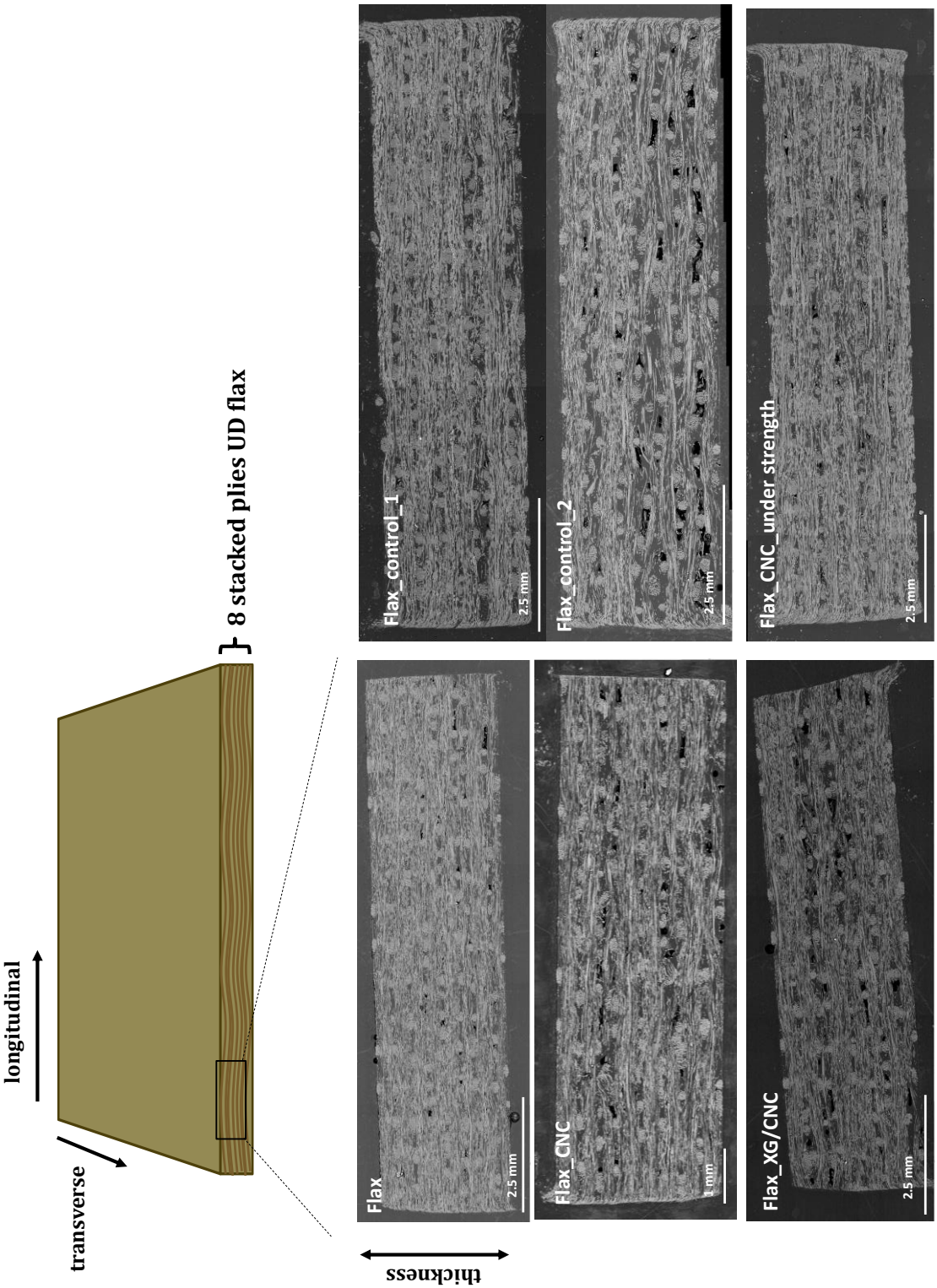

Figure IV-11: SEM mapping of polished cross-sections in longitudinal direction of flax, flax_CNC (free drying of under strength, flax_XG/CNC and flax_control 8 plies reinforced epoxy composite plates. Note that flax_control_1 and flax_control_2 images were taken from the same composite plate.

IV. 3. 5. (Visco-)elastic behaviour

In this part, the effects of treatments applied to flax fabrics are analysed firstly by studying the (visco-)elastic behaviour of the biocomposites by quasi-static longitudinal tensile tests and transverse dynamic thermal analysis; and secondly by studying their ultimate properties by quasi-static longitudinal and transverse tensile tests coupled with SEM observations of failure surfaces.

IV. 3. 5. 1 Longitudinal tensile stiffness

Median stress-strain curves of uniaxial tensile tests are represented in **Figure IV-12** for the different biocomposites and the measured Young's moduli for each biocomposite.

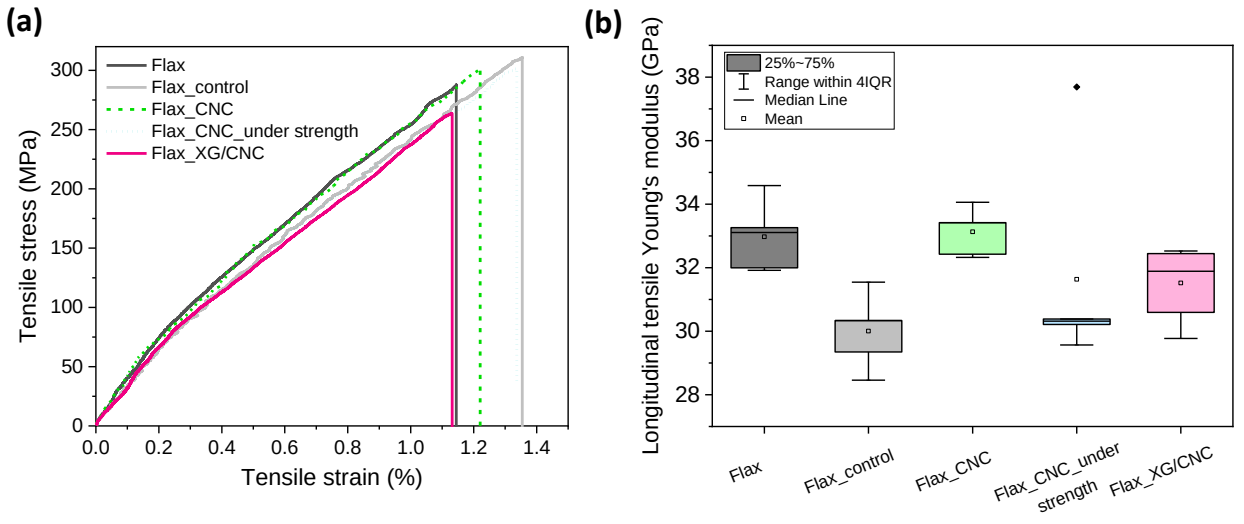

Figure IV-12: Quasi-static longitudinal tensile behaviour of the different biocomposite laminates, (a) stress-strain curves, (b) Young's modulus.

The CNC treatment does not improve the longitudinal stiffness of the biocomposite, with median Young's modulus of 32.4 GPa, as compared to raw flax fabrics with E = 33.1 GPa (**Figure IV-12 b**). XG/CNC tends to decrease slightly the Young's modulus with a median value of 31.9 GPa. Besides, it clearly appears that the dipping/free drying steps induce a pronounced decrease of roughly 8.5 % of the Young's modulus (30.3 GPa for the flax_control fabrics) which has to be related to the shrinkage and destructuration of the flax fabrics and consecutive misalignment of

flax yarns observed for this biocomposite (**Figure IV-11**). This supports that the CNC and XG/CNC treatments can contribute to the dimensional and structural stability of flax fabrics when submitted to functionalizing treatments that involve dipping/free drying steps. Furthermore, it also contributes to maintain the stiffness of the biocomposites. Based on these results, a biocomposite laminate was prepared with flax fabrics treated by CNC and dried under strength to prevent the destructuration and shrinkage of the fabrics during drying step. Despite outlier observed for one specimen (e.g. 37.7 GPa), drying under strength does not improve the final Young's modulus of the biocomposite. This could be explained by the lower packing, i.e. roughly 9.8 % increase in the laminate thickness as compared to raw flax fabrics (**Table IV-3**) and worse fibre dispersion (**Figure IV-8**) obtained with this biocomposite.

It has been shown that the packing has a strong influence on the fibre volume fraction and voids that are key parameters for the mechanical performances of the biocomposite. To take into account variations in packing and fibre volume fraction and their influence on the stiffness of the biocomposite, we used the mixture law (**Equation IV-9**) [1], so as to better evidence the effect of flax fabric treatments. This mixture law allows the back calculation of an ***equivalent Young's modulus of flax fibres*** $E_{f\,eq}$ that is related to (i) the median Young's modulus of the fibres and its eventual variation due to fibre treatments, and (ii) microstructural effects related to alignment of the yarns. Both parameters, i.e. intrinsic properties of the fibres and fibre orientation effects, cannot be discriminated with this approach. Note that interfacial adhesion and porosity are not variables that are considered in the mixture law. Indeed, perfect bonding between fibres and matrix is assumed in this model and their potential contributions of interfacial adhesion and porosity are thus implicit in the calculation of the equivalent Young's modulus of flax fibres. Besides, it should be pointed out that the latter parameters are usually assumed to have little influence when considering the longitudinal stiffness of a UD composite [19], [20].

$$E_c = E_{feq}.V_f + (1 - V_f).E_m \qquad \text{(IV-9)}$$

where E_c and E_{feq} are respectively the measured Young's modulus of the unidirectional composite laminates and the calculated equivalent longitudinal Young's modulus of flax fibres,

V_f the measured fibre volume fraction and E_m the measured Young's modulus of neat epoxy resin (E_m = 3.35 GPa).

The equivalent longitudinal Young's moduli of flax fibres calculated for the different biocomposites are reported in **Figure IV-13**.

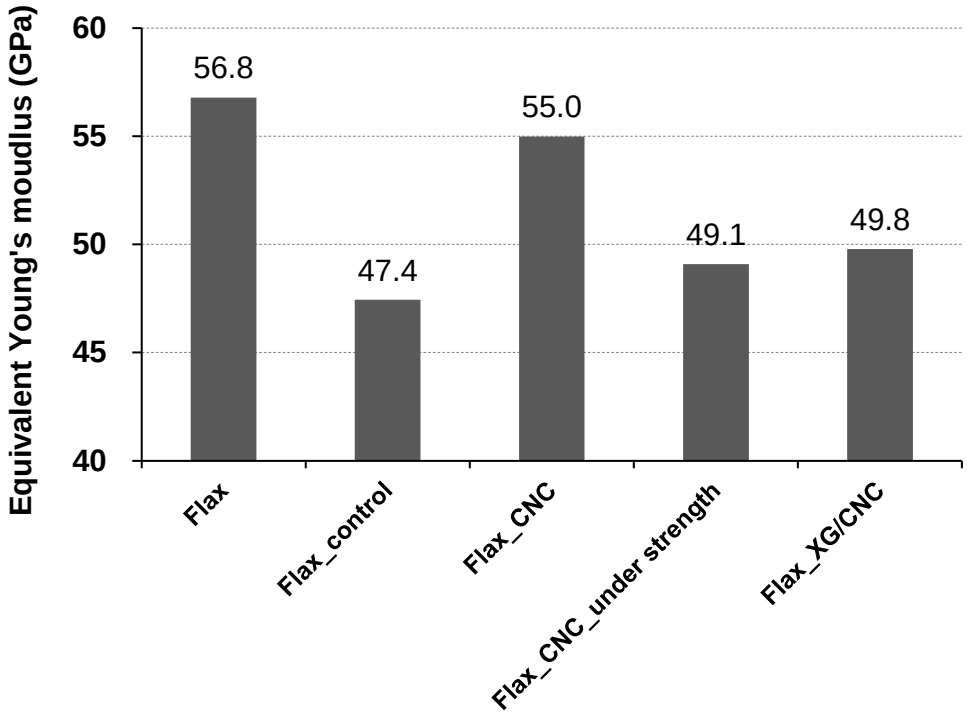

Figure IV-13: Calculated equivalent longitudinal Young's moduli of flax fibres for the different biocomposite laminates.

The highest equivalent Young's modulus is obtained with the raw flax fabric reinforced biocomposite with 56.8 GPa, which highlights the good tensile properties of the UD flax fabric used as well as the optimal orientation of the yarns achieved during the manufacturing of the laminates. As a comparison, Coroller *et al.* [1] measured the Young's modulus of different variety of elementary flax fibres and found the highest Young's modulus for the Marylin (57.1 ± 15.5 GPa), Hermes and Andrea having Young's moduli of 48.9 ± 12.0 GPa and 48.3 ± 13.8 GPa, respectively. The CNC treated flax fabric reinforced composite gave similar equivalent Young's modulus (55 GPa) which points out that the adsorption of CNC on flax fabrics did not allow to improve the

stiffness of flax fibres neither those of biocomposite laminates and that good yarns alignment was also achieved for this composite. In contrast, a strong decrease of the equivalent Young's modulus, with values equivalent to Hermes and Andrea Young's modulus, is observed for the others laminates (flax_control, CNC_under strength and XG/CNC), which is primarily attributed to orientation defects of yarns for the flax_control composite as observed on the polished cross-sections of the laminates (**Figure IV-11**). Besides, as significantly higher pore volume was measured for the XG/CNC treated flax fabric reinforced composite (i.e. 3.8 % versus 2.4 to 3.2% for the other biocomposites), its negative impact on the calculated equivalent Young's modulus of flax fibres cannot be neglected. An analytical model based on thin Laminate Plate Theory (LPT) [56], that would also considered the effect of voids on the elastic properties of the epoxy matrix via Mori-Tanaka micromechanical model [57], would allow to better discriminate the effect of voids and refine the calculation of the equivalent Young's modulus of the fibres.

IV. 3. 5. 2 Transverse dynamic behaviour

Samples were tested over two consecutive heating cycles (noted 1st cycle and 2nd cycle) in dual cantilever bending in transverse direction, so as to better detect the fibre / matrix interface behaviour. Indeed, fibres carry more load in dual cantilever bending, providing a more sensitive detection of the mechanical response in the interphase region [58], [59], especially when the composites is stressed in the transverse direction of the fibres.

The damping factor ($\tan\delta = E''/E'$) is directly related to internal frictions, molecular motions, thermal transitions and relaxations in the material. In the case of composites, the interfacial bonding can be studied through the analysis of *tan δ*, which is strongly affected by the molecular motions of macromolecular chains within matrix but also at the fibre / matrix interface [59]–[61].

- **Effect of CNC and XG/CNC treatments on epoxy resin curing**

Figure IV-14 represents the storage modulus *E'* and the damping factor *tan δ* as a function of the temperature for untreated, control, CNC and XG/CNC treated flax / epoxy composite plates. In overall, the α transition temperature T_α (related to the glass transition temperature T_g) ranges between 76.5°C and 76.7°C for the 1st heating cycle and 80.6°C and 82.9°C for the 2nd heating cycle

(**Table IV-4**). The flax_control sample presents the higher T_α at 82.9°C reached after the 2nd heating cycle. It should be point out that T_α was higher for the neat epoxy resin (i.e. 80.8°C and 88.3°C for the 1st and 2nd heating cycles, respectively), suggesting that the presence of flax fibres whatever their treatment tends to hamper the curing and crosslinking of epoxy.

For all samples, we can observe a shift of T_α to higher temperatures for the 2nd cycle compared to the 1st cycle: + 7.5°C for epoxy resin (not represented in **Figure IV-14**), + 5.4°C for untreated flax / epoxy composite, + 6.4°C for flax_control, + 4.0°C for flax_CNC and flax_XG/CNC epoxy composites. This shift of T_α to higher temperatures can be explained by an incomplete curing of the epoxy resin during the manufacturing of the biocomposites. Then, the heating up to 120°C during 1st cycle allows a post-curing and enhanced cross-linking of the epoxy resin that result in reduced molecular motions of macromolecular chains in the material and hence higher T_α. The presence of CNC and XG/CNC seems to decrease this shift compared to the untreated and control samples, and hence limit this post-curing effect. It is possible that chemical reactions occur between the hydroxyl groups of cellulose nanocrystals adsorbed at the surface of flax fibres and so in contact with the reactive groups of the epoxy resin or the hardener containing amines, inducing a more limited post-curing effect. It should be interesting to study in details the interactions CNC – epoxy matrix during the curing process.

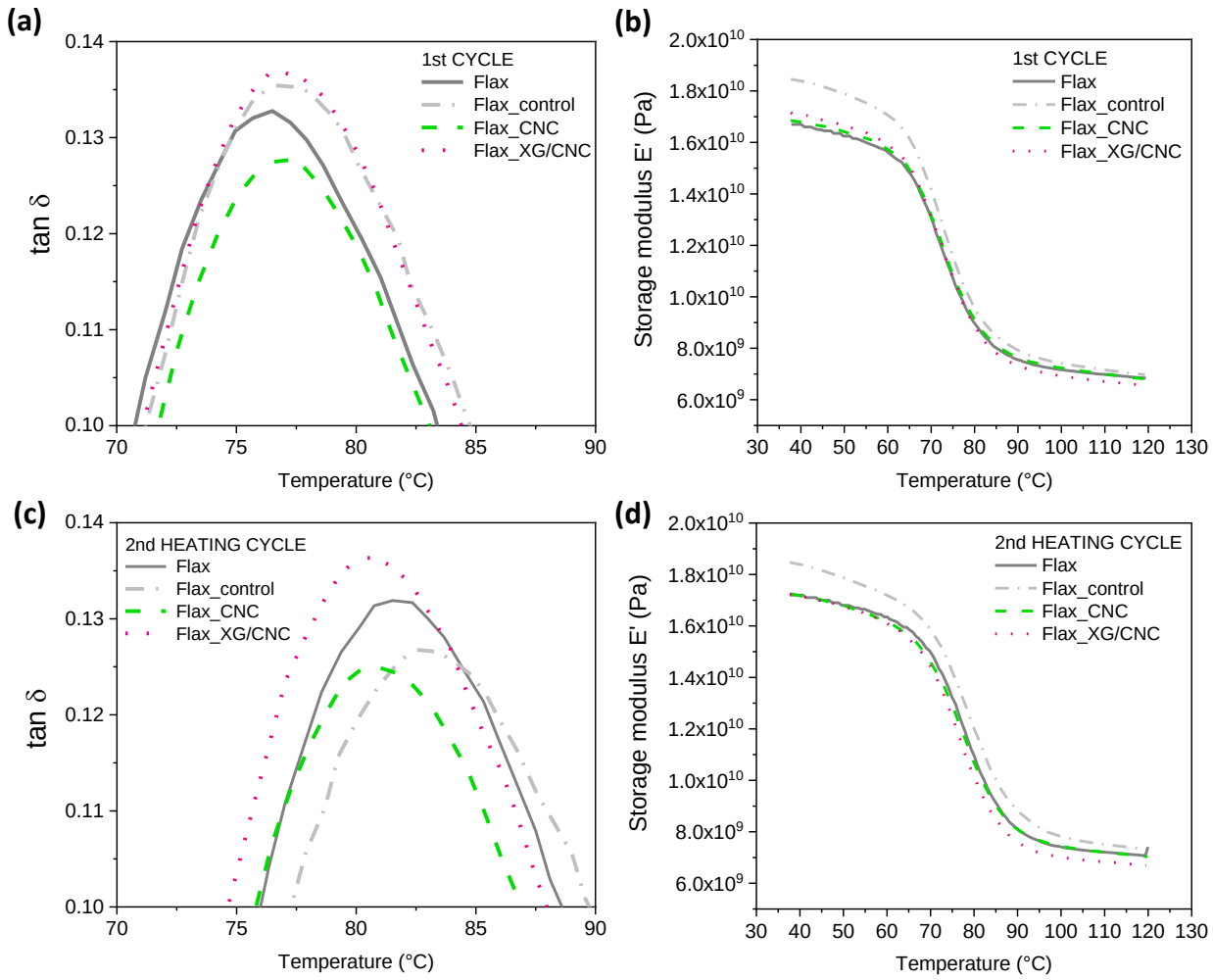

Figure IV-14: DMTA measurements in transverse direction with the damping factor *tan δ* and the storage modulus *E'* as a function of the temperature ranging from 40°C to 120°C for raw, control, CNC and XG/CNC treated flax fabric / epoxy composites for (a)(b) the first heating cycle and (c)(d) the second heating cycle.

When comparing all storage moduli at 40°C, the flax_control / epoxy composite plate displays the highest E' with 18.5 GPa that has to be related to the good fibre dispersion for this sample, and hence higher quantity of fibre/matrix interface. However, the post-curing effect observed between the heating cycles does not have a significant impact on the storage modulus with increases comprised between 0.1% and 3 %.

- **Influence of the CNC and XG/CNC treatments on the damping factor**

Considering the peak intensities of the damping factor at the α transition for all UD flax fabrics / epoxy biocomposites (**Table IV-4**), it is obvious that the presence of flax fibres within the epoxy matrix decreases strongly the damping intensity from 1.02 (neat epoxy resin) to 0.133 (untreated flax / epoxy), due to the dominant elastic response of flax fibres.

Table IV-4: Main results obtained by DMTA (double cantilever transverse bending) on epoxy resin, untreated and control flax fibres, flax_CNC and flax_XG/CNC epoxy composites.

	Cycle	E' @ 40°C (GPa)	Tan δ	Tα (°C)
Epoxy	1st	**2.36** ± 0.4	**1.02** ± 0.010	**80.8** ± 1.1
	2nd	**5.93** ± 0.3	**0.979** ± 0.034	**88.3** ± 0.0
Flax	1st	**16.7** ± 0.2	**0.130** ± 0.004	**76.5** ± 0.1
	2nd	**17.2** ± 0.2	**0.132** ± 0.005	**81.9** ± 0.5
Flax_control	1st	**18.4** ± 0.2	**0.135** ± 0.003	**76.5** ± 0.3
	2nd	**18.4** ± 0.2	**0.127** ± 0.003	**82.9** ± 0.2
Flax_CNC	1st	**16.8** ± 0.3	**0.128** ± 0.004	**76.7** ± 0.4
	2nd	**17.1** ± 0.1	**0.125** ± 0.004	**80.7** ± 0.6
Flax_XG/CNC	1st	**17.1** ± 0.2	**0.137** ± 0.002	**76.6** ± 0.3
	2nd	**17.2** ± 0.2	**0.137** ± 0.002	**80.6** ± 0.3

Considering the 1st heating cycle, it seems that the treatment of flax fabrics by CNC decreases slightly the peak intensity of the damping factor compared to the untreated fibres (0.133 versus 0.128 respectively). This result suggests a possible increase of the interfacial adhesion related to restricted molecular mobility at the interface due to the presence of CNC and their possible (physico-)chemical interactions with the epoxy network. In contrast, the treatment with XG/CNC tends to increase the damping factor of the composite material, possibly due to increased internal frictions and molecular motions at the interface with the presence of XG chains and the above-mentioned extensible network formed by XG/CNC complex (*see **Chapter II***).

Nielsen and Landel [62] proposed a mixture rule which could estimate the damping factor of composite materials *tan* δ_c, in the case of an ideal composite in which interfaces do not contribute to damping but play only their role of transferring loads (**Equation IV-10**):

$$\tan \delta_c = (1 - V_f).\tan \delta_m \quad \text{(IV-10)}$$

where V_f is the volume fraction of fibres and tan δ_m the damping factor (tan δ_m = 1.02 in 1st cycle and tan δ_m = 0.979 in 2nd cycle).

Equation IV-10 does not consider the nature of the interactions occurring at the fibre / matrix interface in biocomposites. However, strong interactions contribute to decrease the damping factor thanks to the formation of an interphase zone with reduced molecular mobility and enhanced mechanical interlocking between fibres and matrix. In our case, the theoretical values of composites damping based on Equation IV-10 should be 0.452, 0.396, 0.426 and 0.393 for the 1st cycle for flax, flax_control, flax_CNC and flax_XG/CNC epoxy composites respectively, which has to be compared to those obtained experimentally, i.e. 0.133, 0.135, 0.128 and 0.137 respectively. This indicates that for all biocomposites, strong interactions occur at the interfaces and tend to reduce the damping due to interactions and specific surface area between the fibres and the matrix, resulting in the formation of an interphase with reduced molecular mobility.

Ziegel and Romanov proposed a modified mixture rule to take into account the effect of this interphase region on damping [63], **Equation IV-11**:

$$\tan \delta_c = (1 - B.V_f).\tan \delta_m \quad \text{(IV-11)}$$

where *B* is an adjusting parameter of the fibre volume fraction that considers the formation of a strong interphase between fibres and matrix. The stronger the interfacial interactions, the thicker the immobilized layer and the higher the value of parameter B (**Table IV-5**). The 2nd heating curing appears to not have influence on the parameter B. The flax fabrics treatment process, i.e. water dipping and drying, decreases the parameter B by around 9.0 % correlated to worse interfacial interactions between flax_control fibres and epoxy resin matrix. However, the presence of CNC of flax fibre surfaces enhances the parameter B by 5.3 % compared to the flax_control composite, inducing higher interactions at the interphase zone. The flax_XG/CNC composite display a

parameter B identical to the flax_control, which can be explained by the presence of the XG biopolymer at the interface.

Table IV-5: Parameter B values of the different flax / epoxy laminates for 1st and 2nd heating cycles.

Parameter B	Flax	Flax_control	Flax_CNC	Flax_XG/CNC
1st cycle	1.56	1.42	1.50	1.41
2nd cycle	1.55	1.42	1.50	1.40

IV. 3. 6. Ultimate mechanical properties

IV. 3. 6. 1 Longitudinal tensile strength

Figure IV-15 represents the longitudinal tensile strength and work of rupture measured for the different manufactured flax / epoxy biocomposite laminates.

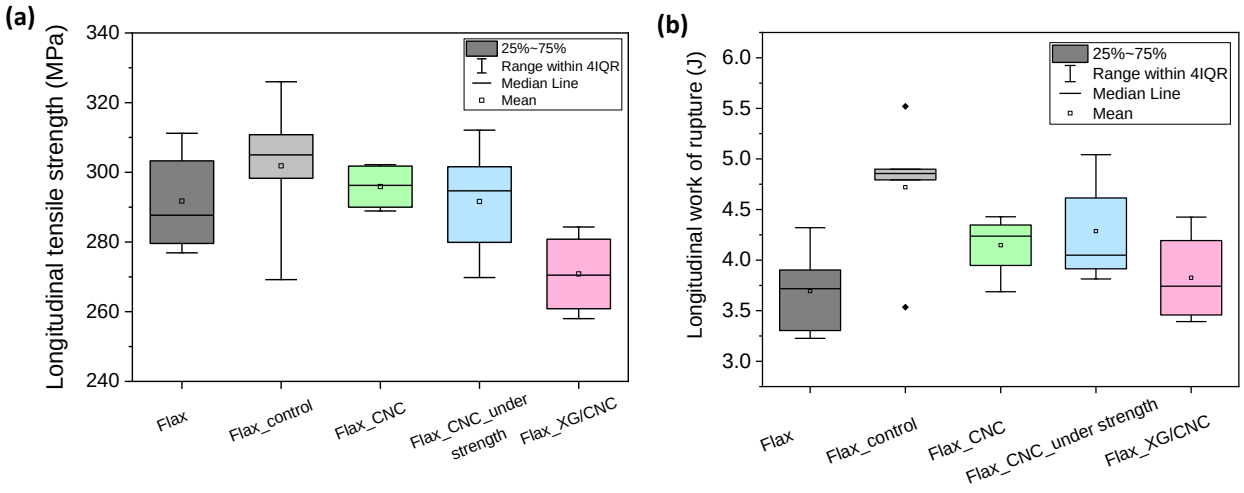

Figure IV-15: Quasi-static longitudinal tensile properties for the different biocomposite laminates (a) tensile strength, (b) work of rupture.

All the biocomposites have similar median tensile strength ranging from 270 to 305 MPa (**Figure IV-15 a**). The CNC treatment improves slightly the tensile strength of the composites by around 3.0 %. Note that XG/CNC treatment led to slightly lower tensile strength with around 6.0 % of decrease.

Based on the microstructural analysis, differences in terms of fibre and pore volume fractions have been evidenced that should influence the tensile strength of the composites. To take into account their influence and better evidence the effect of flax fabric treatments, we used the mixture law (**Equation IV-12**) [1].

$$\sigma_c = V_f . \boldsymbol{\sigma_{feq}} + \left(1 - V_f\right) . \sigma_{feq} . \frac{E_m}{\boldsymbol{E_{feq}}} \qquad \text{(IV-12)}$$

where σ_c and σ_{feq} are respectively the measured tensile strength of the unidirectional composite laminate and calculated equivalent tensile strength of flax fibres in the longitudinal direction, $E_{f\ eq}$ and E_m are respectively the calculated equivalent longitudinal Young's modulus of flax fibres (from **Equation IV-9**) and the measured Young's modulus of the neat epoxy resin (E_m = 3.35 GPa); V_f the measured fibre volume fraction.

This mixture law allows the back calculation of an ***equivalent tensile strength of flax fibres*** $\boldsymbol{\sigma_{f,eq}}$ that is related to (i) the median tensile strength of the fibres and its eventual variation due to fibre treatments, and (ii) microstructural effects related to dispersion and alignment of the yarns. Both parameters, i.e. intrinsic properties of the fibres and microstructural effects, cannot be discriminated with this approach. Also note that interfacial adhesion and pore volume are not variables that are considered in the mixture law and their contributions are thus implicit in the calculation of the equivalent tensile strength of flax fibres. The resulting equivalent tensile strength of flax fibres is thus related to *(i)* intrinsic tensile strength of (non-)treated flax fibres, *(ii)* interfacial adhesion between the fibres and the epoxy matrix as well as *(iii)* microstructural parameters, i.e. yarns dispersion and alignment, and pore volume. Finally, **Equation IV-12** allows to compare the effects of flax fabric treatment independently of the fibre volume fraction and by considering the real matrix strength at fibre breakage [1].

As shown in **Figure IV-16**, equivalent tensile strength of flax fibres are much lower (maximum of 493 MPa reached for raw flax fabrics) than the expected tensile strength of elementary flax fibres ranging from 841 to 1134 MPa as measured by Coroller *et al.* [1] on elementary flax fibres from Hermes, Andrea and Marylin varieties. This suggests that the load transfer within the composites was not optimum to take full advantage of intrinsic tensile strength of flax fibres. In this regard,

Coroller *et al.* [1] also found that the load transfer was not optimum in for flax / epoxy composites with efficiency factors ranging from 0.54 to 0.72 depending on intrinsic properties of flax fibres and their dispersion state within the matrix. It should be pointed out that the discontinuity of the fibres within natural fabrics inherent to dimensional characteristics of plant fibre cells is responsible of lower strength of biocomposites when compared to synthetic fibre reinforced composites, such as glass/polymer composites.

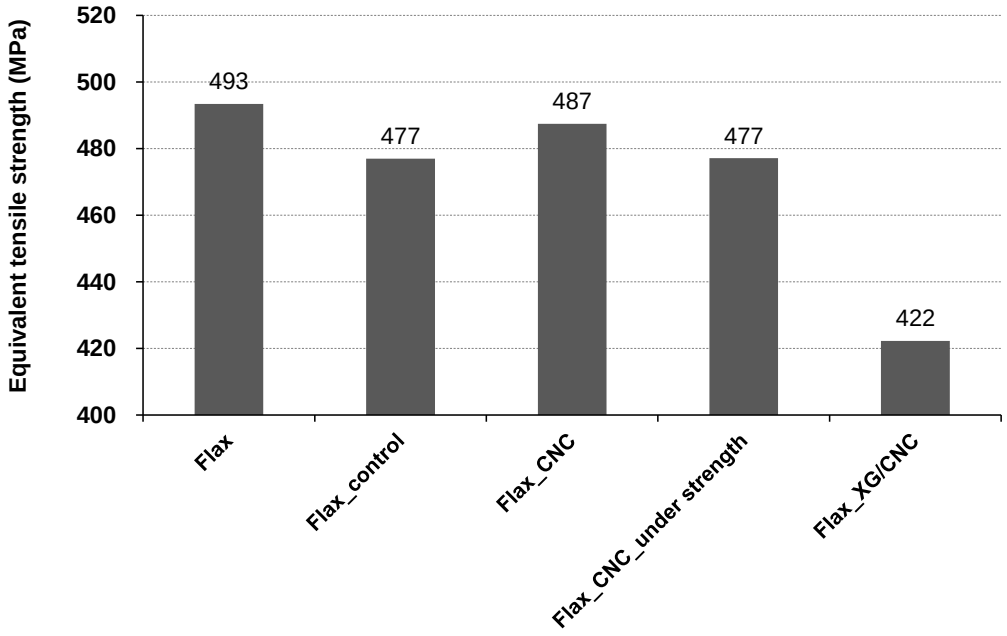

Figure IV-16: Calculated equivalent longitudinal tensile strength of flax fibres for the different biocomposite laminates.

Interestingly, the CNC treatment allows maintaining the equivalent tensile strength obtained with raw flax fabrics, which supports that CNC treatment can improve the dimensional and structural stability of flax fabrics when submitted to functionalizing treatments that involve dipping/free drying steps. Indeed, the control flax fabric reinforced composite has lower equivalent tensile strength of the fibres as compared to the reference biocomposite prepared with raw flax fabric, highlighting the degrading effect of the treatment process. Note that the CNC treated flax fabric dried under strength did not allow any improvement of the equivalent tensile strength. This is

attributed to the worse dispersion of fibre bundles and the presence of porosities and failures in fibre bundles and in the interphase zone fibre / matrix observed for this composite (**Figure IV-8**).

In contrast, XG/CNC treatment leads to much lower equivalent tensile strength which has to be related to the bad dispersion of fibres (**Figure IV-8**) with the above-mentioned formation of fibre bundles (see **Figure IV-5**), but also to the higher voids content obtained with this composite. As shown in **Figure IV-17**, the longitudinal tensile strength of the composites is strongly correlated with the void content measured in composite laminates. Indeed, the failure mechanisms and resulting tensile strength of composite materials are strongly determined by microstructural defects and induced stress concentrations occurring under mechanical solicitations.

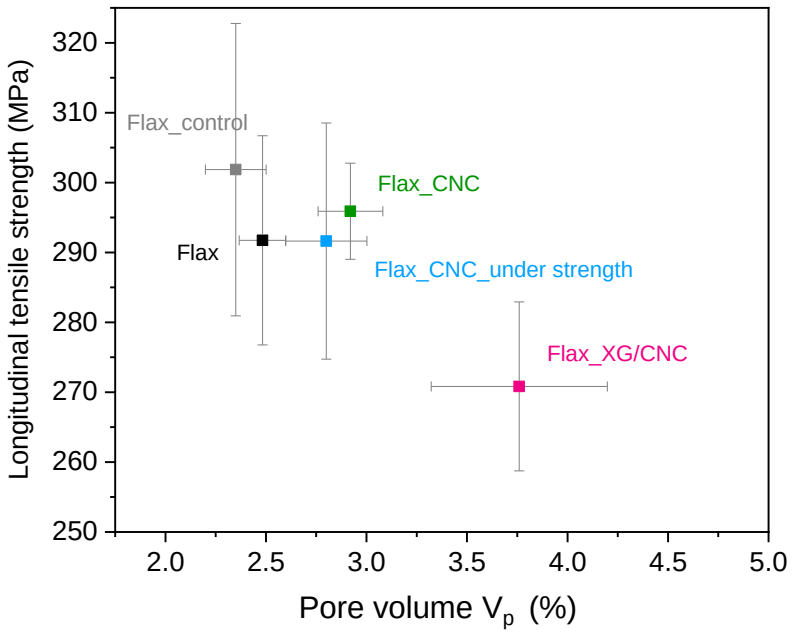

Figure IV-17: Longitudinal tensile strength as a function of the pore volume V_p for the different prepared flax fabrics reinforced epoxy composite plates.

Finally, the work of rupture measured for the different biocomposites (**Figure IV-15 b**) reveals some interesting differences. The control treatment has considerably enhanced the work of rupture with an increase of 30% compared to the reference. The presence of adsorbed CNC on flax fibre surfaces appears also to increase the work of rupture by 14% (free drying) and 11%

(drying under strength) compared to the raw flax fabric. This is primarily due to the higher strain sustained by these composites, hence allowing dissipating more energy upon breakage. It thus appears that creating more interface (case of flax_control fabrics) and/or the nanostructuration at the interface (case of CNC treated fabrics) can modify failure mechanisms and improve the work of rupture even if interfacial adhesion is unchanged.

Concluding, the CNC and XG/CNC treatments did not allow to improve significantly the longitudinal tensile strength of the composites but substantial improvement were found in terms of work of rupture. Interestingly, it was found that CNC treatment can improve the dimensional and structural stability of flax fabrics when submitted to functionalizing treatments that involve dipping/free drying steps. Furthermore, it also contributes to maintain the tensile strength of the biocomposites. Same conclusions were drawn when studying the effect of the treatments on the stiffness of the biocomposites (*see **paragraph 3.4.4.1***).

IV. 3. 6. 2 Transverse tensile strength and surface failures

In the transverse direction of UD fabric reinforced composites, tensile strength is mostly determined by the matrix strength, the residual stresses, and the quality and quantity of fibre / matrix interfaces related to fibre content and distribution, and fibre / matrix interfacial adhesion [64], [65]. Static transverse tensile tests conducted on UD fabric reinforced composites can thus highlight the failure behavior in the interphase zone [66]. Results of the transverse tensile tests on the different prepared biocomposites are represented in **Figure IV-18.**

The addition of CNC on flax fibres, whatever the drying process, decreases strongly the transverse tensile strength by 22 % (free drying) and 30 % (drying under strength). The presence of CNC onto flax fibres induces a more brittle behaviour with a strong decrease of the tensile strain, as shown **Figure IV-18 a**. The treatment XG/CNC on flax fibres seems to have less impact on the tensile strength with a decrease of 9.7 % compared to raw flax / epoxy composites, possibly due to the behavior of the extensible network formed by XG/CNC and their better interactions with cellulosic surfaces. In contrast, the flax_control / epoxy laminate displays higher transverse tensile strength with an increase of 11 % compared to the reference, which is attributed to higher

dispersion and hence larger fibre / matrix interfaces as observed in **Figure IV-8**. Values of transverse work of rupture follow the same trend as the transverse tensile strength with values of 0.89 J (raw flax), 1.04 J (flax_control), 0.38 J (flax_CNC), 0.35 J (flax_XG/CNC) and 0.20 J (flax_CNC_under strength).

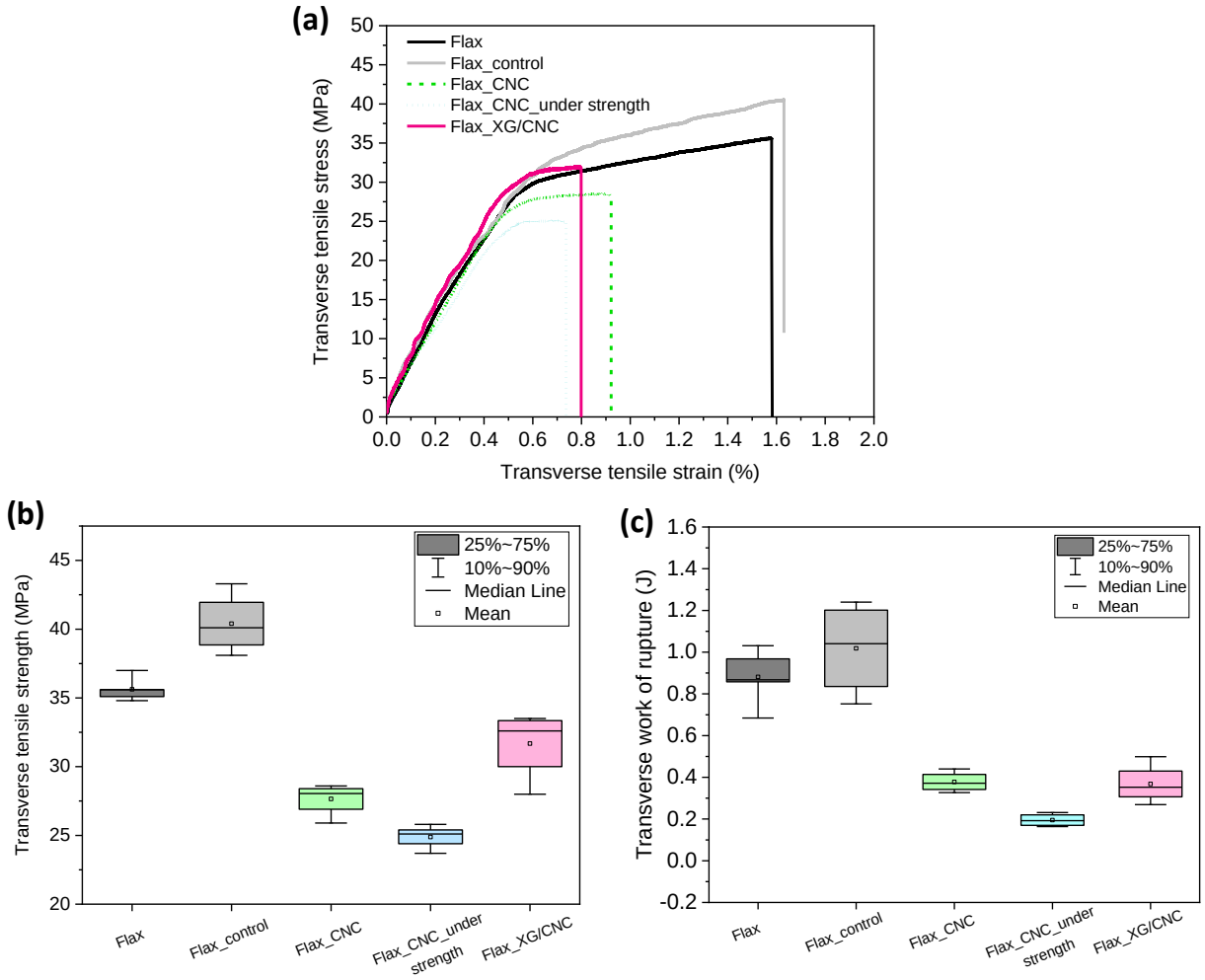

Figure IV-18: Quasi-static transverse tensile properties for the different biocomposite laminates (a) stress-strain curves, (b) tensile strength and (c) work of rupture.

SEM images on fracture surfaces of transverse tensile flax / epoxy specimens are presented in **Figure IV-19**. First, a peeling phenomenon of one or more cell walls of flax fibres has been observed for all specimens (**Figure IV-19 a, b & c**). Many delaminated cell walls in the form of fibrillary ribbons were observed on failure surfaces, especially for the flax_control / epoxy

laminate. Le Duigou *et al.* (2014) studied the complex interphase zone between flax fibres and epoxy resin, and revealed a possible role of the resin penetration in the cell walls to the peeling phenomenon via microbond tests [21]. Moreover, they highlighted in another study an increase of flax fibres fibrillation with the immersion time in water [67]. Indeed, the dipping of flax fibres in water might induce a decrease of the intracellular cohesion within the cell wall structure of flax fibres. Finally, good interfacial adhesion between flax fibre surfaces and epoxy resin would also increase the peeling of fibres, if considering a weaker intracellular cohesion than fibre / matrix interfacial adhesion.

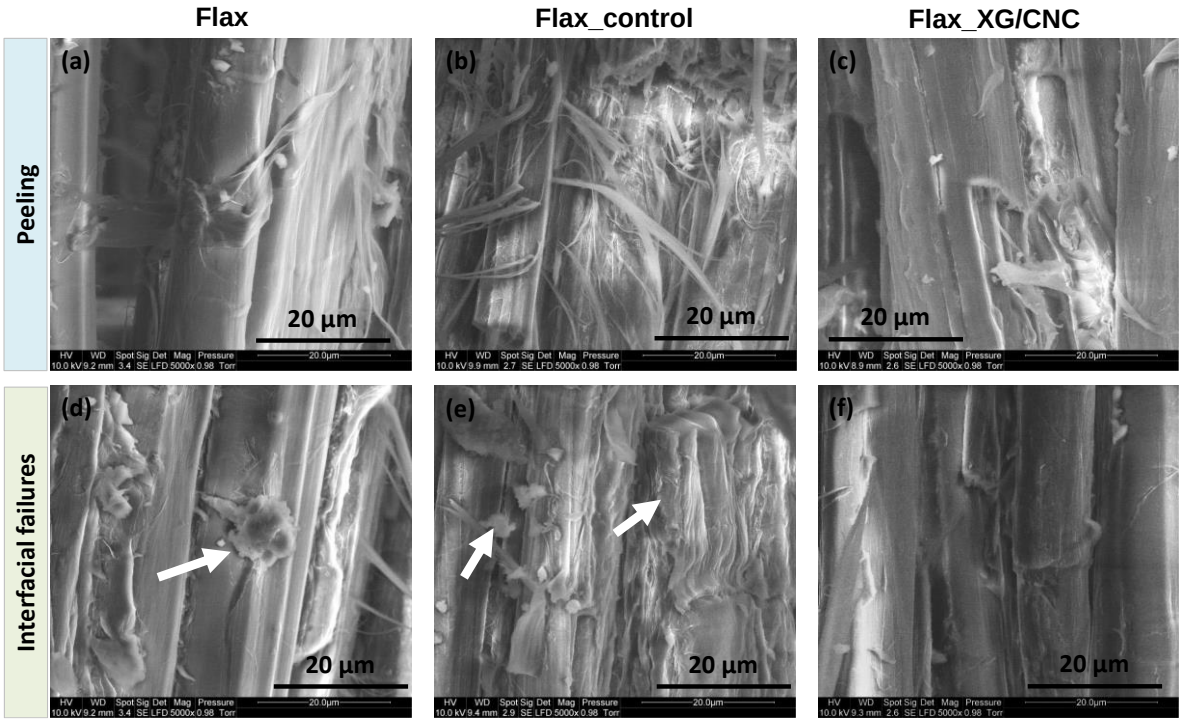

Figure IV-19: SEM images of fracture surfaces (5000x) observed during quasi-static transverse tensile tests on raw, control and XG/CNC treated flax fabrics / epoxy laminates with (a – c) the peeling phenomenon and (d – f) interfaciale failures flax / epoxy (white arrows show epoxy matrix).

Moreover, different interfacial failures have been observed between flax / epoxy laminates (**Figure IV-19 d, e & f**). Some residues of epoxy matrix are visible on untreated flax fibres (white arrow), representative of cohesive interfacial failures but the major part of the fibres seems to be clean, supporting that the main mechanism was adhesive interfacial failure. The fibres treated with

XG/CNC look globally clean with very few residues of matrix on their surface, which is consistent with an adhesive interfacial failure and the decrease of tensile strength observed for flax fibres coated XG/CNC. Finally, the flax_control / epoxy laminate shows more confused fracture surfaces with a mix of epoxy resin and "control" flax fibres, hence supporting a better fibre / matrix cohesion in accordance with the higher transverse tensile strength of the composite. It should be point out that the peeling phenomenon described above could be partly responsible for these improved transverse tensile properties. Indeed, the peeled cell walls ribbons allow to dissipate more energy during crack propagation and sustain more load and strain. The hierarchical structure of cell walls and its controlled destructuration can thus be an advantage in the failure mechanisms and strength of flax fibre reinforced composites.

IV. 4. Conclusions

This *Chapter IV* deals with a multi-scale analysis of the impact of the CNC and XG/CNC treatments on UD flax / epoxy biocomposite laminates. This chapter highlighted the complexity of flax fabric treatments and biocomposite manufacturing process, and their role on the mechanical performances of biocomposites.

At the scale of elementary flax fibre, it has been shown that the surface treatment with CNC decreases the polar character of flax fibres but does not change significantly their wettability and work of adhesion with the epoxy resin. In contrast, the XG/CNC treatment appears to decrease the wettability towards epoxy resin with a slightly higher contact angle.

Considering composite microstructures, CNC and XG/CNC treatment have a strong influence on the dispersion state of fibres and yarns within the manufactured biocomposites. The adsorption of the XG biopolymer, having strong interactions with cellulosic surfaces, creates packed web-like structure between elementary fibres limiting yarns dispersion and the packing ability of fabrics during manufacturing. This is responsible for worse impregnation and substantial increase in porosity, which affects the ultimate mechanical properties of composite plates.

However, the treatment process, i.e. dipping and drying steps, of such fabrics has to be well controlled to avoid any degradation, destructuration and shrinkage of treated fabrics, which could impact negatively final mechanical performances of the composite. In this regard, CNC treatment can contribute to the dimensional and structural stability of flax fabrics when submitted to functionalizing treatments that involve dipping/free drying steps. This allows maintaining the structural properties of the composites in terms of tensile stiffness and strength. Moreover, the CNC and XG/CNC treatments improved the longitudinal work of rupture due to the higher strain sustained by these composites, hence allowing dissipating more energy upon breakage.

In conclusion, improving the mechanical performances of such flax fibres / epoxy biocomposite laminates through interfacial modifications appears as a great challenge with the following key parameters to be controlled for the design of an optimal flax reinforcement:

- Broadening fibres / matrix interfaces via a better dispersion of flax fibres within the matrix while maintaining fibres / yarns orientation and integrity of the fabrics.
- Modifying fibres / matrix mechanical/chemical interactions via reactive molecules and nanostructuration while maintaining good fibre dispersion and good wettability towards the matrix.
- Exploring the controlled destructuration of the hierarchically organized flax cell walls to promote energy dissipation during crack propagation while maintaining the above-mentioned microstructural and wetting characteristics.

IV. 5. References

[1] G. Coroller *et al.*, 'Effect of flax fibres individualisation on tensile failure of flax/epoxy unidirectional composite', *Composites Part A: Applied Science and Manufacturing*, vol. 51, pp. 62–70, Aug. 2013, doi: 10.1016/j.compositesa.2013.03.018.

[2] M. Abida, F. Gehring, J. Mars, A. Vivet, F. Dammak, and M. Haddar, 'Hygro-mechanical coupling and multiscale swelling coefficients assessment of flax yarns and flax / epoxy composites', *Composites Part A: Applied Science and Manufacturing*, vol. 136, p. 105914, Sep. 2020, doi: 10.1016/j.compositesa.2020.105914.

[3] Y. Saadati, G. Lebrun, J.-F. Chatelain, and Y. Beauchamp, 'Experimental investigation of failure mechanisms and evaluation of physical/mechanical properties of unidirectional flax–epoxy composites':, *Journal of Composite Materials*, Jan. 2020, doi: 10.1177/0021998320902243.

[4] M. Kersani, S. V. Lomov, A. W. Van Vuure, A. Bouabdallah, and I. Verpoest, 'Damage in flax/epoxy quasi-unidirectional woven laminates under quasi-static tension', *Journal of Composite Materials*, vol. 49, no. 4, pp. 403–413, Feb. 2015, doi: 10.1177/0021998313519282.

[5] N. Martin, P. Davies, and C. Baley, 'Comparison of the properties of scutched flax and flax tow for composite material reinforcement', *Industrial Crops and Products*, vol. 61, pp. 284–292, Nov. 2014, doi: 10.1016/j.indcrop.2014.07.015.

[6] T. Cadu *et al.*, 'What are the key parameters to produce a high-grade bio-based composite? Application to flax/epoxy UD laminates produced by thermocompression', *Composites Part B: Engineering*, vol. 150, pp. 36–46, Oct. 2018, doi: 10.1016/j.compositesb.2018.04.059.

[7] L. Marrot, A. Bourmaud, P. Bono, and C. Baley, 'Multi-scale study of the adhesion between flax fibers and biobased thermoset matrices', *Materials & Design (1980-2015)*, vol. 62, pp. 47–56, Oct. 2014, doi: 10.1016/j.matdes.2014.04.087.

[8] K. Oksman, 'High Quality Flax Fibre Composites Manufactured by the Resin Transfer Moulding Process', *Journal of Reinforced Plastics and Composites*, vol. 20, no. 7, pp. 621–627, May 2001, doi: 10.1177/073168401772678634.

[9] I. Van de Weyenberg, J. Ivens, A. De Coster, B. Kino, E. Baetens, and I. Verpoest, 'Influence of processing and chemical treatment of flax fibres on their composites', *Composites Science and Technology*, vol. 63, no. 9, pp. 1241–1246, Jul. 2003, doi: 10.1016/S0266-3538(03)00093-9.

[10] Y. Li, Q. Li, and H. Ma, 'The voids formation mechanisms and their effects on the mechanical properties of flax fiber reinforced epoxy composites', *Composites Part A: Applied Science and Manufacturing*, vol. 72, pp. 40–48, May 2015, doi: 10.1016/j.compositesa.2015.01.029.

[11] F. Omrani, P. Wang, D. Soulat, and M. Ferreira, 'Mechanical properties of flax-fibre-reinforced preforms and composites: Influence of the type of yarns on multi-scale characterisations', *Composites Part A: Applied Science and Manufacturing*, vol. 93, pp. 72–81, Feb. 2017, doi: 10.1016/j.compositesa.2016.11.013.

[12] C. Baley, A. Le Duigou, A. Bourmaud, and P. Davies, 'Influence of drying on the mechanical behaviour of flax fibres and their unidirectional composites', *Composites Part A: Applied Science and Manufacturing*, vol. 43, no. 8, pp. 1226–1233, Aug. 2012, doi: 10.1016/j.compositesa.2012.03.005.

[13] U. Huner, 'Effect of Chemical Surface Treatment on Flax-Reinforced Epoxy Composite', *Journal of Natural Fibers*, vol. 15, no. 6, pp. 808–821, Nov. 2018, doi: 10.1080/15440478.2017.1369207.

[14] V. Fiore, T. Scalici, and A. Valenza, 'Effect of sodium bicarbonate treatment on mechanical properties of flax-reinforced epoxy composite materials':, *Journal of Composite Materials*, Jul. 2017, doi: 10.1177/0021998317720009.

[15] CELC European Scientific Commitee, *Flax and Hemp fibres: a natural solution for the composite industry*, JEC Composites. 2012.

[16] R. Rayyaan, W. R. Kennon, P. Potluri, and M. Akonda, 'Fibre architecture modification to improve the tensile properties of flax-reinforced composites':, *Journal of Composite Materials*, Jul. 2019, doi: 10.1177/0021998319863156.
[17] J. L. Thomason, 'Glass fibre sizing: A review', *Composites Part A: Applied Science and Manufacturing*, vol. 127, p. 105619, Dec. 2019, doi: 10.1016/j.compositesa.2019.105619.
[18] *Glass Fibre Sizings by James L. Thomason | Blurb Books UK*. 2015.
[19] N. Le Moigne, B. Otazaghine, S. Corn, H. Angellier-Coussy, and A. Bergeret, *Surfaces and Interfaces in Natural Fibre Reinforced Composites*. Cham: Springer International Publishing, 2018.
[20] B. D. Agarwal, L. J. Broutman, and K. Chandrashekhara, *Analysis and Performance of Fiber Composites*. John Wiley & Sons, 2017.
[21] A. Le Duigou, A. Kervoelen, A. Le Grand, M. Nardin, and C. Baley, 'Interfacial properties of flax fibre–epoxy resin systems: Existence of a complex interphase', *Composites Science and Technology*, vol. 100, pp. 152–157, Aug. 2014, doi: 10.1016/j.compscitech.2014.06.009.
[22] J. Acera Fernández *et al.*, 'Role of flax cell wall components on the microstructure and transverse mechanical behaviour of flax fabrics reinforced epoxy biocomposites', *Industrial Crops and Products*, vol. 85, pp. 93–108, Jul. 2016, doi: 10.1016/j.indcrop.2016.02.047.
[23] I. Van de Weyenberg, T. Chi Truong, B. Vangrimde, and I. Verpoest, 'Improving the properties of UD flax fibre reinforced composites by applying an alkaline fibre treatment', *Composites Part A: Applied Science and Manufacturing*, vol. 37, no. 9, pp. 1368–1376, Sep. 2006, doi: 10.1016/j.compositesa.2005.08.016.
[24] J. A. Fernandez, 'Modification of flax fibres for the development of epoxy-based biocomposites', IMT Mines Alès, 2016.
[25] M. C. Seghini *et al.*, 'Effects of oxygen and tetravinylsilane plasma treatments on mechanical and interfacial properties of flax yarns in thermoset matrix composites', *Cellulose*, vol. 27, no. 1, pp. 511–530, Jan. 2020, doi: 10.1007/s10570-019-02785-3.
[26] P.-J. Liotier *et al.*, 'Role of interface formation versus fibres properties in the mechanical behaviour of bio-based composites manufactured by Liquid Composite Molding processes', *Composites Part B: Engineering*, pp. 86–95, Apr. 2019.
[27] F. Barthelat, 'Architectured materials in engineering and biology: fabrication, structure, mechanics and performance', *International Materials Reviews*, vol. 60, no. 8, pp. 413–430, Nov. 2015, doi: 10.1179/1743280415Y.0000000008.
[28] F. Barthelat, R. Rabiei, and A. K. Dastjerdi, 'Multiscale toughness amplification in natural composites', *MRS Online Proceedings Library Archive*, vol. 1420, ed 2012, doi: 10.1557/opl.2012.714.
[29] M. Lilli *et al.*, 'Tailoring the interfacial strength of basalt fibres/epoxy composite with ZnO-nanorods', *Composite Interfaces*, vol. 0, no. 0, pp. 1–23, Aug. 2020, doi: 10.1080/09276440.2020.1805217.
[30] O. Zabihi, M. Ahmadi, Q. Li, S. Shafei, M. G. Huson, and M. Naebe, 'Carbon fibre surface modification using functionalized nanoclay: A hierarchical interphase for fibre-reinforced polymer composites', *Composites Science and Technology*, vol. 148, pp. 49–58, Aug. 2017, doi: 10.1016/j.compscitech.2017.05.013.
[31] L. Chen *et al.*, 'Role of a gradient interface layer in interfacial enhancement of carbon fiber/epoxy hierarchical composites', *J Mater Sci*, vol. 50, no. 1, pp. 112–121, Jan. 2015, doi: 10.1007/s10853-014-8571-y.
[32] R.-C. Zhuang, T. T. L. Doan, J.-W. Liu, J. Zhang, S.-L. Gao, and E. Mäder, 'Multi-functional multi-walled carbon nanotube-jute fibres and composites', *Carbon*, vol. 49, no. 8, pp. 2683–2692, Jul. 2011, doi: 10.1016/j.carbon.2011.02.057.
[33] H. Wang, G. Xian, and H. Li, 'Grafting of nano-TiO2 onto flax fibers and the enhancement of the mechanical properties of the flax fiber and flax fiber/epoxy composite', *Composites Part A: Applied Science and Manufacturing*, vol. 76, pp. 172–180, Sep. 2015, doi: 10.1016/j.compositesa.2015.05.027.

[34] A. Asadi, M. Miller, S. Sultana, R. J. Moon, and K. Kalaitzidou, 'Introducing cellulose nanocrystals in sheet molding compounds (SMC)', *Composites Part A: Applied Science and Manufacturing*, vol. 88, pp. 206–215, Sep. 2016, doi: 10.1016/j.compositesa.2016.05.033.
[35] Y. Chen, X. Zhou, X. Yin, Q. Lin, and M. Zhu, 'A Novel Route to Modify the Interface of Glass Fiber-Reinforced Epoxy Resin Composite via Bacterial Cellulose', *International Journal of Polymeric Materials and Polymeric Biomaterials*, vol. 63, no. 4, pp. 221–227, Mar. 2014, doi: 10.1080/00914037.2013.830250.
[36] K.-Y. Lee, K. K. C. Ho, K. Schlufter, and A. Bismarck, 'Hierarchical composites reinforced with robust short sisal fibre preforms utilising bacterial cellulose as binder', *Composites Science and Technology*, vol. 72, no. 13, pp. 1479–1486, Aug. 2012, doi: 10.1016/j.compscitech.2012.06.014.
[37] M. F. Pucci, P.-J. Liotier, D. Seveno, C. Fuentes, A. Van Vuure, and S. Drapier, 'Wetting and swelling property modifications of elementary flax fibres and their effects on the Liquid Composite Molding process', *Composites Part A: Applied Science and Manufacturing*, vol. 97, pp. 31–40, Jun. 2017, doi: 10.1016/j.compositesa.2017.02.028.
[38] D. Gay, *Matériaux composites*, 4ème édition. Hermès - Lavoisier, 1997.
[39] E. Doineau *et al.*, 'Adsorption of xyloglucan and cellulose nanocrystals on natural fibres for the creation of hierarchically structured fibres', *Carbohydrate Polymers*, vol. 248, p. 116713, Nov. 2020, doi: 10.1016/j.carbpol.2020.116713.
[40] D. K. Owens and R. C. Wendt, 'Estimation of the surface free energy of polymers', *Journal of Applied Polymer Science*, vol. 13, no. 8, pp. 1741–1747, 1969, doi: 10.1002/app.1969.070130815.
[41] M. F. Pucci, P.-J. Liotier, and S. Drapier, 'Tensiometric method to reliably assess wetting properties of single fibers with resins: Validation on cellulosic reinforcements for composites', *Colloids and Surfaces A: Physicochemical and Engineering Aspects*, vol. 512, pp. 26–33, Jan. 2017, doi: 10.1016/j.colsurfa.2016.09.047.
[42] T. Nahum, H. Dodiuk, S. Kenig, A. Panwar, C. Barry, and J. Mead, 'The effect of composition and thermodynamics on the surface morphology of durable superhydrophobic polymer coatings', *Nanotechnology, Science and Applications*, vol. Volume 10, pp. 53–68, Feb. 2017, doi: 10.2147/NSA.S123447.
[43] S. Li *et al.*, 'Super-Hydrophobicity of Large-Area Honeycomb-Like Aligned Carbon Nanotubes', *J. Phys. Chem. B*, vol. 106, no. 36, pp. 9274–9276, Sep. 2002, doi: 10.1021/jp0209401.
[44] H. Qian, A. Bismarck, E. S. Greenhalgh, G. Kalinka, and M. S. P. Shaffer, 'Hierarchical Composites Reinforced with Carbon Nanotube Grafted Fibers: The Potential Assessed at the Single Fiber Level', *Chem. Mater.*, vol. 20, no. 5, pp. 1862–1869, Mar. 2008, doi: 10.1021/cm702782j.
[45] V. Khoshkava and M. R. Kamal, 'Effect of Surface Energy on Dispersion and Mechanical Properties of Polymer/Nanocrystalline Cellulose Nanocomposites', *Biomacromolecules*, vol. 14, no. 9, pp. 3155–3163, Sep. 2013, doi: 10.1021/bm400784j.
[46] C. L. Pirich, R. A. de Freitas, M. A. Woehl, G. F. Picheth, D. F. S. Petri, and M. R. Sierakowski, 'Bacterial cellulose nanocrystals: impact of the sulfate content on the interaction with xyloglucan', *Cellulose*, vol. 22, no. 3, pp. 1773–1787, Jun. 2015, doi: 10.1007/s10570-015-0626-y.
[47] M. E. Schrader, 'Young-Dupre Revisited', *Langmuir*, vol. 11, no. 9, pp. 3585–3589, Sep. 1995, doi: 10.1021/la00009a049.
[48] D. H. Bangham and R. I. Razouk, 'Adsorption and the wettability of solid surfaces', *Transactions of the Faraday Society*, vol. 33, p. 1459, 1937, doi: 10.1039/tf9373301459.
[49] Wu, *Polymer Interface and Adhesion*. Routledge, 2017.
[50] S. Wu, 'Calculation of interfacial tension in polymer systems', *Journal of Polymer Science Part C: Polymer Symposia*, vol. 34, no. 1, pp. 19–30, 1971, doi: 10.1002/polc.5070340105.
[51] K. R. Ramakrishnan, N. Le Moigne, O. De Almeida, A. Regazzi, and S. Corn, 'Optimized manufacturing of thermoplastic biocomposites by fast induction-heated compression moulding: Influence of processing parameters on microstructure development and mechanical behaviour', *Composites Part A: Applied Science and Manufacturing*, vol. 124, p. 105493, Sep. 2019, doi: 10.1016/j.compositesa.2019.105493.

[52] A. Bourmaud, G. Ausias, G. Lebrun, M.-L. Tachon, and C. Baley, 'Observation of the structure of a composite polypropylene/flax and damage mechanisms under stress', *Industrial Crops and Products*, vol. 43, no. Supplement C, pp. 225–236, May 2013, doi: 10.1016/j.indcrop.2012.07.030.
[53] L. Liu, B.-M. Zhang, D.-F. Wang, and Z.-J. Wu, 'Effects of cure cycles on void content and mechanical properties of composite laminates', *Composite Structures*, vol. 73, no. 3, pp. 303–309, Jun. 2006, doi: 10.1016/j.compstruct.2005.02.001.
[54] B. Madsen, A. Thygesen, and H. Lilholt, 'Plant fibre composites – porosity and volumetric interaction', *Composites Science and Technology*, vol. 67, no. 7–8, pp. 1584–1600, Jun. 2007, doi: 10.1016/j.compscitech.2006.07.009.
[55] B. Madsen and H. Lilholt, 'Physical and mechanical properties of unidirectional plant fibre composites—an evaluation of the influence of porosity', *Composites Science and Technology*, vol. 63, no. 9, pp. 1265–1272, Jul. 2003, doi: 10.1016/S0266-3538(03)00097-6.
[56] J. N. Reddy, *Mechanics of Laminated Composite Plates and Shells: Theory and Analysis, Second Edition*. CRC Press, 2003.
[57] T. Mori and K. Tanaka, 'Average stress in matrix and average elastic energy of materials with misfitting inclusions', *Acta Metallurgica*, vol. 21, no. 5, pp. 571–574, May 1973, doi: 10.1016/0001-6160(73)90064-3.
[58] K. E. Reed, 'Dynamic mechanical analysis of fiber reinforced composites', *Polymer Composites*, vol. 1, no. 1, pp. 44–49, 1980, doi: 10.1002/pc.750010109.
[59] S. Dong and R. Gauvin, 'Application of dynamic mechanical analysis for the study of the interfacial region in carbon fiber/epoxy composite materials', *Polymer Composites*, vol. 14, no. 5, pp. 414–420, 1993, doi: 10.1002/pc.750140508.
[60] J. F. Gerard, S. J. Andrews, and C. W. Macosko, 'Dynamic mechanical measurements: Comparison between bending and torsion methods on a graphite-reinforced and a rubber-modified epoxy', *Polymer Composites*, vol. 11, no. 2, pp. 90–97, 1990, doi: 10.1002/pc.750110204.
[61] N. Le Moigne, M. Longerey, J.-M. Taulemesse, J.-C. Bénézet, and A. Bergeret, 'Study of the interface in natural fibres reinforced poly(lactic acid) biocomposites modified by optimized organosilane treatments', *Industrial Crops and Products*, vol. 52, pp. 481–494, Jan. 2014, doi: 10.1016/j.indcrop.2013.11.022.
[62] R. F. Landel and L. E. Nielsen, *Mechanical Properties of Polymers and Composites*. CRC Press, 1993.
[63] K. D. Ziegel and A. Romanov, 'Modulus reinforcement in elastomer composites. II. Polymeric fillers', *Journal of Applied Polymer Science*, vol. 17, no. 4, pp. 1133–1142, 1973, doi: 10.1002/app.1973.070170411.
[64] A. Bergeret and P. Krawczak, 'Liaison renfort/matrice - Comportement des composites', p. 27, 2006.
[65] A. Bergeret and P. Krawczak, 'Liaison renfort/matrice - Définition et caractérisation', *Techniques de l'Ingénieur*, vol. AM5305v1, 2006.
[66] B. D. Agarwal, L. J. Broutman, and K. Chandrashekhara, *Analysis and Performance of Fiber Composites*. John Wiley & Sons, 2017.
[67] A. Le Duigou, P. Davies, and C. Baley, 'Exploring durability of interfaces in flax fibre/epoxy micro-composites', *Composites Part A: Applied Science and Manufacturing*, vol. 48, pp. 121–128, May 2013, doi: 10.1016/j.compositesa.2013.01.010.

General conclusions and perspectives

I. General conclusions of the PhD project

This PhD project focused on a bio-inspired and innovative treatment surface of flax fibres based on the creation of hierarchical fibres via the adsorption of lignocellulosic biomass by-products, i.e. cellulose nanocrystals and xyloglucan. Moreover, the project went until the elaboration of hierarchical flax fibres based thermoplastic and thermoset composites comprising the CNC and XG/CNC treatments with the aim of increasing mechanical performance. More precisely, this PhD project zoomed in on the interphase zone with the desire to increase the loads transfer within the composites via the CNC and XG/CNC treatments.

The ***Chapter I*** presents the general context of this study and highlights the advantages but also the complexity and limitations of such flax fibres, i.e. heterogeneous and multi-scaled fibres, for their use as reinforcement in composites. Moreover, the desire to increase the compatibility flax fibre / polymeric matrix has been widely studied in the literature but usually employed strategies seem not to enhance sufficiently mechanical performance of flax fibre based composites to target structural applications. A complete but non-exhaustive overview of a bio-inspired strategy is down and highlights the strong potential of nano-objects for the development of hierarchical materials with high mechanical performance, i.e. toughness, strength and interfacial shear strength.

First, the adsorption process of CNC and XG on the surface of flax fibres and interactions flax/XG/CNC have been investigated to better understand the role of each component for their use as treatment of flax fibres (**Table 1**).

Table 1: Research questions and strategies / techniques used to study the adsorption process of XG and CNC on flax fabric.

Adsorption of xyloglucan and cellulose nanocrystals on flax fibres for the creation of hierarchically structured fibres	
Research questions and answers	**Implemented strategies / techniques**
• ***Localization*** *of XG and CNC on flax fabric?* → Homogeneously and randomly adsorbed at the surface of flax fibres. • ***Penetration*** *of the components in the architecture of the fabric?* → Yes. Heterogeneity of XG and CNC adsorbed quantities within the bulk of yarns with their penetration in the yarn. → Complexity to treat such industrial flax fabrics with swelling and destructuration effects.	Coupling of Scanning electron microscopy **(SEM)** + **Confocal microscopy** with the grafting of **fluorescent labelling** (rhodamine B and fluorescein) on XG and CNC 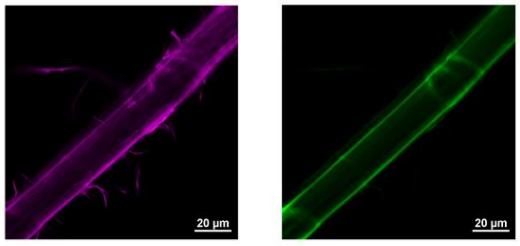
• ***Quantification*** *of adsorbed XG and/or CNC on flax fibres and* ***adsorption kinetic****?* → Around 20 mg/g_{fibres} of XG and CNC were adsorbed on flax fabric. → The presence of XG on fibre surfaces seems to increase the amount of adsorbed CNC at high concentrations.	Use of labeled XG and CNC with fluorescent labelling rhodamine B and supernatant analysis with **Spectroscopy UV** method: → **adsorption isotherms** 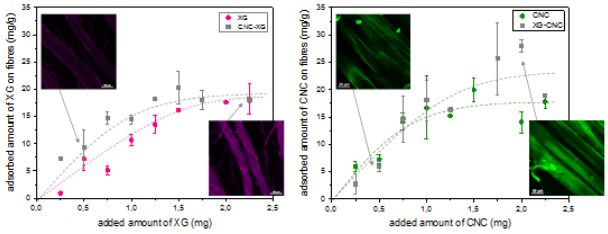
• ***Architecture*** *and* ***affinities*** *between flax/XG /CNC?* → High affinity between XG and cellulose confirmed. → Creation of an extensible network XG/CNC on flax fibres with higher rupture distance CNC-tip / flax fibre+XG.	**Adhesion force measurements** by Atomic force microscopy **(AFM)** → AFM-tip functionalization with XG or CNC for adhesion measurements on flax fibres. 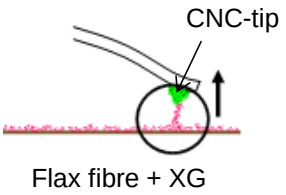

Developed CNC and XG/CNC modified hierarchical flax fibres were adapted at higher scale and for the type of reinforcing flax fibre to create hierarchical composites.

Thermoplastic composites with short flax fibres incorporated in the PP matrix were manufactured by twin-screw extrusion (**Table 2**). The combination of two strategies of flax fibre / matrix interface modification, i.e. nanostructuration with CNC and XG/CNC adsorption and fibre/matrix chemical coupling with maleic anhydride-grafted polypropylene (MAPP) was investigated in terms of microstructural and mechanical properties of composite.

Table 2: Research questions and strategies / techniques used for the study of microstructural and mechanical properties of PP / short flax fibre thermoplastic composites.

Hierarchical thermoplastic biocomposites reinforced with flax fibres modified by xyloglucan and cellulose nanocrystals	
Research questions and answers	**Implemented strategies / techniques**
• *Effect of CNC and XG/CNC treatments on* ***impregnation and interfacial adhesion fibre/matrix*** *in the manufacturing conditions?* → The presence of CNC decreases the polar character of flax fibre surfaces and increases the work of adhesion with PP/MAPP matrix. → The presence of XG seems to counterbalancing those effects, probably due to its strong hydrophilic character.	→ **Tensiometer K100SF:** immersion of elementary flax fibre in testing liquids to obtain surface free energies (polar and dispersive components) of modified fibres. → **Work of adhesion calculations** between PP or MAPP and modified flax fibres at the twin-screw extrusion mixing temperature (190°C) thanks to OWRK and Wu approaches. 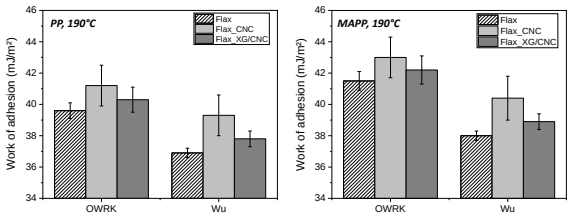

- *Effect of the **combination of 2 strategies of interfacial adhesion modification on microstructural and mechanical behaviour** of composites?*

1) *Creation of hierarchical / nanostructured flax fibres by the adsorption of CNC and XG/CNC*
2) *Incorporation of the coupling agent maleic anhydride grafted polypropylene (MAPP)*

→ Micro-scale: Increase of the work of rupture by 12.5 % and 21.6 % for CNC and XG/CNC treatments, respectively.
Observation of more progressive local failures.

→ Macro-scale: Combine MAPP coupling agent and CNC increases the tensile strength of PP/flax composite, with many covalent bonds between CNC modified fibres and MAPP.

→ **Micro scale**: ***in situ* micro-mechanical tensile SEM tests** (20 wt% fibres)
- Work of rupture measurements
- Observation of the crack propagation within the composite

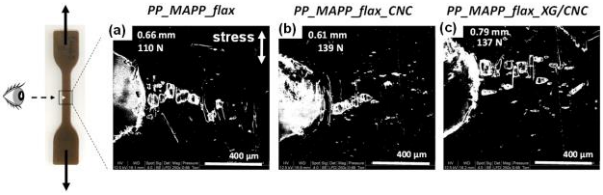

→ **Macro scale**: ***uniaxial tensile test*** (5, 20 and 30 wt% fibres)
- Ultimate strength and stiffness, work of rupture measurements

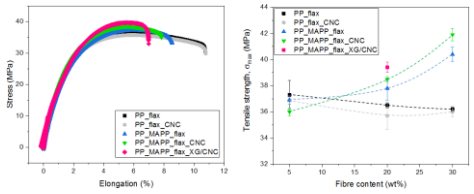

Finally, a multi-scale analysis of epoxy thermoset laminate composites composed of UD flax fabrics modified by CNC and XG/CNC was performed (**Table 3**). It highlights also limitations and impacts of flax fabrics treatment processes on mechanical performances in terms of microstructure and mechanical properties of the final composite.

Table 3: Research questions and strategies / techniques used for the multi-scaled analysis of thermoset laminate composites composed of epoxy / UD flax fabrics.

Multi-scale analysis of hierarchical flax fabric reinforced epoxy biocomposites	
Research questions and answers	**Implemented strategies / techniques**
• *Effect of CNC and XG/CNC treatments on the **morphological aspects of elementary fibres and yarns** within the UD flax fabrics?* → Shrinkage of flax fabrics upon drying step during the treatment process. → Adsorbed amount of CNC and XG/CNC around 3.1 and 6.0 % (depending on fabric architecture and shrinkage effect). → XG/CNC forming polymeric web-like structures surrounding fibres within yarns.	→ **SEM** observations of flax fibres and yarns from treated UD flax fabrics. 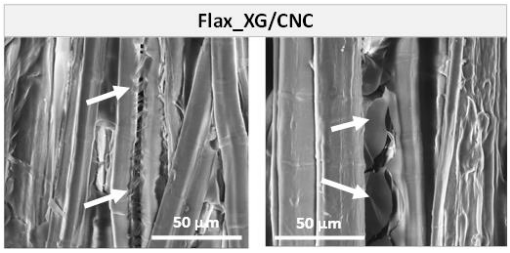 → **Gravimetric/dimensional analysis** of the fabric treatment process (dipping, drying) and the adsorption of CNC and XG/CNC on flax fabrics.
• ***Wettability and impregnation** of the epoxy resin on modified UD flax fabrics during manufacturing process?* → Adsorbed CNC on flax fibres do not change significantly the work of adhesion/wettability towards epoxy resin while XG/CNC increase slightly the contact angle. → XG/CNC treatment induces a worst dispersion by creating fibre bundles caused by the web-like structures between elementary fibres in yarns. → Both CNC and XG/CNC treatments appear to decrease the packing ability of fabrics (bad impregnation and increase of porosities).	→ **Tensiometer K100SF:** contact angle measurement between modified elementary flax fibres and epoxy resin liquid and work of adhesion calculation (Young-Dupré, OWRK and Wu approaches) 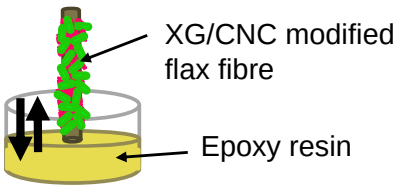 → **Microstructural analysis**: **Dispersion state** of flax fibres and yarns in epoxy resin biocomposites plates; Flax-XG/CNC 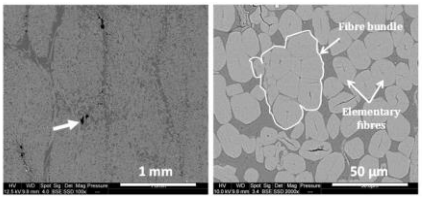 Fibre and pore volumes V_f and V_p **determination** for all composite plates.

- *Effect of **fabric treatment process (water dipping, drying)** on composite properties**?***

→ Destructuration of the fabric and shrinkage.

→ Better dispersion of elementary fibres and yarns provided by the water dipping.

→ Drying by contact under strength induces more packed yarns with CNC and creates porosities and bad dispersion in composite.

→ SEM observations of laminates polished surfaces to study the **flax plies alignment** with an analysis of a **"control" composite.**

→ Use of **2 different fabric drying processes** (free in an oven or by contact under strength)

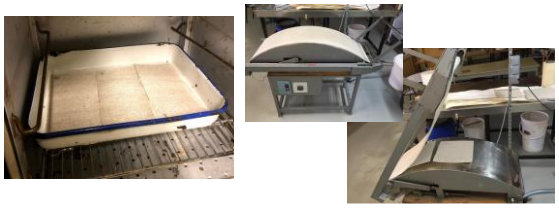

- ***Mechanical behavior** of laminate composites and effect of flax fabric treatments CNC and XG/CNC?*

→ CNC treatment contributes to the dimensional and structural stability of flax fabrics (tensile stiffness and strength) submitted to dipping and drying steps for functionalizing treatments.

→ The presence of CNC on fibres decreases slightly the damping factor in DMTA tests (0.133 versus 0.128), characteristic of a possible better interfacial adhesion with restricted molecular mobility at the interface.

→ Improvements of the longitudinal tensile strength by 3.0 % and the work of rupture by 14 % for CNC treatment (free drying), dissipating more energy upon breakage compared to the reference.

→ More brittle behavior of composites with the addition of CNC on flax fibres: decrease of transverse tensile strength by 22 % and 30 % (free and under strength drying respectively).

→ Peeling phenomenon of cell walls of flax fibres (delaminated cell walls forming fibrillary ribbons) especially for the control composite: participation to the energy dissipation during crack propagation?

→ **Use of mixture rules** to analyze the effect of treatments on mechanical properties.

→ **(Visco-)elastic behavior:** stiffness via longitudinal and transverse quasi-static uniaxial tensile tests, DMTA measurements in transverse specimens.

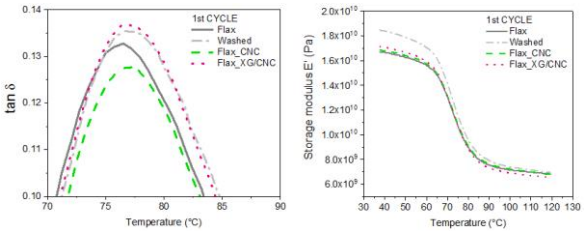

→ **Ultimate behavior:**
Strength via longitudinal and transverse quasi-static uniaxial tensile tests,

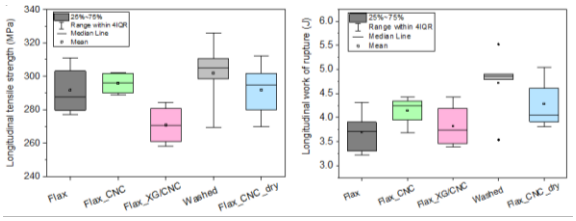

Fracture surfaces, SEM observations of failure fractures in transverse tensile test.

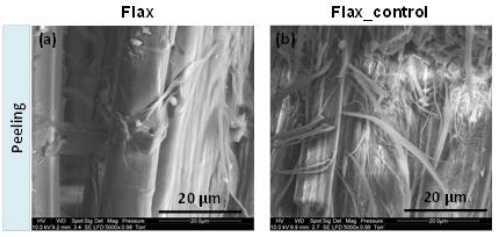

To globally conclude on this PhD project, the adsorption of XG, CNC and XG/CNC on an industrial flax woven fabric was investigated in terms of quantification and localization. This kind of treatment is easy to manage in water solvent and creates hierarchical / nanostructured fibres. However, such fabrics display complex architectures with twisted and entangled yarns which can complicate and influence the adsorption quantity and homogeneity with the penetration of XG and CNC within the yarns. Moreover, some phenomena like swelling and destructuration can occur in water and also modify the morphology and properties of treated fabrics.

CNC and XG/CNC modified hierarchical flax fibres were used in thermoplastic and thermosetting composites. As the processes for manufacturing thermoplastic and thermoset materials are relatively different, this choice has made it possible to highlight certain advantages or limitations of this type of treatment. Indeed, the process of mixing by extrusion of short flax fibres in PP involves a controlled concentration of fibres and very low porosity volumes in the composite. It therefore facilitates the analysis of the interphase zone with few influential parameters resulting from the process. On the other hand, the thermocompression process involves variable fibre volume fractions and voids, influenced by the quality of the fibre/matrix impregnation, and can greatly modify the mechanical behaviour of the prepared laminated composites. However in both cases, improvements of tensile strength and work of rupture were measured in micro- and/or macroscale, which reveal the positive impact of the nanostructuration of flax fibre surfaces by cellulose nanocrystals.

All this work has made it possible to study the processes to be implemented to develop hierarchical flax fibres and their incorporation into composite materials, and to evaluate the potential of these hierarchical plant reinforcements for the development of structural biocomposites.

II. Perspectives

A main perspective of this work could be the **incorporation of CNC in the bulk of the matrix**. Kumar *et al.* (2020) studied the mechanical performance of glass fibre epoxy composites integrating CNC in the matrix [1]. They demonstrated the strong reinforcement of CNC with tensile Young's modulus and strength increased by 14 % and 24 %, respectively for the addition of 2 wt% CNC. Moreover, they observed deposited CNC on glass fibres highlighting the presence of CNC at the interphase zone. Following this strategy, promising results have already been obtained in our project with the addition of CNC in epoxy at 1 wt% and 5 wt%, and measurements of higher transverse tensile strength for the highest amount (5 wt%) (**Figure 1**).

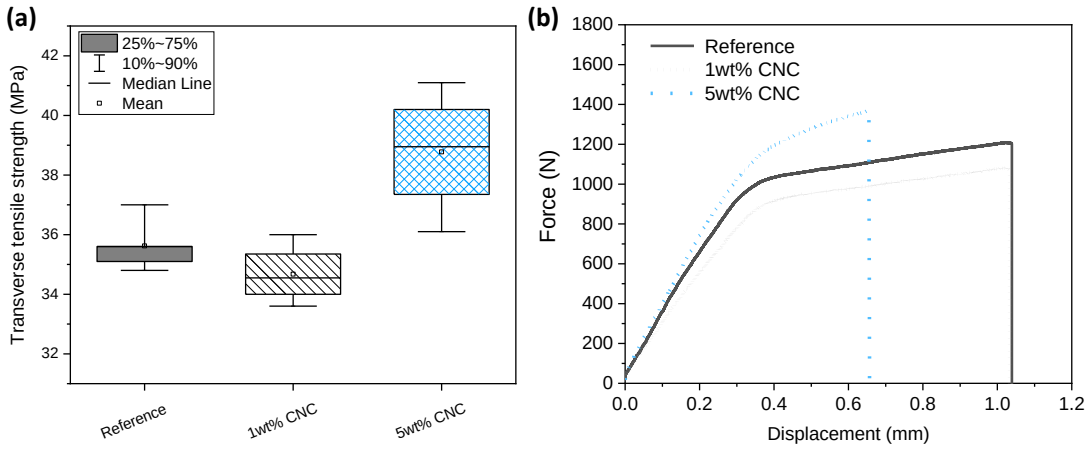

Figure 1: Quasi-static transverse tensile tests of UD flax / epoxy laminate composites with incorporated 1 wt% and 5 wt% CNC in the bulk of the matrix, (a) tensile strength and (b) force-displacement curves.

Other perspectives could be the **oxidation of XG** using periodates or the **functionalization of CNC** depending on the matrix to increase the compatibility fibre / matrix, and hence induce higher mechanical performances of the composite. There are many different types of CNC functionalization which have to be choose according to the matrix [2], [3]. In the case of reactive matrices, adapted reactive groups have to be grafted on CNC to create chemical bonds between modified CNC and the matrix. Considering the epoxy resin matrix, the grafting of epoxy, amine or carboxyl groups can ensure a better compatibilization with the matrix.

Polyolefin matrices such as PE or PP imply the use of different CNC modification strategies: grafting of initiators for living radical polymerization, grafting of reactive groups on CNC which can react with coupling agents (MAPE, MAPP) etc. It has to be noticed that in all cases, the adsorption behaviour of CNC might be influenced by this change of their global surface chemistry.

The **use of cellulose nanofibrils (CNF)** also called microfibrillated cellulose (MFC) depending on dimensions, should be investigated. Flexible structure, degree of fibrillation of CNF and higher aspect ratio (10 – 100) compared to CNC (5 – 30) [4], could be interesting properties to create higher mechanical interlocking with the matrix at the interphase zone.

A strong influence of flax fabric treatment has been observed in the ***Chapter IV*** on mechanical performance of laminated composites. One kind of CNC deposition treatment has been performed, i.e. dipping of fabrics in water suspension, possibly responsible of fabric destructuration. **Other fabric treatment processes should be tested such as spray-coating or padding** avoiding the long-time dipping step.

Finally, it seems that current manufactured industrial flax fabrics display very good mechanical properties that limit maybe the desire to obtain composites with very superior properties by doing modification treatments on theses final products. By keeping in mind the strategy of hierarchical interphases inspired by biological systems, we could maybe think to **the creation of new fabrics with biobased compounds by modern technologies, such as the 3D impression**…

References

[1] S. Kumar, B. G. Falzon, J. Kun, E. Wilson, G. Graninger, et S. C. Hawkins, « High performance multiscale glass fibre epoxy composites integrated with cellulose nanocrystals for advanced structural applications », *Composites Part A: Applied Science and Manufacturing*, vol. 131, p. 105801, avr. 2020, doi: 10.1016/j.compositesa.2020.105801.

[2] A. Dufresne, « Nanocellulose: a new ageless bionanomaterial », *Materials Today*, vol. 16, nº 6, p. 220-227, juin 2013, doi: 10.1016/j.mattod.2013.06.004.

[3] B. L. Peng, N. Dhar, H. L. Liu, et K. C. Tam, « Chemistry and applications of nanocrystalline cellulose and its derivatives: A nanotechnology perspective », *The Canadian Journal of Chemical Engineering*, vol. 89, nº 5, p. 1191-1206, 2011, doi: 10.1002/cjce.20554.

[4] E. J. Foster *et al.*, « Current characterization methods for cellulose nanomaterials », *Chemical Society Reviews*, vol. 47, nº 8, p. 2609-2679, 2018, doi: 10.1039/C6CS00895J.

Scientific contributions (2017-2021)

Publications in scientific journals

1. **Doineau E.**, Bauer G., Ensenlaz L., Novales B., Sillard C., Bénézet J-C., Bras J., Cathala B., Le Moigne N. « Adsorption of xyloglucan and cellulose nanocrystals on natural fibres for the creation of hierarchically structured fibres », *Carbohydrate Polymers*, vol. 248, p. 116713, nov. 2020. doi.org/10.1016/j.carbpol.2020.116713

2. **Doineau E.**, Coqueugniot G., Pucci M. F., Caro A-S., Cathala B., Bénézet J-C., Bras J., Le Moigne N. « Hierarchical thermoplastic biocomposites reinforced with flax fibres modified by xyloglucan and cellulose nanocrystals », *Carbohydrate Polymers*, vol. 254, p. 117403, feb. 2021. doi.org/10.1016/j.carbpol.2020.117403

3. **Doineau E.**, Cathala B., Bénézet J-C., Bras J., Le Moigne N. « Development of bio-inspired hierarchical fibres to tailor the fibre/matrix interphase in (bio)composites », *Polymers*, 13(5), p. 804, mar. 2021. doi.org/10.3390/polym13050804

Oral presentations in conferences

International conferences:

- **Doineau E.,** Le Moigne N., Cathala B., Bénézet J-C., Bras J., "Development of hierarchical interphase in flax/epoxy biocomposites with cellulose nanocrystals: Effects on physical properties of flax fibres and biocomposites", in *EPNOE 6th – International Polysaccharides Conference*. Aveiro (Portugal) – October 21-25th 2019.

- **Doineau E.**, Le Moigne N., Bénézet J-C., Bras J., Cathala B., "Adsorption behaviour of xyloglucan and cellulose nanocrystals on flax fabrics and effects on the mechanical behaviour of flax/epoxy biocomposites", in *ICCS21 – International Conference on Composite Structures 21th*. Bologna (Italy) – September 4-7th 2018.

National conferences:

- **Doineau E.,** Bénézet J-C., Cathala B., Bras J., Le Moigne N., « Fonctionnalisation d'un tissu de lin industriel par adsorption de polysaccharides : Effets sur les propriétés physiques des fibres de lin et des biocomposites lin/époxy », in *GFP Méditerranée 2020, 16ème journée du Groupe Français des Polymères Section Méditerranée*. IMT Mines Alès (France) – March 9-10th 2020.

- **Doineau E.,** Bras J., Le Moigne N., Cathala B., Bénézet J-C., "Adsorption behaviour of xyloglucan and cellulose nanocrystals on flax woven fabrics and effects on the mechanical behaviour of flax/epoxy biocomposites", in *GDR SYMBIOSE – Groupe de Recherche Synhtons et Matériaux Biosourcés*. Ecole Nationale Supérieure de Chimie de Paris (France) – December 18th 2018.

Poster presentation in scientific conferences

- **Doineau E.**, Le Moigne N., Cathala B., Bénézet J-C., Bras J., "Adsorption of xyloglucan and cellulose nanocrystals on flax woven fabrics: Effects on physical properties of flax fibres and flax/epoxy biocomposites", in *JJC Ecocomp - Journée Jeunes Chercheurs Eco-composites et composites biosourcée*. IMT Mines Alès (France) - March 28-29th 2019.

- **Doineau E.**, Le Moigne N., Cathala B., Bénézet J-C., Bras J., "Adsorption of xyloglucan and cellulose nanocrystals on flax woven fabrics: Effects on physical properties of flax fibres and flax/epoxy biocomposites", in *GDR SYMBIOSE – FLOWER Conference*. Nantes (France) – April 24-26th 2019.

Résumé en français

Ce travail de thèse vise à développer un traitement de surface de fibres de lin pour l'amélioration des propriétés mécaniques de biocomposites à matrice polymère et renforts en lin. Cette modification de surface s'inspire des structures hiérarchiques présentes dans les systèmes biologiques (os, nacre ou bois), constitués de nano-objets permettant un meilleur transfert de charges dans ces matériaux. Cette présence d'objets de dimensions nanométriques permet notamment d'atteindre des valeurs de contrainte et ténacité élevées et de limiter la propagation de fissures. Dans ces travaux de recherche, des produits dérivés de la biomasse ligno-cellulosique, à savoir les nanocristaux de cellulose (CNC) et le xyloglucane (XG), ont été choisis pour leurs propriétés et leur affinité mutuelle afin de créer des fibres de lin hiérarchiques. Dans un premier temps, l'adsorption de XG et CNC sur les fibres de lin a pu être localisée et quantifiée grâce à des marqueurs fluorescents. De plus, des mesures de force d'adhésion en microscopie à force atomique ont révélé la création d'un réseau extensible XG/CNC sur la surface de la fibre. Par la suite, deux voies ont été proposées avec l'élaboration de biocomposites thermoplastiques (polypropylène/fibres de lin) et thermodurcissables (résine époxy/tissu de lin) utilisant ces fibres nanostructurées. Dans les deux cas, une augmentation du travail à la rupture a été mesurée en micro-tractions et/ou tractions uniaxiales, permettant une plus grande dissipation de l'énergie lors de la rupture. L'ensemble de ces travaux a permis d'évaluer le potentiel de différents renforts en lin hiérarchiques (tissu unidirectionnel ou fibres courtes) pour le développement de biocomposites structuraux avec un focus fait sur la zone d'interphase fibre / matrice.

Mots-clés : *fibre lin hiérarchique, nanocristaux de cellulose, xyloglucane, interphase, biocomposite.*

English Abstract

This thesis project aims at developing flax fibres surface treatment for the improvement of the mechanical properties of biocomposites with polymeric matrix and flax reinforcements. This surface modification is inspired by the hierarchical structures present in biological systems (bone, nacre or wood), composed of nano-objects which allow a better transfer of loads in these materials. This presence of nano-sized objects makes it possible to reach impressive strength and toughness values and to limit cracks propagation. In this project, products derived from lingo-cellulosic biomass, namely cellulose nanocrystals (CNC) and xyloglucan (XG), were chosen for their interesting properties and mutual affinity to create hierarchical flax fibres. In a first step, the adsorption of XG and CNC on flax fibres was localized and quantified using fluorescent markers. In addition, atomic force microscopy measurements of adhesive force revealed the creation of an extensible XG/CNC network on the fibre surface. Subsequently, two paths were proposed with the elaboration of thermoplastic (polypropylene/flax fibres) and thermoset (epoxy resin/flax fabric) biocomposites using these nanostructured fibres. In both cases, an increase of the work of rupture has been measured by micro- and/or uniaxial tensile tests, allowing dissipating more energy upon breakage. All this work has allowed evaluating the potential of different hierarchical natural reinforcements (unidirectional fabric or short flax fibers) for the development of structural biocomposites with a focus on the fiber/matrix interphase zone.

Keywords : *hierarchical flax fibre, cellulose nanocrystals, xyloglucan, interphase, biocomposite.*